The Expression of Connexins in Neurodegeneration

Ia Chevyreva

A thesis submitted in fulfilment of the requirements

for the degree of Doctor of Philosophy in Anatomy,

The University of Auckland, 2011

ABSTRACT

Changes in connexin expression are thought to play a role in neurological disease and the possible effects of these changes in connexion expression in the disease process are therefore important. The need to screen for connexin expression quickly and cost-effectively has directed attention to microarray technology. The aim of the first section of this study was to design a 'boutique' microarray chip to screen for mRNA for all the reported connexins in the human. Where possible, the probes were designed to be compatible with the rat connexin mRNA. Twenty 50-base length oligonucleotide custom-designed probes, fourteen of them showing cross-species human/rat alignment, and twenty probes for the human connexin sequences designed by the German company MWG were included in the array. The array was tested on rat and on human tissue and the result validated by the Affymetrix GeneChips. Results confirmed that our array design was reliable, had a consistent target binding pattern and that it could detect differential connexin gene expression in both human and rat tissues.

As our goal was to screen human brain tissue for connexin expression, obtaining RNA of sufficiently high quality to be used in microarray experiments became a concern. We investigated whether it was possible to obtain high quality RNA from postmortem human tissue using samples obtained from the New Zealand Neurological Foundation Human Brain Bank. The principle finding was that RNA quality is most strongly affected by the pH of the tissue, with both the pH and the RNA quality being influenced by the mode of death. The best quality RNA samples were then used for the screening of human brain tissue for connexin expression.

One control and five disease samples from the secondarily affected regions of Huntington's (MC), Parkinson's (CN) and Alzheimer's disease, as well as hippocampus samples from two mesial temporal lobe epilepsy patients were screened on the custom-designed connexin array and on the Illumina Sentrix arrays to search for changes in the expression of connexins and inflammatory cytokines. It proved possible to obtain consistent data from the two platforms from samples with a wide range of RNA quality, and certain common patterns in the change of connexins and inflammatory markers were identified

ACKNOWLEDGEMENTS

The biggest credit deservedly goes to my primary supervisor, Associate Professor Louise Nicholson, for the enormous amount of support I received from her in making my project come together. Her boundless energy and dedication has been an inspiration to me. I would also like to thank my other supervisor, Professor Colin Green, for his help with the connexins background, and general moral support.

I would like to thank Professor Richard Faull for kindly providing the postmortem human brain tissue for the study and to Jocelyn Bullock for obtaining the tissue from the Human Brain Bank.

Dr Shamim Shaikh should be credited for the huge amount of time and effort she has put into teaching me all the molecular biology techniques, and keeping me going through all my mistakes and frustrations. Her knowledge in the area is truly amazing, and I would have been lost without her.

I am grateful to Dr Lee Yong Law, who taught me most of what I know about oligonucleotide probe design, to Liam Williams at the SBS Microarray facility who helped me learn microarray techniques and to Dr Mik Black for doing the statistical analysis for me for the first part of my study and teaching me the fundamentals of microarray analysis.

I am extremely thankful to my mother who provided invaluable emotional support as well as applied her considerable linguistic skills to editing and proofreading my thesis.

I wish to acknowledge financial assistance from the University of Auckland Doctoral Scholarship (2004).

I would like to thank the students in the connexin group for great company and everyone else who I have come in contact with during my PhD and who has supported me throughout it.

TABLE OF CONTENTS

LIST OF TABLES

LIST OF FIGURES

LIST OF ABBREVIATIONS

CCD – charge-coupled device

CD11A – alpha L integrin

CD11B – alpha M integrin

CN – caudate nucleus

CNS – central nervous system

DNA – deoxyribonucleic acid

DNase - deoxyribonuclease

GAPDH – glyceraldehyde-3-phosphate dehydrogenase

GCOS – Affymetrix GeneChip® Operating Software

GFAP – glial fibrillary acidic protein

IL-1β – interleukin 1 beta

IL-6 – interleukin 6

IL-10 – interleukin 10

MC – motor cortex

MTG – medial temporal gyrus

HNRPC – heterogeneous nuclear ribonucleoprotein C1/C2

HPRT – hypoxanthine-guanine phosphoribosyltransferase

Oligo – oligonucleotide probe

PMT – photomultiplier tube

qRT-PCR – quantitative real-time polymerase chain reaction

RNA – ribonucleic acid

RNase – ribunuclease

RPS9 – ribosomal protein S9

TCEA1 – transcription elongation factor A (SII) 1

TNF-α – tumour necrosis factor alpha

1 INTRODUCTION

1.1 Gap Junctions and Their Role in Neurological Disease

1.1.1 Gap junctions – structure and function

Gap junctions provide a means for direct cell-to-cell communication. A connexon is a pore in the plasma membrane which aligns with an identical pore on the adjacent cell, forming a conduit between their cytoplasmic compartments. Gap junctions are not finely discriminative in terms of the chemicals that are able to pass through them, the primary limitation being the size of the pore. Gap junction channels serve for diffusional exchange of ions, metabolites such as ATP, ADP, glucose, glutamate and glutathione and second messengers including CAMP and inositol 1,4,5-triphosphate (Kam et al., 1998; Niessen et al., 2000; Goldberg et al., 2002) and other molecules including antigens (Neijssen et al., 2005; Mendoza-Naranjo et al., 2007), contributing towards the integration of metabolic activities by coupling cells into a direct communication network. The coupling of cells via gap junctions occurs by the means of not just one single channel but a plaque which may contain hundreds of gap junction channels (Evans and Martin, 2002; Willecke et al., 2002; Mese et al., 2007; Orthmann-Murphy et al., 2008).

A gap junction is composed of two hemichannels (connexons), one in the plasma membrane of either cell, that then dock together. Each connexon is comprised of six protein subunits called connexins (Cx). A connexin protein is a plasma membrane protein with four transmembrane domains (that have an α-helical conformation) and both amino- and carboxy-termini on the cytoplasmic side. Thus a connexin possesses two extracellular loops and one intracellular loop. Extracellular loops are believed to serve as docking domains for the two hemichannels (See Figure 1) (Goodenough et al., 1996; Kumar and Gilula, 1996; Evans and Martin, 2002; Willecke et al., 2002; Yeager and Harris, 2007).

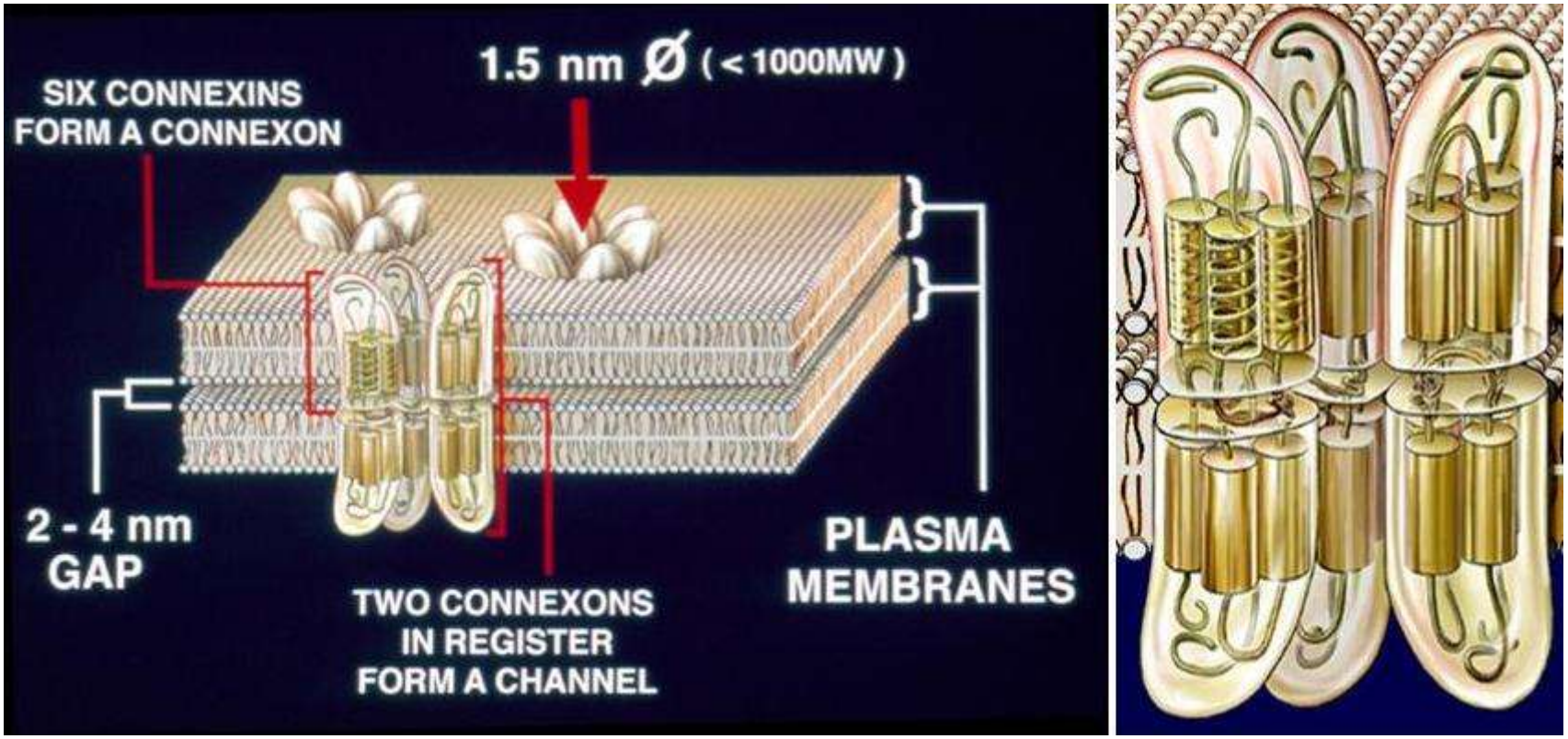

Figure 1. The structure of a gap junction, on the left; the molecular structure of a connexin, on the right (picture kindly provided by Professor Colin R. Green).

It is at the level of the connexin protein that the diversity of gap junctions primarily lies. So far, 21 distinguishable human connexins have been identified (as found on the GenBank database: http://www.ncbi.nlm.nih.gov). The intramembrane regions, extracellular loops, and amino-termini of the various connexins tend to be highly conserved. The variability between different members is mainly present on the cytoplasmic loop and the carboxy-terminus (Willecke et al., 2002; Yeager and Harris, 2007).

There are two different notations in use to describe connexin proteins. One method is based on the molecular weight in kilodaltons (e.g. Cx26 is the connexin protein with the molecular weight of 26 kDa). The other system utilises connexin classes denoted by Greek symbols, depending on the sequence homology and the length of the cytoplasmic loop, and a number in the order of discovery (Cx26 is gap junction beta 2 (GJB2)). (Kumar and Gilula, 1996; Evans and Martin, 2002; Mese et al., 2007). The Greek-symbol nomenclature is preferable in terms of denoting orthologous (i.e. evolutionarily homologous) connexin types between different species (since orthologous proteins tend to differ somewhat in the amino acid composition between species, the molecular weight notation makes it difficult to establish homology).

Human connexin genes often show high sequence identity to their mouse and rat orthologs. For some of the earlier sequenced connexins, the molecular mass is very similar, so that the same abbreviations can be used for both terminologies (e.g. human Cx32 and rat Cx32 are both gap junction beta 1 (GJB1 and Gjb1 respectively), with some of the connexins identified later, considerable molecular mass differences can occur between species. (Evans and Martin, 2002; Willecke et al., 2002; Mese et al., 2007)

When both of the two docked connexons in a gap junction are composed of the same connexin protein, that gap junction is referred to as homotypic. If the gap junction is made up of a different kind of connexin protein within connexon, the gap junction is said to be heterotypic. The possibility also exists for much greater gap junction variability through the formation of heteromeric gap junction channels, i.e. when each connexon subunit contains a mix of connexin types (a homomeric connexon is made up of the same connexin subtype). The protein subunit composition of gap junction channels defines their conductance and permeability properties. Heterotypic and heteromeric gap junctions can differ in their permeability from the corresponding homotypic and homomeric gap junctions. (Willecke et al., 2002; Mese et al., 2007). Gap junctions can show preferential permeability for anions, others for cations and some have no charge selectivity (Elfgang et al., 1995; Cao et al., 1998). Different permeability of gap junctions to signals and metabolites affects their potential physiological function. Uncoupled connexons are also active in single plasma membranes forming hemichannels which

provide a pathway for molecular exchange between the cytoplasm and the extracellular compartment (Saez et al., 2005)

1.1.2 Connexins in the CNS – health and disease

1.1.2.1 Connexin expression in the CNS

The central nervous system expresses a number of different connexins. Neurons have been shown to express Cx36 (expressed exclusively in neurons), Cx45 and Cx57 (Condorelli et al., 1998; Sohl et al., 2005; Collignon et al., 2006; Meier and Dermietzel, 2006). Cx43 is thought to be expressed in neurons during development (Nakase and Naus, 2004; Collignon et al., 2006). The expression of Cx32 in neurons is controversial (Theis et al., 2005), with recent studies using a more specific Cx32 antibody localising its expression in myelinated glial cells rather than neurons (Sohl et al., 2005). Cx31.1 has been shown to be expressed neurons of the mouse brain (Dere et al., 2008) and rodent dopaminergic neurons (Vandecasteele et al., 2006).

Astrocytes express Cx43 (in both white and grey matter) and Cx30 (primarily in the grey matter); Cx 45, Cx40, Cx46 (Scemes et al., 1998; Dermietzel et al., 2000). The expression of Cx26 in astrocytes is uncertain, as its high homology to Cx30 makes it hard to differentiate in immunohystochemical studies. Oligodendrocytes express Cx29 (human Cx30.2), Cx32 and Cx47 (Kleopa et al., 2004; Li et al., 2004a; Orthmann-Murphy et al., 2008; Sargiannidou et al., 2008). Microglia express Cx43 and Cx36 (Parenti et al., 2002; Nakase and Naus, 2004).

Cx31.9 has been shown to be expressed in the cerebral cortex (White et al., 2002) and Cx31 in neuronal cell lines (particularly in differentiated neurons) (Unsworth et al., 2007).

An additional number of connexins present in the brain are expressed by endothelial cells (Cx37, Cx40, as well as Cx43, Cx45 (Brisset et al., 2009) and Cx32 (Okamoto et al., 2009)) and meningeal cells (Cx43 and Cx26) (Nakase and Naus, 2004; Brisset et al., 2009) (See Table 1 for a summary).

Glial cells are extensively coupled via gap junctions, forming a glial syncytium throughout the brain and spinal chord (Dermietzel, 1998; Rouach et al., 2002; Orthmann-Murphy et al., 2007). Gap junction coupling is the most abundant between astrocytes (especially in the grey matter) and less abundant between astrocytes and oligodendrocytes. There is structural fevidence or heterotypic gap junctions between Cx32 in oligodendrocytes and astrocytic Cx26, Cx30, Cx43 and Cx47 (Li et al., 2004b). Gap junctional communication between has been demonstrated in grey but not white matter (Orthmann-Murphy et al., 2007; Orthmann-Murphy et al., 2008). Neurons are extensively coupled during

development but less so in the adult CNS (interneuronal interactions are mainly synaptical), and coupling between neurons and glia generally appears insignificant (Nakase and Naus, 2004; Sohl et al., 2005; Orellana et al., 2009)

1.1.2.1.1 Astrocytes

Astrocytes are known to play a key role in the maintenance of normal physiological function by regulating ion (Na^+ and K^+) homeostasis and removing excess potentially toxic chemicals (such as glutamate) from the extracellular space around neurons. Astrocytes also provide a link between neurons and blood vessels. An important function of astrocytes is the propagation of intercellular Ca^{2+} waves in response to activation. Gap junctions have been shown to be involved in mediating intercellular Ca^{2+} signalling through the glial syncytium resulting in the release of glutamate (Rossi and Volterra, 2009). Connexin hemichannels play a role in the release of adenosine triphosphate (ATP) associated with Ca^{2+} signalling (Cornell-Bell et al., 1990; Charles et al., 1992; Venance et al., 1997; Stout et al., 2002). Astrocytes also provide a link between neurons and blood vessels, producing vasoactive factors in response to neuronal activity causing rapid changes in blood flow depending on changing energy demand. This function is dependent on connexin channels and is strongly reduced by their inhibition (Zonta et al., 2003; Metea and Newman, 2006; Xu and Pelligrino, 2007)

Intercellular communication between astrocytes occurs mainly through gap junction channels. Gap junctions are believed to protect neurons through the spatial buffering of neurotoxic substrates. Moreover, reduced gap-junctional communication between astroglial cells is associated with neurotoxicity (Blanc et al., 1998; Ozog et al., 2002). Unapposed hemichannels however may act in the opposite way, as overactivated glial cells show enhanced hemichannels activity (Retamal et al., 2007) that very likely worsens their neurotoxic effects (Stridh et al., 2008).

Gap junctional channels and hemichannels are under the control of different mechanisms, possibly related to the different molecular compositions of the subcellular compartment where each one is located (Orellana et al., 2009). Under normal physiological conditions the probability of hemichannels opening is low but it can be markedly increased by a drop in extracellular divalent cations Ca^{2+} and Mg^{2+} which occurs in ischaemic brain. Hemichannel opening is also stimulated by oxygen and glucose deprivation and exposure to pro-inflammatory cytokines. Their opening allows the release of molecules such as NAD^+, ATP, glutamate, prostaglandin E2, and glutathione (Stout et al., 2002; Ye et al., 2003; Bruzzone et al., 2005; Cherian et al., 2005; Rana and Dringen, 2007).

In several CNS disorders, astrocytes can be activated by various inflammatory mediators, including cytokines (Thornton et al., 2006; Fogal et al., 2007), lipoteichoic acid (Kinsner et al., 2005), LPS

(McNaught and Jenner, 1999; Zhou et al., 2006), and amyloid-β. (Wang et al., 2007). Some suggested mechanisms that underlie this effect include the release of high levels of NO, peroxynitrite, glutamate, TNF-α and IL-1β (Heales et al., 1999; Bal-Price and Brown, 2001). Astrocyte activation involves changes in cellular phenotype and gene expression which can be deleterious for neurons (Hewett et al., 1994; Bolanos et al., 1997; Bal-Price and Brown, 2001). Accordingly, activated astrocytes increase neuronal death *in vitro* (Chao et al., 1996; Hu et al., 1997; Kingham et al., 1999).

After brain injury, astrocytes adjacent to the cite of injury undergo a process called reactive astrogliosis involving astrocyte proliferation and hypertrophy. The activated astrocytes show an increased level of expression of Cx43 (Haupt et al., 2007). Upregulation of Cx43 is thought to play a significant role in lesion spread. A number of studies demonstrated that blocking connexin hemichannels at the site of an acute injury reduces lesion spread and limits glial activation and astrocytosis (Cronin et al., 2006; Danesh-Meyer et al., 2008; O'Carroll et al., 2008).

1.1.2.1.2 Microglia

Microglia are another cell type where connexin expression changes have been investigated. Microglia have an important role in the CNS, taking part in the reactive gliosis response. They are the most sensitive detectors of threatening conditions in the CNS. When activated by stimuli such as hypoxia/reoxygenation, ischaemia/reperfusion, cytokines, amyloid-β, α-synuclein, glutamate (Kaushal and Schlichter, 2008), lipopolysaccharide (LPS) (Madrigal et al., 2005; Ruano et al., 2006), extracellular proteoglycans (Bussini et al., 2005), prion peptides (Brown et al., 1996; Bate et al., 2002), cell debris (Beyer et al., 2000), amyloid-β peptide, microglia release high levels of pro-inflammatory cytokines, leading to inhibition of astrocytic gap-junctional communication. Two pro-inflammatory cytokines in particular, interleukin-1β (IL-1β) and tumor necrosis factor-α (TNF-α), were shown to be involved in this inhibition (Meme et al., 2006). Activated microglia demonstrate an increase in expression of Cx43 and Cx32 (Takeuchi et al., 2006). Cx32 and Cx43 form hemichannels through which neurotoxic concentrations of glutamate are released (Takeuchi et al., 2006; Retamal et al., 2007) and their neurotoxic effect is blocked with glutaminase or the gap junction blocker CBX (Yawata et al., 2008). Moreover, glutamate induces astrocyte oedema (Koyama et al., 2000; Han et al., 2004) and therefore contributes to the propagation of ischaemic effect as a wave to the periphery of the ischemic injury. Microglia-mediated neurotoxicity is known to be progressive over time (Gao et al., 2003; Huh et al., 2003; McGeer and McGeer, 2003) and may contribute to the progression of various neurodegenerative diseases. In accordance with this notion, immunosuppression reduces delayed cell death (Hailer, 2008).

Since connexin hemichannels are permeable to ATP (De Vuyst et al., 2006; Kang et al., 2008)), it is possible that in microglia they provide a pathway for ATP release which stimulates microglial migration to the sites of injury (Davalos et al., 2005). The existence of Cx36 heterocellular gap junctions between microglia and neurons has been suggested and may provide another mechanism for transfer of death signals from microglia to neurons (Dobrenis et al., 2005).

1.1.2.1.3 Oligodendrocytes

The function of connexins in oligodendrocytes is thought to be metabolic, allowing ions and nutrients to pass to all layers of the myelin sheath (Paul, 1995; Suter and Snipes, 1995; Kleopa et al., 2004). Absence of connexin Cx32 results in demyelination and an enhanced excitability in the CNS (Sutor et al., 2000; Sargiannidou et al., 2009) while vacuolation of nerve fibres was observed in Cx47-null mice, particularly at the site of the optic nerve where axons are first contacted by oligodendrocytes and myelination starts (Odermatt et al., 2003; Ahn et al., 2008).

1.1.2.2 Neurodegenerative diseases

1.1.2.2.1 Alzheimer's disease

Alzheimer's disease is characterised by the accumulation of amyloid-β into amyloid plaques outside and around neurons and formation of neurofibrillary tangles inside neurons. High concentrations of amyloid-β are toxic to a number of neuronal types (Loo et al., 1993; Pike et al., 1995; Parihar and Hemnani, 2004).The mechanisms of amyloid-beta toxicity involve activation of NMDA glutamate receptors, sustained elevations of extracellular calcium and oxidative stress (Alvarez-Maubecin et al., 2000; Ekinci et al., 2000). These effects are similar to those induces by ischaemia/reprefusion but on an extended time scale.

Amyloid plaques in the brains of patients with Alzheimer's disease are closely associated with activated astroglia and microglia (Wisniewski and Wegiel, 1991; Kalaria, 1999). High levels of inflammatory cytokines such as tumour necrosis factor-α (TNF-α), interleukin-1β (IL-1β) and interleukin-6 (IL-6), produced primarily by reactive microglia and astrocytes, are also detected in the brain of patients with Alzheimer's disease (Parenti et al., 2002; Rossi and Volterra, 2009). An increase in Cx43 expression was observed at the site of amyloid plaques (Nagy et al., 1996; Nakase and Naus, 2004). The pro-inflammatory cytokines released by microglia enhance Cx43 hemichannels activity (Retamal et al., 2007), but inhibit gap junction coupling between astrocytes. A reduction in gap-junctional communication adversely affects the buffering capacity of astrocytic networks, while

increased hemichannel activity could influence the viability of neighbouring cells by paracrine interactions. Disregulation of the release and uptake of signalling molecules such as glutamate, arachidonic acid byproducts and prostaglandin E2 probably contributes to neuronal excitotoxicity (Ye et al., 2003; Mergenthaler et al., 2004; Ahmad et al., 2006; Takeuchi et al., 2006). The presence of amyloid-β is likely to have a potentiating effect on these mechanisms and may aggravate astroglial mediated neuronal death. The rise in Ca^{2+} induced by amyloid-β may lead to activation of Cx43 hemichannels in astroglial cells and promote their death in three possible ways - excessive entry of Ca^{2+} through Cx43 hemichannels causing activation of enzymes such as lipases, phosphatases, and proteases, Na^{+} and Cl^{-} influx through the hemichannels leading to osmotic water inflow and astroglial swelling, and release of molecules required in normal cell metabolism (e.g., glucose and derivates, NADH, ATP, ascorbic acid, and reduced glutathione (GSH)) to the extracellular space (Wang et al., 2007; Orellana et al., 2009).

1.1.2.2.2 Parkinson's disease

The precise mechanisms of Parkinson's disease at the molecular level have not been elucidated, but the disease pathogenesis involves oxidative stress and accumulation of α-synuclein (Singleton et al., 2003). The substantia nigra of PD patients shows significant proliferation of reactive amoeboid macrophages and microglia in postmortem studies (McGeer et al., 1988). Activated glial cells in the substantia nigra express inflammatory cytokines such as TNF-α, IL-1β, and IFN-γ (Hunot et al., 1996; Hirsch et al., 1998). In 1-methyl-4-phenyl-1,2,3,6-tetrahydropyridine (MPTP)-lesioned striatum, an animal model of PD, total Cx43 mRNA and astroglial Cx43-immunoreactivity were significantly increased, while astroglial coupling evaluated with dye coupling of patched cells remained unaffected (Rufer et al., 1996). Cx43 is also upregulated in activated microglia of the macrophage phenotype (Shaikh et al., 2007)

As with Alzheimer's disease, it is probable that increased opening of microglial, astroglial, and neuronal hemichannels in Parkinson's disease is associated with a decline in gap junction coupling. Overexpression of α-synuclein inhibits gap junction communication in dopaminergic neuroblastoma cells, and this may increase the susceptibility of α-synuclein overexpressing cells to various toxins (Sung et al., 2007). In addition, α-synuclein binds to Cx32, a connexin that is expressed in the substantia nigra (SiuYi Leung et al., 2001; Vandecasteele et al., 2006) where neurons are electrically coupled (Vandecasteele et al., 2005).

1.1.2.2.3 Huntington's disease

Huntington's disease (HD) is a progressive and fatal neurological disorder caused by an increased number of CAG repeats in the gene coding for the protein huntingtin (1993). The accumulation of this protein within the cell body causes apoptosis of striatal neurons (Paulsen et al., 2001). Similarly to other neurodegenerative diseases, HD causes both microglial (Tai et al., 2007) and astroglial activation (Aguado et al., 1998) and elevated Cx43 expression in the caudate nucleus in HD correlates with astrocytes positive for glial fibrillary acidic protein (GFAP), a cell-specific marker for reactive astrocytes (Vis et al., 1998b).

Astroglia expressing mutant huntingtin aggravate excitotoxic neuronal damage (Shin et al., 2005). Moreover, a fragment of the mutant huntingtin disrupts the microglial transcription program (Giorgini et al., 2008). Thus expression of mutant proteins (e.g., amyloid-β, α-synuclein, and huntingtin) can adversely affect the normal glial response, amplifying the initial injury by damaging susceptible neurons (Lobsiger and Cleveland, 2007). Alternatively, the expression of these mutant proteins in glia causes them to become an important source of neurotoxicity in their own right, potentially independent of the effects of the mutation in neurons (Lobsiger and Cleveland, 2007).

1.1.2.2.4 Epilepsy

In mesial temporal lobe epilepsy a highly significant increase in Cx43 also colocalises with increased glial fibrially acidic protein-positive astrocytes (astrocytosis) (Fonseca et al., 2002). Gliosis is also present at the site of the lesion (Carlen et al., 2000). The pathogenesis of epileptic seizures is associated with abnormal stimulation occurring at a certain brain region causing waves of depolarisation extending to the surrounding cells (Traub et al., 2001). Astrocytes that are extensively coupled by gap junctions are believed to be involved in synchronisation of this electrical activity (Carlen et al., 2000). The increase in Cx43 expression may therefore facilitate the rapid propagation of Ca^{2+} waves between astrocytes and the propagation of currents between excitable cells creating the potential for re-entrant electrical activity (Fonseca et al., 2002). Another study on connexin expression in hippocampal tissue of mesial temporal lobe epilepsy found no change in the expression in Cx36 (expressed in neurons) but downregulation of Cx32 (expressed in oligodendrocytes) (Collignon et al., 2006).

1.1.2.3 Vascular effects in neurodegenerative diseases

The inflammatory response involves an elevation in circulating inflammatory cytokines as well as local inflammation. Disturbances in the integrity of the vascular bed play an important role in the connection between the circulating inflammatory cytokines and neurodegenerative diseases (Green and

Nicholson, 2008). Blood vessel leakiness and disruptions of the blood-brain barrier allow circulating inflammatory proteins and peripheral cells such as cytotoxic T-lymphocytes to enter the brain from the bloodstream. Inflammatory cytokines released by activated microglia possibly also damage brain capillaries which leads to infiltration of peripheral cells (Hirsch and Hunot, 2009).

Parkinson's, Alzheimer's and Huntington's diseases involve pathological changes in the capillaries in the cerebral cortex (Farkas et al., 2000; Hirsch et al., 2005; Grammas et al., 2006). Brain microvessels in Alzheimer's disease have high levels of soluble IL-1β, IL-6, IL-8 and TNF-alpha and also release neurotoxic thrombin (Grammas and Ovase, 2001; Grammas et al., 2004; Haan, 2006; Tripathy et al., 2007). Vascular changes in Parkinson's disease may alter the transport of nutrients and toxic compounds in (Faucheux et al., 1999; Hirsch et al., 2005). Disruption of the blood-brain barrier has also been identified in the 6- hydroxydopamine model of Parkinson's disease (Lindgren et al., 2007). Cx40 expression in vascular endothelium, is increased in Huntongton's disease brains, apparently due to more numerous and smaller blood vessels (Vis et al., 1998a).

Connexins play an important role in lesion spread after acute trauma in the CNS. A raise in chemicals such as glutamate, Ca^{2+} and K^{+} to excitotoxic levels creates a cytosolic wave that spreads to the undamaged neighbouring cells leading to cell death, a so-called bystander effect (Cornell-Bell et al., 1990; Vis et al.). Upregulation of Cx43 is thought to play a significant role in lesion spread. A number of studies demonstrated that blocking connexin hemichannels at the site of an acute injury reduces lesion spread and limits glial activation and astrocytosis (Cronin et al., 2006; Danesh-Meyer et al., 2008; O'Carroll et al., 2008). The chronic inflammatory response and elevated expression of Cx43 in neurodegenerative diseases suggests that regulating connexin expression may afford a potential therapy by interrupting the inflammatory cycle (Green and Nicholson, 2008).

Neurodegenerative diseases have been shown to involve inflammation. Inflammatory markers, both local and circulating, affect the expression levels and the activity of gap junction channels and hemichannels. The relationship between inflammation and connexin expression needs to be elucidated further. The chronic inflammatory response and elevated expression of Cx43 in neurodegenerative diseases suggests that regulating connexin expression may afford a potential therapy by interrupting the inflammatory cycle (Green and Nicholson, 2008).

To monitor connexin expression changes in neurodegenerative diseases and to allow for intervention, the complete connexin expression pattern in both normal and diseased brains needs to be determined. The data available at present are far from complete. This project proposes to identify connexin expression patterns first in the normal human brain and then in brains with various neurodegenerative diseases, including epilepsy, Alzheimer's, Huntington's and Parkinson's diseases

and to correlate is with the expression of inflammatory markers. The focus of this study is on the brain regions secondarily affected by Alzheimer's, Parkinson's and Huntington's disease, because at the end stage of the disease the primary area has suffered an extensive loss of neurons, and our interest is in the levels of expression of the connexins which may lead to or contribute to cell death rather than being a consequence of it.

Table 1. The summary table of the connexins found in the brain by the cell type in which they are expressed.

Cell types / connexins	Cx36	Cx45	Cx57 (Cx62)	Cx43	Cx32	Cx26	Cx30	Cx29 (Cx30.2)	Cx47	Cx37	Cx40	Cx46	Cx31.1	Cx31
Neurons	Yes (exclusively)	Yes	Yes	Yes (during development	?								Yes	Yes (neuronal cell lines)
Astrocytes		Yes		Yes (white and grey matter)		?	Yes (grey matter)				Yes	Yes		
Oligodendrocytes	Yes	Yes			Yes			Yes	Yes					
Microglia	Yes	Yes		Yes										
Brain endothelial cells		Yes		Yes	Yes					Yes	Yes			
Meningial cells				Yes		Yes								

1.2 RNA quality in the human brain

The development of microarrays as a relatively recent technique for the screening of gene expression has highlighted the importance of obtaining high quality RNA, since microarray analysis is more susceptible to variations in RNA integrity than more traditional technologies (Stan et al., 2006; Webster, 2006). RNA quality presents less of a problem when dealing with animal tissue, where the optimal tissue removal and storage techniques, such as quick sacrificing of the animals and immediate freezing in liquid nitrogen, can be employed. When dealing with human tissue, however, there is the need to address special parameters, such as the wide variation in the cause of death, the length of the agonal state (the state of an individual during the time immediately preceeding death) and the postmortem (PM) delay, which tends to be measured in hours. These factors lead to a decrease in both the yield and the quality of the human RNA obtained (Johnson et al., 1986). The above factors make an investigation into the way various parameters affect the quality of the RNA transcripts of paramount importance (Buesa et al., 2004; Stan et al., 2006; Popova et al., 2008).

In the past two decades, a number of studies have investigated the parameters around RNA quality, but with varying results. The one factor most commonly considered is the PM delay. The findings have, however, proved to be contradictory. Studies such as those of Lipska et al. (Lipska et al., 2006) have shown a relationship between the PM interval and RNA quality, while others have concluded that there is at best a modest relationship (Barton et al., 1993; Harrison et al., 1995) or no relationship (Schramm et al., 1999; Cummings et al., 2001; Watakabe et al., 2001; Miller et al., 2004; Catts et al., 2005; Heinrich et al., 2006; Ervin et al., 2007), with Heinrich et al. (Heinrich et al., 2006)} and Schramm et al. (Schramm et al., 1999) having considered PM intervals of up to 118 h and 96 h, respectively.

The other major factor that has been considered is the length and severity of the agonal state, with its concomitant hypoxia leading to acidosis, as measured by the pH of the postmortem tissue. Here the overwhelming conclusion has been that the length and severity of the agonal state and the tissue pH are strongly correlated with the quality of the RNA obtained from the sample (Harrison et al., 1991; Harrison et al., 1995; Kingsbury et al., 1995; Johnston et al., 1997; Lee et al., 2005; Stan et al., 2006). More prolonged agonal states resulted in lower pH of the tissue, while PM delay had no influence on the tissue pH (Stan et al., 2006).

The dependence of RNA stability on the particular type of tissue has also been considered (Watakabe et al., 2001; Lee et al., 2005), with significant variation being found. For example, the RNA in tumours has been found to be less stable than RNA in normal tissue (Von Euler et al., 2005). Surgical tissue has also yielded RNA of poorer quality than postmortem brains. The reason for this is

not clear, but several things have been suggested, such as active RNAses in surgical tissue and the effects of anaesthesia or exposure to air (Stan et al., 2006).

The issue as to whether certain RNA transcripts are more susceptible to degradation, affecting gene expression profiles, has also been investigated. Catts et al. (Catts et al., 2005) concluded that RNA containing the 3'UTR AUUUA motif was preferentially degraded with increased PM delay. Differential susceptibility of housekeeping genes to PM-related degradation has also been observed (Barrachina et al., 2006). It has also been suggested that the severity of the agonal state directly influences gene expression levels in certain pathways (Li et al., 2004a).

Other factors that have occasionally been considered are age, with a reduction in the RNA quality with increasing age (Harrison et al., 1995), sex, with no effect (Johnston et al., 1997) and concomitant psychiatric diagnoses (Johnston et al., 1997; Schramm et al., 1999; Webster, 2006).

The RNA Integrity Number (RIN) produced by the Agilent Bioanalyser system, has been established as the most reliable indicator of the sample RNA quality, and is superior to the older methods used such as the 28S:18S ratio (Imbeaud et al., 2005; Weis et al., 2007).

In the present project, we investigated the quality of human brain tissue from patients with various neurodegenerative conditions (namely Alzheimer's disease, Parkinson's disease and Huntington's disease) as well as normal controls and hippocampal tissue from epilepsy patients obtained during temporal lobectomies. In the case of each of the neurodegenerative conditions, our primary interest was in the brain region secondarily affected (medial temporal gyrus, caudate nucleus and cortex respectively). While all human brain tissue is "precious", tissue from these areas tends to be in demand by a large number of researchers. We propose to employ the little-used region of the cerebellum for primary screening of RNA quality in each of our cases. Stan et al. (Stan et al., 2006) have found that the pH of the cerebellum is representative of the pH of the tissue from other brain regions. We wished to determine whether primary screening in this way could be used as a guide to the RNA quality in the region of interest in the same brain.

We also investigated the effect of PM delay, the duration of the agonal state, the tissue pH, the age at death and the sex of the patient in our study.

1.3 Microarrays

1.3.1 Screening techniques

The research undertaken in this area has highlighted the need for a quick and reliable way to screen for the change in the expression of various (rather than just one or a few) connexins in a quantitative and reproducible manner. The established, more conventional methods for the analysis of gene expression, such as Northern Blotting or quantitative RT-PCR, have high resolution but relatively low throughput. The study of gene expression on the protein level, by techniques such as 2-D gel electrophoresis has similar disadvantages in terms of reproducibility and the limit in the number of proteins that can be analysed at any one time. The most efficient method for high throughput quantitative genetic screening that has become available in the recent year is microarray analysis (Cepko, 2001; Geschwind and Van Deerlin, 2001; Blalock et al., 2005; Mirnics et al., 2006; Chen and Tew, 2008).

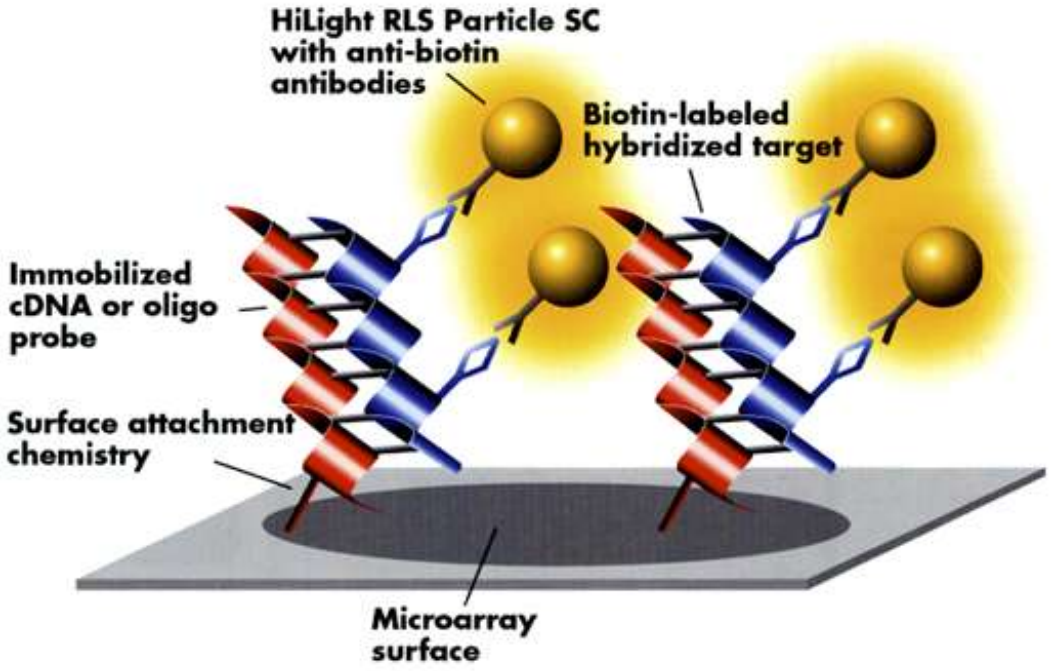

Figure 2. The principle of microarrays: the probe immobilised on the slide and a cDNA or cRNA target incorporating a tag for visualisation (Adapted from the High-Light Microarray System (Qiagen, 2003)).

1.3.2 Microarrays – outline

Microarrays offer a way to screen a large number of samples in a highly reproducible manner, with quantifiable results. They allow for considerable savings in both time and cost, as, once a microarray chip has been designed, slides can be printed and analysed in a highly automated manner. Microarrays offer high sensitivity and the analysis can be performed using a limited amount of tissue (Barrett and Kawasaki, 2003; Loring, 2006).

The basis of microarray technology is the precise spotting of DNA or RNA fragments (probes), complementary to the mRNA of interest, on a solid support (a slide, or chip), with high density, so they can be used as detectors of gene expression (Holloway et al., 2002; Mirnics et al., 2006). The probes can also be synthesised *in situ*, such as in the Affymetrix GeneChip platform (Armstrong and van de Wiel, 2004; Hamadeh and Afshari, 2004). RNA of interest from biological samples is extracted and copied, while incorporating a tag, such as a fluorophore molecule that allows it to be traced. (Butte, 2002; Holloway et al., 2002; Mirnics et al., 2006). The resultant labelled cDNA or cRNA is referred to as target. The target is hybridised to the probe immobilised on a slide (See Figure 2). After washing, the microarray slide is imaged to obtain the complete hybridisation pattern. (Heller, 2002). The fluorescence signal intensity at each spot is proportional to the number of dye molecules and thus to the number of target molecules hybridised to the probes (Cheung et al., 1999).

1.3.3 cDNA *vs* oligonucleotide microarrays

The two main classes of microarrays are cDNA microarrays, that employ cDNA probes (PCR products or genomic clones) of about 1000 bases in length, and oligonucleotide arrays, that use specially designed oligonucleotide probes (complementary to the sequence of interest) from 20-25 (in Affymetrix GeneChip) to 50-70 bases in length (Barrett and Kawasaki, 2003; Loring, 2006).

1.3.3.1 cDNA microarrays

cDNA microarrays were the first to become available. The probes in this type of array are usually PCR products. They do not have to be sequence-verified, which was an advantage at the time when complete or near-complete eukaryotic genome sequences were not known. cDNA clones are generally 100 to 1500 bases in length. They are amplified using two vector universal primers, immobilised on an array surface and then denatured. Because cDNA probes are longer than oligonucleotides, they have better hybridisation properties, but the trade-off is lesser specificity and inability to distinguish between different gene family members or splice variants, since, due to their larger length, they allow for a

significant number of mismatches (Baldwin, 2001; Hughes et al., 2001; Yue et al., 2001; Barrett and Kawasaki, 2003). cDNA microarrays are rarely used now, as they require large cDNA libraries that need to be constantly updated (Loring, 2006).

The length and low selectivity of cDNA probes makes them a not especially suitable medium for a connexin chip design, as connexin mRNA is relatively short (under a 1000b in length in a number of cases) and has a high sequence homology within the connexin gene family (See GenBank database for the connexin gene sequences). These considerations therefore favour the second approach – the shorter oligonucleotide probe arrays. The use of cDNA arrays is becoming increasingly rare in the gene expression field, given the advantages of oligonucleotide arrays (or of PCR-based "arrays" in situations where only small numbers of RNAs are to be studied).

1.3.3.2 Oligonucleotide microarrays

The work on the sequencing of the human genome accomplished in recent years has made DNA sequences for human connexins readily available - a crucial pre-requisite for the design of oligonucleotide probes, which, due to their shorter length, need to be precisely tailored to the target gene sequence (Barrett and Kawasaki, 2003). Oligonucleotide arrays are in turn subdivided into two categories: short oligonucleotides (20-25 bases in length, and long oligonucleotides (generally 50-70 bases in length).

1.3.3.2.1 Short oligonucleotide arrays

Short oligonucleotides are associated with the first widely employed microarray chip platform, the Affymetrix GeneChip. These arrays are referred to as high density microarrays due to the tight packing of array spots onto a chip (a 1.28 x 1.28 cm chip contains up to 500,000 microarray elements, with each spot 18 μm in diameter). The latest chip designs contain sequences for up to 30,000 genes (Lipshutz et al., 1999; Nelson, 2001; Barrett and Kawasaki, 2003; Hamadeh and Afshari, 2004; Schena et al., 2008). The Affymetrix GeneChip technology involves designing multiple 25-mer probe pairs across the mRNA sequence of interest and then synthesising these probes directly on the glass surface using their proprietary photolithographic process (Lipshutz et al., 1999; Lockhart and Barlow, 2001). In the past each Affymetrix probe pair consisted of a perfect match oligo (PM) and a mismatch oligo (MM) created by a single substitution of the complementary nucleotide at the centre (base 13) position. The difference in signal intensity between the two oligonucleotides in the probe pair was used to measure the noise and crosshybridization associated specifically with that sequence (Hollingshead et al., 2005). At present, the mismatch data is no longer used for the analysis of the Affymetrix arrays, Robust

Multichip Average is employed to compute gene expression summary values for Affymetrix Genechip data. The raw intensity values are background corrected, log- transformed and then quantile normalized. Next a linear model is fit to the normalized data to obtain an expression measure for each probe set on each array .

1.3.3.2.2 Long oligonucleotide arrays

50-70 base oligonucleotide arrays combine the advantages of better selectivity associated with oligonucleotides *versus* cDNA, and of better hybridisation properties than the 20-25 base oligonucleotide probes (Hughes et al., 2001).

Newer commercial platforms such as Illumina Sentrix® BeadChips use 50-mer oligonucleotides on glass microspheres ("beads") with the diameter of 3 μm which are coated with hundreds of thousands of copies of a particular oligonucleotide and randomly assembled into wells etched on a silicon wafer (Elo et al., 2006; Loring, 2006). The Illumina process employs the oligonucleotide synthesis methods that are used for spotted long-oligonucleotides arrays. The oligonucleotides are attached to microbeads which are then placed onto microarrays using a random self-assembly mechanism (Gunderson et al., 2004). The Illumina and Affymetrix platforms are also very different in their probe selection and design procedure.

Illumina arrays yield around 30 copies of the same 50-mer oligonucleotide on the array. With Illumina arrays a decoding step is undertaken in which the locations of each probe on the array are determined using a ~30-base address sequence covalently attached to the bead by an amine group. A final difference between the platforms is that multiple (six to eight) Illumina arrays are placed on the same chip. This means that the hybridization and subsequent steps are performed in a parallel fashion, while on the Affymetrix platform each array is processed separately (Barnes et al., 2005).

The custom-made long oligonucleotide platform allows greater flexibility than commercially available oligonucleotide chips, although the array density is usually lower (Nelson, 2001). However, if only a limited number of genes need to be screened (as with the connexin gene family), this is unlikely to present a problem. Custom-designed arrays also offer the advantage of significantly reduced cost. (Barrett and Kawasaki, 2003).

1.3.3.3 Two-colour and one-colour arrays

One-colour array procedure involves the hybridization of a single sample to each microarray after labelling it with a single fluorophore (such as phycoerythrin, Cy3 or Cy5), whereas in a two-colour

procedure, two samples (e.g., experimental and control) are labelled with different fluorophores (usually Cy3 and Cy5 dyes) and hybridized together on a single microarray.

The hybridisation of two samples to the same array allows a direct comparison between the experimental sample and the reference sample, minimizing variability caused by processing multiple microarrays per assay. This reduction in variability theoretically leads to determining levels of differential expression between sample pairs with an increased sensitivity and accuracy. It is also possible to design more complex experimental protocols when using two-colour platforms, such as hybridization with a common reference sample or the use of loop designs. Although dye-specific biases can substantially affect results when the two-colour procedure is used, this can be corrected by performing dye-reversed replicates (dye swaps or fluorophore reversals).

The primary advantages of one-colour array designs are experimental design simplicity and flexibility. Hybridization of a single sample per microarray makes it easier to compare across microarrays and between groups of samples. Data inconsistency across assays due to multiple sources of variability, including microarray fabrication and processing, can be reduced by performing sufficient biological and technical replicates in one-colour array experiments (Patterson et al., 2006).

1.3.3.4 Oligonucleotide design

1.3.3.4.1 Oligonucleotide probe requirements

As mentioned earlier, the sequence data is at present widely available, which allows researchers to design their own probes and arrays. Oligonucleotide microarray probes have to meet stringent criteria in terms of selectivity and specificity to ensure efficient hybridisation with minimal cross-binding. For this reason the question of oligonucleotide design is of utmost importance. It is possible to have oligonucleotide probes designed commercially; however, programs are available in the public domain for the creation of your own sequences (Holloway et al., 2002). The primary requirements for the probe design are similar length and melting temperature (Tm) (G-C content) to ensure quantitative comparison of gene expression. This is necessary to ensure comparable hybridisation properties for the probes across an array. A probe must also not contain homodimer or hairpin structures stable at the Tm, as this reduces binding efficiency.

1.3.3.5 Sensitivity and specificity

The two major properties of microarrays that it is desirable to maximise are specificity, and sensitivity (Hughes et al., 2001; Koltai and Weingarten-Baror, 2008). Specificity refers to the ability of

a probe to bind to a unique target sequence. A specific probe will provide a signal that is proportional to the amount of the target sequence only. A non-specific probe will provide a signal that is influenced by the presence of other molecules. Hybridisation of the probe with molecules other than the target is referred to as non-specific hybridisation. Lower levels of non-specific hybridisation result in higher specificity. Very short probes, such as 25-mers, have an increased chance of random matches to non-target sequences, which decreases specificity. In very long probes, the specificity is also reduced, as there is a higher chance that a probe fragment matches an unwanted target. The fact that biological nucleotide sequences are not random further contributes to this because different targets can share domains of high sequence similarity (Kreil et al., 2006).

A number of studies have been done on the amount of sequence homology between different probes/targets permissible in a chip before cross-hybridisation occurs (Kane et al., 2000; Hughes et al., 2001; Taroncher-Oldenburg et al., 2003). These studies indicate that non-target sequences that are >70-80% similar to the target region contribute to the binding signal intensity; however, there is no agreement on the exact value. Kane et.al. (Kane et al., 2000) also suggested that even if the target region is marginally similar (50-70%), it should not contain a stretch of 15 or more contiguous bases (for 50-base oligonucleotides). Hughes (Hughes et al., 2001) et al showed that 18 or more randomly placed mismatches per 60-mer can reduce hybridisation to background levels. It has also been found that the position, as well as number of mismatches is crucial, with the importance of a nucleotide to hybridisation efficiency being proportional to its distance from the array surface (in situ synthesised or amino-modified probes attach to the microarray surface with either 3' or 5' end, so that hybridisation is less hindered by steric interactions at the end furthest from the slide) (Kane et al., 2000; Hughes et al., 2001; Li and Stormo, 2001).

The gene region from which a probe is selected can also substantially affect specificity and cross hybridization. Coding regions are more conserved between closely related genes. Thus probes selected from coding region are the most prone to cross-hybridization. It is preferable to design oligonucleotides within the final 600 bases at the 3' end, as the oligo-dT primer, used for cDNA target generation, binds to the poly-A tail of mRNA.(Li and Stormo, 2001; Nelson, 2001; Barrett and Kawasaki, 2003), and also in part because the difference in sequence is typically larger in such regions. When more probes are designed to 3' UTR and fewer selected from the coding regions, discrimination among splice variants is however made more difficult (Liu et al., 2010).

The level of noise (random signal variation) decreases with greater probe length. For shorter probes, it is necessary to use replicates from different arrays or multiple probes per array.

The sensitivity is a measure of how little is lost of the signal reflecting specific hybridization between the probe and its target. Sensitivity generally increases with probe length, as the binding energy between the probe and the target is typically higher, e.g. 60-mers detect targets with eightfold higher sensitivity than 25-mers) (Chou et al., 2004).

The detection limit of long oligonucleotide arrays has also been investigated, and the values suggested range from 0.1 mRNA copies per cell (assuming 100,000 transcripts per cell) (Hughes et al., 2001) to 10 mRNA copies/cell (assuming 360,000 mRNA copies per cell) (Kane et al., 2000); or 10 pg of DNA (~107 copies) per target per array (Taroncher-Oldenburg et al., 2003). These values are similar to those found in cDNA array platform or short oligonucleotide arrays (Kane et al., 2000; Barrett and Kawasaki, 2003; Wang et al., 2003). The figures given for the relative amount of change which can be detected with long oligonucleotide arrays range from 1.5- (Mirnics et al., 2001) to 3-fold (Heller, 2002), with better statistical significance achieved upon multiple repetition of the experiments (Mirnics, 2001).

1.3.3.6 Reproducibility

Reproducibility (or repeatability) is the degree to which repeated measurements of the same variable will show the same or similar results. Usually measurements involve an error that makes repeated measurements differ from each other in value. With a set of measurements, the precision is usually calculated by comparing a measure of dispersion (e.g. variance or standard deviation) with zero. An ideally precise technique would have all values exactly equal (zero variance) (Draghici et al., 2006).

Reproducibility is the most readily measurable characteristic of a microarray platform. Good reproducibility does not, however, necessarily mean an accurate measurement of the expression of a particular gene. The repeated measurements for a probe can be perfectly concordant with each other, with all of them reflecting the same measure of cross-hybridisation rather than true gene expression. This can be true both within a particular platform and between platforms. The relative accuracy of the microarray platforms can be assessed using either titrated RNA samples or measurements of gene abundance obtained from different platforms (Shi et al., 2006).

Within-array as well as between-array reproducibility can be measured for platforms with multiple probes per gene per array. Barnes et al. (Barnes et al., 2005) discovered that within-platform reproducibility was substantially higher on the Affymetrix array than on the Illumina array, suggesting that the Affymetrix arrays contains more probe sets which are truly redundant.

1.3.3.7 Accuracy

Accuracy can be defined as the concordance of the true value with its measured quantity. Within a set of measurements, accuracy of a technique is usually calculated by comparing the actual value with the mean or median. In the ideal situation the mean or median would be exactly equal to the true value, but in reality the measurements are affected by a bias that leads to the mean differing from the true value.

Accuracy and precision are completely independent variables. A technique can therefore be accurate but not precise (the mean of several measurements is close to the actual value but the individual measurements vary considerably) and precise but not accurate (the individual measurements are close to each other but their mean is far from the actual value). A valid result is one that is both accurate and precise (Draghici et al., 2006).

Microarrays can be used to measure both absolute target abundance and ratios of expression (relative target concentration). Accurate measures of absolute target abundance would be expected to produce accurate ratio measurements, but the inverse is not necessarily true (Draghici et al., 2006). It is difficult to compare absolute expression values from different platforms due to varying labelling methods and probe sequences. The relative expression level between a pair of sample types should however be maintained between platforms (Shi et al., 2006).

1.3.3.8 Comparison across platforms

The correlation between commercial platforms is the highest for genes known to be differentially expressed, and for genes expressed at a higher level. The correlation is lowest between genes with a low expression level, and filtering out probes with low signal improves concordance (Barnes et al., 2005; Draghici et al., 2006). Different strategies for calling a gene present or absent on an array can however result in different numbers of genes being compared (Shi et al., 2006). The genes that are not differentially expressed between the compared samples are likely to present noisy expression profiles not reproducible between platforms (Barnes et al., 2005; Hester et al., 2009).

The earlier comparison studies which relied on GenBank or UniGene database identifiers produced lower correlation between platforms as it was impossible to check whether the probes aimed at the same gene actually measure the same transcript (Kuo et al., 2002). The probe sequences are necessary to determine whether the same transcripts are being assayed and whether the gene regions they are complementary to are similar. Region and sequence similarity improves correlation between platforms but can increase the chance of similar cross-hybridisation patterns (Draghici et al., 2006).

The largest microarrays platform comparison study was performed within an FDA-initiated program for evaluation of the reproducibility, quality and consistency of microarray platforms (MicroArray Quality Control, MAQC). In this study they compared six commercially available microarray platforms: Applied Biosystems (ABI); Affymetrix (AFX); Agilent Technologies (AGL for two-colour and AG1 for one-colour); GE Healthcare (GEH); Illumina (ILM) and Eppendorf (EPP).Researchers at the National Cancer Institute (NCI) also generated spotted microarrays using oligonucleotides obtained from Operon (Shi et al., 2006). The results demonstrated high agreement between the platforms, including those with differing approaches to measuring expression levels, such as Affymetrix with multiple short oligonucleotide probes and Illumina with beads containing long nucleotide probes. One-colour and two-colour platforms also showed high concordance.

The ability of different microarray platforms to detect subtle rather than large changes in gene expression level is important when investigating tissues where the expected differences are small, such as the human brain. Hollingshead et al. (Hollingshead et al., 2005) screened tissue samples from the same area of two post-mortem human brains, one schizophrenic and one normal control on a two-colour cDNA platforms, Affymetrix GeneChips and one-colour CodeLiml arrays found only a ~50% correlation comparing three microarray platforms (a cDNA microarray and two commercially designed arrays platforms, Affymetrix GeneChip and Amersham CodeLinkR) using postmortem human brain tissue.

Pedotti et al. (Pedotti et al., 2008) compared gene expression patterns in the hippocampus of five wild-type and five transgenic deltaC-doublecortin-like kinase mice using five microarray platforms: Applied Biosystems, Affymetrix, Agilent, Illumina, and LGTC home-spotted arrays and found that small changes in GABA-ergic signalling could be consistently detected.

1.3.3.9 The microarray chip: parameters

An important consideration when designing a microarray chip is the significant potential for variability due to factors such as location bias, hybridisation conditions, or image acquisition artefacts. To obtain reliable data and to make quantitative, rather than qualitative measurements, replications are necessary. A number of oligonucleotide probes (2-3) are commonly designed for each transcript of interest. Each probe is duplicated several times and these are spotted randomly at different locations on the chip. (Hughes et al., 2001; Shmulevich et al., 2003)

1.3.3.9.1 Replicates

The use of replicates helps to distinguish between genes that are truly differentially expressed, and those affected by random signal variation (noise). Averaging between replicates minimizes the effects of random variation and allows evaluation of the extent of experimental variation. Comparison tests use this estimate of variability within the replicates to determine a confidence level as to whether the gene is differentially expressed. Microarray experiments generally involve two types of replicates: technical and biological.

Biological replicates are used to deal with biological variability which is intrinsic to all organisms, due to both genetic variability and varying environmental effects. This makes it necessary to perform repeated hybridizations with RNA samples from independent sources, for example extracting tissue of interest samples from three different rats and hybridizing each to a separate array. The necessary number of replicates varies depending on the variability of the system being studied (e.g. there is less variability between inbred mice or cell lines than between clinical tissue samples). Biological replication allows to obtain gene expression data that is broadly applicable across large numbers of individuals, as well to reduce noise.

Technical replicates deal with variation due to experimental artefacts and measurement errors. There are two possibilities for replicated measurements – replicated features within a slide and replication of hybridization of the same RNA sample to different slides. Dye reversal experiments can also be used as technical replicates for two-colour arrays to reduce systematic bias due to different incorporation and intensities of the two dyes (Armstrong and van de Wiel, 2004; Hackl et al., 2004)

1.3.3.9.2 Controls

It is important to build controls into the chip in order to obtain reliable results. A common form of internal reference is to use the expression of housekeeping genes. However, constancy of their expression cannot always be assumed (Eickhoff et al., 1999; Barrachina et al., 2006; Popova et al., 2008). A more reliable control method is to spike a known amount of reference RNA (which is distinguishable from that normally present in the tissue) into the sample and to use the amount of binding for comparison. The RNA used for this purpose can be a synthetic oligonucleotide (Eickhoff et al., 1999) or RNA derived from a different organism, such as yeast or bacteria (Hill et al., 2001; Evans et al., 2003). The spike-in method of array normalisation offers the advantages of the ability to compare results across different array and experimental designs, allows one to estimate absolute, rather than relative mRNA abundance, and to compare the sensitivity of individual arrays (Kane et al., 2000; Hill et al., 2001; Evans et al., 2003). However, it also has many disadvantages such as the challenges of

performing sufficiently accurate measurement of the spikes, and the risk of relying on such a small number of measurements for the normalisation of the entire data set. Spikes are seldom used alone for array normalisation (Armstrong and van de Wiel, 2004).

1.3.3.10 Oligonucleotide probe synthesis

The synthesis of longer oligonucleotide probes does not require expensive photolithographic masks used by Affymetrix and allows for much greater flexibility (Nelson, 2001). One method of longer nucleotide synthesis involves an *in situ* inkjet printing process. Modified ink-jet pumps, similar to those used for printing, deliver 100-picoliter reagent droplets onto a hydrophobic surface with exposed active hydroxyl groups. The droplets contain phosphoramide DNA monomers which form covalent bonds. The process is repeated after washing and deprotection as many times as necessary to reach the desired length. The process is automated, and the array synthesis can be modified by re-programming the computer with different nucleotide sequences (Hughes et al., 2001; Nelson, 2001; Barrett and Kawasaki, 2003; Schena et al., 2008). Long oligonucleotides can also be synthesised to any length and spotted onto slides in a manner similar to cDNA probes, usually using a robotic arrayer (Nelson, 2001; Barrett and Kawasaki, 2003).

1.3.3.11 Microarray slides

Spotted arrays are typically printed onto glass slides. Glass has continued to be the favourite support medium due to its low cost, non-porous nature and low autofluorescence. Other slides, including nylon and nitrocellulose membranes and plastic are also available. The kind of slide used is usually determined by the particular protocol that is employed (Baldwin, 2001; Holloway et al., 2002; Evans et al., 2003; Schena, 2008). The biggest recent advance in slide manufacture has been the use of a three-dimensional matrix coated onto slides onto which the probes are then bound, comprised of three parts: a long-chain, hydrophilic passivating polymer, a reactive group, and photoreactive chemistry. The result is two-fold; a surface that can be covalently coupled to any substrate of choice and one that prevents nonspecific binding, while concurrently allowing for the homogenous coupling of different types of molecules, including DNA, RNA, protein, and cells

(http://www.surmodicsivd.com/content/activated-microarray-slides).

1.3.3.12 Microarray protocol

1.3.3.12.1 Target generation and labelling

Fluorescence labelling of the target is conducted using reverse transcription of mRNA, either from poly(A) RNA or total RNA. The labelling method used initially was direct incorporation, whereby the reverse transcription step is conducted using fluorescence-labelled nucleotides. However, these nucleotides are bulky and prone to uneven incorporation. A more recent method is to use a modified nucleotide (e.g. amino-allyl dUTP), to which a fluorescent molecule can be coupled at a later time point. The most common dyes used for target labelling in microarray technology are Cy3 and Cy5 due to their easily distinguishable spectra (Cy3 has an absorption peak at 554 nm and an emission peak at 568 nm and Cy5 has the absorption/emission peaks at 649 nm and 666 nm respectively) and the wide availability of lasers necessary to excite them (a green 568 nm laser for Cy3 and a red 647 nm laser for Cy5) (Herman, 1998; Baldwin, 2001; Holloway et al., 2002). More recent alternatives to Cy3 and Cy5 dyes are Alexa Fluor dyes (Alexa488 and Alexa494), the introduction of which has allowed the use of three- and four-channel arrays (Martin-Magniette et al., 2008; Schena, 2008; Mayr et al., 2009).

Dual-colour labelling is used to assess comparative binding between the test sample and the control. This process measures relative, rather than absolute target abundance, e.g. the ratio between gene expression in normal and diseased tissue, thus the use of a normal control sample is required. It is necessary to reverse labelling in repeated experiments to obviate labelling bias (Mirnics, 2001). Another way to account for uneven dye incorporation is to label the same target cDNA with both Cy3 and Cy5 and conduct a control experiment, co-hybridising them on the same chip and comparing the binding signal intensity. A correlation of over 85% (preferably 90%) between the two dyes is desired (Luo and Geschwind, 2001).

Other techniques besides fluorescence exist for the labelling and detection of microarray targets. One example is filter arrays – cDNA arrays on nylon or nitrocellulose membranes that use radiolabelled, rather than fluorescence-tagged samples hybridised to separate filters (Evans et al., 2003). These are sometimes referred to as macroarrays due to their lower probe density and have been used successfully in neuroscience research (Becker, 2001; Mirnics et al., 2001; Holloway et al., 2002; Evans et al., 2003). However, this technique has a number of disadvantages compared to the fluorescence based arrays, including low array density and inability to perform two-colour comparative hybridisation (Becker, 2001).

1.3.3.12.2 Hybridisation

Different hybridisation and washing techniques may be used depending on the microarray protocol (Kane et al., 2000; Hughes et al., 2001; Holloway et al., 2002). Generally the two fluorescence-labelled target samples are co-hybridised on the array overnight, and then the excess target is washed off (Luo and Geschwind, 2001). The hybridisation stringency affects binding specificity, and may need to be optimised for a particular chip design (Hughes et al., 2001; Schena, 2008).

1.3.3.13 Microarray data: extraction, analysis and submission

1.3.3.13.1 Image acquisition

Scanning the slides requires a high-resolution microarray scanner. The systems commonly employed are a laser scanner or a CCD (charge-coupled device). The resolution limit necessary to detect microarray elements is 5-10 μm, which is ten times greater than a traditional flatbed scanner (Baldwin, 2001). It is advisable to use the same scanner (or at least the same model of scanner) for repeated experiments, as different scanners tend to give a subtle difference in results (Holloway et al., 2002).

1.3.3.13.2 Analysis

Commercially available microarray scanners usually come with their own software for the initial data extraction. The fluorescence double-hybridisation data is usually stored as TIFF files, with 16 bit of colour deep per channel (a channel corresponds to a fluorochrome) (Tamames et al., 2002).

1.3.3.13.3 Spot detection

The keystone of the major image analysis programs is adjusting a grid over the image to correspond to the position of microarray spots. The spot position is usually easy to define due to the regular printing pattern. However, the precise detection of the spot edges can present a problem. A common way of defining spot boundaries is to overlay circular masks onto the elements, with a user-defined radius to enclose all possible signal pixels (Wang et al., 2001). However, this method can generate significant errors if the spot is not perfectly circular or positioned off-centre, with small regions of hybridisation being judged as background and *vice versa* (although an improvement in the printing processes has simplified this). An alternative method to the use of a circular mask is to analyse the change in the greyscale value between adjacent pixels in an image (this is usually significant at a spot edge). The first step is to amplify contrast, then the image is filtered with a Gaussian smoothing filter, and the spot edge can be detected from the modified image. The area immediately outside the edge is

stored as background and is used in calculating background subtraction (Kim et al., 2001; Shimokawa et al., 2008).

1.3.3.13.4 Background correction

The background intensity quantifies the amount of unspecific binding to the glass slide, even where no spotted material is available. This intensity value will be added to the true intensities of all spots in the slide. Background correction is performed in order to improve the accuracy of the expression values. There are several methods to estimate local and global background (Perou et al., 2000). The most common approaches to remove the background effect are: filtering out those genes for which the estimator of the background intensity is higher than the estimator of the foreground intensity. For the rest of the genes, the background intensity will be overall much lower than the foreground intensity so the subtraction of the background intensity from the foreground intensity will not be necessary; subtracting the background intensity from the foreground intensity. A problem may arise because negative values could be obtained if the very low intensity spots were not previously removed (Huber et al., 2002). If background intensity is bigger than foreground intensity the reason can be that the estimators provided by the image analysis software for either the foreground (usually the median of the pixels within the spot) or the background were not correct. Kooperberg et al. (Kooperberg et al., 2002) present a novel algorithm based on Bayesian Statistics to estimate the foreground and background from the pixel intensities.

1.3.3.13.5 Spot quantification

The precise quantification of the spots can be based on the mean pixel intensity of each spot after removing the calculated background (this is usually used with the circular masks method of boundary detection). The more complex algorithms take into account the exact shape of the spots and the distribution of pixel values within a spot for the estimation of hybridisation quality (Jain et al., 2002). The ability of the image processing programme to detect low-quality spots (those with very irregular boundaries or a lack of detectable intensity due to poor hybridisation) and discard them is important (Tamames et al., 2002; Stekel, 2003; Shimokawa et al., 2008).

1.3.3.14 Data analysis

1.3.3.14.1 Log transformation

The DNA microarrays data is normally transformed from raw intensities into log intensities before proceeding with analysis. There are several reasons for this transformation – to achieve a reasonably even spread of features across the intensity range, a constant level of variability at all intensity levels, an approximately normal distribution of experimental errors and an approximately bell-shaped distribution of intensities (Stekel, 2003; Steinhoff and Vingron, 2006). Logarithms to base 2 are usually used in microarray analysis. The reason is that the ratio of the raw Cy5 and Cy3 signal intensities is transformed into the difference between the logs of the intensities of the Cy3 and Cy5 channels. Thus genes upregulated 2-fold correspond to a log ratio of +1 and 2-fold downregulated genes correspond to a ratio of -1.

1.3.3.14.2 Normalisation

Microarray experiments generate a substantial amount of experimental variation, making it difficult to identify biological variation. The process of normalisation involves removing non-biological variation introduced in the measurements and minimizing the random errors.

One of the basic issues is whether only a small fraction of genes on the array or a large fraction are expected to be differentially expressed A specialized array containing a small number of genes of interest is likely to have many or most genes changed in the experiment. For normalizing data from such arrays, it is necessary to use housekeeping genes, internal controls or a reference sample On a whole genome array, only a small fraction of genes would be expected to change, thus the overall expression levels across the array are expected to be equal (Steinhoff and Vingron, 2006).

Global mean normalisation of array signal intensities results in the mean ratio for all array experiments being equivalent. Global methods assume that the red and green intensities are related by a constant factor, i.e. R = kG, and the centre of the distribution of log ratios is shifted to zero

$\log2R/G \rightarrow \log2R/G - c = \log2R/(kG)$

A common choice for the location parameter c = log2k is the median or mean of the intensity log ratios M for a particular gene set (Yang et al., 2002b). Much experimental variation present in gene expression data is however not constant across the range of element signal intensities and hence cannot be addressed by global normalisation (Colantuoni et al., 2002a).

The fit of a lowess function to the data scattered in a M-A plot (where M=log2(R/G) and A=1/2 (log2R + log2G)) is a common practice to normalize microarray data (Yang et al., 2002b). Another

common normalisation method estimates Ki for every gene but based on linear regression methods (Quackenbush, 2001). In most of the cases, the relationship between both channels is not linear so the use of non-linear techniques such as lowess (linear) or loess (quadratic) is more suitable (Steinhoff and Vingron, 2006). In addition, the regressive approach is very sensitive to outliers and lowess/loess offers a more robust estimation. Although lowess performs well, some new non-linear fittings have been proposed lately (Workman et al., 2002; Wilson et al., 2003).

Spatial normalisation

In addition to global variation of intensities across the whole array, another source of systemic bias is regional inhomogeneity of intensity measurements over the surface of the array. Non-biological spatial artefacts include uneven washing and temperature gradient or the array being not completely horizontal in the scanner (Stekel, 2003; Chai et al., 2010). One method of spatial normalisation is to perform a loess regression on each grid of the array separately. Local mean normalisation is a methodology that normalizes element signal intensities to a mean intensity calculated locally across the surface of a DNA microarray (Colantuoni et al., 2002a).

Quantile normalisation

Quantile normalisation is currently the most common normalisation method used for Affymetrix arrays. Quantile normalisation assumes that the distribution of miR abundances is approximately the same in all samples. For convenience, an artificial reference chip is created by pooling intensities across all to produce an intensity reference distribution in that particular experiment. This reference distribution is described by a distribution function F_2. To normalize each chip, the distribution of miR intensities for that chip (e.g. denoted by the distribution function F_1) is transformed to equal the reference intensity distribution. In practice, this transformation is accomplished by determining the quantile in the chip's intensity distribution for each signal intensity on the chip and replacing that value with the value having that quantile in the reference distribution. In a formula, the transform is

$$x_{norm} = F_2^{-1}(F_1(x)),$$

where F_1 is the distribution function of the actual chip for which the calculation is being made and F_2 is the distribution function of the reference chip (Zhao, 2010).

1.3.3.14.3 Analysis

The particular data analysis methods employed depend on the experimental design, and may involve pairwise (each slide) or pooled-sample (across different slides) comparisons (Armstrong and van de

Wiel, 2004). The main aim of the initial analysis stage is to determine whether the ratios between the intensities of the two channels, or channel intensities from single-colour arrays, are statistically significant in the context of the entire arrays. The statistical significance of a particular ratio is a more important consideration than the actual magnitude of the ratio, as the amount of within-slide variation has to be taken into account (Vacha, 2003). The data then can be further organised and clustered to answer the experimental question (Quackenbush, 2001; Butte, 2002; Sheffler et al., 2005; Tomlinson et al., 2008).

1.3.3.14.3.1 Corrections for multiple testing and false discovery error

The p-value calculated for each individual gene needs to be adjusted based on the total number of tests performed. The reason for this is that the p-value calculated for each individual gene represents the probability of a similar difference in expression level occurring purely due to chance and this risk is cumulative for all tests that are performed. That is, if 10,000 tests are conducted and a p=0.05 significance threshold is used for the raw p value, 500 false positives would be expected. If there were 100 differentially expressed genes, it would be impossible to separate the real differential expression from the false-positive results. Reducing the cut-off to e.g. 1% or lower, would lead to a high false-negative rate and a failure to identify important genes (Lee et al., 2008).

Corrections for multiple testing allow the user to adjust the p-value based on the number of tests performed. These adjustments help to reduce the number of false positives in an experiment. Family wise error rate (FWER) corrections adjust the p-value by evaluating the probability that at most one false positive is included at the cutoff level of a test statistic among all candidates (Lee et al., 2008), so that it reflects the chance of at least one false positive being found in the list. Therefore, if 500 genes with an adjusted FWER p-value of 0.05 are identified, then there is a 5% chance of having 1 false positive amongst the 500. Bonferonni and Holm are examples of FWER methods. The FWER methods are more conservative than the false-discovery rate control methods.

False discovery rate control (FDR) adjust the p value so that it reflects the frequency of false positives in the list. Therefore, if 500 genes with an adjusted FDR p value of 0.05 are identified, then there will be an estimated 25 false positive in the list of 500. Examples of FDR methods include Benjamini and Hochberg and SAM (Significance analysis of microarrays). The FDR methods are usually acceptable for “discovery” experiments; i.e., where a small number of false positives is acceptable (Olson, 2006; Steinhoff and Vingron, 2006).

1.3.3.14.3.2 Further analysis

In the most basic analyses, two sets of data (e.g., from normal and diseased tissue) are examined for differential gene expression through statistical testing (including *t*-tests and empirical Bayesian approaches) followed by multiple-comparison corrections. A downside of these methods is the fact that each gene is examined individually, despite there being a well-established biological relationships between genes. The expression of genes may better be addressed by viewing the genes as related components of a biological system (Beyene et al., 2007) incorporating existing biological knowledge and considering known pathways rather than individual genes (Braun et al., 2008). Multi-gene effects are often approached through the use of multivariate analysis (Szabo et al., 2002; Xiao et al., 2004) that attempts to identify associated groups of genes.

Multivariate analysis methods can be divided into two general classes, designated supervised and unsupervised. Supervised methods aim to determine genes or samples which fit a predetermined pattern and unsupervised methods involve analysis to characterize the components of the data set without the *a priori* knowledge (Eisen et al., 1998; Hackl et al., 2004).

1.3.3.14.3.2.1 Unsupervised methods

Unsupervised methods attempt to identify relatively homogenous groups or clusters of genes that behave similarly across a range of conditions or samples. One of the unsupervised methods is the Principal Components Analysis. Principal Components Analysis (PCA) is a multivariate data analysis system that involves a transformation of a number of likely correlated variables into a smaller number of uncorrelated variables known as principal components. Principal components analysis can then be used to define a summary expression level for the genes known to be involved in a particular pathway in order to reduce the dimensionality of the problem (Jolliffe, 1986).

Canonical correlation analysis is designed to explain or summarise the relationship between two sets of variables by identifying linear combinations of each set of variables that generates the highest possible correlation between the composite variables for each set of data.

Cluster analysis is used for classification of data when class labels are unknown (Beyene et al., 2007). Clustering can be described as the process of separating a set of objects into a number of subsets on the basis of their similarity (Gilbert et al., 2000). The aim is to generally define clusters that minimize intracluster variability while maximizing intercluster distances, i.e. finding clusters whose members are similar to each other, but distant to members of other clusters in terms of gene expression based on the used similarity measurement. The motivation to find such clusters is driven by the

assumption that genes that demonstrate similar patterns (coexpressed genes) share common characteristics, such as common function, common regulatory elements, or common cellular origin (Hackl et al., 2004).

1.3.3.14.3.2.2 Supervised methods

Supervised methods are generally used for finding genes with expression levels which are significantly different between groups of samples and finding genes which actually predict a characteristic of samples.

Linear discriminant analysis incorporates class labels and maximises a transformed ratio of between-class covariance to within-class covariance. Gene voting (Golub et al., 1999) is a technique that aggregates the weighted votes from all modelling gene signatures; the advantage of this technique is that it can be easily implemented without complicated computing and statistical arguments (Lee et al., 2008).

1.3.3.15 Microarray data publication

A set of guidelines, for the publication of microarray data, known as MIAME, has been developed by the Microarray Expression Database Group (http://www.mged.org/Workgroups/MIAME/miame.html). The guidelines refer to the necessary format of microarray data for submission and require information about:

- experimental design;

- array design;

- the extraction, preparation and labelling of samples used for hybridisation;

- hybridisation conditions;

- measurements such as image acquisition and quantification;

- normalisation controls.

Adherence to these guidelines is now essential for the publication of microarray data in a number of journals (Holloway et al., 2002; Shimokawa et al., 2008).

1.4 Beyond microarrays

Over the past few years rapid advancement in high-throughput gene expression analysis technologies has taken place. Microarrays have been used widely in research on neurodegenerative diseases and have provided much of the information known today about the transcriptional profiles associated with various neurodegenerative disorders. RNA-seq is a newer technology promising even more reliability, accuracy and reproducibility.

1.4.1 RNA-Seq

RNA-Seq is a new transcriptome profiling technology that utilizes next-generation sequencing platforms, including the Roche 454 Life Science Genome Sequencer FLX System, the Illumina Genome Analyzer and the Applied Biosystems SOLiD system (Janitz, 2008). RNA-Seq employs a sequencing strategy where transcripts are reverse transcribed into cDNA, and adapters are then ligated to each end of the resulting molecule. Sequencing can be either unidirectional (single-end sequencing) or bidirectional (paired-end sequencing). The sequencing data are then aligned against a reference genome or assembled *de novo*, with the final product being a genome-wide expression profile and/or structural transcript map (Courtney et al., 2010).

RNA-Seq provides a number of advantages over microarray technology. First, RNA-Seq is not dependent on genome sequence data. RNA-Seq can provide information regarding transcript structure, including single base-pair resolution of transcript boundaries and boundaries between exons. It is also possible to detect variations among sequences, such as SNPs, with RNA-Seq, making it useful for genotyping and linkage analysis (Wang et al., 2009b).

A second major advantage of RNA-Seq over microarrays is that it addresses the problems of saturation and background signal. Each molecule is sequenced individually and mapped to unique regions of the genome, providing a quantification technique with no upper or lower limit. The result is that RNA-Seq has a much larger dynamic range of detection than microarray. An RNA-Seq analysis of the *Saccharomyces cerevisiae* transcriptome estimated a greater than 9000-fold range of transcript abundances (Nagalakshmi et al., 2008), while the range of transcript detection in a mouse transcriptome analysis spanned five orders of magnitude (Mortazavi et al., 2008). By comparing these findings to the smaller dynamic range (100-fold to a few 100-fold) of microarrays the superiority of RNA-Seq is well illustrated. Validation techniques such as quantitative PCR (qPCR) (Nagalakshmi et al., 2008) and

spike-in RNA (addition of samples of RNA of known concentration) (Mortazavi et al., 2008) provide evidence that RNA-Seq is extremely accurate. Other advantages include high levels of reproducibility with reduced laboratory work; since there are no cloning steps and a smaller RNA sample is required.

Due to RNA-Seq being a young technology, there are bioinformatic challenges related to storing, retrieving and processing such large amounts of data. The first obstacle to data analysis is short-read mapping to the reference genome. For complex transcriptomes, such as in humans that that span splice junctions become extremely difficult to map and read due to extensive alternative splicing and trans-splicing events. Thus the short read sequencing technologies are the most appropriate tool when sensitivity is very important, and when sensitivity is not the limiting factor, it may be more suitable to use DNA microarrays (Courtney et al., 2010).

1.4.2 Non-coding RNAs

Several hundred small RNA molecules have been identified recently in almost all eukaryotic organisms. New classes of small RNAs are being discovered all the time, even as previously unknown functions are being attributed to already known small RNAs (Matera et al., 2007). Some of these classes of ncRNAs are well known, such as ribosomal RNAs (rRNAs) and transfer RNAs (tRNAs), whose roles in mediating the pathogenesis of CNS disorders (e.g., mitochondrial enchephalopathies) have been at least partially characterized (Sproule and Kaufmann, 2008).

Additional classes of ncRNAs that have been identified more recently include a wide range of long ncRNAs (lncRNAs) and a number of types of short ncRNAs (microRNAs piwiRNAs, small nucleolar RNAs, promoter- associated small RNAs and transcription initiation RNAs among others) (Taft et al., 2010).

The most studied of these small RNAs is a class of 19–23 nt naturally occurring RNA molecules – miRNAs – that contribute to post-transcriptional regulation of gene expression. These RNA molecules are produced by enzymatic processing of longer precursor RNA molecules transcribed from intergenic noncoding transcripts or noncoding regions of protein-coding transcripts largely by RNA polymerase II (Lee et al., 2004). miRNAs are loaded onto the RNA-induced silencing complex, RISC, and guide this complex to their target mRNAs via base-pairing interactions. 6–7 nts at the 5’ end of the miRNA, the so-called ‘seed sequence’, and are thought to determine most of their target specificity. The catalytic component of the RISC complex is an Argonaute (Ago) proten,, and depending on the type of Argonaute present and the degree of complementarity between the miRNA and its target sequence, the target mRNA may be endonucleolytically cleaved and degraded or translationally repressed. Translational repression often leads to target mRNA degradation via decapping and subsequent

exonucleolytic degradation (Filipowicz et al., 2008). Recent findings also indicate that miRNAs can upregulate their targets (Vasudevan et al., 2007; Orom et al., 2008). The average miRNA is predicted to have the ability to act on target sites in hundreds of genes, so each miRNA could potentially regulate a large number of mRNA targets (Bushati and Cohen, 2007).

In the central nervous system, many miRNAs are expressed, often in a temporally and/or spatially regulated manner during development (Kosik, 2006; Kapsimali et al., 2007; Landgraf et al., 2007). To date, more than 400 miRNAs have been identified in human and chimpanzee brain, and it is estimated that approximately 1000 miRNAs are expressed in the human brain (Berezikov et al., 2006).

There is now some evidence for the possible involvement of miRNAs in the aetiology of neurodegenerative diseases. Kim et al. (Kim et al., 2007) identified a miRNA, miR-133b, that is expressed specifically in midbrain dopaminergic neurons and is deficient in midbrain tissue from patients with Parkinson's disease. Hebert et al. (Hebert et al., 2008) investigated changes in miRNA expression profiles of sporadic Alzheimer's disease patients and found that in diseased brain several miRNAs potentially involved in the regulation of amyloid precursor protein (APP) and BACE1 protein component of the enzyme BACE1/beta-secretase responsible for the cleavage of APP into amyloid-beta expression appeared to be decreased.

At present it remains unclear whether miRNAs are actively involved in the aetiology or progression of neurodegenerative disorders. The disregulation of miRNA expression may well be either causative or a consequence of disruption of various cellular processes in neurodegenerative diseases. Identification of causative links opens up the possibility for therapeutic intervention by replacing miRNAs that are lacking or blocking the activity of overexpressed miRNAs (Bushati and Cohen, 2008).

1.4.3 Biointegrative approaches to neurodegenerative diseases

Traditional biological methods of investigating neurodegenerative diseases involved analysis of one or several genes. It has become evident that this is insufficient, as neurodegenerative diseases involve complex molecular interactions involving both genomes and environmental determinants. A systems biology approach represents a deeper integrated investigation of molecular interactions. This allows gaining a complete perspective on the diseases by combining genomic, transcriptomic and proteomic data. This has only recently become feasible due to the development of high thoroughput technologies including microarrays, mass spectrometry analyses of proteins together with rigorous bioinformatics.

With the emergence of new generation sequencing such as RNA-seq the boundaries of knowledge in this area will expand even faster (Noorbakhsh et al., 2009; Courtney et al., 2010).

In this project we designed our own 'boutique' microarray chip to screen for connexin mRNA with long oligonucleotide probes and a Cy3 and Cy5-labelled cDNA target. The chip is to be used for cross-species application for both human and rat tissue. The primary purpose of the chip is to screen normal human central nervous system tissue to establish connexin expression patterns and then use this knowledge for comparative studies to determine how the connexin expression is up- or downregulated in a number of neurodegenerative diseases (e.g. Huntington's and Alzheimer's diseases and epilepsy). This will ascertain if connexins have a role in the progression of these devastating diseases and add significantly to the current body of knowledge, which is growing rapidly with the application of new techniques.

The applications of this custom array, however, are by no means restricted to human neurodegenerative disease. The cross-species design will allow the use of the chip to screen rat tissue, for instance, rat disease models. Researchers interested in connexin expression in various tissues and organs can apply the same platform to their studies, and save vast amounts of time, since microarrays allow tissue screening in a highly parallel fashion.

The transcriptome profiling technology has proved to be one of the fastest developing technology fields within molecular biology. Two important considerations are the number of genes that can be analysed with new technologies, and cost. New sequencing technologies such as RNA-seq have recently become available. For a smaller gene set it is possible to us a TaqMAN RT-PCR approach which allows analysis of up to 96 different RNAs simultaneously. Microarrays however still have their place in the gene expression profiling field

Hypothesis

Connexin expression in the human brain changes in neurodegenerative disease in such a way that common patterns can be detected. These changes correlate with changes in the level of inflammatory markers. It is possible to detect these expression changes using microarray technology.

Aims

1. To build a boutique connexin array.
2. To use the boutique array to screen for connexin expression in different neurodegenerative diseases, such as Alzheimer's disease, Parkinson's disease, Huntington's disease and epilepsy.
3. To validate the data obtained from the boutique arrays using the Illumina Sentrix® whole genome array.
4. To correlate the changes in connexin expression with the changes in the expression of inflammatory markers using the data from the Illumina Sentrix® array.

2 METHODOLOGY

2.1 Methods for Chapter 3 – Connexin Microarray Chip Design and Validation in Rat and Human

2.1.1 Design

2.1.1.1 Oligonucleotide probe design

2.1.1.1.1 Background

An oligonucleotide probe for a cDNA microarray is a single-stranded DNA sequence 50-70 bases in length, complementary to the transcript of interest. As the array target is cDNA generated from mRNA by reverse transcription, the probe is a part of the sense, rather than antisense coding sequence. The primary requirements for probe design within a set are similar length, GC content, low homology to other probes and non-target cDNA, and the absence of hairpin loops and homodimer formations stable at the melting temperature (Tm).

2.1.1.1.2 Overview of the design process

The first stage of this project was to design human-specific connexin oligonucleotide probes, 2-3 per connexin, dependent on whether suitable unique regions of sequence could be identified. These probes were an average of 70 nucleotides in length, with the number of bases adjusted to the optimal melting temperature.

From the point of cost and reliability, a German company called MWG was chosen to supply the probes. This company has a 30,000 gene human array, with one oligo per gene. Their probe sequences are, however, kept confidential.

The 30,000 gene human chip database on the MWG website (www.the-mwg.com) was searched for the oligonucleotides which target connexin gene expression using the MWG CGX (compact gene index) search tool. Twenty oligonucleotides were identified (Table 2. MWG connexin oligonucleotide probes). A decision was made to order 20 of the MWG connexin probes and design 20 of our own, so that the two sets could act as controls for each other and ensure better internal data reliability.

MWG probes are 50-mer in length due to constraints inherent in the process of mass spectrometry purification. Thus our design had to be tailored to the 50-base length.

The possibility of designing a cross-species human-rat array was also investigated. The feasibility of such a design depended primarily on the degree of homology between orthologous human and rat connexins. All the probes were designed to obtain one cross-species human-rat oligonucleotide, where possible.

Table 2. MWG connexin oligonucleotide probes.

Connexin	Catalogue number
GJA1 – Cx43	mwghuman30K#A:06282
GJA3 – Cx46	mwghuman30K#A:04569
GJA4 – Cx37	mwghuman30K#A:07540
GJA5 – Cx40	mwghuman30K#A:10765
GJA8 – Cx50	mwghuman30K#A:05284
GJA9 – Cx59	mwghuman30K#B:1437
GJA10 – Cx62	mwghuman30K#B:1576
GJB1 – Cx32	mwghuman30K#C:0976
GJB2 – Cx26	mwghuman30K#A:09852
GJB3 - Cx31	mwghuman30K#A:04777
GJB5 – Cx31.1	mwghuman30K#A:07766
GJB6 – Cx30	mwghuman30K#A:06957
GJB7 – Cx25	mwghuman30K#C:7834
GJC1 – Cx45	mwghuman30K#A:08425
GJC2 – Cx47	mwghuman30K#A:06598
GJC3 – Cx30.2	mwghuman30K#C:1285
GJD2 – Cx36	mwghuman30K#A:06477
GJD4 – Cx40.1	mwghuman30K#C:1752
Cx?*	mwghuman30K#C:0547
Cx?*	mwghuman30K#C:0548

* These two probes appear to be designed to incomplete coding sequences posted on the GenBank database as unidentified ‘human connexin’ (accession numbers AF251047_1 and AF251048_1 respectively), that do not hybridise to any known human connexin.

2.1.1.1.3 Controls

The next step was to select appropriate controls. The MWG 30,000 human gene array contains pre-designed positive control probes (complementary to the sequences of commonly expressed genes) and negative control probes (*Arabidopsis*). Ten control oligos were ordered from the MWG, 5 positive and 5 negative (See Table 3).

Table 3. Array controls.

Catalogue number	**Gene**
Positive human controls	
mwghuman10K#11002	glyceraldehyde phosphate dehydrogenase (GAPDH)
mwghuman10K#11004	hypoxanthine-guanine phosphoribosyltransferase (HPRT)
mwghuman10K#11006	ubiquitin
mwghuman10K#01731	heterogeneous nuclear ribonucleoprotein C1/C2 (HNRPC)
mwghuman10K#08383	transcription elongation factor A (SII), 1 (TCEA1)
Negative *Arabidopsis* Controls	
mwgaracontrol#001	ara_a48#1
mwgaracontrol#004	ara_b184#1
mwgaracontrol#007	ara_b455#1
mwgaracontrol#009	ara_b605#1
mwgaracontrol#012	ara_c335#1

2.1.1.1.4 Design protocol for custom oligonucleotides

The first stage of oligo design is to obtain the coding sequences for the genes of interest from the GenBank database on the National Centre for Biotechnology Information website (http://www.ncbi.nlm.nih.gov) - in this case human and rat connexins. After all the sequences required have been downloaded, it was then necessary to convert them into FastA format, so that they could be read by the oligo design software (this removes spaces, line breaks and extra characters and gives each sequence a special identifier). The conversion was done using GeneWorks Release 2.5.1 software that is a nucleic acid and protein sequence analysis program. The sequences in the FastA format were then loaded into the oligonucleotide design software OligoWiz Version 1.0.8. This program analyses the sequences in their entirety and picks out good regions in terms of uniqueness of each sequence, melting temperature deviation from the desired mean, and the position within the coding sequence (proximity to the 3' end is preferred as oligo-dT primers are used for cDNA generation). Each oligonucleotide sequence of the desired length within these regions is given a score from 0 to 1 based on the abovementioned parameters, with the best oligo having the highest score. Our 50-mer probe sequences were then chosen from the highlighted optimal regions manually.

2.1.1.1.5 Cross-species design

To investigate the possibility of having human-rat connexin oligos, orthologous human and rat connexin coding sequences were aligned in GeneWorks Release 2.5.1. For the cross-species design, it was important that human connexin sequence regions with good scores in the OligoWiz software (see above) coincided with regions of good human-rat alignment. The aim was to obtain an oligo with more than eighty percent homology and a stretch of contiguous nucleotides of more than 15 bases (as this would ensure rat mRNA hybridisation (Kane et al., 2000; Hughes et al., 2001; Taroncher-Oldenburg et al., 2003). If this proved impossible, cross-species design of the probe for this particular connexin was abandoned.

2.1.1.1.6 Checks for cross-hybridisation

A nucleotide-nucleotide BLAST search (BLASTn) was performed on the National Centre for Biotechnology Information website (http://www.ncbi.nlm.nih.gov) for all the probes. The probes that cross-hybridised to non-target connexin sequences were discarded and new ones selected using the process described above. A BLASTn search was once again performed to ensure that there was no possibly cross-hybridisation, and the process repeated until all the selected probes were unique to their target sequence.

The final step was to ensure the absence of secondary structures and homodimer formation. For this purpose, a computer program called Oligo 4.0-S was used. This software provides a list of parameters for a given nucleotide sequence, including melting temperature and the stability of loop and dimer structures (See Figure 3).

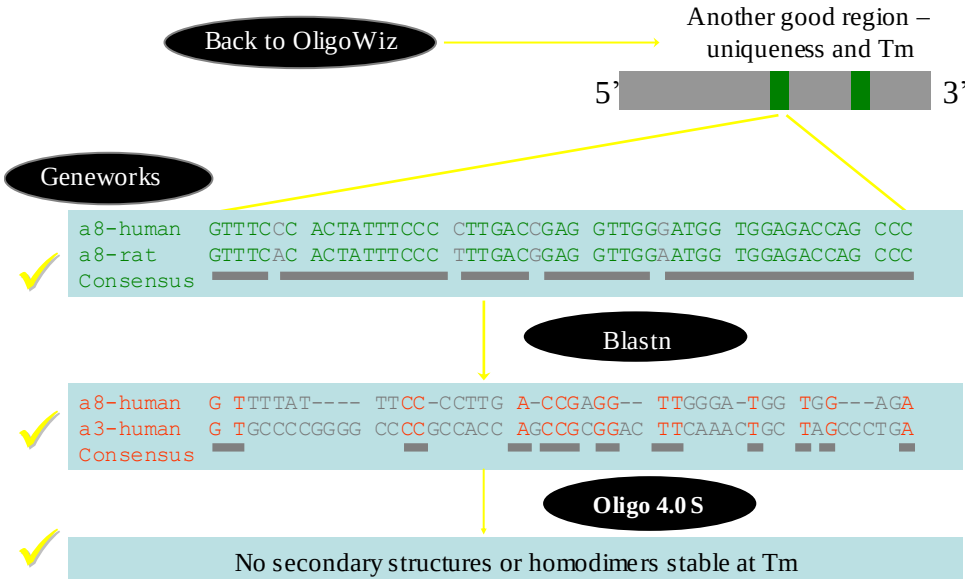

Figure 3. Overview of the oligonucleotide design protocol.

2.1.1.1.7 Oligonucleotide probe synthesis

Once suitable probes were selected, an order for the oligonucleotide sequences was placed with MWG. The MWG oligos are synthesised to the HPSF® (high purity salt-free) standard, to ensure that they are free from salts and metal ions. This standard also guarantees that the proportion of truncated chains for each given nucleotide is less than 0.1%. The composition of the oligonucleotides is checked using MALDI TOF® mass spectrometry. The oligonucleotides are 5'-end amino modified by introducing amino modifier C6 at the synthesis scale of 0.01 μmol. This modifier has a primary amino group at the end of a six-carbon spacer. This amino modifier is called a linker and is used for attaching the probe to the microarray surface.

2.1.1.1.8 Reconstitution

All the oligos were shipped from Germany liophylised in a 96-well plate. On receiving the plate, the oligos were reconstituted in 100 μl of double-distilled water in each well so that the final concentration was 100 pmol/μl.

2.1.1.2 Microarray chip Design

2.1.1.2.1 Array layout

A 4-block array was designed with each 10 x 10 block containing the 50 probe spots (20 MWG connexin oligos, 20 custom-designed oligos, 5 positive controls, 5 negative controls) in a different pattern (See Figure 4). The four-block pattern was designed for a four-pin printer setup, so that each pin would print each oligo once. The 4-block pattern was, in turn, repeated 4 times on the chip, comprising sections 1 to 4, to provide opportunity for data normalisation with a greater number of spots for comparison.

2.1.1.2.2 Printing

A 384-well stock tray was made by transferring 20 μl of 100 pmol/μl probe stocks from each well of the shipping tray in the order that was later used for printing. From each well of the stock tray, 2.5 μl was then transferred into the corresponding wells in a 384-well printing tray, and 2.5 μl of 5x SSC was added to a final concentration of 50 pmol/μl, with 5 μl total in each well.

The first batch of array slides was printed on poly-L-lysine-coated microscope slides, however, the print quality turned out to be poor and the slides would not block properly. To overcome this problem, better quality epoxy-coated slides had to be purchased from the MWG to use for the array printing. The

slides were printed on the MicroGrid II (BioRobotics Ltd.) quill-pin arrayer, using four MicroSpot 2500 pins that have a tip diameter of 100 μm, fill volume of ~65 nl, and a deposition volume of ≤0.05 nl. The diameter of each circular printed spot was ~180 μm

.

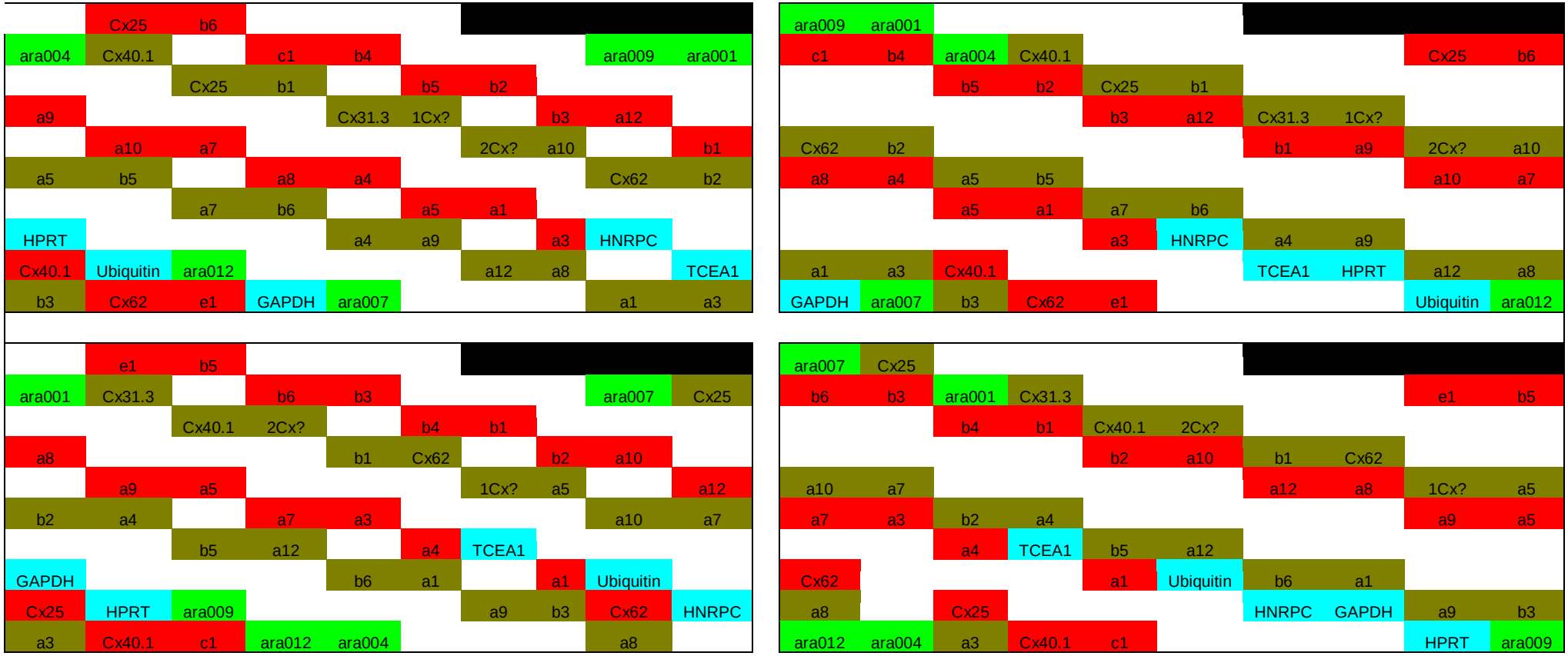

Figure 4. Microarray printing pattern: one section.

2.1.2 Validation

The microarray chip was validated using rat and human tissue.

2.1.2.1 Handling RNA - general considerations

The microarray technology involves screening for RNA expressed in a tissue. The primary consideration when working with RNA is the ubiquitous presence of ribonucleases (RNases) that degrade RNA. It is essential that tissue intended for RNA extraction must be frozen as soon as possible in liquid nitrogen. Proper precautions and appropriate techniques must always be used when handling RNA, and gloves worn at all times. All reagents must be molecular biology grade and free of endonucleases. All solutions must be prepared in double-distilled water treated with 0.1% diethyl pyrocarbonate (DEPC) (Bowtell and Sambrook, 2003).

2.1.2.2 Preliminary validation in rat and human Tissue

2.1.2.2.1 Tissue collection and preparation

2.1.2.2.1.1 Human tissue

Human brain tissue was obtained from the New Zealand Neurological Foundation Human Brain Bank in the Department of Anatomy with Radiology, University of Auckland. Tissue from one normal patient (i.e. diagnosed with no known neurological disease) was used in this study. The patient data is given in Table 4. Full ethical approval was obtained for the study of post-mortem human tissue from the University of Auckland Human Subjects Ethics Committee. Following autopsy, the brain was taken immediately to the Department of Anatomy, University of Auckland. The brain was separated into individual hemispheres and dissected into previously defined tissue blocks. These blocks were then frozen on powdered dry ice, double-wrapped in aluminium foil and stored at -80°C until required for RNA extraction.

Table 4. Source of human tissue for RNA extraction.

Case number	Age, years	Sex	Postmortem delay*, hours	Cause of death
H128	34	F	18.5	Myocardial infarction

*Postmortem delay is defined as the time interval between death and freezing of the tissue.

2.1.2.2.1.2 Animal tissue

Full Ethical Approval was obtained for the study of rat tissue from the University of Auckland Animal Ethics Committee (Application Number N920). Four 21-day-old white Wister rats were

euthanised by carbon dioxide inhalation. Numbers 1 to 4 were assigned to the four animals for tissue identification. The organs (brain, heart, liver, and lens) were removed immediately, rinsed in 0.1 M PBS to remove excess blood, cut into small pieces for ease of RNA extraction and snap-frozen in liquid nitrogen. The pieces were then transferred into pre-weighed and labelled 1.5 ml Eppendorf tubes and stored in –80°C freezer until required for RNA extraction.

2.1.2.2.2 RNA extraction

2.1.2.2.2.1 Initial extraction

The tissues were removed from the -80°C storage freezer and held on dry ice. Tissue samples of 100-200 mg were then crushed in liquid nitrogen and transferred into 1 ml ice-cold TRIzol® reagent (TRIzol® reagent (Invitrogen) is a monophasic mixture of phenol and guanidine isothiocyanate used for the isolation of total RNA). The tissue was then further homogenised using a rotor-stator tissue homogeniser (Omni International, Inc.) until no coarse particles were present in solution. Chloroform (200 μl) was then added to the mixture, the sample was vortexed for 15 seconds, until all phases were thoroughly mixed and left for 2-3 minutes on ice. The sample was then centrifuged at 13,000 rpm at 4 °C for 15 minutes, achieving separation into 2 phases with an interface. The top (aqueous) phase was then collected into a separate tube, while the bottom (phenolic) phase and the interface were discarded. A volume of ice-cold isopropanol equal to the volume of the aqueous phase was added, the sample mixed by inversion and left at -20°C for a minimum of 3 hours to achieve precipitation of the RNA. Where necessary, an overnight precipitation in isopropanol was used to ensure a higher RNA yield. After the elapsed time, the sample was removed from the freezer and centrifuged at 13,000 rpm at 4 °C for 15 minutes to separate the RNA pellet from the suspension. The supernatant was then discarded and the pellet washed with 70% ethanol in water treated with diethyl pyrocarbonate (DEPC) to inactivate RNases, then centrifuged at 10.000 rpm at 4 °C for 7 minutes. The ethanol wash step and subsequent precipitation were repeated.

2.1.2.2.2.2 DNase treatment

The pellet was then dried until semi-translucent and dissolved in DNase mix: 10 units DNase I, 80 units RNase inhibitor, 8 μl 10x New England Biolabs NEBuffer 2 (100 mmol Tris-HCl, 100 mmol $MgCl_2$, 500 mmol NaCl, 10 mmol dithiothreitol (DTT)) and DEPC-treated 0.2 μm filtered water to a volume of 80 μl. The sample was incubated for 15 minutes at room temperature to digest double-stranded DNA. After 15 minutes the reaction was stopped by the addition of 2 μl 200 mmol ethylenedinitrilotetraacetic acid disodium salt dihydrate (EDTA), pH 8.0.

2.1.2.2.2.3 RNA purification

The extracted RNA was purified using the TRIzol® method. A 500 μl volume of the TRIzol® reagent and 100 μl of chloroform were added to the DNase treated sample. The sample was vortexed for 15 seconds to thoroughly mix the phases, left for 2-3 minutes and then centrifuged at 13,000 rpm at 4 °C for 15 minutes. The top aqueous phase was then transferred into a separate tube and an equal volume of ice-cold isopropanol added to precipitate the RNA. The sample was left at -20°C overnight, then centrifuged at 13,000 rpm at 4°C for 15 minutes. The supernatant was discarded, and the pellet washed with 500 μl of 70% ethanol in DEPC-treated water. The sample was then centrifuged at 10,000 rpm at 4°C for 7 minutes and washed twice more in 70% ethanol, each time centrifuging at 10,000 rpm for 7 minutes. The pellet was dried till semi-translucent and re-suspended in a volume of DEPC-treated 0.2 μm-filtered water dependent on the pellet size.

2.1.2.2.2.4 Spectrophotometry

The RNA was then checked for contamination and the concentration determined using a quantitative spectrophotometer. RNA absorbs at 260 nm, with an absorbency of 1 equal to a concentration of 40 μg/ml. The ratio of the optical densities at 260 nm and 280 nm provides an estimate of RNA purity with respect to contaminants such as protein, which are absorbed in the UV range. Pure RNA in 10 mmol tris(hydroxymethyl)aminomethane hydrochloride (Tris-HCl), pH 7.5, has a ratio of 1.9-2.1 (Qiagen Bench Guide, 2001). RNA with a ratio below 1.8 was not used for the subsequent labelling steps.

2.1.2.2.3 RNA integrity monitoring using a denaturing gel electrophoresis

The purified RNA was checked for its integrity by fractionating on a denaturing formaldehyde agarose gel. Good quality, undegraded mammalian RNA shows 3 bands: 28s, 18s and 5s, with the intensity of the 28s band twice the intensity of the 18s band. No smaller sized bands or smearing should be present, as this indicates degradation of the RNA sample. Since RNA has a high degree of secondary structure a denaturing gel is optimal. Formaldehyde in the gel disrupts the secondary structure, so that the RNA molecules can be properly separated on the basis of their charge (Qiagen Bench Guide, 2001).

To perform the gel electrophoresis, 3 μg of RNA was loaded per well. This amount of RNA was added to 7.5 μl of freshly prepared resuspension buffer (10% 10x denaturing buffer*, 50% deionised formamide, 6.48% formaldehyde, made in DEPC water) and 1 μl of 250 mg/l ethidium bromide. The samples were incubated at 55°C for 20 minutes to remove impurities and RNA secondary structure. Prior to loading, 4 μl of ice-cold loading dye (50 mmol HEPES pH 7.0, 50% glycerol, 0.002% w/v bromophenol blue) was added to each sample. The samples were microfuged for a few seconds and loaded into wells of a formaldehyde agarose gel.

The formaldehyde agarose gel was prepared by mixing 50 mmol HEPES pH 7.0, 20 mmol Na phosphate buffer pH 7.0 and 1.2% w/v agarose, microwaving for 30 seconds to melt agarose, cooling to 55 °C, and then adding 7.2% formaldehyde. Formaldehyde cannot be added at a higher temperature as it is denatured by heat. The gel was poured into a casting tray and left to set for two hours before loading the sample.

The electrophoresis was run at 40 V for approximately 3 hours, or until bromophenol blue had run approximately 2/3 of the gel length. The gel was then rinsed in water and visualised under UV light to detect the ribosomal bands (See Figure 5).

2.1.2.2.4 cDNA target synthesis and fluorescent dye labelling

For this study, a two-step amino-allyl cDNA labelling process was employed, using the Amersham Biosciences CyScribe Post-Labelling Kit for microarray hybridisation. In this process, cDNA with one modified amino-allyl nucleotide is first generated from the RNA sample. The fluorescent dyes (Cy3 and Cy5) are coupled to the modified nucleotide in the second stage, thus producing fluorescently-labelled cDNA (Ausubel and et al., 2000).

---

* 10x denaturing buffer: 200 mmol N-[2-Hydroxymethyl]piperasine-N'-[2-ethanesulfonic acid (HEPES), 50 mmol Na acetate, 10 mmol EDTA in DEPC-treated water, pH 7.0.

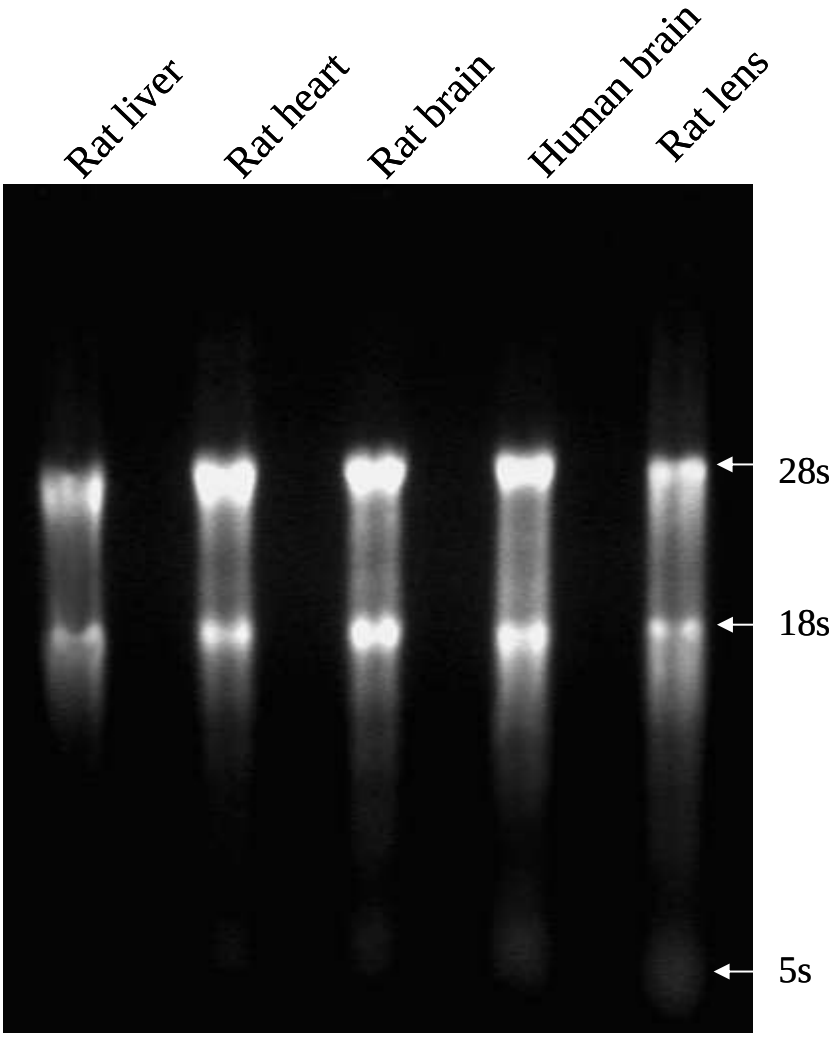

Figure 5. A denaturing RNA gel of the rat liver, rat heart, rat brain, rat lens and human brain samples, showing the 28s, 18s and 5s bands with the 28s/18s band ratio of ~2.

2.1.2.2.4.1 Amino-allyl cDNA generation

The first stage of this process was the generation of amino-allyl modified cDNA from total RNA. An oligo-dT primer was used for the cDNA production to ensure that only poly-A mRNA was converted into cDNA.

For primer annealing, 30 μg of total RNA was incubated with 3 μl of anchored oligo-dT primer at 70°C for 5 minutes, then cooled to room temperature for 10 minutes and microcentrifuged briefly. For the extension reaction, 4 μl of 5x CyScript™ buffer, 2 μl of 0.1M DTT, 1 μl of CyScribe Post-Labelling nucleotide mix, 1 μl of CyScribe Post-Labelling Amino-Allyl dUTP, and 1 μl of CyScript Reverse Transcriptase were added to the sample. The components were mixed gently and incubated at 42°C for 1.5 hours. To cleave and degrade mRNA from the mRNA-cDNA hybrid, 7.5 μl of 2.5M NaOH was added to the sample and incubated for 15 minutes at 37°C. The reaction was terminated by adding 37.5 μl 2M HEPES.

The labelled cDNA was purified using Amicon Microcon® YM-30 columns. Firstly, enough water was added to the sample to a final volume of 500 μl. The sample was added to the column and spun at 13,000 xg for approximately 10 minutes at room temperature (until the volume left on the column was about 15 μl). The reservoir was then removed from the collection vial and inverted over a new vial. The column was then centrifuged at 900 xg for two minutes to recover the cDNA.

2.1.2.2.4.2 Florescent labelling of amino-allyl cDNA

One aliquot of CyScribe Cy3 reactive dye and one aliquot of CyScribe Cy5 reactive dye from Amersham Biosciences (the dye molecules contain NHS-esters that interact with the amino-allyl group on the modified cDNA) were each re-suspended in 30 μl of sterile 0.1M sodium bicarbonate, pH 9.0. Each dye sample was then divided into two 15 μl aliquots. A 15 μl volume of either Cy3 or Cy5 dye was added to the purified cDNA sample, mixed and incubated in the dark at room temperature for 1 hour. After this time, 15 μl of 4M hydroxylamine was added to inactivate any unreacted Cy dye molecules, the sample mixed and incubated in the dark for further 5 minutes at room temperature. Unreacted Cy dye was removed from the sample by Amicon Microcon® YM-30 column purification, employing the method given above, except that the sample was washed with 450 μl water and centrifuged 3 times before collection. After the final wash, the volume was brought down to 12 μl.

2.1.2.2.5 Hybridisation

2.1.2.2.5.1 Blocking of the slides

Blocking of the printed slides was necessary to render the slide surface non-reactive, so that the cDNA target only hybridises to the spotted oligo probes. The printed slides were placed into stainless steel racks and immersed in a glass container containing 0.1% SDS (sodium dodecyl sulphate) solution in double-distilled water at 95°C for 1 minute with constant agitation, then washed in a 5% solution of 95% ethanol in double-distilled water for 1 minute with constant agitation. Then the slides were washed in double-distilled water for 1 minute with constant agitation. The slides were not allowed to dry out between the washing steps, so transferred from one solution to the next immediately.

The printed and blocked slides can be stored for ≤ 3 months for future use in hybridisation experiments.

2.1.2.2.5.2 Hybridisation to the slide

The microarray platform to be employed uses two-colour competitive hybridisation. Two cDNA aliquots obtained as above, one Cy3-labelled and one Cy5-labelled, are co-hybridised to the same slide.

One Cy3 and one Cy5-labelled sample (12+12 μl) were mixed together in the same tube, then 3.0 μl of 20x SSC (saline-sodium citrate) buffer, then 1 μl of 5% SDS and 2 μl of oligonucleotide dA_{80} (to prevent the poly-T tail of cDNA interacting non-specifically with A-rich regions of the probes) was added. The sample was denatured at 95°C for 2 minutes. The coverslip for the slide was washed with ethanol, 1% SDS water and then air-dried. The hybridisation sample (30 μl) was transferred onto the coverslip, avoiding the formation of bubbles, an inverted printed slide was placed over the coverslip, and the covered slide placed into a hybridisation chamber. A few drops of 3xSSC were added to the chamber to prevent drying out of the slide, the chamber lid screwed on tightly and the slide hybridised at 42°C for 16-24 hours.

2.1.2.2.5.3 Washing

After hybridisation, the slide was immersed in a 2xSSC + 0.2% SDS solution, gently agitated until the coverslip floated, followed by a further 5 minutes agitation. The slide was then washed in 1xSSC for 5 minutes, and for 10 seconds in 0.2xSSC, to remove all traces of SDS, since this is highly autofluorescent. The slide was then centrifuged at 700 rpm for 10 minutes to dry.

After the rat brain/heart array was washed using the above protocol, it was evident that the background fluorescence level was very high. The washing time in 0.2xSSC was therefore increased to 45 seconds for the subsequent rat liver/rat brain and human brain/rat brain slides, then to 90 seconds for the rat heart/rat lens slide and to 180 seconds for the rat heart/rat heart slide.

2.1.2.2.6 Data Acquisition

Slides were scanned in a GenePix 4000B Microarray Scanner (Axon Instruments). Data was acquired at two wavelengths simultaneously, using 532 nm (17 mW) and 635 nm (10 mW) lasers, with emission filters 575DF35 (green, ~557-592 nm), and 670DF40 (red, ~650-690 nm), which are optimised for Cy3 and Cy5 respectively. The detection limit of the GenePix 4000B scanner is 0.1 fluor/μm^2 for Cy3 and Cy5. The dynamic detection range is 4 orders of magnitude, linear over 3 orders.

Scan times were about 5 minutes for a preview scan of an entire slide at 10 micron resolution (and under 12 minutes for a scan at 5 micron resolution). Scans of the microarray feature areas at 5 microns were usually less than 30 seconds. A pixel intensity histogram was used during scanning to balance the signal in the red and green channels. The fluorescence intensities were digitised using 16 bits per colour channel.

The scanned image was analysed using the GenePix Pro 4.0 software. This software uses a set of proprietary algorithms to find the microarray features on the slide, and assigns each pixel in the region to either the feature or the background. The background was estimated locally (the mean pixel intensity of the area immediately surrounding each spot). The fluorescent signal was quantitated either as mean or median (median was used as less sensitive to the presence of outliers) pixel intensities per feature (spot). The software also calculated standard deviation from the mean for each spots for both Cy3 and Cy5 signal. This first-analysis data were then downloaded as a GenePix Array Results (GPR) file into data analysis software for secondary analysis.

2.1.2.2.7 Data Analysis

2.1.2.2.7.1 Normalisation

The microarray data from the slides was normalised by applying a LOWESS (locally weighed scatterplot smoother) function to an MA plot, where:

$M = \log R - \log G$, and

$$A = \frac{1}{2} \times (\log R + \log G),$$

with R and G representing the red and green channel intensity values for positive and negative controls (assuming equal representation on both channels). No background correction was done, as the background was uniform on all arrays.

2.1.2.2.7.2 Analysis

The natural logarithms of the values for the red and green channel intensities for all sixteen spots representing each oligo on the array were averaged before and after normalisation. Ratios of normalised red and green (geometric) mean intensities and difference between the log values of the red and green means were calculated. The geometric mean instead of the arithmetic mean, as the former controls better for possible outlying values and abundance differences between the different genes (Vandesompele et al., 2002).Standard deviation for the normalised red and green intensities for the 16-spot set representing each probe was calculated, as well as standard deviation of the normalised red minus green signal for each set.

After normalisation, a pairwise t-test was used to assess whether the difference between the red and green channel intensities for each oligo was significant, based on a Bonferroni correction with n=50 and alpha=0.01. The connexin was considered differentially expressed if the p-value was less than 0.01.

A second test was performed to estimate whether the mean signal intensity for each oligo was significantly greater than that of the brightest negative control in each of the two channels. This was done using a one sample t-test to compare the mean intensity across the 16 spots for each oligo with the intensity of the brightest negative control spot on the array that was itself treated as a constant for the array

2.1.2.3 Validation of the Custom Designed Microarray Chip in Rat Heart vs Human Heart

2.1.2.3.1 Animal tissue collection

The tissue was collected as described in Section 2.1.2.2.1.2 *Animal Tissue Collection*, except that three 7-day-old white Wister rats were used and the organs collected were heart and liver.

2.1.2.3.2 RNA extraction and purification

The RNA was extracted and purified using a combination of the TRIzol® reagent method reagent and the RNeasy® Mini kit from Qiagen. Buffer RPE is supplied as a concentrate in the kit and was reconstituted by adding 4 volumes of 100% ethanol.

The tissues were removed from the -80°C storage freezer and held on dry ice. Tissue samples of 100 mg were then crushed in liquid nitrogen and transferred into 1ml of ice-cold TRIzol® reagent. The tissue was then further homogenised using a rotor-stator tissue homogeniser (Omni International, Inc.) until no coarse particles were present in solution. Chloroform (200 μl) was then added to the mixture,

the sample vortexed for 15 seconds until all phases were thoroughly mixed, and then left for 2-3 minutes on ice. The sample was then centrifuged at 13,000 rpm at 4 °C for 20 minutes, achieving separation into 2 phases with an interface. The top (aqueous) phase was then collected into a separate tube. An equal volume of 70% ethanol (made with DEPC water and 100% ethanol) was added; the mixture was vortexed and loaded onto a Qiagen RNeasy® Mini Silica membrane column. The column was centrifuged for 15 seconds at 10,000 rpm. If the initial sample volume exceeded 700 µl the remaining sample volume was added to the same RNeasy spin column and centrifuged once more for 15 seconds at 10,000 rpm, discarding the flow-through and re-using the collection tube. A 700 µl aliquot of wash buffer RW1 was loaded onto the RNeasy® spin column and the column was centrifuged at 15 seconds at 10,000 rpm, re-using the collection tube from the previous step and discarding the flow-through. Then two successive 500 µl aliquots of wash buffer RPE were added to the spin column and the column centrifuged for 15 seconds at 10,000 rpm, re-using the collection tube from the previous step and discarding the flow-through each time. Then the RNeasy spin column was placed onto a new 1.5 ml collection tube, 30-40 µl of DEPC-treated water was added directly to the spin column membrane and the column was centrifuged for 1 minute at 10,000 rpm to elute the RNA. If the expected RNA yield was more than 30 µg, the previous step was repeated using another 30 µl of DEPC-treated water, re-using the same collection tube.

The concentration and purity of the RNA was determined using the Nanodrop ND-1000 Spectrophotometer.

2.1.2.3.3 RNA Quality Assessment

The RNA quality was assessed by using the Agilent Bioanalyser 2100 to generate an electropherogram by detecting fluorescently labelled RNA eluting from a molecular sieve. The quantity of RNA used to generate the electropherogram was 200-700 ng applied in a 1 µl volume to an RNA 6000 Nano LabChip following the steps in the Agilent Bioanalyser protocol. The RNA Integrity Number (RIN) was taken as the measure of the RNA quality (the RIN is a value out of 10, with 10 being the highest value, calculated by the bioanalyser software according to the area and distribution of fluorescence peaks on the electropherogram) (See Figure 6).

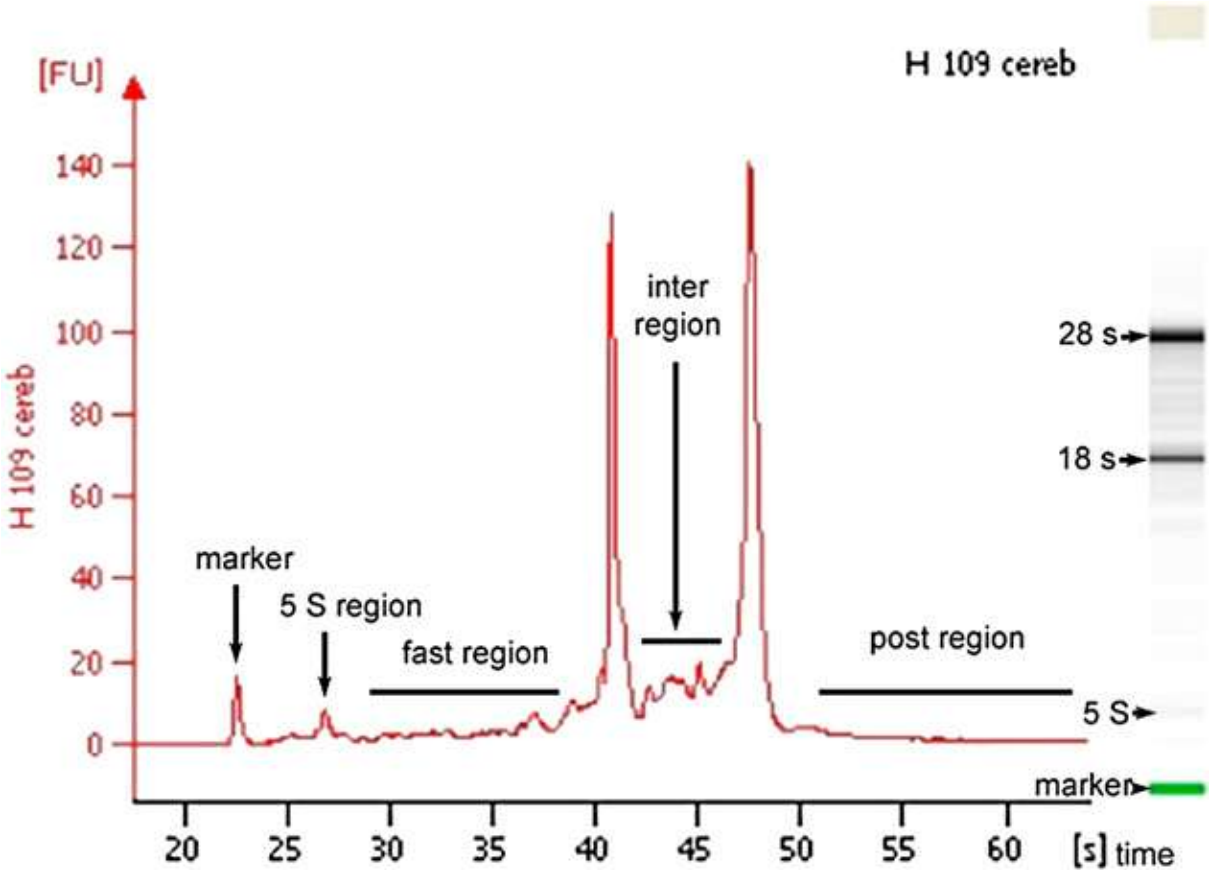

Figure 6. An example of an electropherogram generated by the Agilent Bioanalyser 2100.

2.1.2.3.4 cDNA target synthesis and fluorescent dye labelling

For this project, a two-step amino-allyl cDNA labelling process was employed, using the SuperScript™ Indirect cDNA Labeling System kit to generate fluorescent dye-coupled cDNA for microarray hybridisation. In this process, cDNA with one modified amino-allyl nucleotide is first generated from the RNA sample. Then fluorescent dyes (Cy3 and Cy5) are coupled to the modified nucleotide in the second stage, thus producing fluorescently-labelled cDNA (Ausubel and et al., 2000).

2.1.2.3.4.1 Amino-allyl cDNA generation

The first stage of this process is the generation of amino-allyl modified cDNA from total RNA. An anchored oligo-dT primer was used for the cDNA production to ensure that only poly-A mRNA was converted into cDNA.

The Loading and Wash buffers were supplied in the kit as concentrates. Loading buffer was reconstituted by adding 3 volumes of 100% isopropanol. Wash buffer was reconstituted by adding 3 volumes of 100% ethanol.

For primer annealing, 5-20 μg of total RNA and 2 μl of Anchored Oligo$(dT)_{20}$ Primer (2.5 μg/μl) were added to a 1.5 μl RNase-free tube, the volume was made up to 18 μl with DEPC-treated water and the mixture incubated at 70°C for 5 minutes, then placed on ice for at least 1 minute. For the extension reaction, 6 μl of 5xFirst-strand buffer, 1.5 μl of 0.1M DTT, 1.5 μl of dNTP mix (including amino-modified nucleotides), 1 μl of RNaseOUT™ (40 U/μl) and 2 μl of SuperScript™ III Reverst Transcriptase (400 U/μl) were added to the tube on ice . The components were mixed gently and incubated at 42°C for 3 hours. To cleave and degrade mRNA from the mRNA-cDNA hybrid, 15 μl of 1N NaOH was added to the sample, mixed thoroughly and incubated at 70°C for 10 minutes. To neutralise the pH 15 μl of 1N HCl was added, and the sample mixed gently. Then 20 μl of 3 M Sodium Acetate, pH 5.2 was added to the contents and mixed gently.

The labelled cDNA was purified using S.N.A.P.™ columns supplied in the kit. Loading buffer (500 μl) was added and the contents of the tube vortexed. The sample was then loaded onto the S.N.A.P.™ column and centrifuged at 14,000 xg for approximately 60 seconds at room temperature. The flow-through was discarded. The S.N.A.P.™ column was placed onto the same collection tube and 700 μl of Wash buffer was loaded onto the column, the column was centrifuged at 14,000 xg for 60 seconds. The flow-through was discarded and the column was placed onto the same collection tube. Then the previous step was repeated and the column then placed onto the same collection tube and centrifuged one more time at 14,000 xg for 15 seconds to dry out the membrane, the collection tube and the flow-

through discarded. The column was placed onto a new 1.5 ml microcentrifuge tube, 50 µl of DEPC-treated water was added to the column and the column incubated at room temperature for 1 minute. The column was centrifuged at 14,000 xg for 1 minute at room temperature. This step was repeated using the same 1.5 ml collection tube.

3 M Sodium Acetate (10 µl), pH 5.2 and 2 µl of 20 mg/ml glycogen was added to the collection tube from the previous step and the contents of the tube were mixed. Ice-cold 100% ethanol (300 µl) was added to the tube and the tube was incubated at -20°C overnight.

Then the tube was centrifuged for at 14,000 xg at 4° C for 20 minutes. The supernatant was carefully removed and discarded. Ice-cold 75% ethanol (250 µl, made up with 100% ethanol and DEPC water) was added to the tube and the tube was centrifuged at 14,000 xg for 2 minutes. The supernatant was carefully removed and discarded. The sample was air-dried for 10 minutes and then re-suspended in 5 µl of 2X Coupling Buffer.

2.1.2.3.4.2 Florescent labelling of amino-allyl cDNA

One aliquot of Amersham CyScribe Cy3 reactive dye and one aliquot of CyScribe Cy5 reactive dye (the dye molecules contain NHS-esters which interact with the amino-allyl group on the modified cDNA) were each re-suspended in 30 µl of DMSO (dimethyl sulfoxide) supplied in the Invitrogen SuperScript™ labelling kit. Each dye sample was then divided into six 5 µl aliquots. A 5 µl volume of either Cy3 or Cy5 dye was added to the purified cDNA sample from the ethanol precipitation step, mixed and incubated in the dark at room temperature overnight. After this time, 20 µl of 3 M Sodium Acetate, pH 5.2 was added to the tube, followed by 500 µl of Loading buffer, the sample was vortexed and loaded onto the S.N.A.P.™ Column. The amino-allyl cDNA was purified following the purification protocol described in the previous section. After the final wash, the column was placed onto a 1.5 ml amber collection tube, 50 µl of DEPC-treated water was loaded onto the column membrane and the column incubated for 1 minute at room temperature. The column was centrifuged at 14,000 xg for 1 minute at room temperature, the flow-through containing the dye-coupled cDNA collected. The concentration of the cDNA and the amount of coupled dye was determined using the Nanodrop ND-1000 Spectrophotometer. The labelled cDNA was stored at -20°C.

2.1.2.3.5 Hybridisation

2.1.2.3.5.1 Blocking of the slides

Blocking of the printed slides is necessary to render the slide surface non-reactive, so that the cDNA target only hybridises to the spotted oligo probes. The printed slides were placed into black plastic racks with a black (non-transparent) plastic container and immersed in 0.1% Triton X-100 solution in

double-distilled water at room temperature for 5 minutes with constant agitation, then immediately transferred to a new container with 1.2 mmol HCl solution in double-distilled water for 5 minutes with constant agitation. The slides were then placed into 1.2 mmol HCl solution in a new container for 5 more minutes with constant agitation. After this step the slides were transferred to a new container with 100 mmol KCl solution in double-distilled water and left for 10 minutes with constant agitation. Then the slides were washed in double-distilled water in a new container for a 1 minute with constant agitation. Next the slides were placed in a new container with 4 x SSC solutions at 50°C for 15 minutes with constant agitation and washed once again in double-distilled water for 1 minute. The slides were dried by centrifuging at 1,200 rpm for 5 minutes at room temperature. The slides were not allowed to dry out between the washing steps, but transferred from one solution to the next immediately.

The printed and blocked slides can be stored for ≤ 3 months for future use in hybridisation experiments.

2.1.2.3.5.2 Hybridisation to the slide

The microarray platform to be employed uses two-colour competitive hybridisation. Two cDNA aliquots obtained as above, one Cy3-labelled and one Cy5-labelled, were co-hybridised to the same slide.

One Cy3 and one Cy5-labelled sample (5+5 μl) were mixed together in the same tube, then 1.5 μl of 20 x SSC buffer, 0.5 μl of 5% SDS, 2 μl of ultra-pure water and 1 μl of oligonucleotide dA_{80} (to prevent the poly-T tail of cDNA interacting non-specifically with A-rich regions of the probes) were added to the tube. The sample was denatured at 95°C for 3 minutes. The LifterSlip coverslip (Erie Scientific Company) was washed with double distilled water and wiped clean with a lint-free tissue. The hybridisation sample (15 μl) was transferred onto the coverslip, avoiding the formation of bubbles, an inverted printed slide was placed over the coverslip, and the covered slide placed into a hybridisation chamber. A few drops of 3 x SSC were added to the chamber to prevent drying out of the slide, the chamber lid screwed on tightly and the slide hybridised at 55°C for 16-24 hours.

2.1.2.3.5.3 Washing

After hybridisation, the slide was immersed in a 2 x SSC + 0.2% SDS solution, agitated until the coverslip floated, followed by a further 5 minutes agitation. The slide was then washed twice in 1 x SSC for 2.5 minutes, and then for 2 minutes in 0.2 x SSC, to remove all traces of SDS, since this is highly autofluorescent. The slides were not allowed to dry out between the washing steps, but

transferred from one solution to the next immediately. The slide was then centrifuged at 1200 rpm for 5 minutes to dry.

2.1.2.3.6 Data Acquisition

The data was acquired as in Section 2.1.2.2.6 *Data Acquisition.*

2.1.2.3.7 Data Analysis

2.1.2.3.7.1 Normalisation

The background intensity value for Cy3 and Cy5 signal for each spot was subtracted from the mean Cy3 and Cy5 intensity value for the spot. Background subtracted signal intensity for each spot was divided by the mean signal intensity for the array for Cy3 and Cy5 channels separately. The SNOMAD (Standardisation and Normalisation of MicroArray Data) statistical package was used for data normalisation and is a collection of algorithms for the normalisation and standardisation of gene expression datasets, SNOMAD includes two non-linear transformations that correct for bias and variance which are non-uniformly distributed across the range of microarray element signal intensities: local mean normalisation and local variance correction (Z-score generation using a locally calculated standard deviation). Local mean normalisation across the array surface was performed to correct for spatial hybridisation artefacts – mean signal intensity for Cy3 and Cy5 channels for each spot was divided by the local mean signal intensity calculated based on the X and Y coordinates of the spot on the array to produce a local mean normalised intensity. Local variance correction across element signal intensity function was used to correct for any differences in the variance of Log(Ratios) across the range of gene expression levels. This was done by dividing each Log(Ratio) value by the locally calculated standard deviation of the Log(Ratio) values. Because the variance correction entails division by the standard deviation, the resulting values are Z-scores (i.e. in standard deviation units). Because the standard deviation is calculated locally across gene expression level (X axis), the Z-scores reflect values relative to the amount of variance in the Log(Ratio) values at particular points along the X axis, i.e. variance in the log(ratio) values at particular expression levels (Colantuoni et al., 2002b).

Corrected Log (Ratio) / Local Stadard Deviation =

Local Z-Score

The data was log-transformed to make the variation of intensities or differences less dependent on the absolute magnitude and evens out highly skewed distributions and to convert multiplicative errors into additive ones. Logarithm to base 2 was calculated for each Cy5 and Cy3 feature intensity values to transform Cy5 and Cy3 signal intensities into the difference between the logs of the intensities of the Cy3 and Cy5 channels. Thus genes upregulated 2-fold corresponded to a log ratio of +1 and 2-fold downregulated genes corresponded to a ratio of -1 (Steinhoff and Vingron, 2006). LOWESS function transformation was performed to correct for intensity-dependent imbalance between Cy3 and Cy5

signals. This was done by applying a LOWESS (locally weighed scatterplot smoother) function to an MA plot, where:

$M = \log_2 R - \log_2 G$, and

$$A = \frac{1}{2} \times (\log_2 R + \log_2 G),$$

with R and G representing the Cy5 and Cy3 feature intensity values. This produces corrected log ratios between Cy5 and Cy3 signal intensities. Local variance correction across feature signal intensities was performed to correct for variance differences across the intensity spectrum, based on the local standard deviation values for corrected log ratios.

2.1.2.3.7.2 Analysis

As in Section 2.1.2.2.7.2 *Data Analysis***,** an one sample t-test to estimate whether the mean signal intensity for each oligo was significantly greater than that of the brightest negative control in each of the two channels was performed by comparing the mean intensity across the 16 spots for each oligo with the intensity of the brightest negative control spot on the array, that was treated as a constant for the array.

A pairwise t-test was used to assess whether the difference between the red and green channel intensities for Cx43, Cx40, Cx32 and Cx26 was significant, based on a Bonferroni correction with n=50 and alpha=0.01. The connexin was considered differentially expressed if the p-value was less than 0.01. Pearson correlation coefficients were calculated to estimate whether there was concordance between dye reversals, sample repeats and biological repeats.

2.1.2.4 Validation of the custom-designed microarray chip using the commercial Affymetrix platform

Two GeneChip® Rat Genome 230 2.0 Arrays were used to compare connexin gene expression in rat heart and rat liver. One total RNA liver sample and one total RNA heart sample from the same 7 d.o. rat (rat 1 in Section 2.1.2.3. Validation of the custom designed microarray chip in rat heart *vs* human heart was used).

2.1.2.4.1 Array manufacturing technology

Affymetrix arrays use photolithography for direct oligonucleotide synthesis *in situ* on silicon wafers. The method is based on selective deprotection of surface-bound DNA bases by illumination with UV light through holes in a photolithographic mask. Because this method achieves poor coupling efficiencies, the length of oligonucleotides is limited to 25-mers. However, because of the precision of the photolithographic process, Affymetrix arrays contain a very large number of features compared to spotted cDNA microarrays. The standard array from Affymetrix contains almost 500,000 18x18 μm rectangular oligonucleotide features within a 1.28x1.28 cm area (See Figure 7). Up to 20 "perfect-match" nucleotides are selected for each gene, as well as a corresponding "mismatch nucleotide" for each, in which a single mismatch is based at the centre of the nucleotide (homomeric substitution). The mismatch oligonucleotide is used to monitor non-specific cross-hybridization (Hisham K. Hamadeh, 2004).

The Rat Genome 230 2.0 Array I is comprised of 31,042 probe sets, analyzing 30,248 transcripts and variants from 28,757 well-substantiated rat genes. Sequences used in the design of the array are selected from GenBank®, dbEST, and RefSeq databases. Eleven pairs of oligonucleotide probes are used to measure the level of transcription of each sequence.

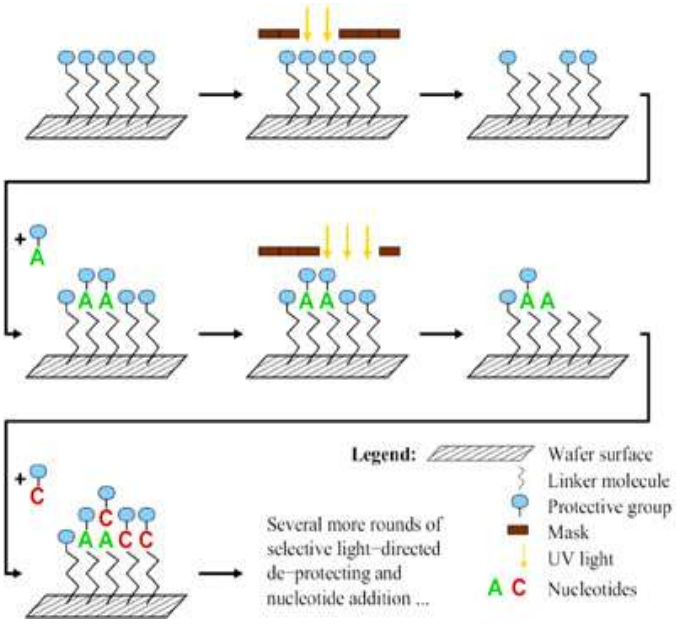

Figure 7. Photolithographic synthesis of Affymetrix arrays. (Picture source (Tomlinson et al., 2008)).

A silicon wafer substrate with linker molecules capped by photoprotective groups is aligned with a photolithographic chrome-coated mask with rectangular holes. UV light is shone through the mask, resulting in selective removal of the photoprotective groups and generation of active sites. The substrate is then washed through with a solution containing a DNA monomer capped with a photoprotective group, and the monomer selectively attaches to the active areas. The process is repeated, using different masks and monomers in each step, until the oligonucleotide probe is assembled.

2.1.2.4.2 Controls

The chip uses two kinds of control probe sets – rat housekeeping genes and bacterial spike controls that represent procaryotic material added to ("spiked into") the sample during preparation.

Housekeeping genes on the chip include rat glyceraldehyde phosphate dehydrogenase (GAPDH), rat hexokinase 1 and beta-actin. Housekeeping gene controls are expected to be present above the detection level in all samples and are used to estimate the quality of the RNA sample.

The first set of spike controls are unlabelled polyA control probe sets (*dap, lys, phe, thr, trp)* which correspond to *Bacillus* genes that have been modified by the addition of Poly(A)+ tails, then cloned into the pBluescript phagemid cloning vector. They are added to the sample immediately preceding the reverse transcription step and amplified and labelled in the same reaction as the sample, and thus act as tracers for the success of the reaction process.

The second set of spike controls is hybridisation controls that are added to the hybridization mix at staggered concentrations to assess hybridization quality. These are probe sets for prokaryotic genes. *bio*B, *bio*C, *bio*D probe sets represent genes of the biotin synthesis pathway from *E.coli*. *cre* is the recombinase gene from P1 bacteriophage. *bio*B is at the resulting concentration of 1.5 pmol and is at the detection limit for most expression arrays and is anticipated to be detected at least 70% of the time. The other controls should be detected all of the time, with increasing signal values (*bio*C (5 pmol), *bio*D (25 pmol) and *cre* (100 pmol)). If these controls are not detected, or the signal value is too low, this indicates a potential problem with the hybridisation reaction or subsequent washing and staining steps.

In addition to the regular probe sets, which are usually designed to be complementary to the region within 500 base pairs of the 3' end of transcripts, maintenance genes and the polyA controls also have 5' and in some cases M (middle) probe sets included on the arrays. These probes give an indication of the integrity of the starting RNA, and efficiency of the first strand cDNA synthesis. In general, the signal for the 3' probe sets would be expected to be somewhat higher than that for the M and 5' probe sets (i.e. resulting in a ratio just greater than 1.0)s a result of the direction of cDNA synthesis during the RT reaction. A ratio of more than 3 for the 3'/5' signal values indicates a potential problem during RNA sample preparation and/or the cDNA synthesis reaction.

2.1.2.4.3 Overview of the Affymetrix GeneChip® Assay hybridisation and labelling procedure

The Affymetrix GeneChip® Assay protocol requires a minimum of 5 μg of total RNA. The samples are reverse transcribed using a T7-oligo(dT) primer and double-stranded cDNA is then synthesized. The double-stranded cDNA, with the incorporated T7 promoter, is then used as a template in any subsequent *in vitro* transcription reaction. Biotinylated UTP and CTP nucleotides are incorporated into cRNA during the *in vitro* transcription reaction. Biotin-labelled cRNA is then fragmented and hybridised to the chip. cRNA bound to the chip is stained with streptavidin-phycoerythrin. The staining protocol includes a signal amplification step that employs an anti-streptavidin antibody (goat) and biotinylated goat IgG antibody. The fluorescence emission is detected using the GeneChip® Scanner 3000 and the images processed and data extracted using Affymetrix GeneChip® Operating Software (GCOS).

2.1.2.4.4 Data Analysis

The rat liver and rat heart scanned array images were analysed using GCOS. A signal value for each probe set was generated and a detection *p*-value was evaluated against a defined cut-off to determine the Detection call. This call indicates whether a transcript is reliably detected (Present) ($p<0.05$), not detected (Absent) ($p>0.65$) or detected at a marginal level (Marginal) ($0.05<p<0.65$). For each probe pair in a set the "mismatch" (non-specific hybridisation) signal is subtracted from the "perfect match" probe signal, with the resultant p-value being lower for the probe set where the signal difference is large. An Array Report was produced for each array, containing information on parameters such background levels, noise levels, statistical thresholds used to for Detection Calls, percentages of present, absent and marginal probe sets, average signal for the array and performance of array controls.

The log signal values for Cx43, Cx40, Cx32 and Cx26 for the rat heart array were subtracted from log signal values for the rat liver array. Positive difference values indicated greater connexin expression in the liver, while negative values indicated greater connexin expression in the heart.

2.2 Methods for Chapter 4 - RNA Quality of Human Brain Tissue.

2.2.1 Tissue collection and preparation

Human brain tissue was obtained from the New Zealand Neurological Foundation Human Brain Bank in the Department of Anatomy with Radiology, University of Auckland. Tissue from eight normal cases (i.e. diagnosed with no known neurological disease), nine cases with Alzheimer's, seven cases with Parkinson, seven with Huntington's disease and three cases with epilepsy were included in the study.

For all the cases except epilepsy, the brain area used was the cerebellum. Brain regions, known to be secondarily affected in specific neurological diseases, such as the caudate nucleus (CN) for Parkinson's disease, the motor cortex (MC) for Huntington's disease and the medial temporal gyrus (MTG) for Alzheimer's disease, and the corresponding areas from normal controls were also used in the study. The epilepsy tissue samples were removed from the hippocampus of patients with intractable mesial temporal lobe epilepsy during temporal lobectomies (Fonseca et al., 2002) (For patient data see Table 5, Table 6, Table 7, Table 8, Table 9, Table 10).

Full ethical approval was obtained for the study of postmortem human tissue from the University of Auckland Human Subjects Ethics Committee. Following autopsy, the brain was taken immediately to the Department of Anatomy with Radiology, University of Auckland. The brain was separated into the two hemispheres and dissected into previously defined tissue blocks. These blocks were then frozen on powdered dry ice, double-wrapped in aluminium foil and stored at −80 °C until required for RNA extraction.

2.2.2 RNA extraction and purification

The RNA was extracted as in Section 2.1.2.3.2 *RNA extraction and purification.*

2.2.3 RNA quality assessment

The quality of the RNA was assessed as in Section 2.1.2.3.3 *RNA Quality Assessment*.

2.2.4 Tissue pH measurement

The measurement of the brain tissue pH was carried out by thawing and macerating a small amount of fresh frozen sample and applying it to a Merck 4.0–7.0 pH strip with the gradation of 0.2 units until

full saturation, then comparing it to the colour table. This method provides a direct measure of the pH of the extracellular and cytoplasmic components of the tissue combined, and avoids dilution with any medium that might affect pH readings.

2.2.5 Statistical analysis

In order to investigate which factors might influence the RNA integrity in the cerebellum, a multiple regression analysis was performed, including all recorded variables thought to possibly influence RNA integrity in any one analysis. The explanatory variables were age (continuous) sex (male, female), mode of death (fast, slow), postmortem delay (continuous), pH level (continuous) and disease group, with cerebellar RNA integrity as the outcome.

Bland and Altman plots (Bland and Altman, 1986, 1999) (the difference between the cerebellum RIN and the secondary brain region RIN in each case plotted against the mean RIN value for the cerebellum and the secondary region RNA pairs in each case) were constructed for each disease group to investigate the magnitude and bias of the difference in RNA integrity in the different brain regions, and whether the difference was related to the integrity level

.

Table 5. Normal control cases.

Case	Age	Sex	Cause of Death	PM, h
H116	18	F	Asphyxia	10
H155	61	M	Ischemic heart disease	7
H109	81	M	Coronary atherosclerosis	7
H112	79	M	Bleeding stomach ulcer	8
H123	78	M	Ruptured abdominal aortic aneurism	7.5
H126	36	F	Asphyxia	11

Table 6. Alzheimer's disease cases

Case	Age	Sex	Cause of Death	PM, h
AZ30	77	M	Myocardial infarction	14.5
AZ32	75	F	Bronchopneumonia	3
AZ38	80	M	Respiratory arrest/bronchopneumonia/emphysema/advanced Alzheimer's disease	5.5
AZ48	63	F	Bronchopneumonia	7
AZ53	85	F	Bilateral bronchopneumonia	2
AZ54	84	M	Bronchopneumonia	3
AZ55	51	M	Bilateral bronchopneumonia	4

Table 7. Parkinson's disease cases

Case	Age	Sex	Cause of Death	PM, h
PD6	69	F	Pneumonia	7
PD8	56	M	Asphyxiation/aspiration pneumonia	4
PD13	70	M	Bronchopneumonia/coma	12
PD15	76	M	Bronchopneumonia	11
PD16	79	M	Pneumonia	8.5
PD18	98	F	Bronchopneumonia	14

Table 8. Huntington's disease cases

Case	Age	Sex	Cause of Death	PM, h
HC84	43	F	Acute renal failure	3.5
HC91	63	F	Huntington's disease	5.5
HC92	72	M	Pneumonia	5
HC107	75	M	Bronchopneumonia	3
HC109	59	F	Bronchopneumonia	7

Table 9. Epilepsy cases

Case	Hippocampus RIN
E46	6.6
E113	7.7
E118	7.2

Table 10. Cases for the postmortem delay range study.

Case	Age	Sex	Cause of Death	PM, h
HC110	44	M	Aspiration Pneumonia	29
HC87	45	M	Bronchopneumonia	18
AZ24	82	F	Pneumonia	97
H157	66	M	Ischaemic heart disease	15
H127	59	F	Pulmonary embolism	21

2.3 Methods for Chapter 5 – Screening of Human Brain Tissue for Connexin Expression

2.3.1 Using the custom-designed microarray chip to screen for connexin expression

2.3.1.1 RNA sources

Human brain RNA obtained in Section 2.2.1 *Tissue collection and preparation* was used in the following experiments (excluding the cerebellum and the postmortem delay range study cases). See Tissue collection and preparation, p.72, and Table 5, Table 6, Table 7, Table 8, Table 9 and Table 10 for patient data.

2.3.1.2 cDNA target synthesis and fluorescent dye labelling

cDNA target synthesis and luorescent dye labelling was carried out as in 2.1.2.3.4 *cDNA target synthesis and fluorescent dye labelling*.

2.3.1.3 Microarray chip

2.3.1.3.1 Array layout

Due to the necessity of printing the slides at a different facility with different equipment, it was necessary to design a new array layout.

A 16-block array was designed with each block containing 36 (6 x 6) probe spots, producing a total of 576 spots. Each block contained oligonucleotide probes in a different pattern (Figure 8). Each of the 50 oligonucleotide probes (20 MWG-designed connexin oligos, 20 custom-designed oligos, 5 positive controls, 5 negative controls) was repeated 12 times on the array, except for custom-designed oligos for Cx30.3, Cx31.1, Cx30, Cx31.9, Cx30.2, Cx25, Cx40.1 and Cx62, which were repeated nine times.

2.3.1.3.2 Printing

The 100 pmol/µl oligonucleotide stocks were diluted to 33 pmol/µl with ultra-pure water in a separate 96-well plate, then 5 µl of the solution was transferred into a 384-well plate and desiccated. Oligos were re-suspended in 5 µl of 1x MWG Spotting buffer A catalogue #1190-100100 (final concentration 35uM).

The slides were printed on a ESI SDDC2 microarray printer using 16 ArrayIt stealth Micro spotting pins catalogue # SMP3. They were printed onto epoxy slides from Schott - Schott Nexterion slide E catalogue #1064016.

2.3.1.3.3 Hybridisation

Hybridisation was carried out according to the protocol in Section 2.1.2.3.5 *Hybridisation.*

2.3.1.3.4 Data acquisition

The data was acquired as in Section 2.1.2.2.6 *Data Acqusition.*

2.3.1.4 Data Analysis

2.3.1.4.1 Normalisation

The data was normalised as in Section 2.1.2.3.7.1 *Normalisation.*

2.3.1.4.2 Analysis

The geometric mean and standard deviation for the normalised log Cy3 and Cy5 intensities for all the spots representing each oligo was calculated, as well as the geometric mean and standard deviation for the difference between log Cy3 and Cy5 intensities.

For each array, a two-sample unequal variance t-test was performed to assess where the normalised log Cy3 and Cy5 intensity values for all spots representing each oligo were significantly brighter than the brightest negative control in each channel.

Then a pairwise t-test was used to assess whether the difference between the Cy3 and Cy5 channel intensities for each oligo was significant, based on a Bonferroni correction with n=50 and alpha=0.01.

Correlation between dye reversals was examined using Pearson correlation coefficients (Stekel, 2003).

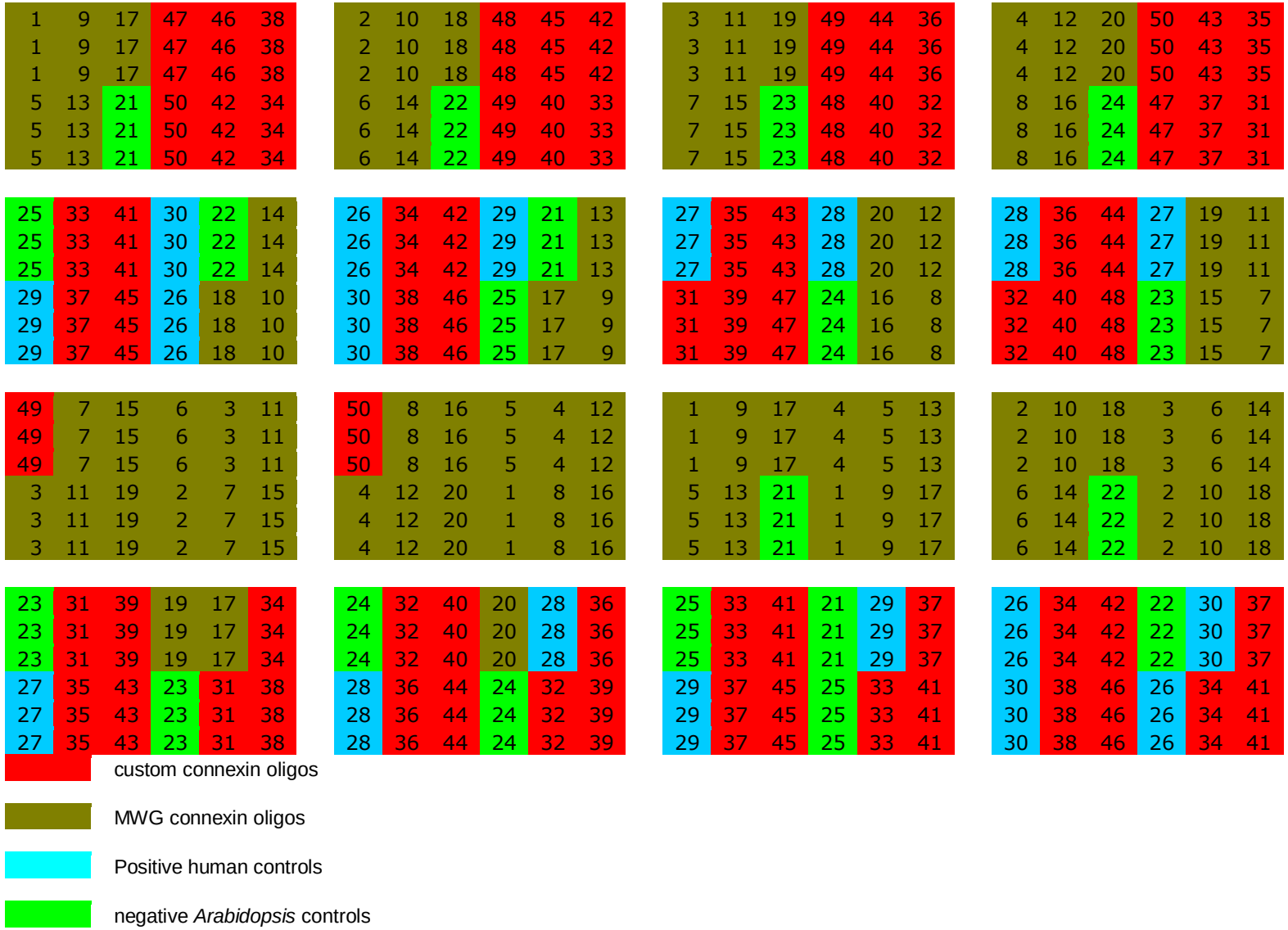

Figure 8. New custom array layout.

Table 11. MWG-designed oligos.

	Name	MWG Catalogue number
1	Connexin 46	A:04569
2	Connexin 31	A:04777
3	Connexin 50	A:05284
4	Connexin 43	A:06282
5	Connexin 36	A:06477
6	Connexin 47	A:06598
7	Connexin 30	A:06957
8	Connexin 37	A:07540
9	Connexin 31.1	A:07766
10	Connexin 45	A:08425
11	Connexin 26	A:09852
12	Connexin 40	A:10765
13	Connexin 59	B:1437
14	Connexin 62	B:1576
15	Connexin	C:0547
16	Connexin	C:0548
17	Connexin 32	C:0976
18	Connexin 31.9	C:1285
19	Connexin 40.1	C:1752
20	Connexin 25	C:7834

Table 12. Positive and negative controls.

Negative *Arabidopsis* controls		
	Name	**MWG catalogue number**
21	ara_a48#1	mwgaracontrol#001
22	ara_b184#1	mwgaracontrol#004
23	ara_b455#1	mwgaracontrol#007
24	ara_b605#1	mwgaracontrol#009
25	ara_c335#1	mwgaracontrol#012
Positive controls		
26	X01677 Human GAPDH	mwghuman10K#11002
27	V00530 Human HPRT1#1	mwghuman10K#11004
28	M26880 Human UBI131 ubiquitin	mwghuman10K#11006
29	M16342 HNRPC	mwghuman10K#01731
30	X73534 TCEA1	mwghuman10K#08383

Table 13. Custom-designed oligos.

	Name and sequence position	ID
31	GJA1 828-877	Cx43
32	GJA3 338-387	Cx46
33	GJA4 835-884	Cx37
34	GJA5 1017-1066	Cx40
35	JGC1 1020-1069	Cx45
36	GJA8 820-869	Cx50
37	GJD2 125-174	Cx36
38	GJA9 1409-1458	Cx59
39	GJC2 796-845	Cx47
40	GJB1 698-747	Cx32
41	GJB2 349-398	Cx26
42	GJB3 349-398	Cx31
43	GJB4 410-459	Cx30.3
44	GJB5 501-550	Cx31.1
45	GJB6 595-644	Cx30
46	GJD3 665-714	Cx31.9
47	GJC3 710-759	Cx30.2
48	GJB7 46-95	Cx25
49	GJD4 838-887	Cx40.1
50	GJA10 838-887	Cx62

2.3.2 Using the Illumina Sentrix® commercial platform to validate the custom-designed microarray chip data for the human brain.

To commercially validate our custom-made connexin microarray chip, 18 samples (one control and five disease samples for each of Huntington's (MC) Parkinson's (CN) and Alzheimer's (MTG)), were hybridised to commercial Illumina Sentrix® Human-6 BeadChip arrays.

2.3.2.1 Array manufacturing technology

Illumina Sentrix® BeadChips are built on a different principle to other commercial arrays. Glass microspheres ("beads") 3 μm in diameter are coated with hundreds of thousands of copies of a particular oligonucleotide synthesised using a proprietary technology. Then the beads are allowed to randomly assemble into wells etched on a silicon wafer. The oligonucleotide probe consists of two parts – a ~30-base address sequence covalently attached to the bead by an amine group, and a 50-mer probe designed for a particular gene sequence. The probe is hybridised to biotin-labelled cRNA (See Figure 9).

Each Human-6 BeadChip contains 6 two-strip arrays designed for 6 separate samples to be hybridised to the chip. Each array contains probes for 47,296 different human gene transcripts selected from primarily the RefSeq Database, but also using Gnomon and Unigene-163 databases. There are on average 30 copies of a bead containing each probe on the array.

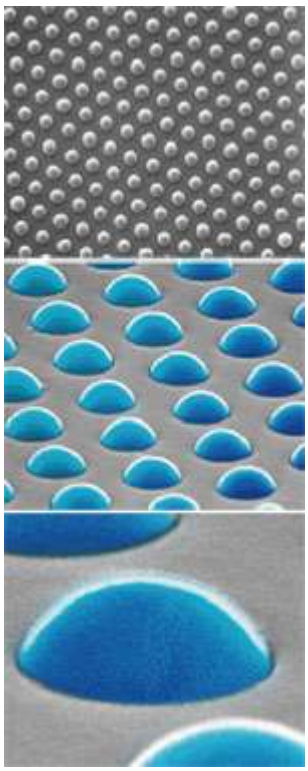

Figure 9. Picture of the Illumina Sentrix® array surface showing nucleotide-coated beads embedded in wells on the silicon wafer surface. (Picture source http://www.centerforgenomicsciences.org).

2.3.2.2 Controls

The BeadChip arrays use a number of different kinds of controls. Sample-independent (spike) controls are used to monitor the efficiency of the hybridisation, washing and staining. Negative control probes which are not complimentary to any transcripts in the hybridisation sample are used to estimate the level of background noise. Housekeeping genes are used to estimate the quality of the sample itself.

Housekeeping genes on the array include ubiquitin C, ribosomal protein S9, glyceraldehyde-3-phosphate dehydrogenase (GAPDH), beta 2-tubulin and thioredoxin.

Unlabelled poly-A controls (*lysA, pheA, thrB, trpF)* which correspond to *Bacillus* genes that have been modified by the addition of Poly(A)+ tails, and then cloned into the pBluescript phagemid cloning vector. They are added to the sample immediately preceding the reverse transcription step and amplified and labelled in the same reaction as the sample, and thus act as tracers for the success of the reaction process.

There are three types of hybridisation controls – Cy3-Labelled, Low-Stringency and High-Stringency. Cy3-Labelled hybridisation controls consist of ten probes with corresponding Cy3-labelled oligonucleotides present in the hybridisation buffer. Following successful hybridization, they produce a signal independent of both the cellular RNA quality and success of the sample prep reactions. Target oligonucleotides for the Cy3 hybridisation controls are present at three concentrations (low, medium, and high), yielding gradient hybridization responses.

The Low Stringency controls consist of 4 probes (corresponding to the medium-and high-concentration Cy3 hybridisation control targets), each of which contains two mismatched bases in its sequence. These controls yield very low signal at adequate hybridisation stringency. If their signal approaches the signal of the respective perfect match Cy3 hybridisation control probes, this indicates that the hybridisation stringency is too low.

The High Stringency control consists of two probes corresponding to a Cy3-labelled oligonucleotide target. The probe/target sequence has a very high GC content and should hybridise even if the hybridisation stringency is too high. If a signal is present from this control in the absence of signal from other hybridisation control probes, this indicated too-high hybridisation stringency.

The Signal Generation Controls (Biotin Controls) consist of two probes with complementary biotin-tagged oligonucleotides present in the Hybridisation buffer. Successful secondary staining is indicated by a positive hybridization signal from these probes.

2.3.2.3 Overview of the Illumina BeadChip Assay hybridisation and labelling procedure

The biotin-labelled cRNA is prepared using the Illumina® TotalPrep RNA Amplification Kit from Ambion, Inc. This process requires 50-100 ng total RNA. The samples are reverse transcribed using a T7-oligo(dT) primer and double-stranded cDNA is synthesized. The double-stranded cDNA, with the incorporated T7 promoter, is then used as a template in the subsequent *in vitro* transcription and amplification reaction. Biotinylated UTP nucleotides are incorporated into cRNA during the *in vitro* transcription reaction. The biotin-labelled cRNA is then hybridised to the array and stained with streptavadin-Cy3. Fluorescence emission by Cy3 is quantitatively detected by the Illumina Bead Station 500 scanner and images are processed using the BeadStudio software.

2.3.2.4 Data Analysis

For each sample on the array the Illumina BeadStudio® software produced an output file giving the average fluorescence signal and the detection threshold p-value for each oligonucleotide probe (with ~30 repeats for each probe), computed from the background model characterizing the chance that the target sequence signal was distinguishable from the negative controls. The Quality Control report for each array consisted of a summary of the performance of different categories of array controls. Averaging normalisation was performed to correct for intensity differences for the six arrays on the chip. The average signal intensity for each array was divided by the average intensity across all of the six arrays. Each probe signal intensity value was multiplied by the resulting scaling factor.

For each array containing the six samples for each disease (Huntington's (MC) Parkinson's (CN) and Alzheimer's (MTG)), one control and five disease samples, each of the connexin genes was marked as expressed or not expressed based on the *p*-value threshold of 0.05, and for the expressed connexins the difference between the log (to base 2) signal values for each of the disease samples and for the control sample was calculated. A positive difference indicated greater connexin expression in the disease sample.

3 CUSTOM CONNEXIN MICROARRAY CHIP DESIGN AND VALIDATION

3.1 Microarray Chip Design

3.1.1 MWG-designed connexin oligonucleotides

After searching the MWG 30,000 human gene array database, 20 oligonucleotides that target connexin expression were identified. However, of these, only 18 represent recognised human connexins. Two out of the 20 probes appeared to be designed to incomplete coding sequences posted on the GenBank database as unidentified "human connexins" (accession numbers AF251047_1 and AF251048_1 respectively), and do not hybridise to any known human connexin (checked by performing a BLAST search). In addition, probes for connexins Cx30.3 and Cx31.9 are missing from the MWG 30,000 human gene oligo set.

3.1.2 Custom-designed oligonucleotides

We designed probes for all 20 distinguishable human connexins. Cx23 was not discovered at the time. The cross-species design proved to be possible for 13 out of the 20 oligonucleotides, although, several of the cross-species oligos contain a significant number of mismatched bases (up to nine for connexin Cx30.3). Oligos for connexins Cx26 and Cx30, while having significantly fewer mismatches (three and four respectively), contain a mismatch close to the 3' end, which may impede hybridisation. Obtaining a closer-matched oligonucleotide probe for these connexins was not possible due to insufficient human-rat homology in the regions unique for that connexin within the connexin gene family, so the sequences with the mismatch close to the 3' end were used.

The primary reason for the difficulties in the design of cross-species oligonucleotides for all connexins was the absence of rat orthologs for the recently reported human connexins of the gamma and delta classes. The human Cx30.2 and rat Cx29 connexins have extremely poor homology.

Most of the oligonucleotides were designed towards the 3'end of the coding sequence, as there is less homology at the 3' end within the human connexin family.

Oligonucleotides for connexins Cx50, Cx40, Cx47 had to be redesigned aligned with connexin Cx46 after a BLAST search, with Cx47 also cross-hybridising with Cx40. In general, Cx46 is the least unique

of all the connexins, and for this reason it was impossible to identify out a cross-species oligo for this connexin despite a good human-rat alignment; Cx46 had only one very small unique region and there was no alignment with rat Cx46 at this place. Within the beta connexin class, the most common candidate for non specific hybridisation was GJB2, which aligned with both GJB5 and GJB6. None of the newer human connexins cross-hybridised with either alpha or beta connexin classes. All cross-hybridising nucleotides were eventually redesigned successfully (See Table 14).

Table 14. Custom-designed connexin oligonucleotides (human –rat base mismatches are highlighted in red.

Greek	Human	Rat	Base number[3]	Sequence	Acc. number, human[4]	Acc. number, rat[5]
GJA1	Cx43	Cx43	828-877	TCC**C**CTCTCGCCTATGTCTCCTCCTGGGTACAAGCTGGTTACTGG**C**GACA	NM_000165	M_012567.1
GJA3	Cx46	-	338-387	AGCAGCTGAAGAGAGAGAGCCCCAGCCCCAAGGAGCCACCGCAGGACAAT	NM_021954.2	
GJA4	Cx37	Cx37	835-884	CCCACCTACA ATGGGCTCTCATCCA**G**TGAGCA**G**AACTGGGCCAACCTGAC	NM_002060.1	NM_021654.1
GJA5	Cx40	Cx40	1017-1066	TGACAAGCG**A**CG**T**CTTAGTAAGGCCAGCAGCAA**G**GCAAGGTCAGATGACC	NM_005266.3	NM_019280.1
GJC1	Cx45	Cx45	1020-1069	GGAGATCAG**G**ATGGC**T**CAGGAACGCTTGGATCT**G**GCA**G**T**T**CAGGCCTACA	NM_005497.1	AF536559.2
GJA8	Cx50	Cx50	820-869	GTTTC**C**CACTATTTCCC**C**TTGAC**C**GAGGTTGG**G**ATGGTGGAGACCAGCCC	NM_005267.2	NM_153465.1
GJD2	Cx36	Cx36	125-174	GGGAGACGGTGTACGATGATGAGCAGACCATGTTTGTGTGCAACACCCTG	NM_020660.1	NM_019281.1
GJA9	Cx59	-	1409-1458	CTGCTGATTCTTTGGGAGGGCTGTCCTTTGAGCCAGGGTTGGTCAGAACC	NM_030772.1	
GJC2	Cx47	Cx47	796-845	CTGGTTATGTA**C**GTGGT**C**AGCTGCCT**G**TGCCTG**C**TGCTCAACCTCTGTGA	AY285161.1	AY233216.1
GJB1	Cx32	Cx32	698-747	CGGGCTTCGGCCACCGCCTCTCACCTGAATACAAGCAGAATGAGATCAAC	BC039198.1	NM_017251.1
GJB2	Cx26	Cx26	349-398	GACATCGA**G**GAGATCAAAACCCAGAAGGTCCG**C**ATCGAAGG**C**TCCCTGTG	NM_004004.1	X51615.1
GJB3	Cx31	Cx31	349-398	TAC**G**A**C**AAC**G**C**A**GGCAAGAAGCACGG**A**GGCCTGTGGTGGACCTACCTGTT	NM_024009.1	NM_019240.1
GJB4	Cx30.3	Cx30.3	410-459	TCAAGGC**C**GC**C**GTGGA**T**G**C**TGG**C**TTCCTCTATATCTTCCAC**C**GC**C**T**C**TAC	NM_153212.1	NM_053984.1
GJB5	Cx31.1	Cx31.1	501-550	**T**CCATGTCCCAA**T**A**T**AGTGGACTGCTTCAT**C**TCCAAGCCCTCAGAGAAGA	NM_005268.1	NM_019241.1
GJB6	Cx30	Cx30	595-644	TCTGTGATTTGCATGCTGCT**T**AA**C**GTGGC**A**GAGTTGTG**C**TACCTGCTGCT	BC038934.1	NM_053388.1
GJD3	Cx31.9	-	665-714	AGCGTGACAACCGCTGCAACCGTGCACACGAAGAGGCGCAGAAGCTGCTC	NM_152219.1	
GJC3	Cx30.2	-	710-759	GCACCAGAAGACACAAGAAAGCAACCGATAGCCTCCCAGTGGTGGAAACC	AF503615.1	
GJB7	Cx25	-	46-95	TACTCCACTGGGACTGGATGGATTTGGCTGGCTGTCGTGTTTGTCTTCCG	AJ414563.1	
GJD4	Cx40.1	-	838-887	CGTACATCCAGGGTGTCAGGGCACACGAAGATTCCGGATGAGGATGAGAG	AJ414564.1	
GJA10	Cx62	Cx57	1367-1416	CCTGCTTGGATTTTCC**T**CA**C**TGGGAAAACAGCCC**C**TCACCTCTGCCTTCA	AJ414565.1	XM_232859.2

[3] Position on the human coding sequence

[4] GenBank Accession number for the human coding sequence

[5] Gen Bank Accession number for the rat coding sequence

3.2 Preliminary Validation in Rat and Human Tissue

3.2.1 Microarray slides

Data from nine microarray slides were acquired and analysed. Of the nine slides, six represented three pairs of 'dye reversals', where two RNA samples (rat liver *vs* rat brain, human brain *vs* rat brain (choroid plexus) and rat heart *vs* rat lens) were labelled with Cy3 and Cy5 respectively for hybridisation to the first slide, and with Cy5 and Cy3 respectively (labelling reversal) for hybridisation to the second slide. This dye reversal was performed to eliminate dye bias and to ensure consistency of results. The fourth pair of slides consisted of two rat heart samples hybridised onto one slide, and the ninth slide being a rat heart sample hybridised against itself. The latter was done to check for internal array consistency. Rat heart (Cy3) and rat brain (Cy5) samples were hybridised to the ninth slide.

There was no substantial variation between the signal intensity in the sixteen 50-oligonucleotide blocks on all nine arrays. This can be judged by the small standard deviation for both red and green channel intensities for each of the 16-spot sets representing an oligonucleotide probe. The background was also uniform across the slide for each array; no background correction was required for analysis.

Negative controls showed signal intensity at the level higher than the background level on all arrays. The signal intensity of the negative controls was clustered at the low end of the intensity scale. The amount of non-specific signal at these spots was taken into account by using a t-test for evaluating whether the intensity of each probe was significantly greater than that of the brightest negative control. All of the nine arrays also demonstrated a greater fluorescence signal for the Cy3-labelled target than for the Cy5-labelled target. This colour imbalance required normalisation based on the intensity values of positive and negative controls in each channel.

The high amount of non-specific signal at the negative controls was also paralleled by the appearance of oversaturated spots on the array, representing oligos with mean log signal intensity values of approximately twice that of the negative controls; the number of such spots was however small. The oligos that demonstrated such oversaturation were largely consistent within each array and across the nine arrays: the MWG-designed connexin Cx50 probe and the custom-designed Cx46 probe showed intensity values at the top of the scale and were significantly brighter than the brightest positive control in both channels on all nine arrays. The custom-designed Cx25 oligo was below the brightest positive control on only one of the arrays (human brain *vs* rat brain). Neither of the custom-designed oligos in question (Cx46 and Cx25) hybridises to the orthologous rat connexin (a rat Cx25 has not been reported), thus the binding to these probes must be assumed to be non-specific. The sequence of the MWG-designed Cx50 probe is not known, but it has also been designed to align with the human and not the rat connexin sequence. The human brain *vs* rat brain array dye reversal pair (the only arrays

using human tissue), demonstrated that the excessive binding to all three of these oligonucleotides (Cx25, Cx50, Cx46) is biased towards the rat tissue.

The five positive controls showed a very consistent intensity distribution pattern across all the arrays, with ubiquitin always having the highest signal magnitude, followed by GAPDH, with HPRT showing the lowest intensity, and was not significantly expressed on any of the arrays. TCEA1 and HNRPC alternatively take the third and fourth places. The three arrays (rat liver/rat brain, human brain/rat brain, and rat brain/rat heart) that showed differential expression for any of the positive controls also showed differential expression for at least one negative control.

3.2.1.1 Rat heart 2 (Cy3) vs rat heart 2 (Cy5) array

The primary purpose of Rat heart 2 (Cy3) *vs* rat heart 2 (Cy5) and Rat heart 2 (Cy3) *vs* rat heart 3 (Cy5) arrays was to test the consistency of target binding and evaluate the extent of influence on the microarray data of using samples from one animal *versus* two different animals (i.e. of individual animal variation).

This array has the highest concordance between the red and green channels (standard deviation of red/green mean signal intensity ratios for all 50 oligos is 0.21). The correlation between the two samples was 0.958. All of the positive controls except HPRT showed significant signal on this array. The amount of internal variation, as measured by the mean standard deviation of intensities for all the 16-spot sets representing an oligo in the red and green channels was 0.439, the second lowest of all slides.

The number of the oligos showing differential expression for the slide was five (three custom- and two MWG-designed) all showing higher expression in the red channel, and the total number of expressed connexins is 34 (20 custom- and 14 MWG-designed), with 26 higher in the red channel and eight in the green channel (See Table 15, Figure 11). Of the custom-designed probes, Cx46, Cx59, Cx25, Cx30.2 and Cx31.9 are not rat-specific.

3.2.1.2 Rat heart 2 (Cy3) vs rat heart 3 (Cy5)

This slide showed the second highest concordance between the red and green channel intensities, with the standard deviation of red/green mean signal intensity ratios for all 50 oligos of only 0.22. The correlation between the two heart samples was also high (Pearson correlation coefficient 0.987 for normalised log intensities). All of the positive controls except HPRT showed significant signal on this array. The amount of internal variation, as measured by the mean standard deviations of intensities for

all the 16-spot sets representing an oligo in the red and green channels, was the median among the slides, at 0.631.

The number of differentially expressed genes for this slide was low, with only two oligos showing differential expression (custom-designed Cx40 and Cx30, both of these probes gave a higher intensity value in the red channel (heart 3) after normalisation).The total number of expressed connexins was 30, with 21 higher in the red channel and nine in the green channel (See Table 15, Figure 10). Of the custom-designed probes, Cx46, Cx58, Cx25, Cx30.2 and Cx31.9 are not rat-specific.

In conclusion, there were 30 oligos showing significant expression in both arrays, 21 custom- and nine MWG-designed. Of the custom-designed probes, Cx46, Cx58, Cx25, Cx30.2 and Cx31.9 are not rat-specific. Two connexins were differentially expressed in both arrays (custom-designed Cx31.1 and Cx30), both higher in the red channel.

Table 15. Connexins expressed in the rat heart slides.

Heart 2vs Heart 3				Heart 2vs Heart 2				Combined	
Expressed Connexins				Expressed Connexins				Expressed Connexins	
Higher in Heart 2		Higher in Heart 3		Higher in Red		Higher in Green		Custom	MWG
Custom	MWG	Custom	MWG	Custom	MWG	Custom	MWG		
Cx31 Cx31.9 Cx25 Cx30.2	Cx37 Cx40 Cx31	Cx43 Cx46 Cx40 Cx45 Cx36 Cx58 Cx47 Cx32 Cx26 Cx30.3 Cx31.1 Cx30 Cx62	Cx43 Cx50 CX47 Cx32 Cx31.1 Cx25	Cx43 Cx46 Cx40 Cx45 Cx36 Cx58 Cx47 Cx32 Cx26 Cx30.3 Cx31.1 Cx30 Cx40.1 Cx62 TCEA1	Cx43 Cx46 Cx45 Cx50 Cx58 Cx47 Cx32 Cx31.1 Cx25 Cx40.1 Cx62	Cx37 Cx31 Cx31.9 Cx25 Cx30.2	Cx37 Cx40 Cx31	Cx43 Cx46 Cx36 Cx58 Cx47 Cx32 Cx26 Cx31 Cx30.3 Cx31.1 Cx30 Cx31.9 Cx25 Cx62 Cx30.2 GAPGD	Cx43 Cx37 Cx40 Cx50 Cx47 Cx32 Cx31 Cx31.1 Cx25
Subtotal: 4	3	13	6	15	11	5	3	16	9
Controls				Controls				Controls	
GAPDH HNRPC		TCEA1 Ubiquitin		TCEA1 Ubiquitin		GAPDH HNRPC		HNRPC TCEA1 Ubiquitin	
Differentially Expressed Connexins				Differentially Expressed Connexins				Differentially Expressed Connexins	
Higher in Heart 2		Higher in Heart 3		Higher in Red		Higher in Green		Custom	MWG
Custom	MWG	Custom	MWG	Custom	MWG	Custom	MWG		
		Cx31.1 Cx30		Cx31.1 Cx30 Cx40.1	Cx45 Cx40.1			Cx31.1 Cx30	
Subtotal: 0	0	2		3	2	0	0	2	0
Controls				Controls				Controls	

3.2.1.3 Rat heart (Cy3) vs rat lens (Cy5) array

This array had the largest scatter of red/green ratios from the mean (SD for the R/G normalised means is 2.29, which is higher than the others by an order of magnitude). The mean SD for the red and green signal level for each 16-spots per oligo was also the highest (SD=1.323), having the most significant within-slide variability of the nine arrays. This slide also had the lowest expression signal intensities overall for both green and red channels. Of the five positive controls, only ubiquitin gave a signal above the significance threshold – this is the lowest number of positive controls expressed of all (See Table 16, Figure 12).

A total of four connexins were differentially expressed on this array; one at a higher level in the heart (MWG-designed Cx47) and three (custom-designed Cx36, Cx58, and the MWG-designed Cx43) in the lens. The custom-designed Cx31 and Cx58 showed very high red (lens) *vs* green (heart) ratios (7.941 for Cx58 and 15.689 for Cx31), which were significantly larger than any red/green ratios on any of the other arrays. The number of significantly expressed connexins was second lowest for this slide after the rat lens *vs* rat heat dye reversal (the total of 12, seven custom- and five MWG-designed). Custom-designed Cx46 and Cx25 probes are not rat-specific.

3.2.1.4 Rat lens (Cy3) vs rat heart (Cy5) array

This array had an intermediate scatter of red/green ratios from the mean (SD for the R/G normalised means is 0.547). The mean SD for the red and green signal level for each of the 16-spots per oligo was also intermediate (SD=0.596). This slide also had the third lowest overall expression signal intensities for both green and red channels. This slide expressed two positive controls (ubiquitin and GAPDH) which was the second lowest number of controls after the rat heart *vs* rat lens array (See Table 16, Figure 13).

The number of connexins showing differential expression on this array was four (one custom- and two MWG-designed oligos showed higher expression in the lens and one MWG-designed connexin in the heart). The total number of expressed connexins for this slide was eight, which was the lowest of all slides, four custom- and four MWG-designed.

This array pair gave the lowest number of significantly expressed connexins of all the arrays, with the first slide expressing only one, and the second - two positive controls. Three connexins were expressed in both of the slides (custom-designed Cx46 and MWG-designed Cx37 and Cx50), however, custom-designed Cx46 and MWG-designed Cx50 showed very high levels of non-specific binding on

all arrays. None of the connexins were differentially expressed on both the original slide and the dye reversal.

Table 16.Connexins expressed in the rat heart and rat lens slide pair.

Rat Heart *vs* Lens				**Lens *vs* Rat Heart**				**Combined**	
Expressed Connexins				**Expressed Connexins**				**Expressed Connexins**	
Higher in Rat Heart		**Higher in Rat Lens**		**Higher in Rat Heart**		**Higher in Rat Lens**		Custom	MWG
Custom	MWG	Custom	MWG	Custom	MWG	Custom	MWG		
Cx46 Cx62	Cx40 Cx47 Cx31	Cx36 Cx58 Cx47 Cx31 Cx25	Cx37 Cx50	Cx46	Cx50	Cx30.3 GAPDH Ubiquitin	Cx43 Cx37 Cx31.1	Cx46	Cx37 Cx50
Subtotal: 2	3	5	2	1	1	3	3	1	2
Controls				**Controls**				**Controls**	
		Ubiquitin				GAPDH Ubiquitin			
Differentially Expressed Connexins				**Differentially Expressed Connexins**				**Differentially Expressed Connexins**	
Higher in Rat Heart		**Higher in Rat Lens**		**Higher in Rat Heart**		**Higher in Rat Lens**		Custom	MWG
Custom	MWG	Custom	MWG	Custom	MWG	Custom	MWG		
	Cx47	Cx36 Cx58 Cx31			Cx50	Cx30.3	Cx37 Cx31.1		
Subtotal:	1	3	0	0	1	1	2	0	0

3.2.1.5 Rat brain (Cy3) vs rat heart (Cy5) array

There was no dye reversal pair for this slide. The slide had both the third lowest intra-slide variation (red and green intensity SD mean of 0.54), and the third lowest red/green ratio variation (after the rat heart *vs* rat heart array, R/G standard deviation of 0.274). As this slide was washed under the least stringent conditions, it had the highest value for the brightest negative control. All of the positive controls had significant binding intensities except for HPRT. Ubiquitin had a considerably higher signal level in the brain sample than in the heart sample, resulting in a number of oligos giving a higher signal than the brightest negative control in the heart but not in the brain (the MWG-designed Cx31, Cx40, Cx31.1, Cx37, and custom-designed Cx30.2) (See Table 17, Figure 14).

There were 11 probes showing differential binding in this array, ten at a higher level in the brain and one (Cx62 (Cx57)) in the liver. The number of significantly expressed connexins was 28 (12 MWG- and 16 custom-designed) (See Table 17, Figure 14). Of the custom-designed oligos, Cx46, Cx58, Cx25 and Cx30.2 do not hybridise to rat connexin targets.

Table 17. Connexins expressed in the rat heart and rat brain slide.

Brain *vs* Heart			
Expressed Connexins			
Higher in Brain		**Higher in Heart**	
Custom	MWG	Custom	MWG
Cx43 Cx46 Cx37 Cx40 Cx45 Cx36 Cx58 Cx47 Cx26 Cx31 Cx30.3 Cx31.1 Cx30 Cx25 Cx62	Cx43 Cx46 Cx37 Cx50 Cx47 Cx25 Cx62	Cx32	Cx40 Cx32 Cx31 Cx31.1 Cx62
Subtotal: 15	7	1	5
Controls			
GAPDH Ubiquitin		HNRPC TCEA1	
Differentially Expressed Connexins			
Higher in Brain		**Higher in Heart**	
Custom	MWG	Custom	MWG
Cx37 Cx40 Cx45 Cx36 Cx58 Cx47 Cx31 Cx30	Cx43 Cx25		Cx62
Subtotal: 8	2	0	1
Controls			
Ubiquitin			

3.2.1.6 Rat liver (Cy3) vs rat brain (Cy5) array

This array had the lowest internal variation, with the mean SD for the 16 spots per oligo of 0.415. The standard deviation for normalised ratios for this array was intermediate among the nine, at SD=0.306. All the positive controls except HPRT were expressed on this array, with TCEA1 differentially expressed in the brain (See Table 18, Figure 15).

This array gave significant expression levels for the greatest number of connexins (35, with the only oligos not showing a significant signal being unknown MWG-designed connexins, the MWG-designed Cx30 and custom-designed Cx50) and the highest number of differentially expressed connexins (12 (seven custom- and five MWG-designed) showing a higher expression level in the liver and four (three custom- and one MWG-designed) showing a higher level of expression in the heart). Of the custom-designed oligonucleotides, Cx30.2, Cx46, Cx25 and Cx59 are not rat-specific.

3.2.1.7 Rat brain (Cy3) vs rat liver (Cy5) array

This array had the fourth highest internal variation, with the mean SD for the 16 spots per each oligo of 0.724. The standard deviation for normalised ratios for this array was next highest after the liver *vs* brain array among the nine, at SD=0.403. All the positive controls except HPRT were expressed on this array, with HNRPC showing a higher level of expression in the liver and TCEA1 in the heart (see Table 18, Figure 16).

There were 35 expressed connexins on this array, with the expression pattern being similar to the previous array. There are seven differentially expressed connexins, with six connexins (four custom- and two MWG-designed) showing a higher expression level in the liver, and one (custom-designed Cx40) in the brain.

This slide pair shows a higher expression level in the liver compared to the brain in both the red and the green channels. Five custom- and one MWG-designed connexins were differentially expressed in both slides.

Table 18. Connexins expressed in the rat liver and rat brain slide pair.

Liver *vs* Brain				**Brain *vs* Liver**				**Combined**	
Expressed Connexins				**Expressed Connexins**				**Expressed Connexins**	
Higher in Liver		**Higher in Brain**		**Higher in Liver**		**Higher in Brain**		Custom	MWG
Custom	MWG	Custom	MWG	Custom	MWG	Custom	MWG		
Cx43 Cx46 Cx45 Cx36 Cx58 Cx47 Cx32 Cx31 Cx30.3 Cx31.1 Cx30 Cx31.9 Cx25 Cx40.1	Cx43 Cx46 Cx37 Cx45 Cx36 Cx58 Cx47 Cx32 Cx26 Cx31 Cx31. 1 Cx30. 2	Cx37 Cx40 Cx26 Cx62 Cx30.2	Cx40 Cx50 Cx25 Cx40.1	Cx43 Cx46 Cx45 Cx36 Cx58 Cx47 Cx32 Cx31 Cx30.3 Cx31.1 Cx30 Cx31.9 Cx25 Cx40.1	Cx43 Cx46 Cx37 Cx45 Cx58 Cx47 Cx32 Cx26 Cx31 Cx31.1 Cx30.2 Cx62	Cx37 Cx40 Cx26 Cx62 Cx30.2	Cx40 Cx50 Cx25 Cx40.1	Cx43 Cx46 Cx37 Cx40 Cx45 Cx36 Cx58 Cx47 Cx32 Cx26 Cx31 Cx30.3 Cx31.1 Cx30 Cx31.9 Cx25 Cx40.1 Cx62 Cx30.2	Cx43 Cx46 Cx37 Cx40 Cx45 Cx50 Cx58 Cx47 Cx32 Cx26 Cx31 Cx31.1 Cx25 Cx30.2 Cx40.1 Cx62
Subtotal: 14	12	5	4	14	12	5	4	19	16
Controls				**Controls**				**Controls**	
GAPDH HNRPC		Ubiquitin TCEA1		GAPDH		Ubiquitin		GAPGD HNRPC Ubiquitin	
Differentially Expressed Connexins				**Differentially Expressed Connexins**				**Differentially Expressed Connexins**	
Higher in Liver		**Higher in Brain**		**Higher in Liver**		**Higher in Brain**		Custom	MWG
Custom	MWG	Custom	MWG	Custom	MWG	Custom	MWG		
Cx45 Cx58 Cx47 Cx31 Cx30 Cx25 Cx30.2	Cx37 Cx36 Cx58 Cx47 Cx31	Cx46 Cx40 Cx31.1	Cx50	Cx45 Cx47 Cx31.1 Cx30	Cx58 Cx62	Cx40		Cx40 Cx45 Cx47 Cx31.1 Cx30	Cx58
Subtotal: 7	5	3	1	4	2	1	0	5	1
Controls				**Controls**				**Controls**	
		TCEA1		HNRPC		TCEA1		TCEA1	

3.2.1.8 Human brain (Cy3) vs rat brain (Cy5) array

This array had the third-highest intra-slide variability after the heart *vs* lens slide (red and green intensity mean SD=1.05) and the fourth highest point scatter (R/G ratio variability, SD=0.464). All of the positive controls except for HPRT showed significant expression in both channels, with GAPDH differentially expressed in human brain (See Table 19, Figure 17).

This array had 14 probes with differential binding (ten custom- and four MWG-designed), all of them with a higher intensity value in the human brain. There were 25 oligos showing significant but non-differential binding levels (20 custom- and five MWG-designed). Of the above probes, the custom designed Cx30.2, Cx58, Cx46, Cx25 hybridise to human connexins only.

3.2.1.9 Rat brain (Cy3) vs human brain (Cy5) array

This array had the second-highest intra-slide variability after the heart *vs* lens slide (red and green intensity mean SD=1.12) and the second-highest point scatter, also after the heart *vs* lens slide (R/G ratio variability, SD=0.674). Of the positive controls, only GAPDH and ubiquitin were expressed on this array (See Table 19, Figure 18).

This array had ten probes with differential binding (seven custom- and three MWG-designed), all of them with a higher intensity value in the human brain. There were 22 other oligos showing non-differential binding levels (16 custom- and six MWG-designed). Of the above probes, the custom designed Cx30.2, Cx58, Cx46, Cx25 hybridise to human connexins only.

There were five connexins differentially expressed in both of these slides, four custom-designed (Cx43, Cx46, Cx37, Cx62) and one MWG-designed (Cx31) and 15 connexins that were expressed above the significance cut-off threshold in both slides (ten custom- and five MWG-designed). This slide pair showed a significant bias for human brain tissue in terms of connexin expression levels which was independent of dye labelling.

Table 19. Connexins expressed in the human brain and rat brain slide pair.

Human brain *vs* Rat brain				**Rat brain *vs* Human brain**				**Combined**	
Expressed Connexins				**Expressed Connexins**				**Expressed Connexins**	
Higher in Human Brain		**Higher in Rat Br**		**Higher in Human Brain**		**Higher in Rat Brain**		**Custom**	**MWG**
Custom	MWG	Custom	MWG	Custom	MWG	Custom	MWG		
Cx43 Cx46 Cx37 Cx45 Cx36 Cx58 Cx47 Cx30.3 Cx31.1 Cx30 Cx25 Cx62 Cx30.2	Cx43 Cx37 Cx50 Cx47 Cx31 Cx31. 1	Cx40 Cx31		Cx43 Cx46 Cx37 Cx58 Cx47 Cx32 Cx30.3 Cx31.1 Cx62 Cx30.2	Cx43 Cx37 Cx40 Cx31 Cx31.1	Cx25	Cx50	Cx43 Cx46 Cx37 Cx58 Cx47 Cx30.3 Cx31.1 Cx25 Cx62 Cx30.2	Cx43 Cx37 Cx50 Cx31 Cx31.1
Subtotal: 14	6	5		10	5	1	1	10	5
Controls				**Controls**				**Controls**	
		HNRPC TCEA1 Ubiquitin		GAPGH Ubiquitin				GAPGH Ubiquitin	
Differentially Expressed Connexins				**Differentially Expressed Connexins**				**Differentially Expressed Connexins**	
Higher in Human Brain		**Higher in Rat Brain**		**Higher in Human Brain**		**Higher in Rat Brain**		Custom	MWG
Custom	MWG	Custom	MWG	Custom	MWG	Custom	MWG		
Cx43 Cx46 Cx37 Cx36 Cx58 Cx47 Cx30 Cx62 Cx30.2	Cx43 Cx37 Cx47 Cx31			Cx43 Cx46 Cx37 Cx32 Cx30.3 Cx31.1 Cx62	Cx40 Cx31 Cx31.1			Cx43 Cx46 Cx37 Cx62	Cx31
Subtotal: 10	4			7	3	0	0	4	1
Controls				**Controls**				**Controls**	
GAPDH									

3.2.2 Summary

The rat heart *vs* rat heart (control) slides showed the highest concordance between the red and green channel intensities and the highest correlation between the signal intensities for the two samples (Pearson correlation coefficient 0.987 for the heart 2 *vs* heart 3 slide and 0.957 for the heart sample against itself). Use of the same heart RNA sample, as opposed to two separate heart samples, did not result in a lower amount of variation, suggesting that this is due to experimental error and not to biological differences.

When the same RNA sample was used on a number of arrays (a rat brain sample was used both on a brain *vs* liver array and in combination with human brain, and the same heart sample was used on the two heart *vs* heart arrays), the correlation coefficient was calculated for the signal intensities for that sample across the two arrays, giving very high correlation coefficients (See Table 20), confirming the consistency of results across arrays.

The calculations of differential connexin expression between the two samples on a slide and of statistical significance of the signal intensity at each connexin probe were dependent on the slide quality, as determined by internal variation across a slide. This led to differences in estimation of differential expression and statistical significance within the dye reversal slide pairs.

Table 20. Pearson correlation coefficients for normalised log mean intensities of RNA samples on different arrays.

1. Dye reversals					
Rat liver vs rat brain		*Rat brain vs human brain*		*Rat hear vs rat lens*	
liver	brain	rat brain	human brain	heart	lens
0.906	0.899	0.901	0.903	0.803	0.717
2. Control heart *vs* heart slides					
Heart sample 2 against itself		*Heart sample 2 vs sample 3*			
0.957		0.987			
3. Comparison across non-paired slides					
Heart sample across two slides		*Brain sample across two slides*			
0.931		0.958			

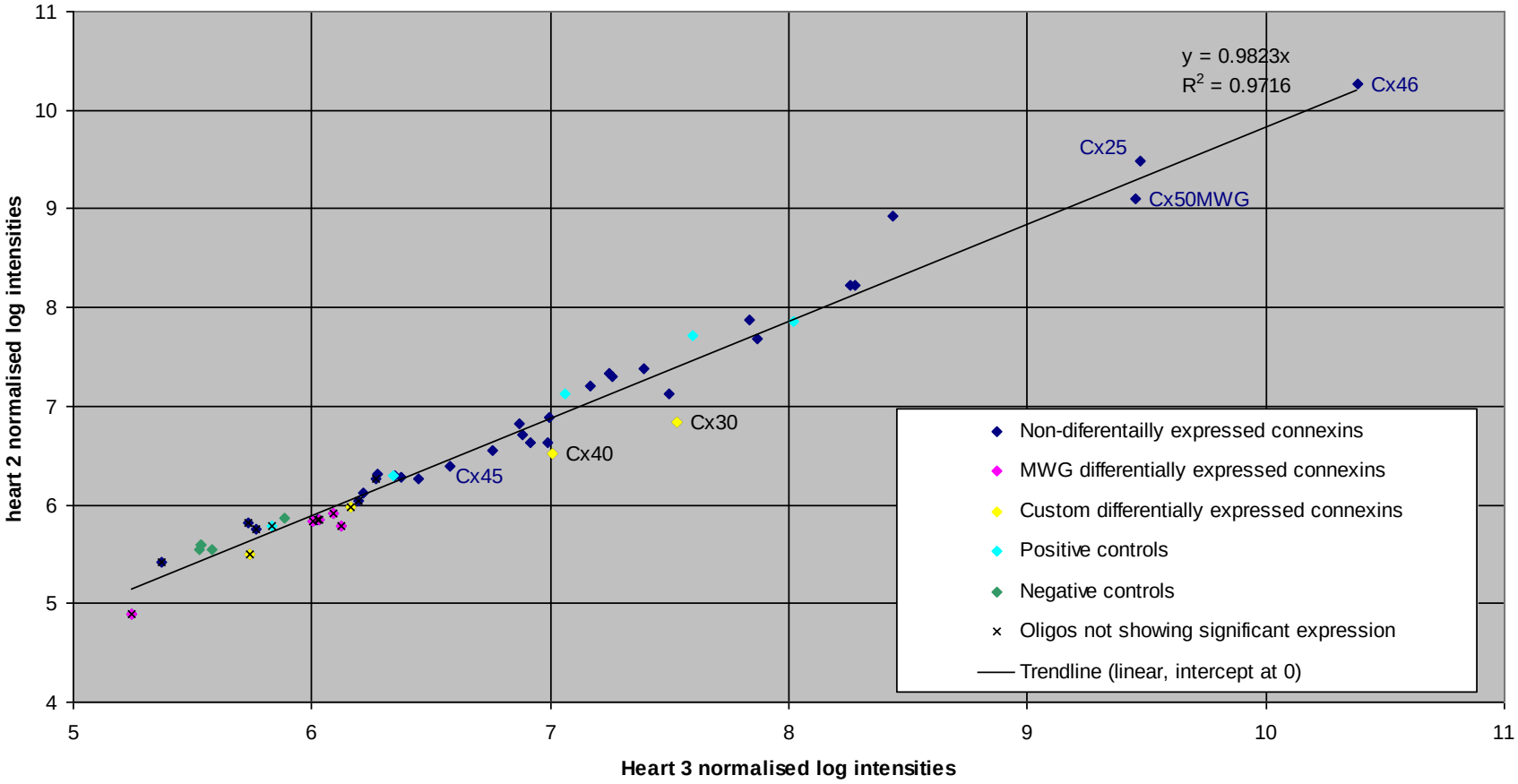

Figure 10. The rat heart2 *vs* rat heart3 normalised log intensity data shows the relative distribution of signal intensities in the red (x axis) and green (y-axis) channel representing two different heart samples.

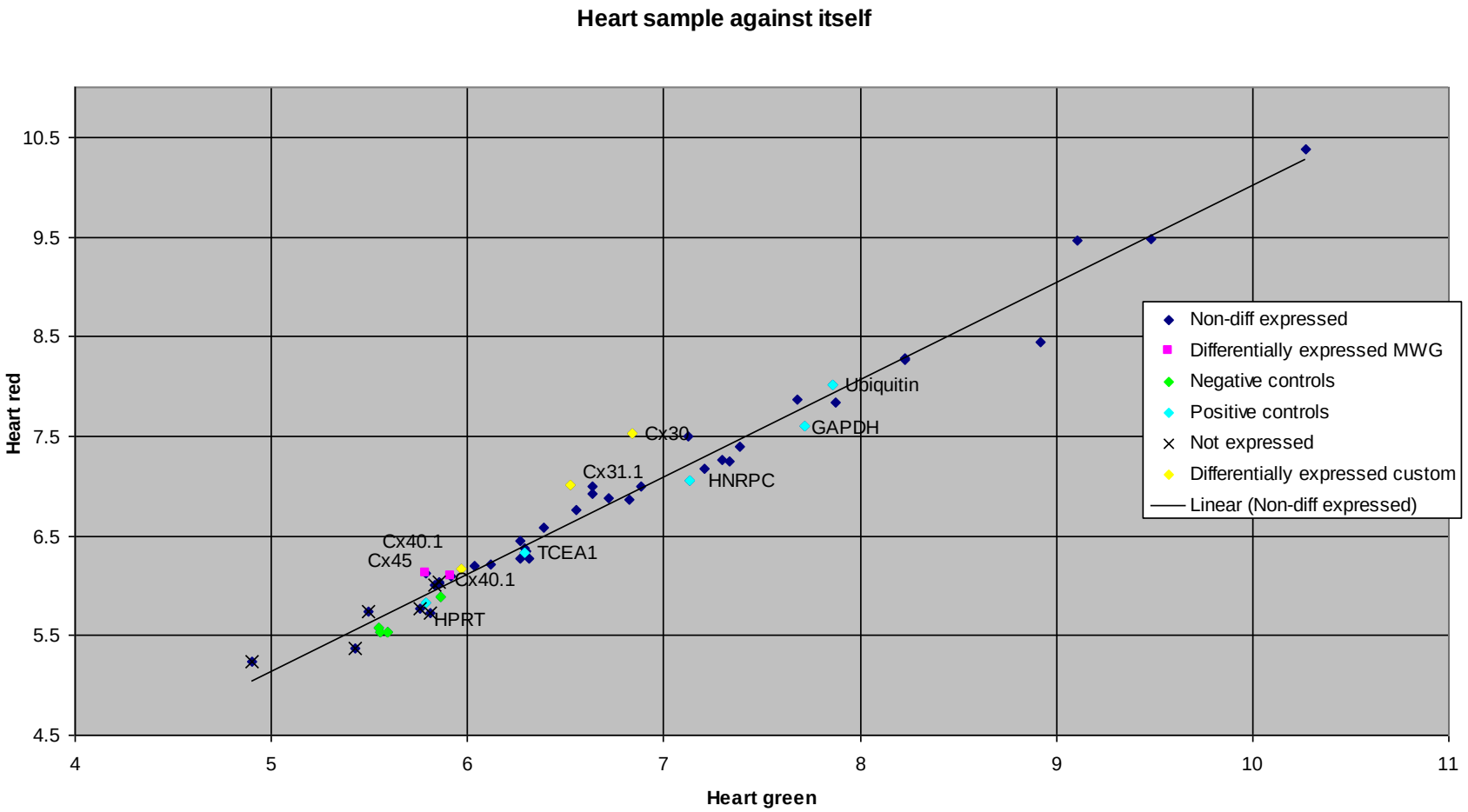

Figure 11. The rat heart 2 *vs* rat heart 2 normalised log intensity data shows the relative distribution of signal intensities in the red (x axis) and green (y-axis) channel representing the same sample labelled with Cy3 and Cy5.

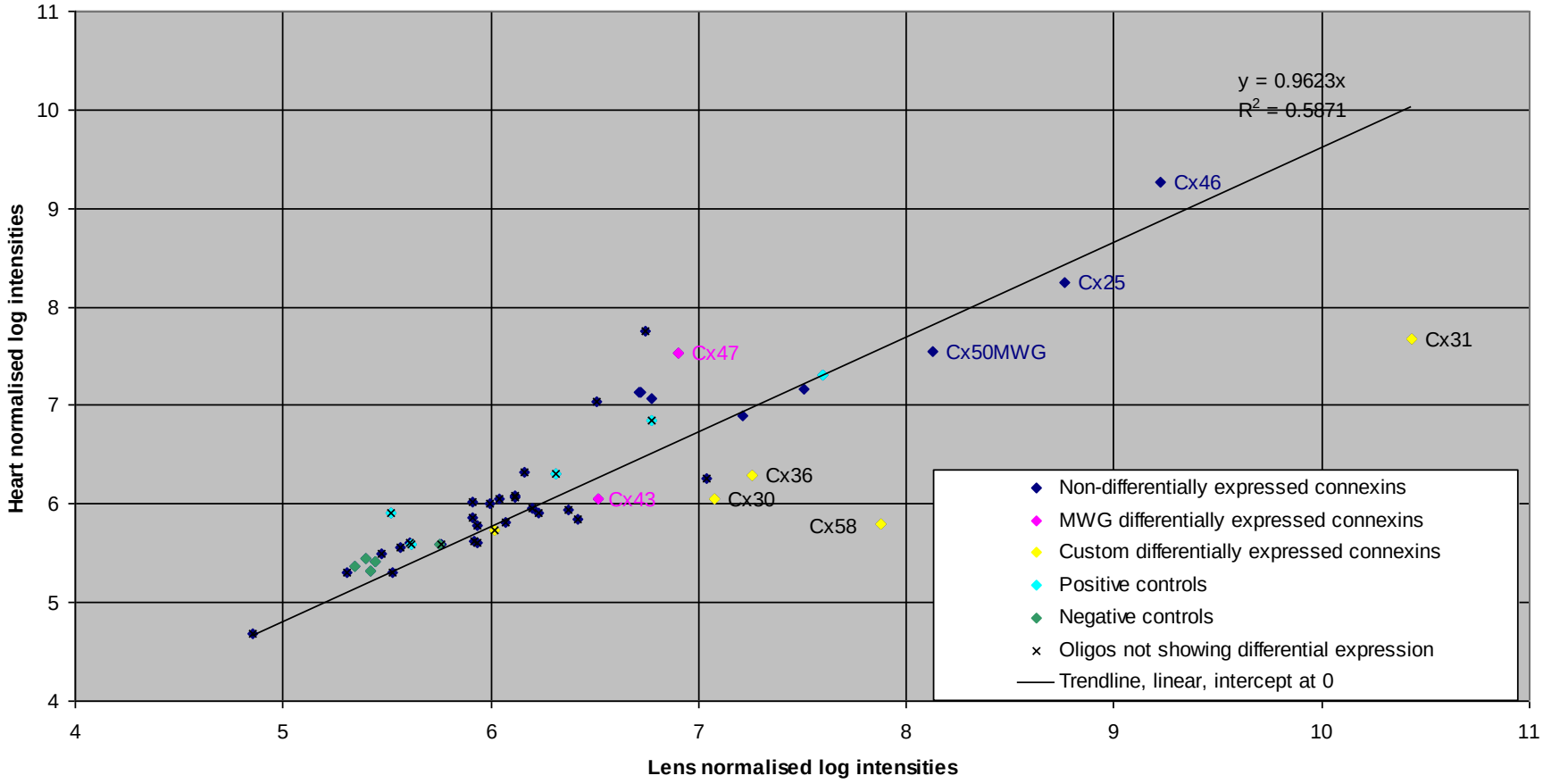

Figure 12. The rat lens *vs* rat heart normalised log intensity data shows the relative distribution of signal intensities in the red (x axis) and green (y-axis) channel representing two different tissue samples.

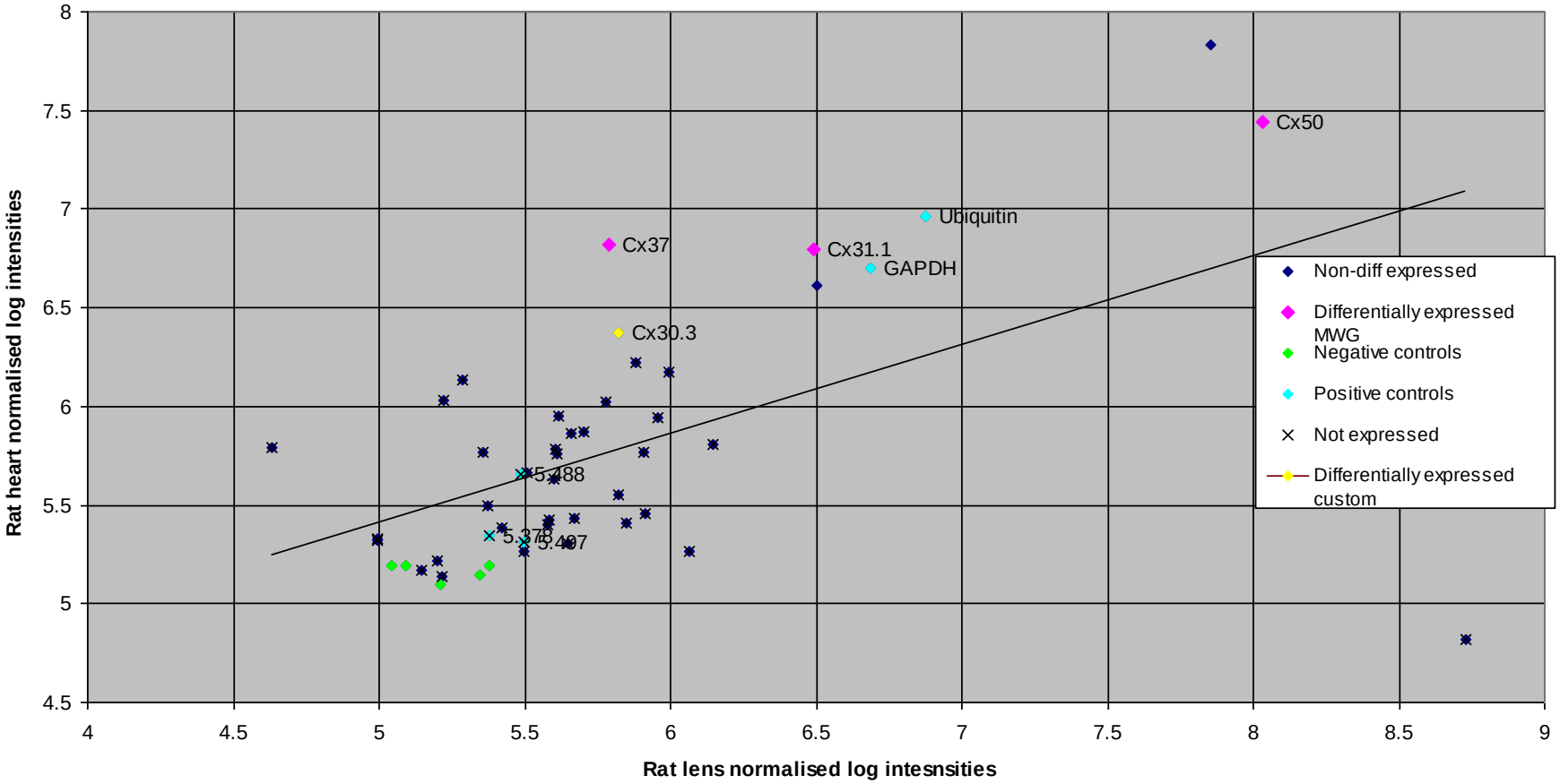

Figure 13. Rat lens *vs* rat heart (dye reversal) normalised log intensity data shows the relative distribution of signal intensities in the red (x axis) and green (y-axis) channel representing two different tissue samples.

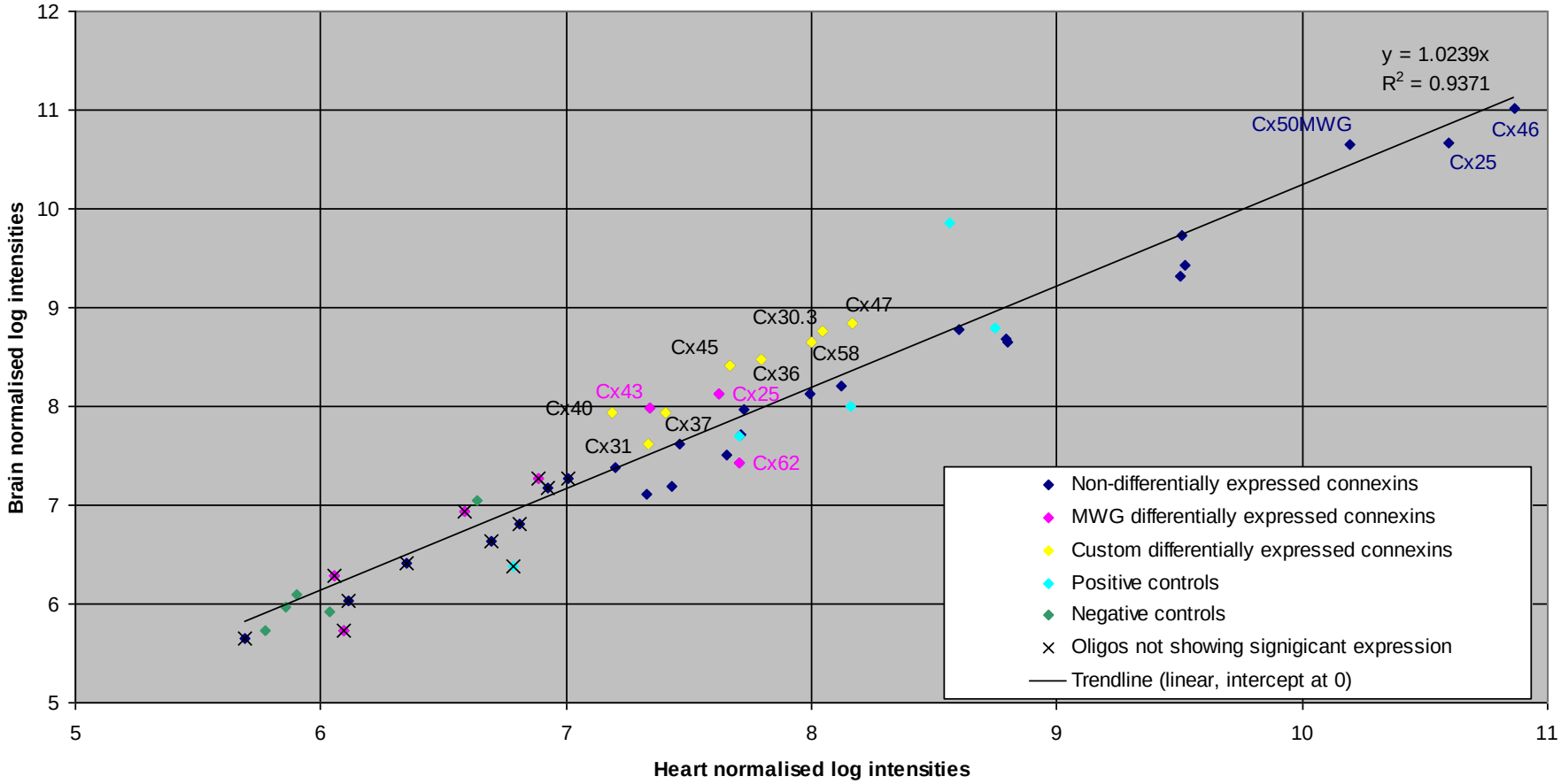

Figure 14. The rat heart *vs* rat brain normalised log intensity data shows the relative distribution of signal intensities in the red (x axis) and green (y-axis) channel representing two different tissue samples.

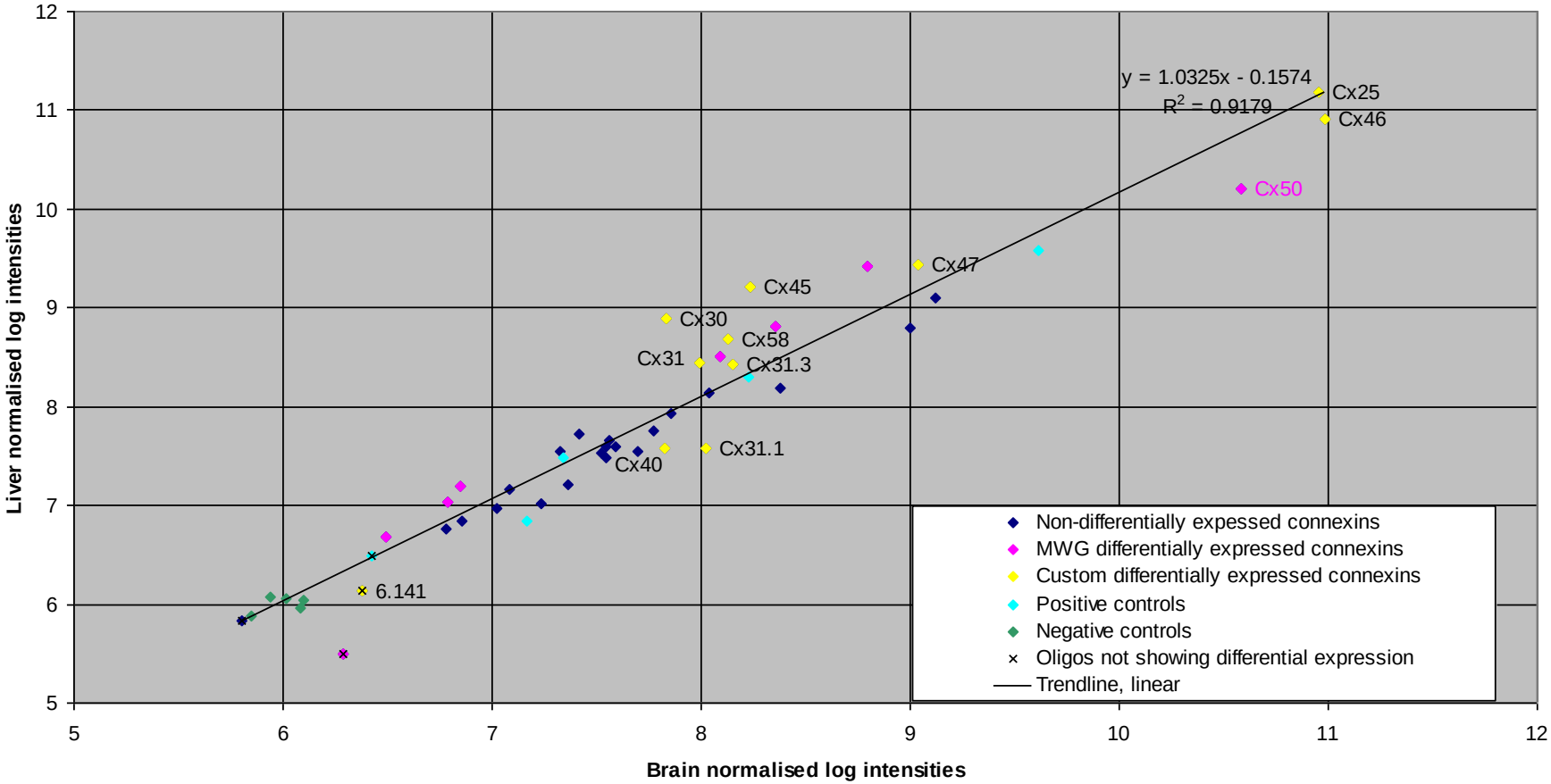

Figure 15. The rat brain *vs* rat liver normalised log intensity data shows the relative distribution of signal intensities in the red (x axis) and green (y-axis) channel representing two different tissue samples.

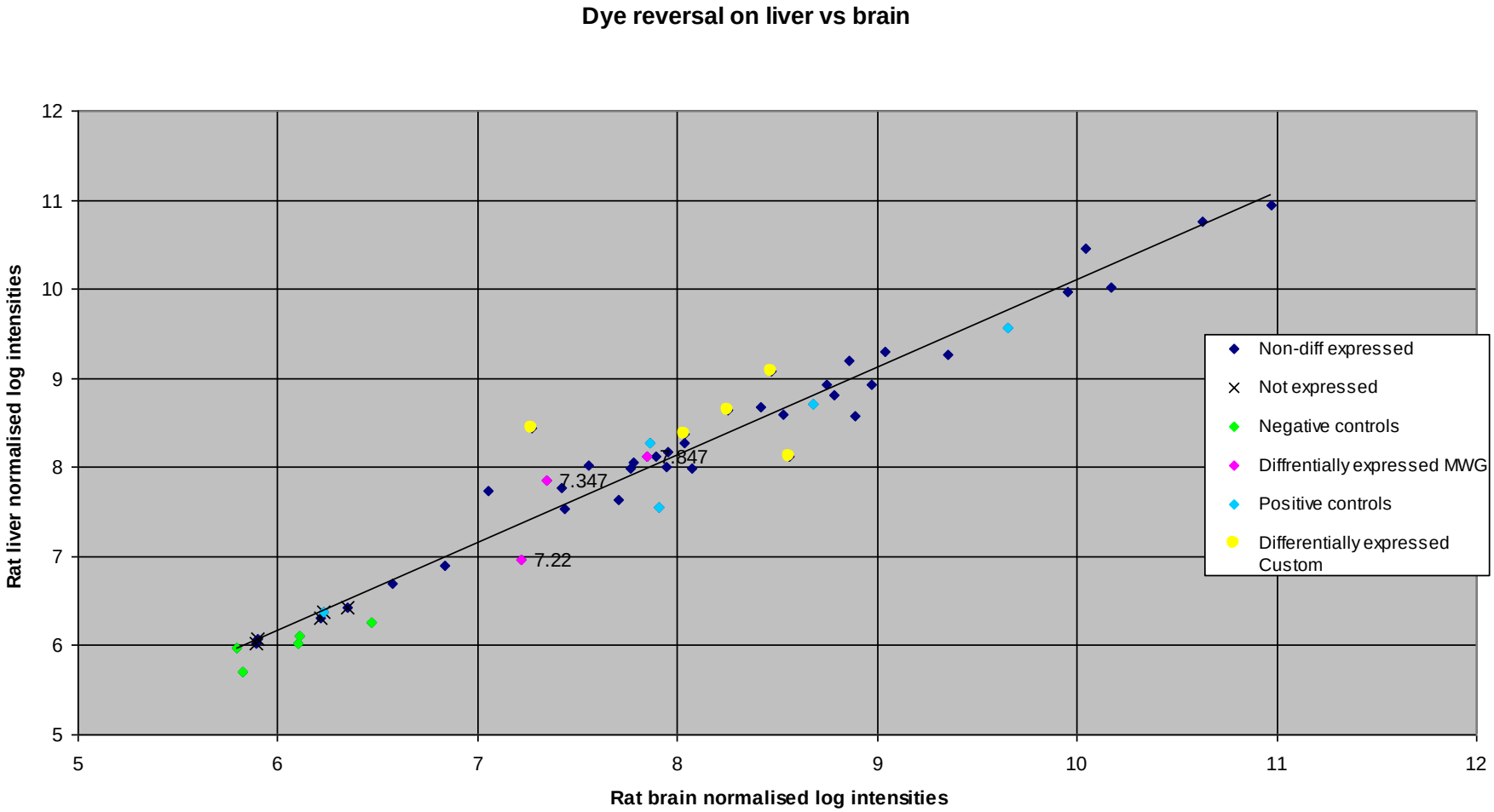

Figure 16. The rat brain *vs* rat liver (dye reversal) normalised log intensity data shows the relative distribution of signal intensities in the red (x axis) and green (y-axis) channel representing two different tissue samples.

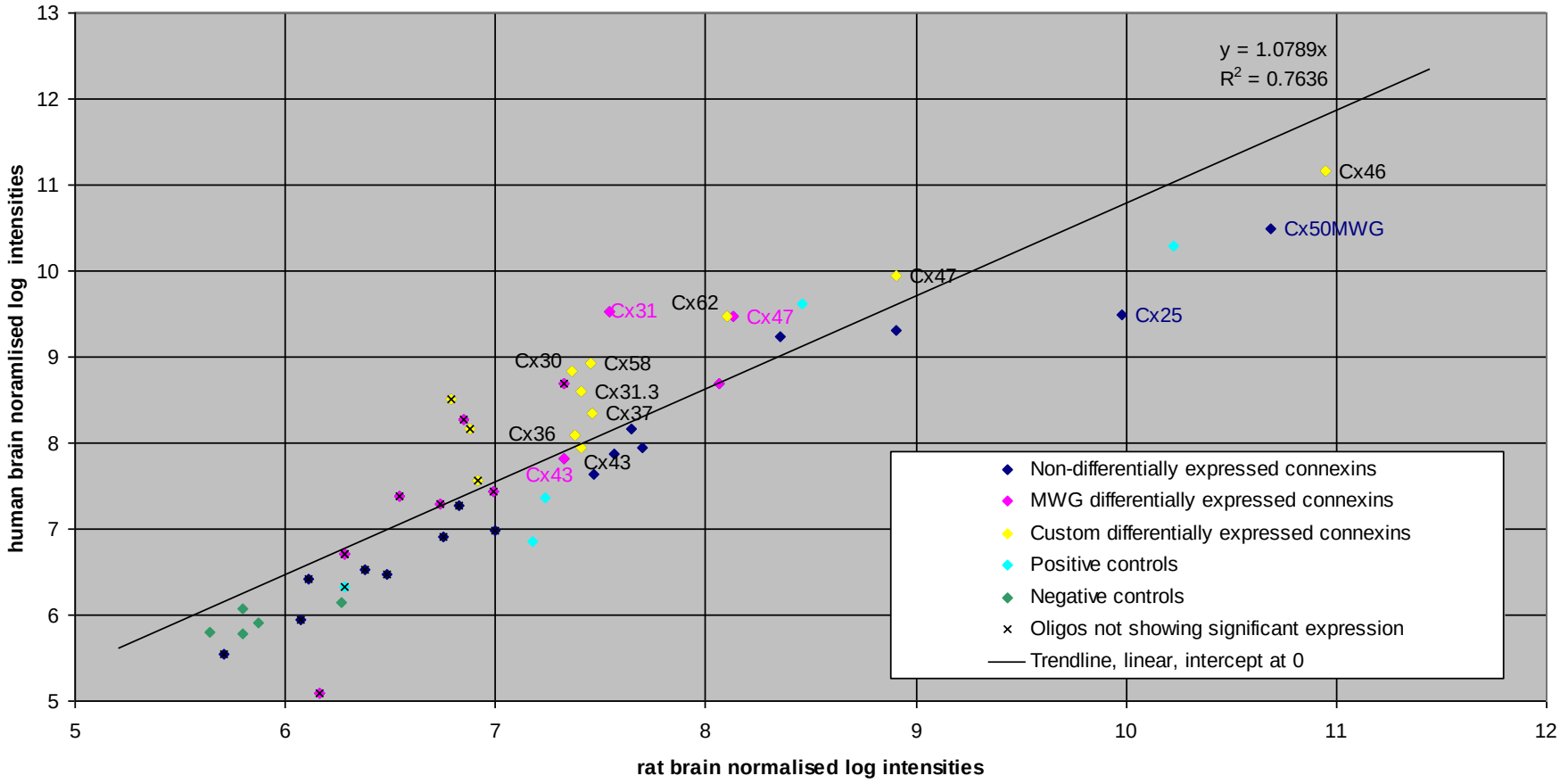

Figure 17. The rat brain *vs* human brain normalised log intensity data shows the relative distribution of signal intensities in the red (x axis) and green (y-axis) channel representing two different tissue samples.

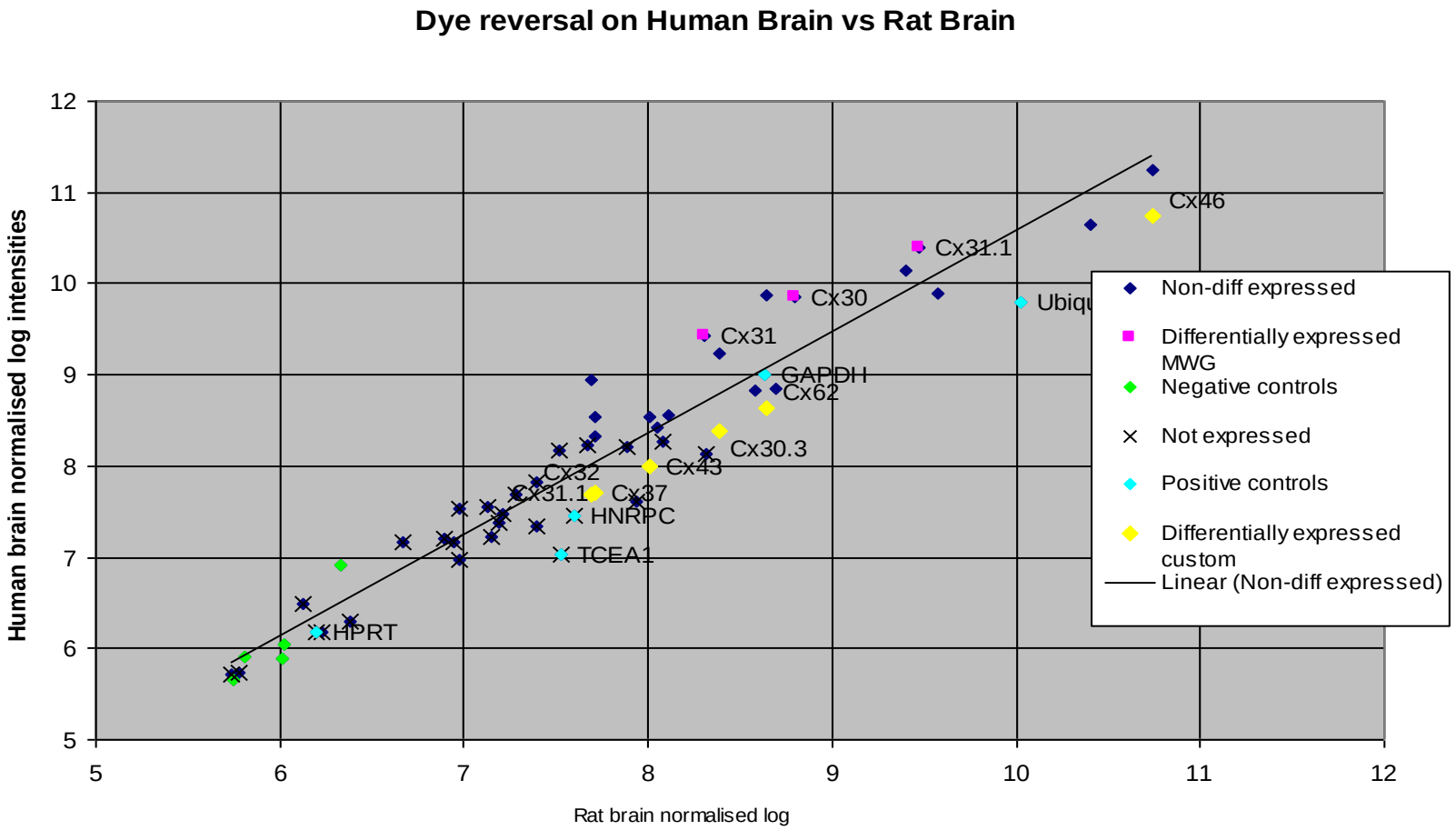

Figure 18. The rat brain vs human brain (dye reversal) normalised log intensity data shows the relative distribution of signal intensities in the red (x axis) and green (y-axis) channel representing two different tissue samples.

3.3 Validation in Rat Heart and Rat Liver

3.3.1 Custom-designed array

This section of the custom array validation involved taking RNA from the heart and liver tissue from three 7 day old Wister rats and co-hybridising Cy3 and Cy5-labelled heart and liver samples for each rat to the same slide. The aim of this study was to evaluate the reliability of the custom-designed array in terms of detecting connexin expression that was well known to occur at a higher level in the heart (Cx43, Cx40) and the liver (Cx32, Cx26) and to determine whether the results from sample repeats, biological repeats and dye reversals correlated with each other to a significant degree. The connexin was considered differentially expressed if the t-test p-value was less than 0.01.

The experimental design was as follows: rat 1 - liver (Cy3) *vs* heart (Cy5) (slides 1, 7, 10) and heart (Cy3) *vs* liver (Cy5) (slides 13, 16, 19); rat 2 – liver (Cy3) *vs* heart (Cy5) (slides 2, 8, 11); rat 3 - liver (Cy3) *vs* heart (Cy5) (slides 3, 6, 12), i.e. three sample repeats, three biological repeats and two dye reversal repeats for one of the animals (See Table 21.Experimental design - three biological repeats, three sample repeats for each of the animals and tree dye reversal repeats for one of the animals.).

All arrays demonstrated higher levels of Cy3 signal as opposed to Cy5 signal, which was especially pronounced at lower signal intensities and which therefore required normalisation. The pattern seen in Section 3.2 *Preliminary validation in rat and human tissue*, with three oligos showing high levels of non-specific binding (the MWG-designed Cx50 and the custom-designed Cx46 and Cx25) was also present in this set of slides, however, as overall signal intensities from these slides were lower, there was no oversaturation.

3.3.2 Connexin expression

3.3.2.1 Cx43

3.3.2.1.1 Custom-designed oligo

The custom-designed oligonucleotide for Cx43 showed significant preferential expression in the heart in all arrays. The average log difference for the nine liver (Cy3) *vs* heart (Cy5) slides was 0.56 (higher in the heart) and the average standard deviation for the 12 oligo spots for each slide was 0.22 for the Cy5 channel and 0.32 for the Cy3 channel. For the three dye reversal slides the average log difference was 0.25 and the average standard deviation was 0.20 for the Cy5 and 0.31 for the Cy3 channel. (See Figure 19, Figure 20, Figure 21 and subsequent connexin expression analyses).

3.3.2.1.2 MWG-designed oligo

The MWG-designed Cx43 oligo did not show a consistent pattern of expression (higher in the heart for 3 slides, higher in the liver for 5 slides, no significant difference in 4 slides). The average log difference for the nine liver (Cy3) *vs* heart (Cy5) slides was 0.04 (higher in the heart) and the average standard deviation for the 12 oligo spots for each slide was 0.25 for the Cy5 channel and 0.34 for the green channel. For the three dye reversal slides the average log difference was 0.46 (higher in the liver) and the average standard deviation was 0.37 for the Cy5 channel and 0.24 for the Cy3 channel.

3.3.2.2 Cx40

3.3.2.2.1 Custom-designed oligo

The custom-designed Cx40 oligo did not show a consistent expression pattern (one slide showed higher expression in the heart, two in the liver and no significant difference across the nine slides). The average log difference for the nine liver (Cy3) *vs* heart (Cy5) slides was 0.06 (higher in the liver) and the average standard deviation for the 12 oligo spots for each slide was 0.24 for the Cy5 channel and 0.27 for the green channel. For the three dye reversal slides the average log difference was 0.11 (higher in the heart) and the average standard deviation was 0.38 for the Cy5 channel and 0.55 for the Cy3 channel.

3.3.2.2.2 MWG-designed oligo

The MWG-designed Cx40 oligo did not show a consistent pattern of expression (higher in the heart for seven slides, no significant difference in five slides). The average log difference for the nine liver (Cy3) *vs* heart Cy5) slides was 0.16 (higher in the heart), the average standard deviation for the 12 oligo spots for each slide was 0.34 for the Cy5 channel and 0.38 for the green channel. For the three dye reversal slides the average log difference was 0.67 (higher in the heart) and the average standard deviation was 0.36 for the Cy5 channel and 0.40 for the Cy3 channel.

3.3.2.3 Cx32

3.3.2.3.1 Custom-designed oligo

The custom-designed oligonucleotide for Cx32 showed significant preferential expression in the liver in all but one of the arrays. The average log difference for the nine liver (Cy3) *vs* heart (Cy5) slides was 0.53 (higher in the liver) and the average standard deviation for the 12 oligo spots for each slide was 0.18 for the Cy5 channel and 0.39 for the Cy3 channel. For the three dye reversal slides the average log difference was 0.73 (higher in the liver) and the average standard deviation was 0.54 for the Cy5 and 0.30 for the Cy3 channel.

3.3.2.3.2 MWG-designed oligo

The MWG-dsigned Cx32 oligo did not show a consistent expression pattern (three slides showed higher expression in the heart, three in the liver and there was no significant difference in six slides). The average log difference for the nine liver (Cy3) *vs* heart (Cy5) slides was 0.12 (higher in the heart); the average standard deviation for the 12 oligo spots for each slide was 0.23 for the Cy5 channel and 0.35 for the green channel. For the three dye reversal slides the average log difference was 0.36 (higher in the liver) and the average standard deviation was 0.46 for the Cy5 channel and 0.30 for the Cy3 channel.

3.3.2.4 Cx26

3.3.2.4.1 Custom-designed oligo

The custom-designed Cx26 oligo showed significant preferential expression in all slides. The average log difference for the nine liver (Cy3) *vs* heart (Cy5) slides was 0.28 (higher in the liver) and the average standard deviation for the 12 oligo spots for each slide was 0.16 for the Cy5 channel and 0.19 for the Cy3 channel. For the three dye reversal slides the average log difference was 0.30 (higher in the liver) and the average standard deviation was 0.32 for the Cy5 and 0.44 for the Cy3 channel.

3.3.2.4.2 MWG-designed oligo

The MWG-designed Cx26 oligo did not show a consistent expression pattern (significantly higher in the liver on two slides and no significant difference in ten slides). The average log difference for the nine liver (Cy3) *vs* heart (Cy5) slides was 0.06 (higher in the heart) and the average standard deviation for the 12 oligo spots for each slide was 0.40 for the Cy5 channel and 0.36 for the Cy3 channel. For the three dye reversal slides the average log difference was 0.24 (higher in the liver) and the average standard deviation was 0.33 for the Cy5 and 0.40 for the Cy3 channel.

3.3.3 Connexins summary

None of the MWG-designed connexin oligos showed a consistent expression pattern, but for the custom-designed oligos, a clear pattern of expression in the expected direction was demonstrated for Cx43 (with significantly higher expression level in the heart), Cx32 and Cx26 (with significantly higher expression level in the liver) (for both the original and the dye reversal slides), but not for Cx40. The custom-designed Cx43 oligo contained two mismatches to the rat connexin sequence (base numbers 4 and 46) and the oligo for Cx40 contained three mismatches to the rat connexin sequence (positions 10, 13 and 34). The custom-designed oligo for Cx32 was a perfect match while the oligo for Cx26 contained 3 mismatches (base numbers 9, 33, 42) (See Table 14).

Of the custom-designed connexin oligos, Cx43 showed the highest level of expression in the heart (0.82 for Cy5 and 0.54 for Cy3) and Cx32 showed the highest level of expression in the liver (0.39 for Cy3 and 0.78 for Cy5). Cx26 showed the lowest level of expression in the heart (-0.08 for Cy5 and -0.19 for Cy3) and the second highest in the liver (0.19 for Cy3 and 0.10 for Cy5) while Cx40 demonstrated the lowest level of expression in the liver (0.21 for Cy3 and 0.06 for Cy5) and the second highest in the heart (0.15 for Cy5 and 0.05 for Cy3).

Of the MWG-designed connexin oligos, Cx40 showed the highest level of expression in the heart (1.48 for Cy5 and 1.79 for Cy3) and in the liver (1.33 for Cy3 and 1.12 for Cy5 while Cx43 showed the second-highest level of expression in the heart (0.82 for Cy5 and 1.01 for Cy3) and the liver (0.78 for Cy3 and 1.47 for Cy5). Cx32 showed the second lowest level of expression in the heart (0.18 for Cy5 and -0.03 for Cy3) and the second lowest in the liver (0.05 for Cy3 and 0.34 for Cy5) and Cx26 demonstrated the lowest level of expression in the heart (-0.96 for Cy5 and -1.35 for Cy3) and the lowest in the liver (-1.02 for Cy3 and -1.11 for Cy5). Cx26 expression level was below the significance threshold for nine of the 12 slides.

3.3.4 Controls

Ubiquitin demonstrated the highest level of expression, followed by GAPDH. TCEA was third highest, HNRPC was fourth highest, and HPRT the lowest. TCEA demonstrated a bias towards the heart samples in both the original and the dye reversal slides (significantly higher level of expression in the heart in all slides), and ubiquitin was significantly more expressed in the liver in ten out of 12 slides. The other three controls did not show a consistent pattern of preferential expression.

3.3.5 Correlation coefficients

The slides showed good concordance for dye reversal, sample repeats and biological repeats.

Table 21.Experimental design - three biological repeats, three sample repeats for each of the animals and tree dye reversal repeats for one of the animals.

Biological repeats	Sample repeats			
	Heart Cy5	Liver Cy3	Heart Cy3	Liver Cy5
Rat 1	+	+	+	+
	+	+	+	+
	+	+	+	+
Rat 2	+	+		
	+	+		
	+	+		
Rat 3	+	+		
	+	+		
	+	+		

Table 22. Average connexin expression values, nine heart Cy5 vs liver Cy3 slides and three heart Cy3 vs liver cy5 slides (dye reversals). Orange – significantly higher expression in the heart, green – significantly higher expression in the liver, grey – no change. LogDif – log difference.

	Heart	**Liver**	**LogDif**	**Fold Change**
a1 - Cx43	0.82	0.25	0.56	1.49
a1 - Cx43M	0.82	0.78	0.04	1.04
a5 - Cx40	0.15	0.21	-0.06	0.96
a5 - Cx40M	1.48	1.33	0.16	1.12
b1 - Cx32	-0.14	0.39	-0.53	0.71
b1 - Cx32M	0.18	0.05	0.12	1.10
b2 - Cx26	-0.08	0.19	-0.28	0.83
b2 - Cx26M	-0.96	-1.02	0.06	1.05
Dye reversals				
	Heart	Liver	LogDif	Fold Change
a1 - Cx43	0.54	0.29	0.25	0.84
a1 - Cx43M	1.01	1.47	-0.46	1.40
a5 - Cx40	0.05	-0.06	0.11	0.92
a5 - Cx40M	1.79	1.12	0.67	0.63
b1 - Cx32	0.04	0.78	-1.04	0.73
b1 - Cx32M	-0.03	0.34	-0.36	1.30
b2 - Cx26	-0.19	0.10	-0.30	1.23
b2 - Cx26M	-1.35	-1.11	-0.24	1.18

Table 23. Correlation coefficients for dye reversals, sample repeats and biological repeats.

1. Sample repeats					
Rat 1		*Rat 2*		*Rat 3*	
heart	liver	heart	liver	heart	liver
0.887	0.899	0.935	0.914	0.925	0.912
2. Biological repeats					
Heart 1-3		*Liver 1-3*			
0.957		0.987			
3. Dye reversals					
Heart 1		*Liver 1*			
0.931		0.958			

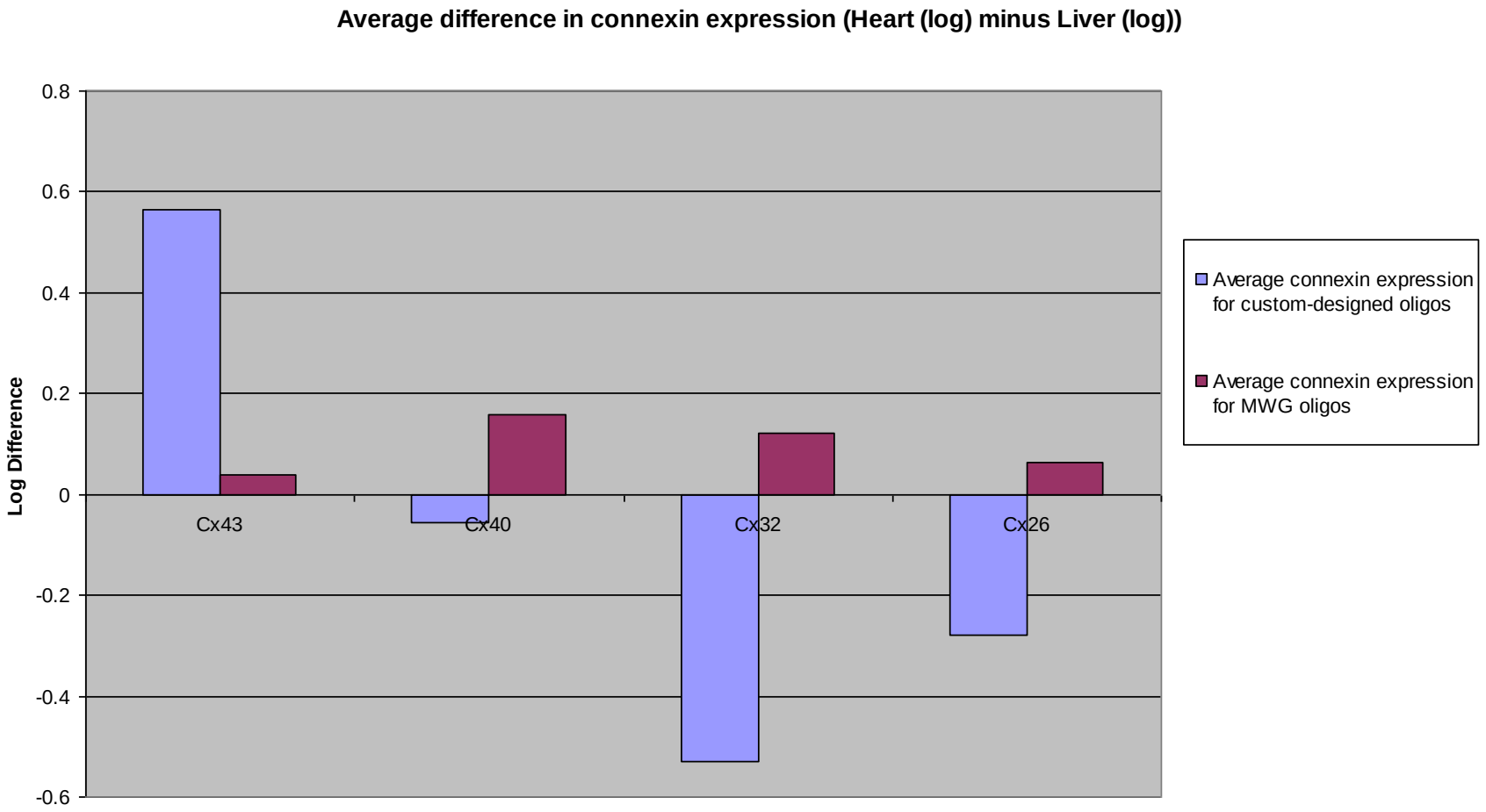

Figure 19. Average difference in connexin expression in the heart and the liver. Three rats (biological replicates) and three sample replicates for each.of the animals were used. Positive difference indicates higher expression in the heart and negative difference indicates higher expression in the liver.

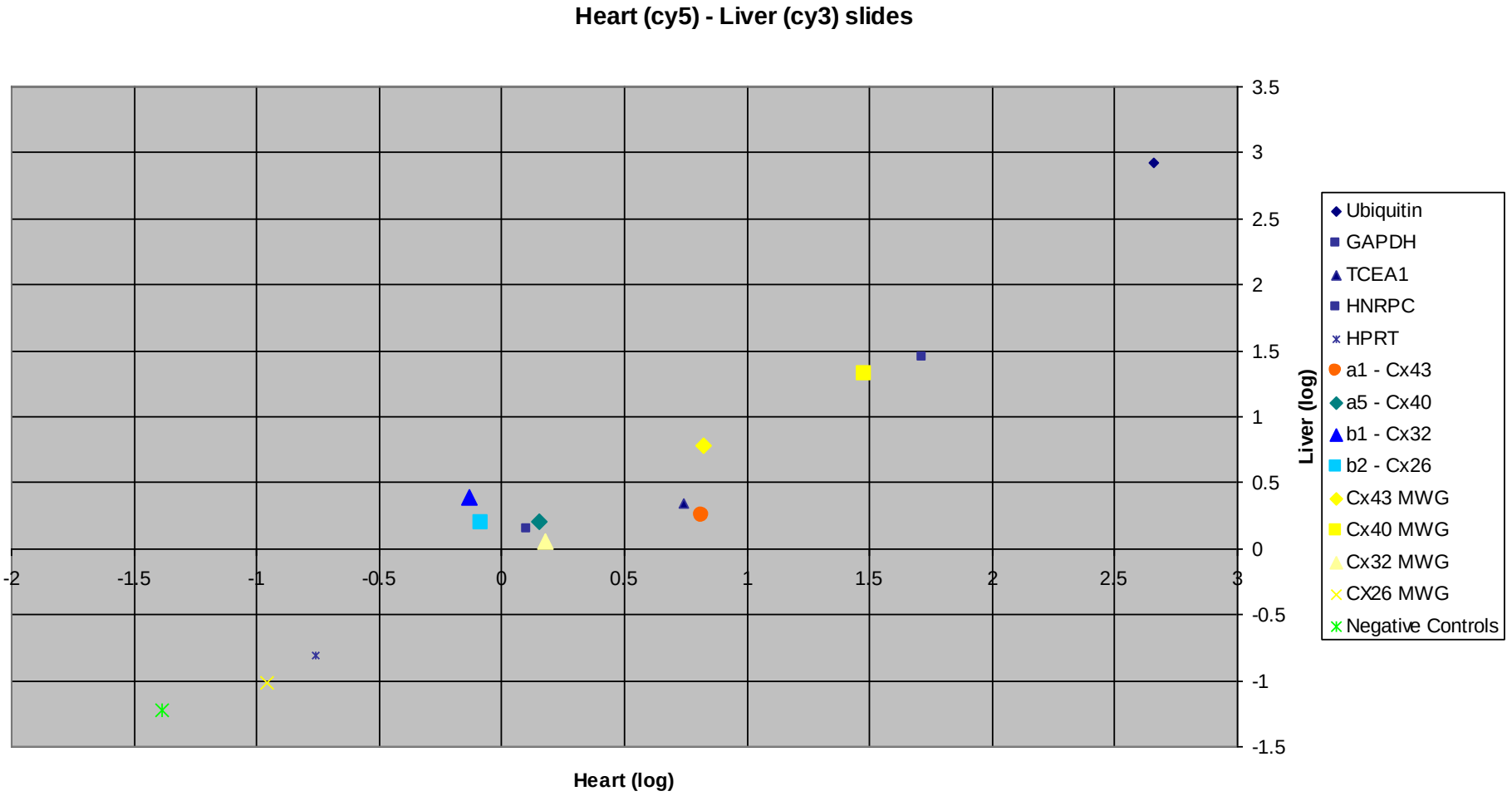

Figure 20. Connexin expression for the nine heart (Cy5) *vs* liver (Cy3) slides. Three rats (biological replicates) and three sample replicates for each.of the animals were used.

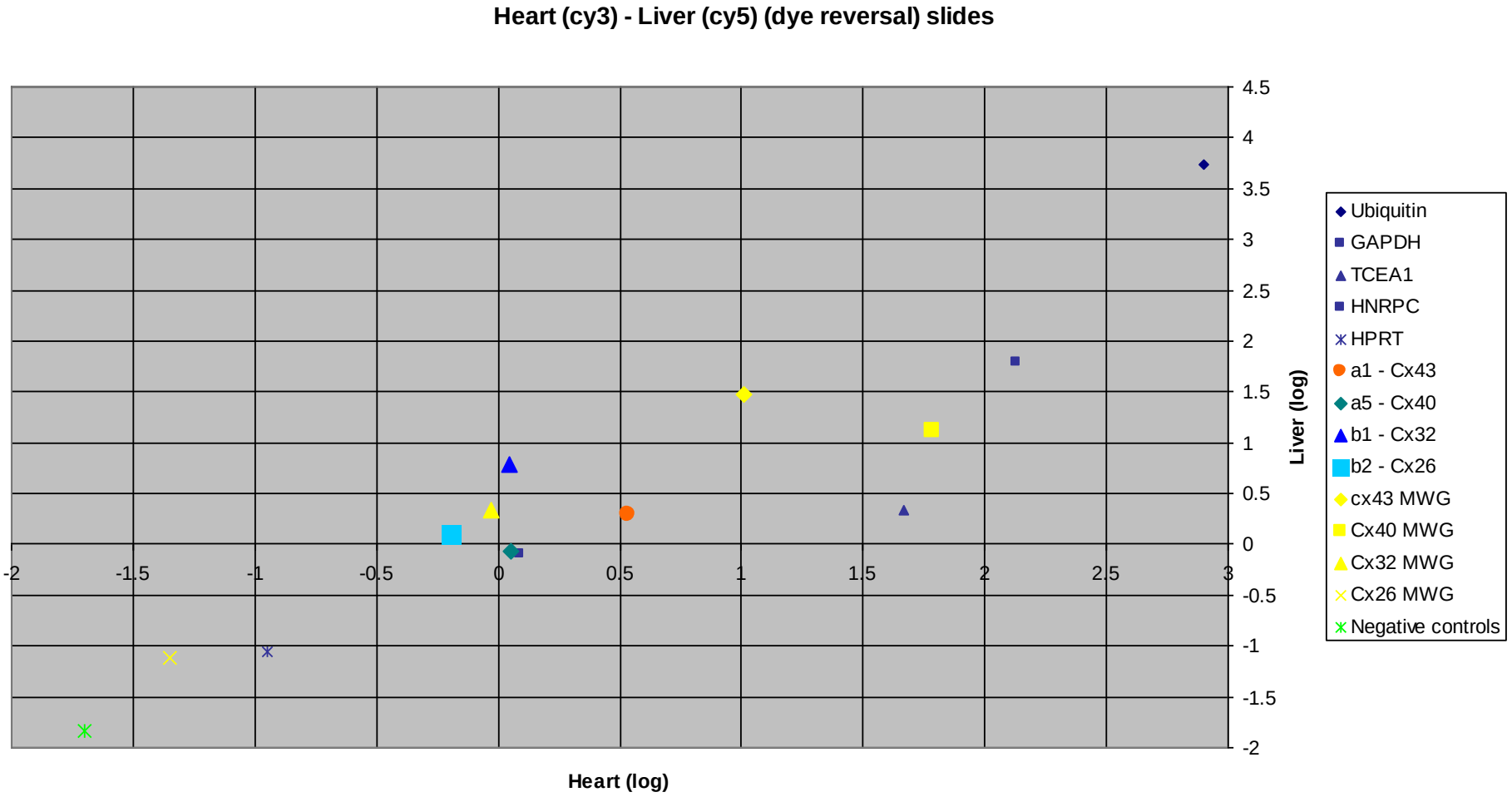

Figure 21. Connexin expression for the three heart (Cy3) *vs* liver (Cy5) slide. Three sample replicates were used.

.

3.3.6 Affymetrix arrays

Two commercially available GeneChip® Rat Genome 230 2.0 Arrays were used to compare connexin gene expression in rat heart and rat liver. One total RNA liver sample and one total RNA heart sample were used from the same 7 d.o. rat (Rat 1).

3.3.6.1 Rat heart array

All of the housekeeping controls (rat glyceraldehyde phosphate dehydrogenase (GAPDH), rat hexokinase 1 and beta-actin) showed significant expression levels on this array. Hybridisation controls that were added to the hybridisation mix at staggered concentrations (*bio*B (1.5 pmol), *bio*C (5 pmol), *bio*D (25 pmol) and *cre* (100 pmol)) were all present with expression levels increasing in accordance with their final concentrations in the hybridization mix. Unlabelled polyA spike controls (*dap, lys, phe, thr, trp)* showed significant expression, except for *thrp* (See Table 23, Table 24, Table 25).

Number of probes present is higher (59.60%), while the average probe signal was somewhat lower (8.50) than for the rat liver array.

The 3'/5' expression ratio (providing an indication of the integrity the starting RNA and efficiency of the first-strand cDNA synthesis) was between 1 and 3 as expected, except for *Lys* that showed the lowest expression level of all spike controls (3'/5' ratios are less reliable for probes with lower expression levels).

3.3.6.2 Rat liver array

Of the housekeeping controls, rat glyceraldehyde phosphate dehydrogenase (GAPDH) and beta-actin showed significant expression levels on this array while rat hexokinase 1 showed significant expression only for the 3' probe set.

Hybridisation controls (*bio*B (1.5 pmol), *bio*C (5 pmol), *bio*D (25 pmol) and *cre* (100 pmol)) were all present with expression levels increasing in accordance with their final concentrations in the hybridization mix. Compared to the heart array the controls showed somewhat higher signal levels. This was paralleled by a larger average signal for the array (8.91), while the number of probes present was somewhat lower (51.00%) than for the rat heart array.

Unlabelled polyA spike controls (*dap, lys, phe, thr, trp)* showed significant expression, except for *thrp* (See Table 22, Table 23, Table 24).

The 3'/5' expression ratio was between 1 and 3 except for *Lys* which showed the lowest expression level of all spike controls, same as in the rat heart array.

3.3.6.3 Connexins

Probes present on the array were Cx43, Cx46, Cx37, Cx40, Cx45, Cx36, Cx32, Cx26, Cx31, Cx30.3, Cx30.2, Cx30. Connexins that showed significant expression in the heart were Cx43, Cx46, Cx37, Cx40, Cx30.2 (marginal); in the liver - Cx43, Cx37, Cx40, Cx32, Cx26. Cx30.3. Cx46, Cx30.2 (marginal) were expressed in the heart only. Cx43, Cx37, Cx40 were expressed at a higher level in the heart than in the liver. Connexins expressed in liver only were Cx32, Cx26 and Cx30.3. No connexins expressed in both tissues were expressed at a higher level in the liver (See Table 25 for a list of connexin probes represented on the array and their expression levels).

The Affymterix array confirmed the results obtained in our custom arrays for the oligos that showed a consistent preferential expression pattern (custom-designed Cx43, Cx32 and Cx26). The custom-designed Cx40, that did not show a consistent pattern of expression, also showed the smallest expression difference in the Affymetrix arrays (See Figure 22 for the Affymetrix data with the relative expression levels for the connexins analysed for both the custom-designed and the Affymetrix arrays).

.

Table 24. The expression levels of housekeeping controls for the heart and liver Affymetrix arrays. Detection: P - present, A - absent, M - marginal.

Heart								
Probe Set	Signal (5') (log)	Det(5')	Signal (M') (log)	Det(M')	Signal (3') (log)	Det(3')	Signal (all) (log)	Sig(3'/5')
AFFX_RAT_GAPDH	12.77	P	12.54	P	12.85	P	12.72	1.06
AFFX_RAT_HEXOKINASE	7.06	P	7.33	P	7.98	P	7.51	1.90
AFFX_RAT_BETA-ACTIN	12.09	P	12.20	P	12.52	P	12.28	1.35
Liver								
Probe Set	Signal (5') (log)	Det(5')	Signal (M') (log)	Det(M')	Signal (3') (log)	Det(3')	Signal (all) (log)	Sig(3'/5')
AFFX_RAT_GAPDH	12.81	P	12.51	P	12.79	P	12.71	0.99
AFFX_RAT_HEXOKINASE	4.30	A	4.59	A	5.56	P	4.92	2.41
AFFX_RAT_BETA-ACTIN	12.24	P	12.91	P	13.04	P	12.77	1.74

Table 25. The expression levels of hybridisation controls for the heart and liver Affymetrix arrays. Detection: P - present, A - absent, M - marginal.

Heart								
Probe Set	Signal (5') (log)	Det(5')	Signal (M') (log)	Det(M')	Signal (3') (log)	Det(3')	Signal (all) (log)	Signal (3'/5')
AFFX-BIOB	4.84	P	5.66	P	5.31	P	5.31	1.39
AFFX-BIOC	7.45	P			7.69	P	7.58	1.18
AFFX-BIOD	8.76	P			10.13	P	9.60	2.58
AFFX-CRE	11.43	P			11.68	P	11.57	1.19
Liver								
Probe Set	Signal (5')	Det(5')	Signal (M') (log)	Det(M')	Signal (3') (log)	Det(3')	Signal (all) (log)	Signal (3'/5')
AFFX-BIOB	5.44	P	6.49	P	6.07	P	6.06	1.55
AFFX-BIOC	8.21	P			8.20	P	8.20	1.00
AFFX-BIOD	9.13	P			10.10	P	9.69	1.96
AFFX-CRE	12.25	P			12.65	P	12.46	1.31

Table 26. The expression levels of unlabelled polyA controls for the heart and liver Affymetrix arrays. Detection: P - present, A - absent, M - marginal.

Heart								
Probe Set	Sig(5') (log)	Det(5')	Sig(M') (log)	Det(M')	Sig(3') (log)	Det(3')	Sig(all) (log)	Sig(3'/5')
AFFX-DAP	8.60	P	9.37	P	9.86	P	9.37	2.39
AFFX-LYS	5.54	P	6.16	P	7.23	P	6.48	3.24
AFFX-PHE	6.29	P	6.66	P	7.34	P	6.83	2.07
AFFX-THR	7.07	P	7.19	P	7.73	P	7.36	1.58
AFFX-TRP	0.77	A	1.85	A	-0.74	A	0.99	0.35
Liver								
Probe Set	Sig(5') (log)	Det(5')	Sig(M') (log)	Det(M')	Sig(3') (log)	Det(3')	Sig(all) (log)	Sig(3'/5')
AFFX-DAP	9.32	P	9.75	P	10.09	P	9.75	1.71
AFFX-LYS	5.48	P	6.60	P	7.60	P	6.81	4.35
AFFX-PHE	6.89	P	6.77	P	7.35	P	7.03	1.37
AFFX-THR	7.39	P	7.33	P	8.16	P	7.68	1.71
AFFX-TRP	1.07	A	2.98	A	0.68	A	1.95	0.79

Table 27. The expression levels for connexins in the heart and liver Affymetrix arrays. Detection: P - present, A - absent, M - marginal. The genes for connexins analysed for both the Affymetrix and the custom-designed arrays are highlighted in blue. The signal levels for probes detected as present on the array are highlighted in green, for probes detected as marginally present – in blue, and for probes which were not detected – in grey.

Symbol	Gene Title	7DHeart_Signal (log)	7DH_Detection	7DLiver_Signal (log)	7DL_Detection	Heart-Liver (log)
Gja1	gap junction membrane channel protein alpha 1(Cx43)	10.73	P	6.35	P	4.39
Gja1	gap junction membrane channel protein alpha 1(Cx43)	12.66	P	9.53	P	3.13
Gja3	gap junction membrane channel protein alpha 3 (connexin46)	5.93	P	4.45	A	1.48
Gja4	gap junction membrane channel protein alpha 4 (Cx37)	8.44	P	6.45	P	1.98
Gja5	gap junction membrane channel protein alpha 5 (Cx40)	7.64	P	6.04	P	1.59
Gja5	gap junction membrane channel protein alpha 5 (Cx40)	5.17	M	4.45	P	0.72
Gja6	gap junction membrane channel protein alpha 6 (Cx45)	2.32	A	1.43	A	0.89
Gja9	gap junction membrane channel protein alpha 9 (Cx36)	1.32	A	1.38	A	-0.06
Gjb1	gap junction membrane channel protein beta 1 (Cx32)	4.04	A	12.31	P	-8.27
Gjb2	gap junction membrane channel protein beta 2 (Cx26)	2.10	A	8.32	P	-6.21
Gjb3	gap junction membrane channel protein beta 3 (Cx31)	3.71	A	4.74	A	-1.03
Gjb4	gap junction membrane channel protein beta 4 (Cx30.3)	0.58	A	4.58	P	-4.00
Gjb5	gap junction membrane channel protein beta 5 (Cx31.1)	4.10	M	0.49	A	3.61
Gjb6	gap junction protein, beta 6 (Cx30)	-0.74	A	-1.00	A	0.26

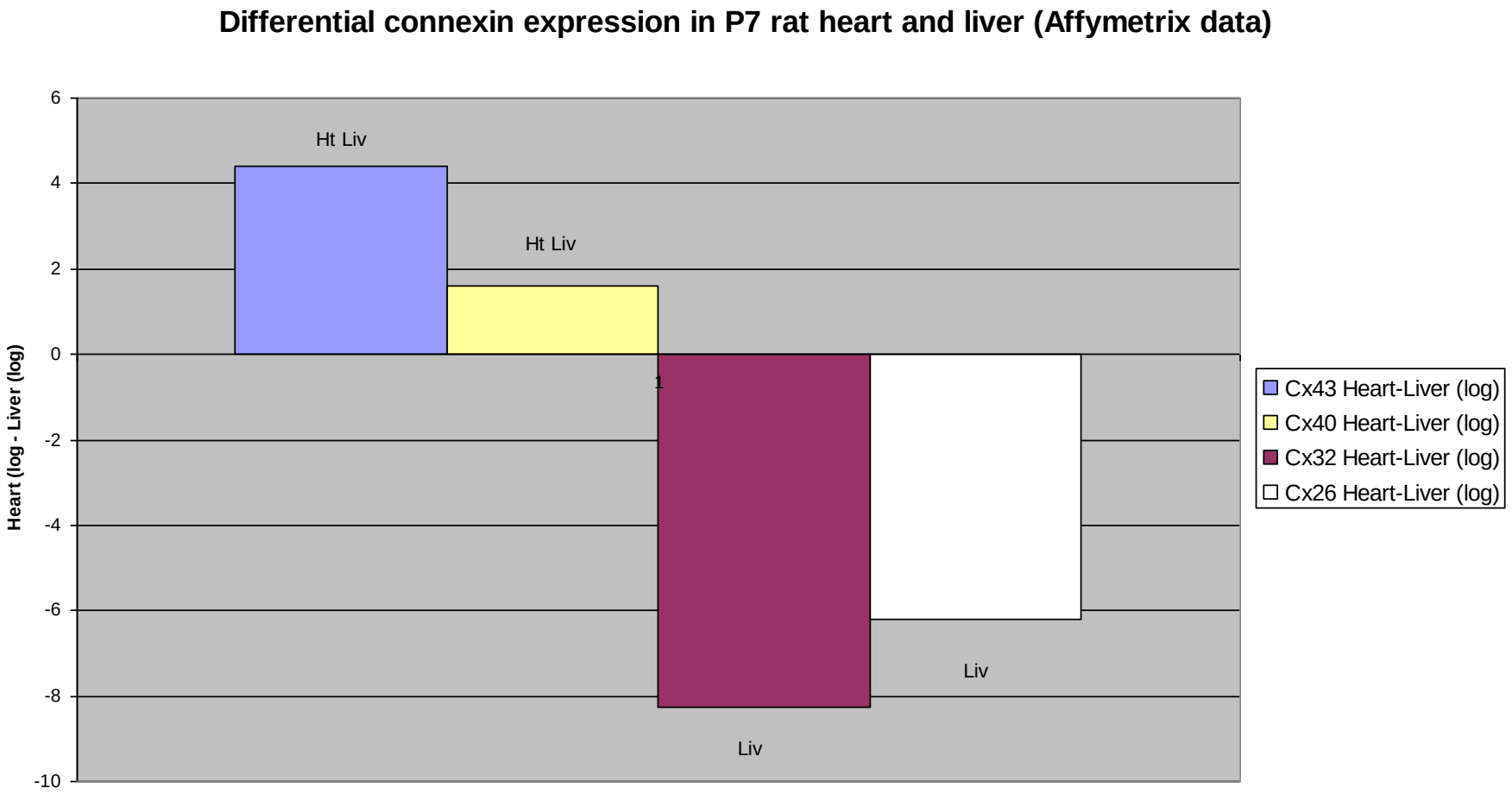

Figure 22. Average difference in connexin expression in the heart and the liver. Positive difference indicates higher expression in the heart and negative difference indicates higher expression in the liver. One heart and one liver sample from the same rat was used. Ht Liv – expressed in both the heart and the liver. Liv – expressed in liver only.

4 RNA QUALITY OF THE HUMAN BRAIN TISSUE

This part of my research work involved screening RNA extracted from human brain tissue from patients with various neurodegenerative conditions (namely Alzheimer's disease, Parkinson's disease and Huntington's disease) as well as normal controls and hippocampal tissue obtained during temporal lobectomies from patients with intractable epilepsy. The initial screening of the human brain tissue was performed using samples taken from the cerebellum. The brain region, secondarily affected in Alzheimer's disease, Parkinson's disease and Huntington's disease (medial temporal gyrus, caudate nucleus and motor cortex respectively) was then investigated. The number of cases for each condition ranged from 3 (epilepsy) to 8 (Alzheimer's). Another part of the study was to investigate RNA stability using cerebellar tissue from normal control cases with a broad range of postmortem delays. Factors that influence RNA quality were assessed, and included postmortem delay, the duration of the agonal state, the tissue pH, the age at death and the sex of the patient.

4.1 Normal Controls

The normal control samples evaluated (See Table 26) had the second longest postmortem (PM) delay (mean=8.42 hours) but the second highest cerebellar RNA quality of all the groups under consideration (mean RIN=8.2 for the subjects for which both the cerebellar RIN and the caudate nucleus RIN values were available) (See Figure 27). The range of the postmortem delays was relatively small (SD=1.69 hours). Samples from the largest number of different regions were evaluated for the normal controls and the trend for variability of the RNA quality between different regions was most evident in these control samples. However, a sufficient number of cases were considered for cerebellum and caudate nucleus only. The quality of samples for the caudate nucleus was lower than for the cerebellum (mean caudate nucleus RIN=7.5), but a smaller number of cases were evaluated in the former instance (four versus six). The mean difference between the cerebellar RIN and the caudate nucleus RIN was 0.7 and with a range from −0.1 to 1.3 (Figure 23, Figure 27 and the Bland and Altman plot, Figure 28).

For the one case where samples from four different brain regions were evaluated (H109, Table 26), the RIN values ranged from 7 to 9.1; the value for MTG was the lowest at 7, the CN the next highest at 7.8, the MC at 8.1, and the cerebellum the highest at 9.1

4.2 Alzheimer's Disease

Eight cerebellar samples were assessed for this disease. The Alzheimer's cases had the second shortest postmortem delay (mean= 5.83 hours) and the largest standard deviation for the postmortem delay (SD=4.29 hours, PM range from 2 to 14.5 hours) (Table 27). The cerebellar RNA quality was the second lowest (mean RIN=8.2 for the subjects for which both the cerebellar RIN and the medial temporal gyrus RIN values were available) (See Figure 27). The mean difference between the cerebellar RIN and the medial temporal gyrus RIN was 1.87, by far the largest of all disease groups, and its range was from 1.4 to 3.1 (See Figure 24, Figure 27 and the Bland and Altman plot, Figure 28).

4.3 Parkinson's Disease

Six cerebellar samples were taken for Parkinson's disease (See Table 28). The longest mean PM delay was 9.5 hours and the sample had second-largest PM variation (SD=3.33 hours). The cerebellar RNA quality was also the lowest, with a mean RIN of 7 for the subjects for which both the cerebellar RIN and the caudate nucleus RIN values were available (See Figure 27). The Parkinson's disease cases represented the only instance where the mean RNA quality of the secondary brain region was higher than the mean cerebellar RNA quality (mean CN RIN=7.3, mean cerebellar RIN=7.0), from the four CN cases evaluated. The mean difference between the cerebellar RIN and the CN RIN was −0.2, and the range of the difference was from −0.9 to 0.4 (See Figure 25, Figure 27 and the Bland and Altman plot, Figure 28).

4.4 Huntington's Disease

The Huntington's disease group had the smallest number of cerebellar samples (five) (See Table 29), the shortest mean PM delay (4.8 hours) and the lowest PM SD (1.6 hours). The mean cerebellar RNA quality was the highest (mean RIN=8.6, See Figure 27), with the mean MC RIN at 8.1 (also 5 samples evaluated). The mean difference between the cerebellar RIN and the MC RIN was 0.5, and the range of the difference was from −0.8 to 2.6 (See Figure 26, Figure 27 and the Bland and Altman plot, Figure 28). There appears to be no apparent relationship between the disease Grade and the RIN values; however, taking into account the small sample size and the fact that three out of the five cases were Grade 3, it is unlikely that such a relationship would be evident.

4.5 Epilepsy

Three hippocampus samples taken during temporal lobectomies were evaluated for RNA quality and had low RIN values (mean=7.2). The PM was not applicable here as the samples were obtained from living patients during surgery (See Table 30).

4.6 The Postmortem Delay Range Study

Cerebellar samples from an additional number of long PM delay cases (ranging from 15 to 97 hours) were evaluated for RNA quality in order to determine if progressively longer PM delays affect the quality of the RNA. Overall, there was surprisingly little difference in the RNA quality of these different cerebellar samples (with the RIN range from only 7.1 to 7.6) (See Table 31).

4.7 The Effect of the Agonal State

The effect of the length of the agonal state on the RNA quality was assessed by separating the cases into those with a fast (n=7) and with a slow (n=17) mode of death, thus creating a binary distribution. Slow mode of death had a significantly lower pH (acidic) than those with a fast mode of death (p=0.017). No correlation between the PM delay and the pH of the tissue was found.

4.8 The Variables Associated with the Cerebellar RNA Integrity

The multiple regression analysis showed a relationship of the cerebellar RIN value to the mode of death, with faster deaths resulting in higher RNA quality (p=0.03), PM delay, with longer PM leading to lower RIN (p=0.04), and, most significantly, to pH, with higher pH resulting in higher RNA quality (p=0.006). No relationship was found with age (p=0.33) or sex of the patient (p= 0.70) or disease group (p=0.32).

In summary, The RNA quality in this study was most closely related to the pH of the tissue. The primary determinant of the tissue pH was the mode of death. The PM delay did not demonstrate a large effect on the RNA quality as evidenced by the PM delay range study, although the multiple regression analysis showed some correlation Cerebellar RNA quality was generally reflective of the RNA quality of the tissue of interest, however, there was no exact correlation.

Table 28. The patient data and the RNA quality (RIN) values for the normal control cases (h - hours).

Case	Age	Sex	Cause of Death	Mode Of death	Cerebellum pH	PM, h	Cerebellum RIN	Motor Cortex RIN	Caudate Nucleus RIN	Medial Temporal Gyrus RIN
H116	18	F	Asphyxia	F	6.2	10	8.7			
H155	61	M	Ischemic heart disease	F	5.9	7	8.3			
H109	81	M	Coronary atherosclerosis	F	5.7	7	9.1	8.1	7.8	7
H112	79	M	Bleeding stomach ulcer	S	5.5	8	6.8		6.9	
H123	78	M	Ruptured abdominal aortic aneurism	F	5.7	7.5	7.5		7.1	
H126	36	F	Asphyxia	F	6.2	11	9.2		8.2	
			Mean			8.42	8.27	8.10	7.50	7.00
			SD			1.69	0.95		0.61	

Table 29. The patient data and the RNA quality (RIN) values for the Alzheimer's disease cases (h - hours).

Case	Age	Sex	Cause of Death	Mode Of death	Cerebellum pH	PM, h	Cerebellum RIN	Medial Temporal Gyrus RIN
AZ30	77	M	Myocardial infarction	F	5.9	14.5	8.6	6.5
AZ32	75	F	Bronchopneumonia	S	5.9	3	8.5	5.4
AZ38	80	M	Respiratory arrest/bronchopneumonia/emphysema/advanced Alzheimer's disease	S	5.7	5.5	7.2	
AZ48	63	F	Bronchopneumonia	S	5.9	7	7.2	
AZ53	85	F	Bilateral bronchopneumonia	S	5.8	2	7.9	6.5
AZ54	84	M	Bronchopneumonia	S	5.5	3	7.8	5.3
AZ55	51	M	Bilateral bronchopneumonia	S	5.8	4	8.3	6.3
			Mean			5.83	7.87	6.00
			SD			4.29	0.58	0.60

Table 30. The patient data and the RNA quality (RIN) values for the Parkinson's disease cases (h - hours).

Case	Age	Sex	Cause of Death	Mode Of death	Cerebellum pH	PM, h	Cerebellum RIN	Caudate Nucleus RIN
PD6	69	F	Pneumonia	S	5.9	7	7.9	8.8
PD8	56	M	Asphyxiation/aspiration pneumonia	S	5.7	4	7.2	7.4
PD13	70	M	Bronchopneumonia/coma	S	5.6	12	6.3	
PD15	76	M	Bronchopneumonia	S	5.3	11	5.1	5.3
PD16	79	M	Pneumonia	S	5.7	8.5	7.9	7.5
PD18	98	F	Bronchopneumonia	S	5.6	14	6.6	
			Mean			9.42	6.83	7.25
			SD			3.64	1.07	1.45

Table 31. The patient data and the RNA quality (RIN) values for the Huntington's disease cases (h - hours).

Case	Age	Sex	Cause of Death	Mode Of death	Cerebellum pH	PM, h	Cerebellum RIN	Motor Cortex RIN	Disease grade
HC84	43	F	Acute renal failure	F	6	3.5	9.3	8.7	3
HC91	63	F	Huntington's disease	S	5.7	5.5	8	7.7	3
HC92	72	M	Pneumonia	S	6.2	5	8.7	8.8	1
HC107	75	M	Bronchopneumonia	S	5.5	3	8.3	9.1	3
HC109	59	F	Bronchopneumonia	S	6	7	8.7	6.1	4
			Mean			4.80	8.60	8.08	
			SD			1.60	0.49	1.23	

Table 32. Case ID and the RNA quality (RIN) values for epilepsy.

Case	Hippocampus RIN
E46	6.6
E113	7.7
E118	7.2
Mean	7.17
SD	0.55

Table 33. The patient data and the RNA quality (RIN) values for the long postmortem delay range cases (h - hours).

Case	Age	Sex	Cause of Death	PM, h	Cerebellum RIN
HC110	44	M	Aspiration Pneumonia	29	7.4
HC87	45	M	Bronchpneumonia	18	7.2
AZ24	82	F	Pneumonia	97	7.1
H157	66	M	Ischaemic heart disease	15	7.6
H127	59	F	Pulmonary embolism	21	7.5
			Mean	36.00	7.36
			SD	34.50	0.21

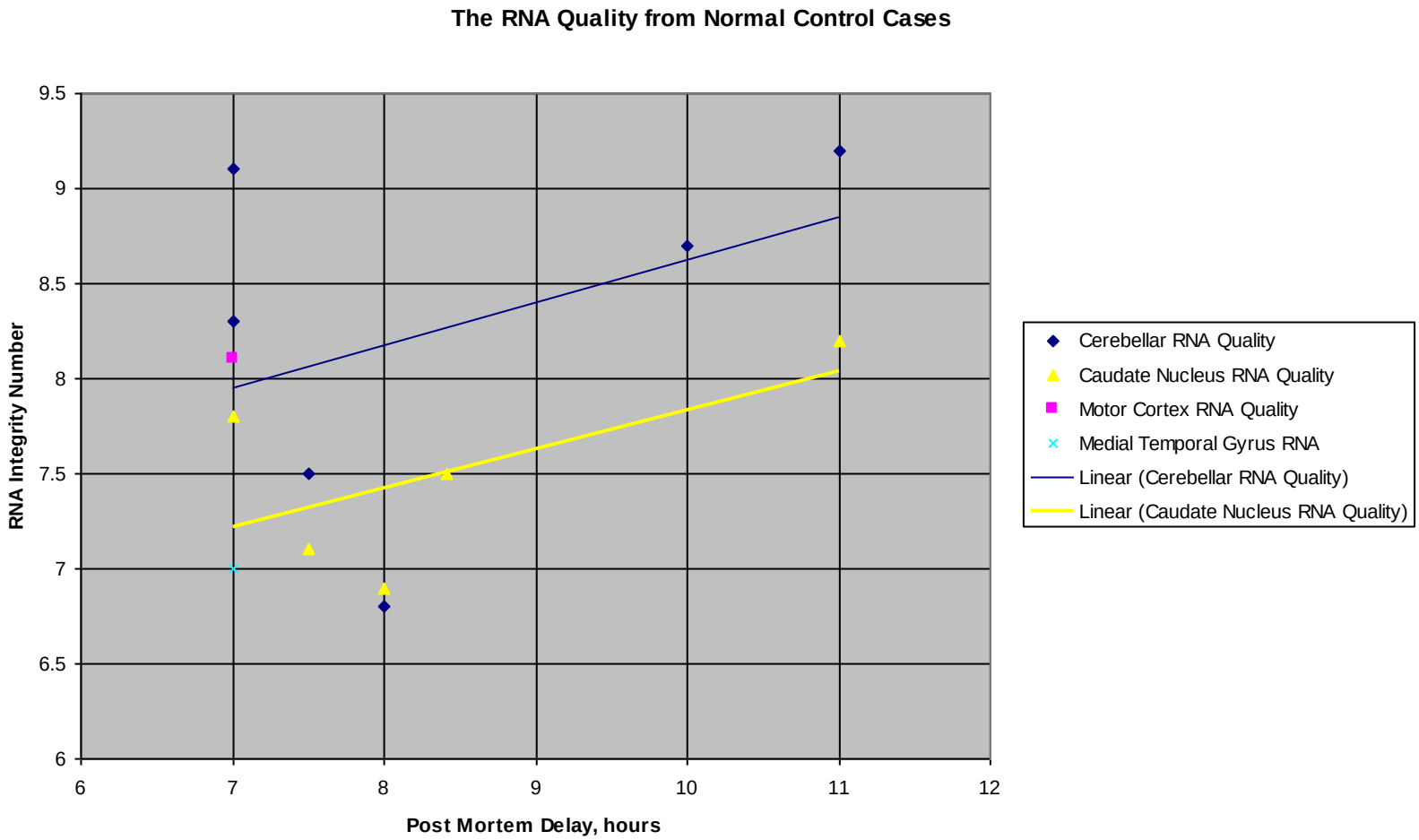

Figure 23. The RNA quality values and trends in relation to the length of postmortem delay for the normal control cases. Six cerebellum samples, four CN sample, one MC sample, one MTG samples were screened.

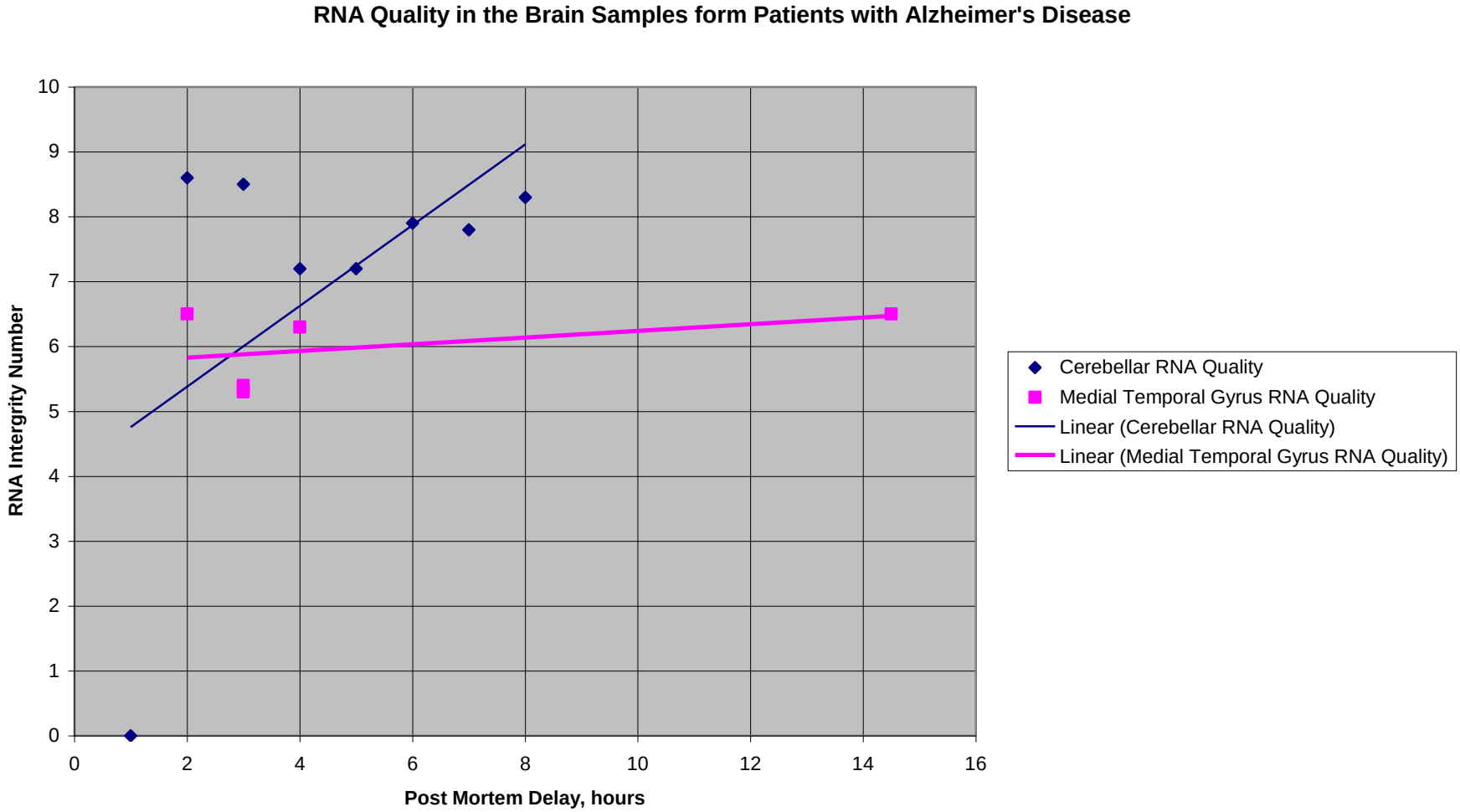

Figure 24. The RNA quality values and trends in relation to the length of postmortem delay for the Alzheimer's disease cases. Cerebellum samples from seven patients and MTG samples from five patients were screened.

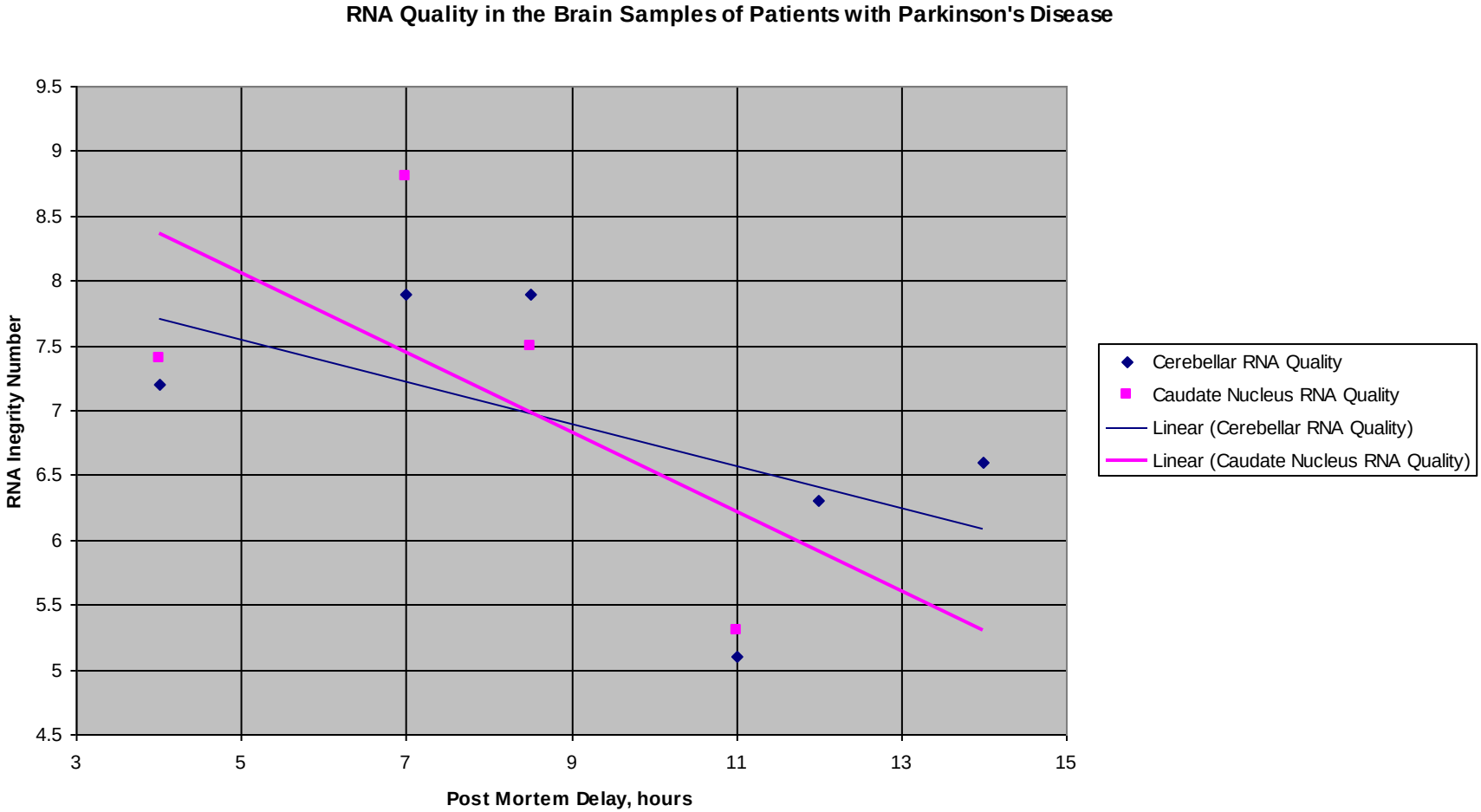

Figure 25. The RNA quality values and trends in relation to the length of postmortem delay for the Parkinson's disease cases. Cerebellum samples from six patients and CN samples from four patients were screened.

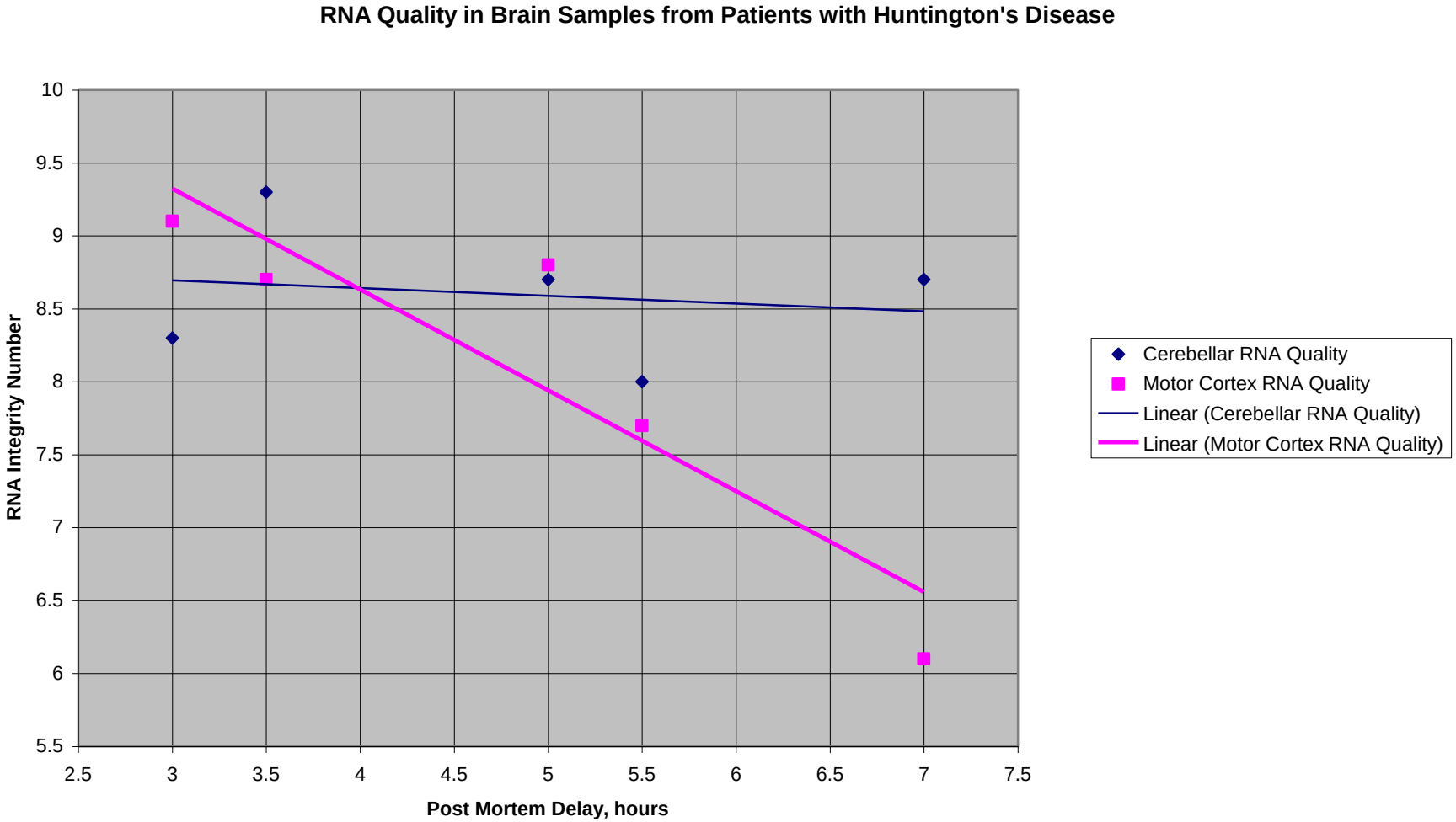

Figure 26. The RNA quality values and trends in relation to the length of postmortem delay for the Huntington's disease cases. Cerebellum samples from five patients and MC samples from five patients were screened.

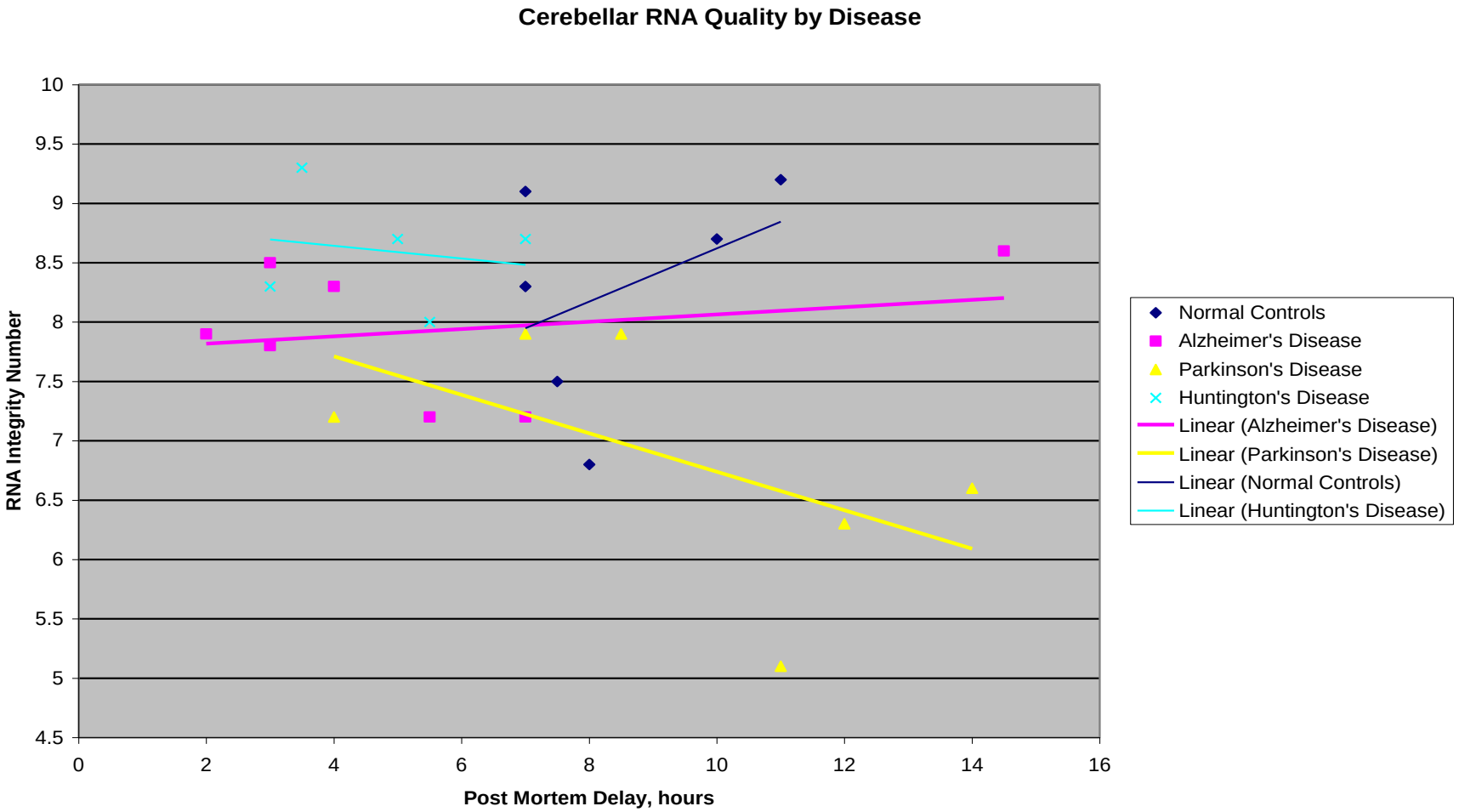

Figure 27. Trends in cerebellar RNA quality by disease and control group in relation to the length of postmortem delay. Normal control samples from five patients, Alzheimer's disease samples from seven patients, Parkinson's disease samples form six patients and Huntington's disease samples from five patients were used. Individual RNA quality was variable both within and between all groups with Huntington's disease cases having the highest mean for RNA quality (mean RIN=8.6), second only to normal controls (mean RIN=8.2). Although the sample sizes were small and variable between disease groups, there is a trend towards a decrease in RNA quality relative to postmortem delay in disease groups with the correlation between postmortem delay and cerebellar quality inverted in the control group.

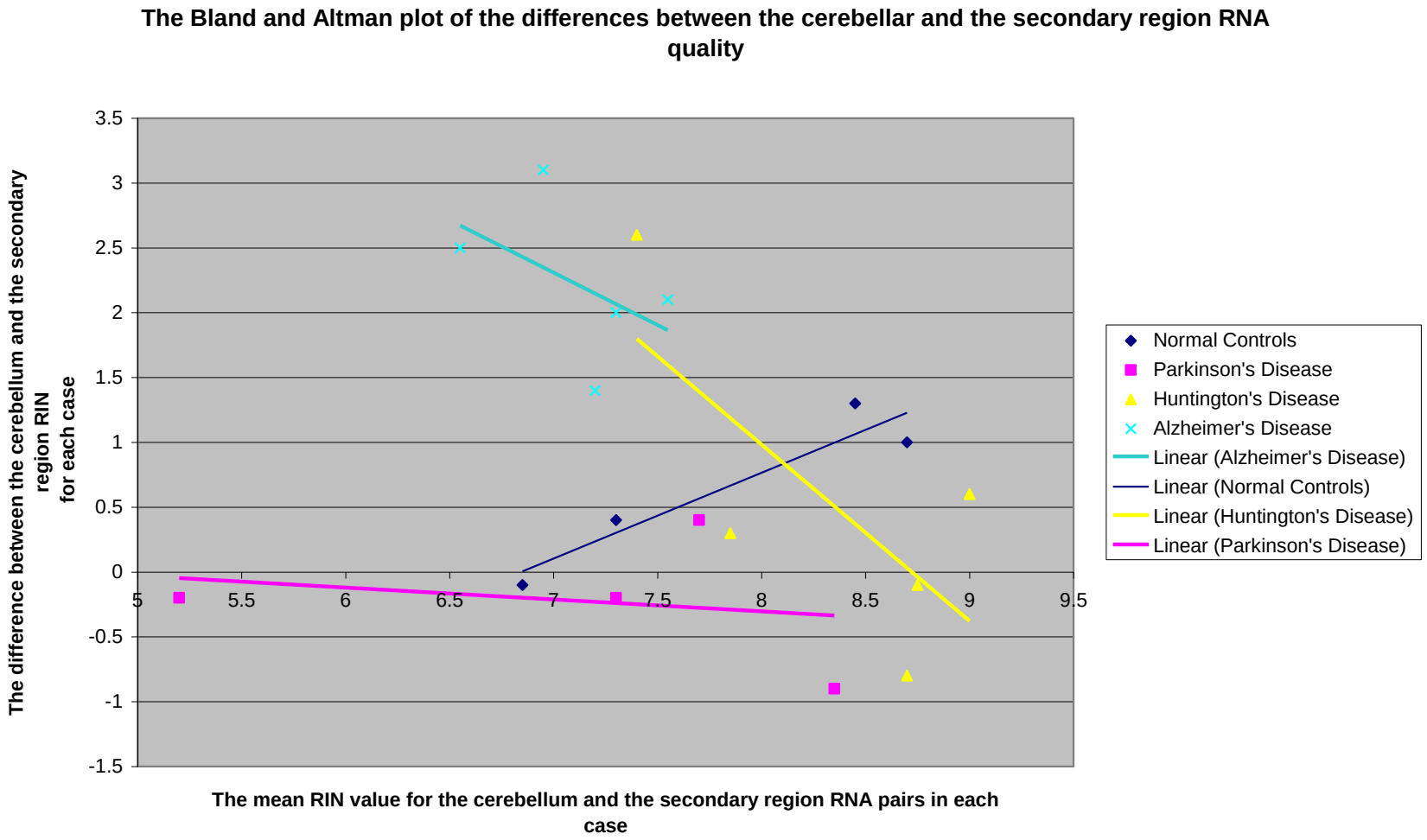

Figure 28. A Bland and Altman plot of the differences between cerebellar and secondary region RNA quality plotted against the mean RIN value for the cerebellum and the secondary region RNA pairs in each case. Five patient sample pairs for each disease were used. The higher the RNA quality for the two samples, the smaller the difference is likely to be. For example, in Huntington's disease and normal controls, both cerebellar and motor cortex samples had high mean values and RIN differences between the sample pairs were close to zero. By contrast, for Alzheimer's disease where the cerebellar RNA quality and that of the medial temporal gyrus were low, the difference between the pairs was large. Thus higher quality cerebellar RNA appears to be a better predictor of RNA quality in the secondarily affected brain region.

5 SCREENING THE HUMAN BRAIN

This chapter describes the use of two gene array technologies, a custom designed boutique gene array and a commercially available IlluminaSentrix array, to screen the secondarily affected brain areas of a number of neurodegenerative diseases for the expression of connexins (and for the Illumina array also the expression of inflammatory markers).

Replication is a key concept in experimental design and statistical analysis. If two populations are being compared, replication allows the assessment of variation within each population, which is essential for the calculation of the statistical significance of any difference observed between the population means (Winer et al., 1991). There are two types of replication used in microarray analysis: technical replication and biological replication (Stekel, 2003).

Examples of technical replication include using multiple probes for the same gene on a single microarray, or hybridising the same RNA to a microarray multiple times. It is also possible to assess technical stability on each chip by using spot replicates. Technical replication provides an estimate of the precision of microarray measurements, and is especially important when new microarray methods are being developed and tested. Statistical significance can also be sought between the multiple negative controls (and technical replicates) and genes of interest within an array. This should make it possible to assess whether a gene is being expressed in the sample of interest at a level above a negative control threshold.

Examples of biological replication include comparing the brains of multiple individuals with a disease with the brains of multiple individuals without that disease, or comparing multiple distinctly different cell lines treated with an active drug, with the same set of cell lines treated with a control drug. Biological replication allows the assessment of the biological variance within each of the groups being compared. This is useful if we wish to draw conclusions about the biological importance of any difference observed between the groups being compared. Biological replication can provide support for generalising our conclusions to a larger population. For example, if gene expression differences were seen consistently between several healthy brains and the brains of a number of patients with a neurodegenerative disease, we can be more confident in generalising our conclusions to all patients with that neurodegenerative disease. Without biological replication to show that differences between the two groups of brains are significantly greater than the differences observed within each group, this generalisation would be difficult to support.

When assessing of the custom-designed connexin microarray developed in this chapter, we use technical replication to confirm that our microarray has relatively low technical variability and therefore has sufficient precision to be useful for investigating connexin expression in neural tissues. We then illustrate the usefulness of our new microarray by comparing connexin gene expression in a single control brain with connexin gene expression in multiple diseased brains. Although due to limited tissue availability, our experiment lacked the biological replication that would be provided by using several control brains from different individuals, the results presented in this chapter lend strong support to using this custom-designed connexin microarray in fully replicated experiments in the future. It is important to note though in reading this chapter that the use of a single control does impose limitations on data interpretation.

5.1 Screening Human Brain for Connexin Expression Using the Custom-Designed Array

The experimental approach used here involved screening affected brain areas for each disease (MC for Huntington's disease, CN for Parkinson's disease and MTG for Alzheimer's disease) against a control sample from the same brain region taken from a normal patient. MC, CN and MTG samples from patient H109 were used as normal controls. HC84, HC91, HC92, HC107, HC109 MC samples were screened against H109 MC sample; PD3, PD6, PD8, PD15, PD16 CN samples were screened against H109 CN sample and AZ30, AZ32, AZ53, AZ54, AZ55 MTG samples were screened against H109 MTG sample. E113 and E118 hippocampus samples were screened against the Alzheimer's disease control as matching hippocampus samples from unaffected patients were not available. Dye reversals were performed to check for dye bias (see Table 34).

Table 34. The samples used in the human brain screening experiments.

Disease	Brain region	Control	Samples
Huntington's	MC	H109	HC84, HC91, HC92, HC107, HC 109
Parkinson's	CN	H109	PD3, PD6, PD8, PD15, PD16
Alzheimer's	MTG	H109	AZ30, AZ32, AZ53, AZ54, AZ55
Epilepsy	Hippocampus	H109	E113, E118

5.1.1 Huntington's disease

5.1.1.1 Controls

The Huntington's disease samples expressed all five positive controls (ubiquitin, GAPDH, HNRPC, TCEA and HPRT), with the exception of HC92, which did not express HPRT. Housekeeping controls were downregulated overall relative to the single control used, with HC107 having the highest level of downregulation of positive controls. Ubiquitin did not appear to change in any of the samples. GAPDH expression was lower in samples HC92 and HC109 compared to control H109 while HNRPC was downregulated in HC92 and showed no change in the others. TCEA mRNA was lower in HC92 and HC107. HPRT appeared to be downregulated in all the four samples in which it was expressed (See Figure 29).

5.1.1.2 Connexins

Connexins that were expressed in the Huntington's samples relative to the five negative control thresholds were Cx43 (both custom- and MWG-designed), Cx46 (MWG-designed), Cx37 (both custom- and MWG-designed), Cx40 (both custom- and MWG-designed), Cx32 (both custom- and MWG-designed), Cx26 (both custom- and MWG-designed), Cx31 (both custom- and MWG-designed), Cx30.3, Cx31.1 (custom-designed only), Cx30 (custom-designed only), Cx25 (MWG-designed), Cx45 (both custom- and MWG-designed), Cx47 (both sets), Cx36 (custom-designed only), Cx31.9 (custom-designed only, expressed in all samples except HC109), Cx40.1 (both sets), Cx30.2 (both sets), Cx62 (both sets).

The custom-designed oligo for Cx43 showed a higher signal in HC84, HC91, HC107 and HC109, and less binding in HC92. The MWG-designed oligo was showed a lower level of binding in HC91, HC92, HC107, and a higher level in HC84 and HC109 compared to the single control used. Cx46 that was represented only by the MWG-designed oligo did not show a change in any of the samples. Cx37 expression was higher for the custom-designed oligo in samples HC92, HC107 and HC109, and for the MWG-designed oligo was higher for the same three samples. Custom-designed oligo for Cx40 did not show a change in message levels, and the MWG-designed oligo for Cx40 showed less Cx40 mRNA in samples HC84, HC91, and HC107. Cx32 message was higher in sample HC91 and lower in HC92 and HC109 for the custom-designed oligo, and for the MWG-designed oligo it was higher in HC91, HC107 and lower in HC92 and HC109. Cx26 mRNA was less in all the samples except HC91 for the custom-designed oligo, and for the MWG-designed it was less in all the samples. Cx31.1 (custom-designed only) did not show a change in any of the samples. Cx30 message (custom-designed only) was decreased in HC91, HC92, HC107.

Cx25 mRNA levels were the same in all of the samples. Cx45 message was higher in HC91, HC107 and HC109 for the custom-designed oligo and for the MWG-designed oligo appeared increased in HC84, HC91, HC107 and downregulated in HC109. The amount of Cx47 mRNA was lower in all the samples for the custom-designed oligo and also for all the samples except HC107 for the MWG-designed oligo. The amount of Cx36 mRNA was not changed in any of the samples relative to the single control used. Cx40.1 mRNA was lower in HC91 and HC107 for the custom-designed oligo, and for the MWG-designed oligo it was lower in all the samples. Cx30.2 and Cx62 were not changed for either the custom-designed oligo or the MWG-designed oligo relative to the control sample. The amount of Cx30.3 mRNA (custom-designed only) was lower in HC109. Cx31.9 mRNA level was lower in HC107 and not changed in the other samples relative to the control. Cx31.9 mRNA was not different to the control except in HC107, where it appeared to be lower (See Figure 30, Figure 31, Figure 32 and Figure 33).

5.1.2 Parkinson's disease

5.1.2.1 Controls

The Parkinson's disease samples expressed four positive controls out of five (ubiquitin, GAPDH, HNRPC and TCEA), with the exception of PD16 that expressed HPRT but not TCEA. PD8 showed the highest level of binding to the five positive control oligonucleotides relative to the human H109 control, and PD15 the lowest. This means PD8 had the greatest mRNA concentration and PD15 the lowest. Ubiquitin mRNA level was higher in PD16 than in the one normal control and appeared downregulated in PD6 and PD15, and to a lesser degree in samples PD3 and PD8. GAPDH was lower in all the samples relative to the control~~and significantly downregulated in samples PD3, PD15 and PD16~~. HNRPC expression was decreased in PD3 and increased in PD6 and PD8, while showing no change in PD15 and PD16. TCEA was upregulated in PD8. HPRT was only expressed in one Parkinson's sample, PD16, but was still at much lower levels than in the single control (See Figure 36).

5.1.2.2 Connexins

Connexins that showed marked expression in the Parkinson's disease samples relative to the five negative control threshold were Cx43 (both custom- and MWG-designed), Cx46 (MWG-designed), Cx37 (both custom- and MWG-designed), Cx40 (both custom- and MWG-designed), Cx32 (custom-designed in all samples, MWG-designed in all samples except PD6), Cx26 (custom-designed in all samples, MWG-designed only in samples PD15 and PD16), Cx31 (both custom- and MWG-designed), Cx30.3 (custom-designed only), Cx31.1 (custom-designed only), Cx30 (custom-designed only), Cx25 (MWG-designed), Cx45 (custom- and MWG-designed), Cx47 (both sets), Cx36 (custom-designed

only), Cx31.9 (custom-designed only), Cx40.1 (both sets, except for PD6 which did not express it), Cx30.2 (custom-designed for all Parkinson's samples - MWG-designed was not expressed in PD6), Cx62 (custom- and MWG-designed).

The binding for the custom-designed oligo for Cx43 was higher in all the disease samples compared to the H109 control sample; the MWG-designed oligo binding was lower in sample PD3 and demonstrated no change in the rest of the samples. Cx46 that was represented only by the MWG-designed oligo did not show a change in any of the samples compared to the normal control. Cx37 expression was increased for the custom-designed oligo in samples PD8, PD15 and PD16, and for the MWG-designed oligo showed higher binding in PD6, PD8, PD15 and PD16. Custom-designed oligo for Cx40 was higher in PD15 compared to the control and showed no change in the others, and the MWG-designed oligo signal was lower in all the samples. Cx32 expression was lower in all samples except PD3 for the custom-designed oligo, and for the MWG oligo it was lower in PD16 relative to the control. Cx26 mRNA signal was lower for all the samples compared to the one control for the custom-designed oligo, and for the MWG-designed oligo it was lower in PD15 and PD16. Cx30.3 mRNA level was higher in PD3, PD6 and PD16; Cx31.1 was expressed al a lower level in PD8. Cx30 binding (custom-designed only) appeared higher in PD3, PD8 and PD15. Cx25 was lower in all samples. Cx45 (custom designed only) showed lower signal in PD15 and no change in others compared to the control. However, Cx45 for the MWG-designed oligo showed higher binding in PD8 and PD15 relative to the control. Cx47. expression was elevated in PD8 and lower in PD16 for the custom-designed oligo relative to the control sample and much lower in PD15 and PD16 for the MWG-designed oligo. Cx36 cDNA binding was higher in PD8 and PD15. Cx40.1 gave lower signal in PD3, PD8 and PD16 for the custom-designed oligo and in PD3, PD8 and PD16 for the MWG-designed oligo. Cx30.2 appeared to show higher expression in PD8 and PD16 for the custom-designed oligo relative to the control sample and at a higher level in PD3, and was reduced in PD16 for the MWG-designed oligo. Cx62 binding was reduced in PD15 and PD16 for the custom-designed oligo and in PD16 for the MWG-designed oligo relative to the control sample. Cx31 showed higher binding in PD3, PD8 and PD16 for the custom-designed oligo and for the MWG-designed it was higher in PD3 and lower in PD16. Cx31.9 mRNA levels were lower in PD6, PD15 and PD16 compared to the control (See Figure 37, Figure 38, Figure 39 and Figure 40).

5.1.3 Alzheimer's disease

5.1.3.1 Controls

The Alzheimer's disease samples showed binding for all five positive control oligonucleotides (ubiquitin, GAPDH, HNRPC, TCEA and HPRT). Ubiquitin binding appeared to be increased in AZ55 but not changed in all the other samples compared to the H109 control. GAPDH expression appeared to

be lower in samples AZ32, AZ53 and AZ54. HNRPC oligonucleotide binding was markedly higher in all the samples except AZ54 relative to the single control sample. TCEA showed lower binding in AZ30 and AZ54, but binding was increased in AZ32. HPRT expression was lower than in the control in all the samples (See Figure 43).

5.1.3.2 Connexins

Connexins that showed marked expression (level of binding compared to the five negative control oligonucleotide based threshold) in the Alzheimer's samples were Cx43 (both custom- and MWG-designed), Cx46 (MWG-designed), Cx37 (both custom- and MWG-designed), Cx40 (both custom- and MWG-designed), Cx32 (both custom- and MWG-designed), Cx26 (custom-designed in all samples and MWG-designed in AZ30, AZ53, AZ55), Cx31 (both custom- and MWG-designed), Cx30.3 (custom-designed only), Cx31.1 (custom- and MWG-designed), Cx30 (custom-designed only), Cx25 (MWG-designed), Cx45 (both custom- and MWG-designed), Cx47 (both sets), Cx36 (custom-designed only), Cx31.9 (custom-designed only), Cx40.1 (both sets), Cx30.2 (both sets), Cx62 (both sets).

Custom-designed oligo for Cx43 gave higher signal for all the Alzheimer's samples compared to the single control, while MWG-designed oligonucleotides showed reduced binding for AZ30 and an increase for the other four samples. Cx46 that was represented only by the MWG-designed oligo showed higher expression in AZ32 and AZ55 compared to the control. Cx37 binding was higher for the custom-designed oligo in all samples except AZ30, and for the MWG-designed oligonucleotide was higher in samples AZ32, AZ53, AZ55. The custom-designed oligo for Cx40 showed higher binding in AZ32 and AZ53, while the MWG-designed oligo was not changed in any of the samples relative to the control. Cx32 binding was higher in all the samples for both oligonucleotides. Cx26 mRNA was lower in all the samples except AZ32 for the custom-designed oligo, and for the MWG-designed, was reduced in the three samples where it was expressed (AZ30, AZ53, AZ55) compared to the control. Cx31.1 (custom-designed only) had lower expression in AZ32 and AZ53. Cx30 (custom-design oligonucleotide only) was higher in AZ30, AZ53, and was decreased in AZ54 and AZ55. Cx25 expression was reduced in samples AZ53 and AZ54. Cx45 binding was increased in all the samples except AZ55 for the custom-designed oligonucleotide and for the MWG the binding was higher in all the samples relative to the control. Cx47 produced a higher signal for all the samples for both oligos. Cx36 expression was higher for AZ53, AZ54 and AZ55. Cx40.1 binding was higher for AZ30 and AZ55 for the custom-designed oligo, and for the MWG-designed oligo it was reduced in AZ53 and increased in AZ55 relative to the control sample. For the custom-designed oligonucleotide Cx30.2 had a lower signal in AZ30, AZ32, and AZ53, but a higher signal in AZ55 and was unchanged for AZ54. For the MWG-designed oligonucleotide Cx30.2 was unchanged in all samples. Cx62 expression was increased in AZ30, AZ54, AZ55 for both oligonucleotides, and decreased in AZ53 for the custom-

designed oligo. Cx31 binding was increased in AZ32, AZ53 and AZ55 for the custom-designed oligonucleotide and also in AZ30 and AZ55 for the MWG-designed oligonucleotide. Cx30.3 was increased in AZ55. Cx31.9 had higher levels of expression in AZ30 and lower in AZ32 (See Figure 44, Figure 45, Figure 46 and Figure 47).

5.1.4 Epilepsy

5.1.4.1 Controls

The epilepsy samples expressed mRNA for all five positive control genes (ubiquitin, GAPDH, HNRPC, TCEA and HPRT). Ubiquitin expression was higher in E118 compared to the H109 normal control sample. HPRT was decreased in E113 and E118, while other positive controls were unchanged relative to the normal control brain sample H109 (See Figure 50).

5.1.4.2 Connexins

Connexins that showed marked expression (level of binding compared to the five negative control oligonucleotide based threshold) in the Epilepsy samples were Cx43 (both custom- and MWG-designed), Cx46 (MWG-designed), Cx37 (both custom- and MWG-designed), Cx40 (both custom- and MWG-designed), Cx32 (both custom- and MWG-designed), Cx26 (custom-designed only), Cx31 (both custom and MWG-designed), Cx30.3 (custom-designed only), Cx31.1 (custom- and MWG-designed), Cx30 (custom-designed only), Cx25 (MWG-designed), Cx45 (both custom- and MWG-designed), Cx47 (both sets), Cx36 (custom-designed only), Cx31.9 (custom-designed only), Cx40.1 (both sets), Cx30.2 (both sets), Cx62 (both sets).

Both custom-designed and the MWG-designed oligos for Cx43 demonstrated higher binding than the one normal control for all the samples. Cx46, which was represented only by the MWG-designed oligo, showed no change. Cx37 was higher for both oligos in E113 and E118 compared to the control. Both custom-designed oligo and MWG-designed oligo for Cx40 gave lower signal in E113, and did not change in E118. Cx32 binding was higher in all the samples for both oligonucleotides. Cx26 (custom-designed only) was expressed at a lower level in E113 but not in E118 relative to the control sample. Cx31.1 (custom-designed only) was not changed. Cx30 (custom-designed only) was higher in all the samples. Cx25 expression was lower in sample E118 but not in E113. Cx45 binding was higher in both samples for both oligonucleotides. Cx47, Cx30 and Cx62 were not changed for both sets of oligos compared to the control sample. Cx36 was higher in both sets. Cx40 had a higher level of binding in E113 and did not change in E118 in both sets. (See Figure 51, Figure 52, Figure 53 and Figure 54).

5.1.5 Summary

All arrays demonstrated higher levels of Cy3 signal as opposed to Cy5 signal, which was especially pronounced at the lower signal levels. The custom-designed oligos for Cx46 and Cx25, and the MWG-designed oligos for Cx50, Cx36 and Cx31.1 consistently demonstrated high levels of what appeared to be non-specific binding, being considerably above the level of the brightest positive control.

Housekeeping controls (the five positive control genes ubiquitin, GAPDH, HNRPC, TCEA and HPRT) on average had lower binding levels compared to binding levels for their respective normal control regions of the brain for each disease. Connexins on average showed higher levels in Alzheimer's disease and epilepsy and no change in Parkinson's and Huntington's disease compared to their respective normal control regions. Epilepsy samples showed the lowest overall signal relative to negative controls oligonucleotides, and Huntington's disease the highest indicating higher mRNA levels overall in the Huntington's disease samples.

5.1.5.1 Controls

Ubiquitin oligonucleotide showed the highest signal in MC, CN and hippocampus, but GAPDH gave a higher signal in MTG. HNRPC oligonucleotide gave intermediate signal in all regions while HPRT gave the lowest signal in CN and MC, and TCEA1 in MTG and hippocampus (See Figure 57).

Ubiquitin and HNRPC binding was higher overall compared to the normal control. GAPDH, TCEA1 and HPRT were lower overall. HPRT showed the most markedly decreased positive control binding relative to the normal control samples for each disease. TCEA1 was lower in Huntington's and epilepsy and unchanged in others compared to their respective control. HNRPC was upregulated in Alzheimer's and unchanged in others. GAPDH was downregulated in Huntington's, Parkinson's and Alzheimer's and unchanged in epilepsy relative to the respective control for each. Ubiquitin was upregulated in epilepsy and unchanged in others (See Figure 55).

5.1.5.2 Connexins

Eighteen connexins were expressed in all diseases (Figures 58 and 59) and of these eleven showed expression in both sets, five in the custom-designed oligonucleotide set only and two in the MWG-designed oligonucleotide set only in all diseases except epilepsy. In epilepsy 12 connexins showed expression in both sets, four in the custom-designed only and two in the MWG-designed only.

Cx43, Cx37, Cx40, Cx32, Cx26, Cx45, Cx47, Cx31, Cx40.1, Cx62 and Cx30.2 were expressed in both sets in all diseases, Cx31.9, Cx36, Cx30, Cx30.3, Cx31.1 in the custom-designed only and Cx46

and Cx25 in the MWG-designed set only. Cx30 was expressed in both sets in epilepsy and in all other diseases was expressed in the custom-designed set only.

For all diseases on average Cx43, Cx37, Cx32, Cx30, Cx45, Cx36 and Cx31 mRNA levels were higher relative to the sample from each of their respective control brain regions. Cx26 and Cx31.9 were lower. Cx40 and Cx40.1 were lower in the MWG-designed set and unchanged in the custom-designed set. Other connexins were unchanged relative to their control region samples., Cx43 binding was higher in the disease sample compared to control in the custom-designed set and lower than the control in the MWG-designed set for Huntington's and Parkinson's diseases. Cx30 was downregulated in the custom-designed set and was upregulated in the MWG-designed set for Huntington's disease. Other connexins did not show changes in opposite directions in both sets of oligos (See Figure 59, Figure 60).

5.2 Screening Human Brain Tissue Using the Commercially Designed Illumina Array.

To commercially validate our custom-designed connexin microarray chip, 18 samples (one control and five disease samples for each of Huntington's (MC) Parkinson's (CN) and Alzheimer's (MTG) diseases), were hybridised to commercial Illumina Sentrix® Human-6 BeadChip arrays.

Controls

5.2.1.1 Huntington's disease

All in-built process controls were positive and labelling (negative) controls were negative as expected in all samples., In HC84 the negative control signal was so low as to be undetectable. Cy3 hybridisation controls showed the highest level of binding, followed sequentially by the housekeeping controls, low stringency, biotin and finally negative controls. All of the controls showed a higher signal level in the disease samples as compared to their respective brain region control samples. The exceptions were the housekeeping controls that were much lower in the HC107 and HC109 samples compared to their control region..

The positive control genes included unbiquitin, GAPDH, beta 2A tubulin, beta 2B tubulin, beta 2C tubulin, thioredoxin, beta-actin, HPRT, HNRPC, TCEA1 and ribosomal protein S9 (RPS9).

Ubiquitin was the positive control with the highest level of expression in Huntington's disease, followed by beta-actin, TCEA gave the lowest signal and HNRPC the second lowest. These are as compared to the negative oligonucleotide binding levels.

The housekeeping control mRNA levels were lower in the disease samples compared to the normal control, with the exception of ubiquitin, which showed a slightly higher level, and the ribosomal protein S9, which was unchanged. The control mRNA with the lowest level relative to the control sample was beta-actin, followed by HPRT (See Figure 56, Figure 58).

5.2.1.2 Parkinson's disease

All in-built process controls were positive and labelling (negative) controls were negative as expected in all samples. In PD16 the negative control signal was so low as to be undetectable. Cy3 hybridisation controls showed the highest level of binding, followed sequentially by the housekeeping controls, low stringency, biotin and finally negative controls. The controls did not show any notable up-

or downregulation, with the exception of sample PD15, in which all the controls were upregulated with the exception of housekeeping controls which were downregulated.

Ubiquitin was the positive control with the highest expression level, followed by beta 2B tubulin; TCEA gave the lowest signal level and HNRPC the second lowest. These are as compared to the negative oligonucleotide binding levels.

The positive control mRNA levels did not show a consistent pattern of change. Beta 2B tubulin, thioredoxin, TCEA1 and ribosomal protein S9 were higher in the disease samples compared to the normal control, and the levels of the remaining positive controls were decreased. The control mRNA with the highest level relative to the control sample was ribosomal protein S9; HPRT had the lowest level compared to the control (See Figure 56, Figure 58).

5.2.1.3 Alzheimer's disease

All in-built process controls were positive and labelling (negative) controls were negative as expected in all samples. Cy3 hybridisation controls showed the highest level of binding, followed sequentially by the housekeeping controls, low stringency, biotin and finally negative controls. All of the controls showed a lower signal level in the disease samples as compared to their respective brain region control samples

Ubiquitin was the positive control with the highest expression level, followed by beta 2B tubulin; TCEA gave the lowest signal level and HNRPC the second lowest relative to the negative control threshold.

The mRNA levels of HPRT and thioredoxin were considerably lower in the disease samples as compared to the negative control sample. Beta 2A tubulin, beta-actin, and TCEA1 levels were also decreased. The GAPDH levels were the least changed between the disease samples and the normal control (See Figure 56, Figure 58).

5.2.2 Connexins

5.2.2.1 Huntington's disease

Connexins that were expressed in all Huntington's disease samples included Cx43, Cx37, Cx32, Cx26, Cx30, Cx45, Cx47 and Cx31.9. Cx40 and Cx40.1 were expressed in the control sample and three of the disease samples (HC84, HC92 and HC109). Cx40.1 was expressed in the control sample and one disease sample (HC107).

Connexins that appeared to be consistently higher in all of the disease samples compared to the single control sample included Cx40 and Cx45; connexins that appeared to be consistently lower in all disease samples included Cx26 and Cx47. The rest of the connexins showed higher levels is some samples but lower levels in others relative to the control sample. Connexins that showed the strongest decrease in mRNA levels relative to the control sample were Cx26 and Cx30. The biggest increase relative to control was demonstrated by Cx45 and Cx37, with Cx31.9 showing the least change between the control and disease samples (See Figure 34).

5.2.2.2 Parkinson's disease

Connexins that were expressed in all Parkinson's disease samples included Cx43, Cx37, Cx40, Cx32, Cx26, Cx30, Cx45, Cx47 and Cx31.9. Cx46 was expressed only in the control sample and in the PD6 disease sample. Cx30.2 was expressed in the control, PD3 and PD16 samples.

Connexins that appeared to be consistently higher in all of the disease samples compared to the single control sample included Cx43 and Cx37; connexins that appeared to be consistently lower in all disease samples included Cx26, Cx30 and Cx31.9, the other connexins did not have a consistent pattern of change. Connexins that showed the most significant downregulation were Cx26 and Cx32; the most significant upregulation was demonstrated by Cx43 and Cx37, and Cx45 showed the least change between the control and disease samples (See Figure 41).

5.2.2.3 Alzheimer's disease

Connexins that were expressed in all Alzheimer's disease samples included Cx43, Cx32, Cx26, Cx30, Cx45, Cx47 and Cx31.9. Cx37 was expressed in four samples (excluding control and AZ30). Cx40 was expressed in the control sample, AZ32, AZ53 and AZ55.

Connexins with a higher mRNA level in all of the disease samples compared to the normal control sample were Cx40, Cx32, Cx45, Cx47, and Cx31.9. None of the connexins had a lower level of expression in all of the disease samples. Cx43, Cx26 and Cx30 showed an inconsistent pattern of change. Connexins with the highest mRNA level in the disease samples were Cx43 and Cx37; Cx26 was the only connexin with a reduced average level of expression, and Cx30 showed the least change between the control and disease samples (See Figure 48).

5.2.3 Inflammatory markers

Of the inflammatory markers investigated, CD11A and CD11B, IL-1β and IL-6 were found in Alzheimer's Huntington's and Parkinson's disease tissue. TNF-α and IL-10 was present in Huntington's disease only; and CD11C, interferon-gamma and colony stimulating factor 2 (granulocyte-macrophage) was not present in any of the samples.

5.2.3.1 Huntington's disease

The inflammatory markers found in Huntington's disease motor cortex were TNF-α, CD11A CD11B, IL-1β, IL-6 and IL-10. None of the inflammatory markers were expressed all five cases, but they were all found in two – four cases. The control sample expressed TNF-α, IL-1β, IL-6 and IL-10 at levels above the negative control threshold, but not CD11A and CD11B. IL-1β was expressed in the control sample and all the disease samples except HC109; CD11A and CD11B were expressed in four disease samples (except HC84). IL-6 was expressed in four samples also (except HC84 and HC109). TNF-α was expressed in three samples (control, HC84 and HC107) and IL-10 only in two (control and HC84).

IL-6 was increased compared to the control sample in three of disease samples in which it was expressed. CD11B was the least expressed of all the markers (three out of four disease samples, the fourth one showing slight increase compared to the control sample). CD11A was lower in all the samples in which it was expressed. TNF-α was higher to a small extent in the two disease samples in which it was expressed and IL-1β was at very high levels in one sample and at lower levels in three others. IL-10 was only expressed in one sample where it was slightly higher.

The overall level of expression of the inflammatory markers was low compared to both connexins and positive controls. Overall, CD11B showed the highest mRNA level of the inflammatory markers and IL-10 the lowest (See Figure 35).

5.2.3.2 Parkinson's disease

The inflammatory marker genes expressed in Parkinson's disease were CD11A, CD11B, IL-1β and IL-6. CD11A and CD11B were expressed in all of the samples. The control sample expressed CD11A and CD11B, but not IL-1β or IL-6. IL-1β was expressed in four samples (not in the control and PD15). IL-6 was expressed in four samples (except control and PD3).

All of the inflammatory markers were higher overall compared to the normal control sample (CD11A was lower in PD8 and slightly lower in PD3). IL-6 was expressed to the greatest extent.

CD11B showed the highest expression level compared to negative control oligonucleotides, followed by IL-6, CD11A and IL-1β (See Figure 42).

5.2.3.3 Alzheimer's disease

The inflammatory marker genes expressed in Alzheimer's disease were CD11A, CD11B, IL-1β and IL-6. CD11B was expressed in all of the samples. The control sample expressed CD11B and IL-1β, but not CD11A or IL-6. CD11A was expressed in all of the disease samples (but not in the control). IL-1β was expressed in the control and AZ30 and AZ53 samples. IL-6 was expressed in four samples (excluding AZ30 and the control).

CD11A and CD11B were at higher levels, IL-1β was lower than the normal control brain in both of the Alzheimer's samples in which it was expressed, and IL-6 was higher than the normal control sample in three out of the four Alzheimer's disease samples in which it was identified.

CD11B shows the highest expression level compared to the negative control oligonucleotides, followed by CD11A, IL-6 and IL-1β (See Figure 49).

5.2.4 Summary

Connexins expressed in the areas of the brain secondarily affected in the neurological disorders Huntington's Alzheimer's and Parkinson's as analysed on the Illumina array included Cx43, Cx37, Cx32, Cx26, Cx30, Cx45, Cx47, Cx31.9 and Cx40. Cx40.1 was expressed in the motor cortex in Huntington's disease, while Cx30.2 and Cx46 were expressed in the caudate nucleus in Parkinson's. CN expressed 11 connexins, MC expressed ten connexins, and MTG expressed nine. The probe for Cx45 consistently showed the highest signal in all diseases, and Cx40 gave the lowest signal in Alzheimer's and Huntington's disease, and the second lowest in Parkinson's disease, followed by Cx46.

Huntington's disease MC showed the lowest level of connexins compared to its normal control region, and Alzheimer's – the most highest level.

Inflammatory markers were expressed at lower levels compared to positive control oligonucleotides and connexin levels. Of the inflammatory markers CD11B was expressed at the highest level in all

diseases, and TNF-α and IL-10, which were only detected in Huntington's disease, gave the lowest signal. IL-10 was detected at a level lower than that of the negative controls for the disease.

Huntington's disease samples showed the lowest level of housekeeping controls relative to its control region sample, and the Parkinson's sample showed the least down regulation. No housekeeping oligonucleotide control was higher than the respective control region sample for all diseases. Housekeeping controls at higher levels overall were ubiquitin, beta 2A tubulin and ribosomal protein S9. The lowest expressed housekeeping control in all samples was HPRT.

5.2.5 Connexin expression relative to cell types

In the present study connexins fall in the following pattern of distribution by cell type. Of the connexins that were expressed in all three sets of oligonucleotides (custom- and MWG-designed sets on the custom array and the Illumina array) Cx45 and Cx32 have been reported to occur in neurons; Cx43, Cx30, Cx45, Cx40 and possibly Cx26 in astrocytes; Cx32, Cx30.2 and Cx47 in oligodendrocytes; Cx43 and Cx36 in microglia; Cx37, Cx45, Cx43, Cx40 and Cx32 in brain endothelial cells and Cx31.9 in cerebral cortex. Connexins expressed in both set of oligos on the custom-designed array include Cx62 (neurons), Cx31 (neuronal cell lines) and Cx40.1 (expressed in pancreas, kidney, skeletal muscle, liver, placenta, and heart). Connexins expressed only in the custom-designed set include Cx36 (neurons and microglia), Cx31.1 (neurons) and Cx30.3 (mouse, rat, and rabbit kidney, epidermis and ovarian cells, but not in the brain). Connexins expressed only in the MWG-designed oligo set include Cx46 (astrocytes) and Cx25 (embryonic stem cells). Three of the connexins detected on the arrays (Cx30.3, Cx40.1 and Cx25) have not been previously reported in neural tissues.

Of the connexins that were expressed in neurons, Cx31 and Cx36 were higher than control sample levels in all the diseases investigated. Cx31.1 was unchanged in all the diseases. Cx45 mRNA levels were higher in Huntington's, Alzheimer's disease and epilepsy, and unchanged in Parkinson's disease. Cx32 mRNA levels were lower in Huntington's and Parkinson's disease but higher in Alzheimer's disease and epilepsy. Cx62 was higher compared to the control sample in Alzheimer's disease and unchanged in the other diseases.

Of the connexins that have been found in oligodendrocytes, Cx30.2 was not changed. Cx32 mRNA levels were lower in Huntington's and Parkinson's disease compared to their respective control sample, and higher in Alzheimer's disease and epilepsy. Cx47 was lower in Huntington's and Parkinson's disease, higher in Alzheimer's disease, but unchanged in epilepsy.

Of the connexins that were detected in astrocytes, Cx43 was at higher levels in all the diseases compared to each respective control sample. Cx26 was lower in all the diseases except epilepsy where it was unchanged. Cx45 was higher in Huntington's, Alzheimer's disease and epilepsy, and unchanged in Parkinson's disease. Cx46 expression was higher in Alzheimer's disease and unchanged in the other diseases. Cx30 mRNA levels were lower in Huntington's disease, higher in Parkinson's disease and epilepsy but unchanged in Alzheimer's disease. The expression of Cx40 did not show a consistent pattern in the three oligo sets.

Cx43 and Cx36 that occur in microglia were at higher levels in all the diseases compared to each respective control sample. Of the connexins which had been detected in brain endothelial cells, Cx43 and Cx37 mRNA levels were higher in all the diseases relative to each respective control region sample. Cx40 did not show a clear pattern of differential expression. Cx45 was at higher levels in Huntington's, Alzheimer's disease and epilepsy, but unchanged in Parkinson's disease. Cx32 was appeared to be at lower levels in Huntington's and Parkinson's disease, and higher levels in Alzheimer's disease and epilepsy compared to each control sample.

Cx31.9 has been found in cerebral cortex and was downregulated in Parkinson's disease and epilepsy, but unchanged in Huntington's and Alzheimer's disease.

Of the connexins whose localisation has not been previously reported in the central nervous system, Cx25 was downregulated in Parkinson's, Alzheimer's disease and epilepsy, but unchanged in Huntington's disease. Cx40.1 was downregulated in Huntington's and Parkinson's disease and unchanged in Alzheimer's disease and epilepsy. Cx30.3 appeared to be reduced in Huntington's relative to the single control, increased in three of five Parkinson's disease samples (and marginally lower in two), even more increased in three out of five Alzheimer's patients relative to the Alzheimer's control sample, and no real change in the epilepsy samples. These connexins warrant further investigation.

5.2.6 Platform comparison

The Illumina platform has been experimentally tested in a number of studies and has been shown to have good reproducibility and concordance with other platforms. It has demonstrated the ability to pick up both large (Shi et al., 2006) and subtle (Pedotti et al., 2008) changes in gene expression. The custom array has a narrower focus on connexin genes and is suitable for quick screening which can be performed independently without complicated equipment. While it does not have as many in-built controls at different levels (such as for hybridisation and labelling), the concordance of the results obtained from our custom array gives a degree of confidence in its performance.

The custom-made array was capable of consistently detecting the same changes detected with the Illumina array in spite of variable RNA quality and small overall fold changes. MWG-designed oligos however appeared to be less sensitive in picking up connexin expression in the human brain than custom-designed oligos. There was more concordance between our custom-designed oligos and Illumina oligos than between MWG-designed oligos and Illumina oligos. Custom-designed oligos demonstrated a more consistent pattern of detection of differentially expressed genes, both within the array and between the custom-designed and the Illumina array.

The degree of consistency between different oligo sets appeared to be related to RNA quality. The Parkinson's disease samples had the highest variability with the least concordance between the two sets on the custom-designed array and the Illumina array. The Parkinson's disease samples also had the highest overall range of RNA quality (RIN from 5.3 for PD15 to 8.8 for PD6). The custom-designed chip detected a higher number of connexins than the Illumina chip. We do not know the algorithms used to set the detection levels on the Illumina array and there will be differences in probe sequences which may account for some variability between results obtained from alternative platforms (Barnes et al., 2005).

Custom-designed probes had a better inter-array reproducibility and detection level for genes definitely present in the sample (MWG-designed Cx43 probe gave very low signal in the human tissue experiments). As we do not know the MWG probe sequences, we cannot be sure whether the MWG probes are in fact assaying the same transcripts as the custom-designed probes nor how specific they are. The results of the human brain tissue experiments suggest that the data from the custom-designed probes have more validity than the data from the MWG-designed probes.

In this study there was only a single control for each brain region secondarily effected in Alzheimer's Parkinson's and Huntington's disease. Relative to this single control, some apparent trends have been observed in the expression of connexins and inflammatory markers and these now warrant further investigation. The custom array does however appear to be reliable and consistent, providing an efficient platform for further analysis of connexin expression from different brain regions, and in a greater number of samples.

.

Tables

Table 35. Differential expression of housekeeping controls in Huntington's disease, custom-designed array. Each of the five Huntington's disease samples was screened against the normal control sample. LogDif - log difference between the disease sample and the control sample values. FC - fold change between the disease sample and the control sample values. Colours: orange – upregulated; green – downregulated, - grey – no change.

	HC84				HC91				HC92				HC107				HC109			
Name	**HC84**	**H109**	**LogDif**	**FC**	**HC91**	**H109**	**LogDif**	**FC**	**HC92**	**H109**	**LogDif**	**FC**	**HC107**	**H109**	**LogDif**	**FC**	**HC109**	**H109**	**LogDif**	**FC**
HNRPC	2.36	2.16	0.20	1.15	2.05	2.18	-0.13	0.91	1.87	2.18	-0.32	0.80	2.42	2.29	0.13	1.09	1.98	1.87	0.11	1.08
Ubiquitin	4.06	4.09	-0.03	0.98	3.86	3.93	-0.07	0.95	3.81	3.83	-0.02	0.98	5.25	5.14	0.12	1.08	3.93	3.81	0.12	1.09
HPRT	0.15	0.79	-0.64	0.64	0.26	0.71	-0.46	0.73					0.47	1.68	-1.21	0.43	0.52	1.75	-1.23	0.43
GAPDH	3.21	3.18	0.03	1.02	3.13	3.19	-0.06	0.96	3.08	3.50	-0.41	0.75	3.74	3.82	-0.08	0.94	3.22	2.81	-0.58	0.67
TCEA1	1.66	1.81	-0.15	0.90	1.38	1.63	-0.25	0.84	1.58	2.19	-0.61	0.66	1.32	2.42	-1.10	0.47	2.19	1.76	-0.11	0.93

Table 36. Differential expression of connexins in Huntington's disease, custom-designed set, includes only the connexins that are expressed on the custom-designed array that are also expressed on the Illumina array. Each of the five Huntington's disease samples was screened against the normal control sample. LogDif - log difference between the disease sample and the control sample values. FC - fold change between the disease sample and the control sample values. Colours: orange – upregulated; green – downregulated, - grey – no change.

	HC84				HC91				HC92				HC107				HC109			
Connexins	**HC84**	**H109**	**LogDif**	**FC**	**HC91**	**H109**	**LogDif**	**FC**	**HC92**	**H109**	**LogDif**	**FC**	**HC107**	**H109**	**LogDif**	**FC**	**HC109**	**H109**	**LogDif**	**FC**
a1 - Cx43	2.17	-1.17	0.88	1.84	1.87	1.43	0.44	1.35	1.54	2.46	-0.92	0.53	2.11	1.73	0.39	1.31	3.18	2.61	0.57	1.48
a4 - Cx37	2.91	0.58	-0.13	0.91	3.05	2.94	0.11	1.08	3.50	3.00	0.51	1.42	2.72	2.31	0.41	1.33	2.93	2.68	0.25	1.19
a5 - Cx40	3.35	0.91	-0.02	0.98	3.31	3.25	0.06	1.04	3.25	3.27	-0.02	0.99	3.51	3.45	0.06	1.04	2.75	2.76	-0.01	0.99
b1 - Cx32	3.68	1.24	-0.02	0.98	2.40	1.91	0.48	1.40	3.30	4.36	-1.06	0.48	3.32	3.44	-0.12	0.92	2.61	3.18	-0.57	0.67
b2 - Cx26	2.13	-0.04	-0.29	0.82	2.17	2.31	-0.13	0.91	1.81	2.95	-1.14	0.45	1.92	2.17	-0.25	0.84	2.41	2.78	-0.38	0.77
b6 - Cx30	2.40	-0.26	0.19	1.14	2.67	1.85	-0.83	0.56	1.61	2.50	-0.89	0.54	2.13	1.54	-0.59	0.66	2.47	2.32	0.15	1.11
c1 - Cx45	2.50	0.02	0.01	1.01	2.79	2.36	0.43	1.35	2.81	2.78	0.03	1.02	2.94	2.56	0.38	1.30	2.79	2.51	0.28	1.21
c2 - Cx46.6/47	2.56	1.02	-0.93	0.53	2.34	3.02	-0.68	0.62	2.55	3.20	-0.64	0.64	2.48	2.70	-0.21	0.86	2.52	2.84	-0.32	0.80
d3 - Cx31.9	2.44	-0.03	0.01	1.00	2.25	2.27	-0.02	0.98	2.33	2.45	-0.12	0.92	2.12	2.53	-0.40	0.76				

Table 37. Differential expression of connexins in Huntington's disease, MWG-designed set, includes only the connexins that are expressed on the custom-designed array that are also expressed on the Illumina array. Each of the five Huntington's disease samples was screened against the normal control sample. LogDif - log difference between the disease sample and the control sample values. FC - fold change between the disease sample and the control sample values. Colours: orange – upregulated; green – downregulated, - grey – no change.

	HC84				HC91				HC92				HC107				HC109			
Connexins	HC84	H109	LogDif	FC	HC91	H109	LogDif	FC	HC92	H109	LogDif	FC	HC107	H109	LogDif	FC	HC109	H109	LogDif	FC
a1 - Cx43M	4.42	1.42	0.54	1.45	4.60	4.91	-0.31	0.81	3.78	5.06	-1.28	0.41	4.12	4.34	-0.22	0.86	2.59	2.01	0.58	1.50
a4 - Cx37M	2.75	0.25	0.03	1.02	2.90	2.73	0.18	1.13	3.03	2.56	0.46	1.38	3.10	2.25	0.85	1.80	2.91	2.55	0.36	1.28
a5 - Cx40M	4.36	2.16	-0.27	0.83	4.32	4.93	-0.61	0.65	4.50	4.61	-0.12	0.92	4.28	4.64	-0.37	0.78	3.11	3.20	-0.09	0.94
b1 - Cx32M	0.84	-1.83	0.21	1.15	2.70	2.23	0.47	1.39	1.69	2.62	-0.93	0.53	0.96	0.63	0.33	1.26	2.02	2.57	-0.56	0.68
b2 - Cx26M	0.66	-1.20	-0.61	0.66	0.62	1.27	-0.64	0.64	0.68	1.93	-1.25	0.42	0.38	1.29	-0.91	0.53	1.85	2.25	-0.40	0.76
c1 - Cx45M	1.34	-1.46	0.34	1.26	1.80	1.13	0.67	1.59	1.64	1.49	0.14	1.10	1.48	1.02	0.45	1.37	2.46	2.07	0.40	1.32
c2 - Cx46.6/47M	3.35	1.25	-0.37	0.77	3.62	3.88	-0.26	0.84	3.64	4.12	-0.48	0.72	3.21	3.20	0.00	1.00	2.81	3.11	-0.30	0.81

Table 38. Differential expression of connexins in Huntington's disease, custom-designed set, includes the connexins that are expressed on the custom-designed array, but not on the Illumina array. Each of the five Huntington's disease samples was screened against the normal control sample. LogDif - log difference between the disease sample and the control sample values. FC - fold change between the disease sample and the control sample values. Colours: orange – upregulated; green – downregulated, - grey – no change.

	HC84				HC91				HC92				HC107				HC109			
Connexin	HC84	H109	LogDif	FC	HC91	H109	LogDif	FC	HC92	H109	LogDif	FC	HC107	H109	LogDif	FC	HC109	H109	LogDif	FC
d2 - Cx36	2.61	2.58	0.03	1.02	2.07	1.94	0.13	1.09	2.42	2.37	0.05	1.04	2.34	2.09	0.25	1.19	2.17	2.17	0.28	1.21
b3 - Cx31	1.91	1.87	0.04	1.03	1.99	1.60	0.38	1.30	2.09	2.37	0.14	1.10	2.06	1.90	0.16	1.12	2.09	2.09	-0.01	0.99
b4 - Cx30.3	3.41	3.44	-0.03	0.98	3.63	3.78	-0.16	0.90	3.58	2.37	-0.06	0.96	3.19	3.37	-0.19	0.88	2.95	2.95	-0.37	0.77
b5 - Cx 31.1	2.56	2.56	0.00	1.00	2.55	2.58	-0.03	0.98	2.86	2.37	0.01	1.01	2.37	2.34	0.03	1.02	2.46	2.46	-0.08	0.94
d4 - Cx40.1	1.68	1.86	-0.17	0.89	1.14	1.57	-0.43	0.74	1.72	2.37	-0.10	0.93	1.75	2.07	-0.32	0.80	2.02	2.02	0.16	1.11
a10 - Cx62	3.39	3.34	0.05	1.04	3.20	3.42	-0.22	0.86	3.28	2.37	0.01	1.01	3.05	3.21	-0.16	0.90	3.69	3.69	0.01	1.01
c3 - Cx31.3(30.2)	4.66	4.64	0.02	1.01	4.50	4.56	-0.05	0.97	4.81	2.37	0.13	1.09	4.42	4.47	-0.06	0.96	4.35	4.35	-0.12	0.92

Table 39. Differential expression of connexins in Huntington's disease, MWG-designed set, includes the connexins that are expressed on the custom-designed array, but not on the Illumina array. Each of the five Huntington's disease samples was screened against the normal control sample. LogDif - log difference between the disease sample and the control sample values. FC - fold change between the disease sample and the control sample values. Colours: orange – upregulated; green – downregulated, - grey – no change.

	HC84				HC91				HC92				HC107				HC109			
Connexin	**HC84**	**H109**	**LogDif**	**FC**	**HC91**	**H109**	**LogDif**	**FC**	**HC92**	**H109**	**LogDif**	**FC**	**HC107**	**H109**	**LogDif**	**FC**	**HC109**	**H109**	**LogDif**	**FC**
a3 - Cx46M	1.59	1.83	-0.24	0.85	2.38	2.49	-0.12	0.92					1.47	1.44	0.03	1.02	2.60	2.60	0.05	1.04
b3 - Cx31M	4.04	3.95	0.09	1.07	4.43	4.24	0.19	1.14	4.07	2.37	0.06	1.05	4.03	3.88	0.15	1.11	4.34	4.34	0.17	1.13
b7 - Cx25M	1.98	2.10	-0.12	0.92	2.41	2.43	-0.03	0.98	2.37	2.37	0.03	1.02	2.50	2.43	0.07	1.05	2.50	2.50	0.26	1.20
d4 - Cx40.1M	1.57	2.10	-0.53	0.69	1.62	1.94	-0.32	0.80	1.94	2.37	-0.18	0.88	1.69	1.92	-0.23	0.86	2.16	2.16	-0.24	0.85
a10 - Cx62M	3.19	3.15	0.04	1.03	3.30	3.27	0.04	1.03	3.17	2.37	-0.02	0.98	3.25	3.21	0.04	1.03	3.18	3.18	0.11	1.08
c3 - Cx31.3(30.2)M	1.08	1.20	-0.12	0.92	1.40	1.36	0.04	1.03	1.32	2.37	-0.18	0.88	1.13	1.22	-0.09	0.94	1.97	1.97	-0.39	0.77

Table 40.Differential connexin expression in Huntington's disease, Illumina array. Five Huntington's disease samples were screened against one control sample. LogDif - log difference between the disease sample and the control sample values. FC - fold change between the disease sample and the control sample values.

	HC84				HC91			HC92			HC107			HC109		
Name	**H109**	**HC84**	**LogDif**	**FC**	**HC91**	**LogDif**	**FC**	**HC92**	**LogDif**	**FC**	**HC107**	**LogDif**	**FC**	**HC109**	**LogDif**	**FC**
a1 - Cx43	12.24	13.19	0.94	1.92	12.27	0.02	1.01	11.41	-0.83	0.56	12.53	0.29	1.22	13.11	0.86	1.82
a4 - Cx37	6.64	6.57	-0.07	0.95	6.85	0.21	1.16	7.15	0.51	1.42	7.56	0.92	1.90	7.28	0.64	1.56
a5 - Cx40	6.26	6.28	0.03	1.02			1.00	6.39	0.14	1.10			1.00	6.45	0.19	1.14
b1 - Cx32	7.50	7.40	-0.10	0.93	7.67	0.17	1.13	6.50	-1.00	0.50	7.61	0.11	1.08	6.77	-0.73	0.60
b2 - Cx26	8.35	7.72	-0.63	0.65	7.77	-0.59	0.67	6.97	-1.38	0.38	7.37	-0.98	0.51	7.37	-0.99	0.50
b6 - Cx30	10.95	11.00	0.05	1.03	10.18	-0.77	0.58	9.47	-1.48	0.36	10.49	-0.46	0.73	10.80	-0.15	0.90
a7 - Cx45	13.63	13.82	0.19	1.14	14.51	0.88	1.85	13.83	0.20	1.15	14.21	0.58	1.49	14.33	0.71	1.63
a12 - Cx46.6/47	9.44	8.62	-0.82	0.57	8.82	-0.62	0.65	9.00	-0.44	0.74	9.28	-0.16	0.90	8.99	-0.45	0.73
c1 - Cx31.9	7.32	7.43	0.11	1.08	7.47	0.15	1.11	7.44	0.12	1.09	7.31	0.00	1.00	6.58	-0.74	0.60
d4 - Cx40.1	6.23										6.85	0.63				

..

Table 41. Differential expression of inflammatory markers in Huntington's disease, Illumina array. Five Huntington's disease samples were screened against one control sample. LogDif - log difference between the disease sample and the control sample values. FC - fold change between the disease sample and the control sample values.

		HC84			HC91			HC92			HC107			HC109		
Name	**H109**	**HC84**	**LodDif**	**FC**	**HC91**	**LodDif**	**FC**	**HC92**	**LodDif**	**FC**	**HC107**	**LodDif**	**FC**	**HC109**	**LodDif**	**FC**
TNFa	5.82	5.97	0.16	1.12							6.12	0.31	1.24			
CD11A	6.38				6.33	-0.06	0.96	6.19	-0.20	0.87	6.10	-0.28	0.82	6.07	-0.32	0.80
CD11B	7.56				6.52	-1.04	0.49	7.68	0.12	1.08	6.69	-0.87	0.55	6.71	-0.85	0.55
Interleukin-1b	6.75	6.02	-0.73	0.60	6.39	-0.37	0.77	7.67	0.92	1.89	6.51	-0.25	0.84			
Interleukin-6	6.08				6.39	0.30	1.23	7.14	1.06	2.09	6.74	0.66	1.58			
Interleukin-10	5.46	5.66	0.20	1.15												

Table 42. Differential expression of housekeeping controls in Parkinson's disease, custom-designed array. Each of the five Parkinson's disease samples was screened against the normal control sample. LogDif - log difference between the disease sample and the control sample values. FC - fold change between the disease sample and the control sample values. Colours: orange – upregulated; green – downregulated, - grey – no change.

	PD3				PD6				PD8				PD15				PD16			
Name	**PD3**	**H109**	**LogDif**	**FC**	**PD6**	**H109**	**LogDif**	**FC**	**PD8**	**H109**	**LogDif**	**FC**	**PD15**	**H109**	**LogDif**	**FC**	**PD16**	**H109**	**LogDif**	**FC**
HNRPC	1.83	2.06	-0.23	0.85	2.10	1.90	0.19	1.14	1.49	1.13	0.36	1.28	1.90	1.89	0.01	1.01	1.76	1.62	0.14	1.10
Ubiquitin	1.24	1.39	-0.15	0.90	3.65	3.86	-0.21	0.86	1.73	1.81	-0.08	0.95	1.81	2.42	-0.62	0.65	3.60	3.10	0.50	1.42
HPRT																	1.06	1.58	-0.52	0.70
GAPDH	2.76	3.23	-0.46	0.72	2.91	2.87	0.04	1.03	2.76	2.88	-0.12	0.92	2.34	2.67	-0.34	0.79	2.11	2.41	-0.29	0.82
TCEA1	1.19	1.26	-0.07	0.95	1.28	1.46	-0.18	0.88	1.44	1.01	0.43	1.35	1.20	1.35	-0.15	0.90				

Table 43. Differential expression of connexins in Parkinson's disease, custom-designed set, includes only the connexins that are expressed on the custom-designed array that are also expressed on the Illumina array. Each of the five Parkinson's disease samples was screened against the normal control sample. LogDif - log difference between the disease sample and the control sample values. FC - fold change between the disease sample and the control sample values. Colours: orange – upregulated; green – downregulated, - grey – no change.

	PD3				PD6				PD8				PD15				PD16			
Connexins	**PD3**	**H109**	**LogDif**	**FC**	**PD6**	**H109**	**LogDif**	**FC**	**PD8**	**H109**	**LogDif**	**FC**	**PD15**	**H109**	**LogDif**	**FC**	**PD16**	**H109**	**LogDif**	**FC**
a1 - Cx43	1.91	1.30	0.61	1.53	1.95	1.51	0.44	1.36	2.16	1.61	0.55	1.46	1.83	1.13	0.70	1.62	1.88	1.83	0.04	1.03
a4 - Cx37	2.55	2.64	-0.10	0.93	1.59	1.44	0.15	1.11	2.56	2.34	0.23	1.17	2.78	2.30	0.48	1.39	1.99	2.34	-0.36	0.78
a5 - Cx40	3.04	3.22	-0.18	0.89	3.17	3.16	0.00	1.00	2.38	2.42	-0.04	0.98	3.21	2.68	0.53	1.44	2.47	2.27	0.21	1.15
b1 - Cx32	3.33	3.24	0.09	1.07	2.90	3.10	-0.20	0.87	2.77	3.10	-0.33	0.80	2.68	3.21	-0.54	0.69	2.49	2.14	0.35	1.27
b2 - Cx26	1.58	2.07	-0.49	0.71	1.34	1.99	-0.65	0.64	1.89	2.27	-0.38	0.77	1.91	2.19	-0.28	0.82	2.18	1.85	0.33	1.25
b6 - Cx30	2.11	1.46	0.65	1.57					1.60	1.34	0.26	1.20	2.16	1.39	0.78	1.71	2.12	1.85	0.27	1.21
c1 - Cx45	1.88	1.67	0.21	1.16	1.75	1.88	-0.14	0.91	2.09	2.03	0.06	1.04	2.16	1.59	0.57	1.48	2.17	1.78	0.39	1.31
c2 - Cx46.6/47	2.07	2.23	-0.15	0.90	1.29	1.22	0.07	1.05	2.29	1.96	0.33	1.26	1.86	2.00	-0.13	0.91	2.20	1.80	0.24	1.18
d3 - Cx31.9	1.77	1.95	-0.18	0.88	1.82	2.21	-0.39	0.76	1.60	1.73	-0.13	0.91	1.65	2.03	-0.38	0.77	2.06	1.77	0.29	1.22

Table 44. Differential expression of connexins in Parkinson's disease, MWG-designed set, includes only the connexins that are expressed on the custom-designed array that are also expressed on the Illumina array. Each of the five Parkinson's disease samples was screened against the normal control sample. LogDif - log difference between the disease sample and the control sample values. FC - fold change between the disease sample and the control sample values. Colours: orange – upregulated; green – downregulated, - grey – no change.

	PD3				PD6				PD8				PD15				PD16			
Connexins	**PD3**	**H109**	**LogDif**	**FC**	**PD6**	**H109**	**LogDif**	**FC**	**PD8**	**H109**	**LogDif**	**FC**	**PD15**	**H109**	**LogDif**	**FC**	**PD16**	**H109**	**LogDif**	**FC**
a1 - Cx43M	3.05	3.79	-0.74	0.60	2.53	2.50	0.03	1.02	4.07	4.26	-0.18	0.88	3.20	3.30	-0.10	0.93	2.43	2.48	-0.05	0.96
a4 - Cx37M	2.15	1.96	0.19	1.14	1.59	1.29	0.30	1.23	2.88	2.37	0.51	1.42	2.67	1.44	1.23	2.35	1.92	2.17	-0.25	0.84
a5 - Cx40M	3.99	4.21	-0.21	0.86	3.36	3.73	-0.37	0.77	3.42	4.37	-0.95	0.52	3.64	3.98	-0.34	0.79	2.70	2.63	0.07	1.05
b1 - Cx32M	1.05	1.06	0.00	1.00					1.56	1.37	0.19	1.14	0.51	0.64	-0.13	0.91	1.89	1.49	0.40	1.32
b2 - Cx26M													0.13	0.71	-0.58	0.67	1.67	1.38	0.29	1.22
c1 - Cx45M	1.34	1.26	0.08	1.06	1.15	1.18	-0.03	0.98	1.22	0.95	0.28	1.21	1.29	0.77	0.52	1.44	1.90	1.50	0.40	1.32
c2 - Cx46.6/47M	2.75	3.09	-0.35	0.79	2.54	2.64	-0.10	0.93	2.70	2.81	-0.12	0.92	2.75	3.28	-0.53	0.69	2.48	2.14	0.34	1.27

Table 45. Differential expression of connexins in Parkinson's disease, cusom-designed set, includes the connexins that are expressed on the custom-designed array, but not on the Illumina array. Each of the five Parkinson's disease samples was screened against the normal control sample. LogDif - log difference between the disease sample and the control sample values. FC - fold change between the disease sample and the control sample values. Colours: orange – upregulated; green – downregulated, - grey – no change.

	PD3				PD6				PD8				PD15				PD16			
Connexin	**PD3**	**H109**	**LogDif**	**FC**	**PD6**	**H109**	**LogDif**	**FC**	**PD8**	**H109**	**LogDif**	**FC**	**PD15**	**H109**	**LogDif**	**FC**	**PD16**	**H109**	**LogDif**	**FC**
d2 - Cx36	1.38	1.56	-0.18	0.88	1.35	1.43	-0.07	0.95	2.33	1.86	0.47	1.39	2.18	1.88	0.30	1.23	1.96	1.71	0.26	1.19
b3 - Cx31	1.61	1.13	0.48	1.40	1.56	1.43	0.13	1.09	1.58	1.30	0.28	1.22	1.69	1.52	0.18	1.13	2.02	1.32	0.69	1.62
b4 - Cx30.3	3.35	3.07	0.28	1.22	2.53	2.03	0.51	1.42	2.88	3.01	-0.13	0.91	2.71	2.75	-0.04	0.97	2.81	2.54	0.28	1.21
b5 - Cx 31.1	2.29	2.01	0.28	1.21	2.10	2.21	-0.10	0.93	1.75	1.99	-0.23	0.85	1.80	1.92	-0.13	0.92	1.65	1.80	-0.16	0.90
d4 - Cx40.1	1.76	2.02	-0.26	0.84					1.35	1.63	-0.28	0.82	1.23	1.28	-0.05	0.97	1.41	1.65	-0.24	0.85
a10 - Cx62	3.37	3.14	0.23	1.17	3.23	3.30	-0.08	0.95	2.54	2.58	-0.04	0.97	2.87	3.12	-0.25	0.84	2.63	2.94	-0.31	0.81
c3 - Cx31.3(30.2)	4.53	4.36	0.16	1.12	4.24	4.13	0.10	1.07	3.75	3.98	-0.23	0.85	4.16	4.18	-0.02	0.99	2.68	3.36	-0.68	0.63

Table 46. Differential expression of connexins in Parkinson's disease, MWG-designed set, includes the connexins that are expressed on the custom-designed array, but not on the Illumina array. Each of the five Parkinson's disease samples was screened against the normal control sample. LogDif - log difference between the disease sample and the control sample values. FC - fold change between the disease sample and the control sample values. Colours: orange – upregulated; green – downregulated, - grey – no change.

	PD3				PD6				PD8				PD15				PD16			
Connexin	**PD3**	**H109**	**LogDif**	**FC**	**PD6**	**H109**	**LogDif**	**FC**	**PD8**	**H109**	**LogDif**	**FC**	**PD15**	**H109**	**LogDif**	**FC**	**PD16**	**H109**	**LogDif**	**FC**
a3 - Cx46M	1.92	1.83	0.09	1.07	1.31	1.36	-0.06	0.96	1.83	2.04	-0.22	0.86	1.53	1.72	-0.18	0.88	1.48	1.63	-0.15	0.90
b3 - Cx31M	4.36	3.89	0.47	1.38	3.56	3.52	0.04	1.03	3.54	3.51	0.03	1.02	3.86	3.83	0.03	1.02	2.78	3.32	0.54	1.46
b7 - Cx25M	1.54	2.17	-0.63	0.65	1.83	2.53	-0.70	0.61	0.47	0.97	-0.50	0.71	1.74	2.23	-0.49	0.71	1.34	2.39	-1.05	0.48
d4 - Cx40.1M	1.18	1.46	-0.28	0.82					1.36	1.74	-0.38	0.77	1.09	1.39	-0.30	0.81	1.55	1.75	-0.20	0.87
a10 - Cx62M	3.10	2.81	0.29	1.22	2.65	2.47	0.18	1.14	2.63	2.42	0.21	1.15	2.99	2.72	0.27	1.20	2.08	2.30	-0.22	0.86
c3 - Cx31.3(30.2)M	1.44	1.23	0.21	1.16					1.03	1.19	-0.16	0.90	0.94	1.05	-0.11	0.93	1.21	1.45	-0.24	0.85

Table 47. Differential expression connexins in Parkinson's disease, Illumina array. Five Parkinson's disease samples were screened against one control sample. . LogDif - log difference between the disease sample and the control sample values. FC - fold change between the disease sample and the control sample values.

		HC84			HC91			HC92			HC107			HC109		
Name	**H109**	**HC84**	**LogDif**	**FC**	**HC91**	**LogDif**	**FC**	**HC92**	**LogDif**	**FC**	**HC107**	**LogDif**	**FC**	**HC109**	**LogDif**	**FC**
a1 - Cx43	12.24	13.19	0.94	1.92	12.27	0.02	1.01	11.41	-0.83	0.56	12.53	0.29	1.22	13.11	0.86	1.82
a4 - Cx37	6.64	6.57	-0.07	0.95	6.85	0.21	1.16	7.15	0.51	1.42	7.56	0.92	1.90	7.28	0.64	1.56
a5 - Cx40	6.26	6.28	0.03	1.02			1.00	6.39	0.14	1.10			1.00	6.45	0.19	1.14
b1 - Cx32	7.50	7.40	-0.10	0.93	7.67	0.17	1.13	6.50	-1.00	0.50	7.61	0.11	1.08	6.77	-0.73	0.60
b2 - Cx26	8.35	7.72	-0.63	0.65	7.77	-0.59	0.67	6.97	-1.38	0.38	7.37	-0.98	0.51	7.37	-0.99	0.50
b6 - Cx30	10.95	11.00	0.05	1.03	10.18	-0.77	0.58	9.47	-1.48	0.36	10.49	-0.46	0.73	10.80	-0.15	0.90
a7 - Cx45	13.63	13.82	0.19	1.14	14.51	0.88	1.85	13.83	0.20	1.15	14.21	0.58	1.49	14.33	0.71	1.63
a12 - Cx46.6/47	9.44	8.62	-0.82	0.57	8.82	-0.62	0.65	9.00	-0.44	0.74	9.28	-0.16	0.90	8.99	-0.45	0.73
c1 - Cx31.9	7.32	7.43	0.11	1.08	7.47	0.15	1.11	7.44	0.12	1.09	7.31	0.00	1.00	6.58	-0.74	0.60
d4 - Cx40.1	6.23										6.85	0.63				

Table 48. Differential expression of inflammatory markers in Parkinson's disease, Illumina array. Five Parkinson's disease samples were screened against one control sample. LogDif - log difference between the disease sample and the control sample values. FC - fold change between the disease sample and the control sample values.

		PD3			PD6			PD8			PD15			PD16		
Name	**H109**	**PD3**	**LodDif**	**FC**	**PD6**	**LodDif**	**FC**	**PD8**	**LodDif**	**FC**	**PD15**	**LodDif**	**FC**	**PD16**	**LodDif**	**FC**
CD11A	6.63	6.61	-0.03	0.98	7.37	0.74	1.67	6.31	-0.32	0.80	7.08	0.44	1.36	6.75	0.11	1.08
CD11B	6.99	7.73	0.74	1.67	8.34	1.34	2.54	7.97	0.98	1.97	7.48	0.48	1.40	7.93	0.94	1.92
Interleukin-1b	6.47	6.77	0.30	1.23	8.48	2.01	4.04	8.45	1.99	3.96				6.61	0.15	1.11
Interleukin-6	6.31				7.37	1.07	2.10	8.27	1.97	3.91	7.42	1.12	2.17	7.25	0.94	1.92

Table 49. Differential expression of housekeeping controls in Alzheimer's disease, custom-designed array. Each of the five Alzheimer's disease samples was screened against the normal control sample. LogDif - log difference between the disease sample and the control sample values. FC - fold change between the disease sample and the control sample values. Colours: orange – upregulated; green – downregulated, - grey – no change.

	AZ30				AZ32				AZ53				AZ54				AZ55			
Name	**AZ30**	**H109**	**LogDif**	**FC**	**AZ32**	**H109**	**LogDif**	**FC**	**AZ53**	**H109**	**LogDif**	**FC**	**AZ54**	**H109**	**LogDif**	**FC**	**AZ55**	**H109**	**LogDif**	**FC**
HNRPC	1.87	1.55	0.32	1.25	1.86	1.42	0.44	1.35	1.81	1.27	0.54	1.46	1.27	1.23	0.04	1.03	1.72	1.35	0.38	1.30
Ubiquitin	2.24	2.16	0.09	1.06	1.54	1.38	0.16	1.12	2.18	2.02	0.17	1.12	1.58	1.75	-0.16	0.89	2.49	2.18	0.31	1.24
HPRT	0.45	1.40	-0.95	0.52	-0.65	1.23	-1.88	0.27	0.25	2.15	-1.91	0.27	0.36	1.64	-1.28	0.41	0.39	1.45	-1.06	0.48
GAPDH	2.10	2.16	-0.06	0.96	1.87	2.18	-0.31	0.81	1.75	2.14	-0.39	0.76	1.72	2.89	-1.17	0.44	2.21	2.36	-0.15	0.90
TCEA1	0.73	1.01	-0.28	0.82	1.04	0.65	0.38	1.31	0.96	0.81	0.15	1.11	0.64	1.04	-0.39	0.76	0.74	0.61	0.13	1.10

Table 50. Differential expression of connexins in Alzheimer's disease, custom-designed set, includes only the connexins that are expressed on the custom-designed array that are also expressed on the Illumina array. Each of the five Alzheimer's disease samples was screened against the normal control sample. LogDif - log difference between the disease sample and the control sample values. FC - fold change between the disease sample and the control sample values. Colours: orange – upregulated; green – downregulated, - grey – no change.

	AZ30				AZ32				AZ53				AZ54				AZ55			
Connexins	**AZ30**	**H109**	**LogDif**	**FC**	**AZ32**	**H109**	**LogDif**	**FC**	**AZ53**	**H109**	**LogDif**	**FC**	**AZ54**	**H109**	**LogDif**	**FC**	**AZ55**	**H109**	**LogDif**	**FC**
a1 - Cx43	1.46	1.19	0.28	1.21	2.10	0.84	1.27	2.41	1.37	0.59	0.78	1.71	2.46	1.12	1.34	2.53	1.71	0.85	0.86	1.81
a4 - Cx37	2.40	2.19	0.22	1.16	1.97	1.47	0.50	1.41	2.20	1.66	0.54	1.46	2.23	1.57	0.66	1.58	2.24	1.58	0.66	1.58
a5 - Cx40	2.56	2.79	-0.23	0.85	2.66	2.01	0.65	1.57	2.40	2.00	0.40	1.32	2.52	2.51	0.01	1.01	2.54	2.69	-0.15	0.90
b1 - Cx32	3.41	2.60	0.81	1.75	2.77	2.16	0.61	1.53	3.20	2.51	0.69	1.61	3.56	2.86	0.70	1.62	3.61	2.86	0.74	1.68
b2 - Cx26	1.92	2.22	-0.30	0.81	1.73	1.58	0.15	1.11	1.89	2.40	-0.51	0.70	2.05	2.31	-0.26	0.83	1.40	2.19	-0.79	0.58
b6 - Cx30	2.38	1.98	0.40	1.32	1.91	1.80	0.11	1.08	2.01	1.68	0.32	1.25	1.61	2.09	-0.49	0.71	1.79	2.24	-0.45	0.73
c1 - Cx45	1.83	1.24	0.59	1.50	1.72	1.06	0.66	1.58	2.11	1.45	0.65	1.57	2.41	1.20	1.21	2.32	1.90	1.84	0.06	1.04
c2 - Cx46.6/47	2.41	1.83	0.58	1.50	2.17	1.40	0.77	1.71	2.21	1.12	1.08	2.12	2.24	1.41	0.83	1.78	3.55	2.34	1.21	2.32
d3 - Cx31.9	2.26	2.00	0.27	1.20	1.43	1.89	-0.47	0.72	1.91	1.84	0.06	1.05	2.15	2.16	0.00	1.00	2.24	2.07	0.18	1.13

Table 51. Differential expression of connexins in Alzheimer's disease, MWG-designed set, includes only the connexins that are expressed on the custom-designed array that are also expressed on the Illumina array. Each of the five Alzheimer's disease samples was screened against the normal control sample. LogDif - log difference between the disease sample and the control sample values. FC - fold change between the disease sample and the control sample values. Colours: orange – upregulated; green – downregulated, - grey – no change.

	AZ30				AZ32				AZ53				AZ54				AZ55			
Connexins	**AZ30**	**H109**	**LogDif**	**FC**	**AZ32**	**H109**	**LogDif**	**FC**	**AZ53**	**H109**	**LogDif**	**FC**	**AZ54**	**H109**	**LogDif**	**FC**	**AZ55**	**H109**	**LogDif**	**FC**
a1 - Cx43M	3.27	3.63	-0.36	0.78	3.14	2.14	0.99	1.99	3.77	2.64	1.13	2.20	4.10	3.41	0.69	1.61	3.39	3.01	0.38	1.30
a4 - Cx37M	1.82	1.96	-0.13	0.91	1.84	-0.08	1.92	3.79	2.25	0.71	1.54	2.91	1.83	1.57	0.27	1.20	2.12	1.48	0.64	1.56
a5 - Cx40M	4.04	3.87	0.17	1.13	2.73	2.89	-0.16	0.89	3.31	3.54	-0.24	0.85	4.24	4.27	-0.04	0.97	4.43	4.37	0.05	1.04
b1 - Cx32M	1.21	0.63	0.58	1.50	0.25	-0.58	0.84	1.78	2.24	0.51	1.73	3.31	1.39	0.64	0.75	1.68	1.13	0.57	0.56	1.47
b2 - Cx26M	0.74	1.02	-0.27	0.83					0.70	1.30	-0.60	0.66					0.04	0.97	-0.93	0.52
c1 - Cx45M	1.50	1.10	0.40	1.32	1.23	0.21	1.03	2.04	1.57	1.02	0.55	1.47	2.04	0.91	1.13	2.19	1.24	0.59	0.65	1.57
c2 - Cx46.6/47M	3.24	2.54	0.70	1.62	2.86	2.30	0.56	1.48	3.01	1.96	1.05	2.07	3.17	2.49	0.68	1.60	1.14	0.00	1.15	2.22

Table 52. Differential expression of connexins in Alzheimer's disease, cusom-designed set, includes only the connexins that are expressed on the custom-designed array, but not on the Illumina array. Each of the five Alzheimer's disease samples was screened against the normal control sample. LogDif - log difference between the disease sample and the control sample values. FC - fold change between the disease sample and the control sample values. Colours: orange – upregulated; green – downregulated, - grey – no change.

	AZ30				AZ32				AZ53				AZ54				AZ55			
Connexins	**AZ30**	**H109**	**LogDif**	**FC**	**AZ32**	**H109**	**LogDif**	**FC**	**AZ53**	**H109**	**LogDif**	**FC**	**AZ54**	**H109**	**LogDif**	**FC**	**AZ55**	**H109**	**LogDif**	**FC**
d2 - Cx36	1.65	1.52	0.25	1.19	1.59	1.43	0.32	1.24	1.78	1.48	0.61	1.52	1.75	1.34	0.81	1.75	1.55	1.22	1.42	2.67
b3 - Cx31	1.53	1.60	-0.07	0.95	1.78	1.31	0.94	1.91	1.89	1.43	0.90	1.87	1.49	1.44	0.11	1.08	1.40	1.42	0.44	1.36
b4 - Cx30.3	2.94	2.81	0.25	1.19	2.42	2.40	0.04	1.03	2.67	2.60	0.15	1.11	3.01	3.06	-0.04	0.97	2.95	2.93	0.52	1.44
b5 - Cx 31.1	1.93	1.74	0.38	1.30	0.67	1.04	-0.37	0.77	1.58	1.96	-0.75	0.59	1.95	2.03	-0.08	0.94	2.10	2.05	0.32	1.25
d4 - Cx40.1	1.78	1.50	0.55	1.46	1.08	1.13	-0.05	0.97	1.31	1.45	-0.28	0.83	1.25	1.41	-0.15	0.90	1.63	1.65	0.72	1.65
c3 - Cx31.3(30.2)	3.42	3.67	-0.51	0.70	3.32	3.75	-0.86	0.55	3.13	3.60	-0.47	0.72	4.15	3.96	0.36	1.29	4.08	4.08	0.79	1.73

Table 53 Differential expression of connexins in Alzheimer's disease, MWG-designed set, includes the connexins that are expressed on the custom-designed array, but not on the Illumina array. Each of the five Alzheimer's disease samples was screened against the normal control sample. LogDif - log difference between the disease sample and the control sample values. FC - fold change between the disease sample and the control sample values. Colours: orange – upregulated; green – downregulated, - grey – no change.

	AZ30				AZ32				AZ53				AZ54				AZ55			
Connexins	**AZ30**	**H109**	**LogDif**	**FC**	**AZ32**	**H109**	**LogDif**	**FC**	**AZ53**	**H109**	**LogDif**	**FC**	**AZ54**	**H109**	**LogDif**	**FC**	**AZ55**	**H109**	**LogDif**	**FC**
a3 - Cx46M	2.09	2.10	-0.01	0.99	1.44	0.98	0.92	1.89	2.03	1.88	0.30	1.23	2.16	2.06	0.19	1.14	2.18	2.24	0.68	1.60
b3 - Cx31M	3.74	3.34	0.81	1.75	2.62	2.71	-0.09	0.94	2.86	3.10	-0.24	0.85	3.67	3.53	0.27	1.21	3.77	3.57	0.40	1.32
b7 - Cx25M	1.64	1.73	-0.19	0.88	0.56	0.88	-0.32	0.80	1.39	2.32	-0.93	0.52	1.71	2.07	-0.35	0.78	1.66	2.05	0.41	1.33
d4 - Cx40.1M	1.44	1.61	-0.32	0.80	0.85	0.66	0.37	1.30	1.40	1.66	-0.50	0.71	1.20	1.28	-0.07	0.95	1.52	1.64	0.65	1.57
a10 - Cx62M	2.43	2.03	0.81	1.76	1.86	1.81	0.09	1.07	2.07	2.14	-0.07	0.95	2.46	2.06	0.79	1.73	2.52	2.14	0.60	1.52
c3 - Cx31.3(30.2)M	0.98	1.03	-0.11	0.92					1.04	1.16	-0.12	0.92	1.24	1.19	0.09	1.06	1.13	1.16	0.60	1.52

Table 54. Differential expression connexins in Alzheimer's disease, Illumina array. Five Alzheimer's disease samples were screened against one control sample. . LogDif - log difference between the disease sample and the control sample values. FC - fold change between the disease sample and the control sample values.

		AZ30			AZ30			AZ53			AZ54			AZ55		
Name	**H109**	**AZ30**	**LogDif**	**FC**	**AZ30**	**LogDif**	**FC**	**AZ53**	**LogDif**	**FC**	**AZ54**	**LogDif**	**FC**	**AZ55**	**LogDif**	**FC**
a1 - Cx43	12.65	12.60	-0.05	0.96	14.18	1.53	2.88	14.03	1.38	2.60	13.67	1.02	2.02	13.74	1.08	2.12
a4 - Cx37	6.15			1.00	7.88	1.73	3.31	7.00	0.85	1.80	6.83	0.67	1.59	7.18	1.02	2.03
a5 - Cx40	6.46			1.00	6.91	0.45	1.37	6.57	0.11	1.08			1.00	6.61	0.14	1.11
b1 - Cx32	7.02	7.70	0.68	1.60	7.47	0.45	1.37	8.12	1.10	2.14	7.90	0.88	1.84	8.03	1.01	2.02
b2 - Cx26	7.69	7.87	0.18	1.13	7.63	-0.06	0.96	7.37	-0.32	0.80	7.25	-0.44	0.74	7.02	-0.67	0.63
b6 - Cx30	10.49	11.32	0.82	1.77	10.39	-0.10	0.93	10.89	0.39	1.31	10.06	-0.43	0.74	10.12	-0.37	0.77
c1 - Cx45	14.23	14.71	0.48	1.39	15.03	0.81	1.75	14.90	0.67	1.59	15.19	0.96	1.95	14.83	0.61	1.52
c2 - Cx47	8.84	9.37	0.53	1.44	9.65	0.81	1.75	9.88	1.03	2.04	9.92	1.07	2.10	9.87	1.03	2.04
d3 - Cx31.9	7.17	7.46	0.29	1.23	7.29	0.12	1.09	7.21	0.04	1.03	7.21	0.04	1.03	7.43	0.26	1.20

Table 55. Differential expression of inflammatory markers in Alzheimer's disease, Illumina array. Five Alzheimer's disease samples were screened against one control sample. LogDif - log difference between the disease sample and the control sample values. FC - fold change between the disease sample and the control sample values.

		AZ30			AZ32			AZ53			AZ54			AZ55		
Name	**H109**	**AZ30**	**LodDif**	**FC**	**AZ32**	**LodDif**	**FC**	**AZ53**	**LodDif**	**FC**	**AZ54**	**LodDif**	**FC**	**AZ55**	**LodDif**	**FC**
CD11A	6.35	6.40	0.05	1.04	6.97	0.61	1.53	6.67	0.32	1.25	6.65	0.30	1.23	6.80	0.45	1.36
CD11B	7.00	7.57	0.58	1.49	7.35	0.35	1.28	7.68	0.68	1.61	7.24	0.24	1.18	7.62	0.62	1.54
Interleukin-1b	6.52	6.39	-0.12	0.92				6.41	-0.10	0.93						
Interleukin-6	6.44				6.69	0.25	1.19	6.62	0.18	1.13	6.58	0.14	1.10	6.36	-0.08	0.95

Table 56. Differential expression of housekeeping controls in epilepsy, custom-designed array. Each of the two epilepsy samples was screened against the normal control sample. LogDif - log difference between the disease sample and the control sample values. FC - fold change between the disease sample and the control sample values. Colours: orange – upregulated; green – downregulated, - grey – no change.

	E113				E118			
Name	**E113**	**H109**	**LogDif**	**FC**	**E118**	**H109**	**LogDif**	**FC**
HNRPC	1.15	1.00	0.15	1.11	1.04	1.08	-0.04	0.97
Ubiquitin	2.04	1.99	0.05	1.04	2.78	2.16	0.62	1.54
HPRT	-0.54	0.34	-0.88	0.54	0.41	0.91	-0.50	0.71
GAPDH	1.76	1.69	0.06	1.04	1.14	1.34	-0.20	0.87
TCEA1	0.25	0.45	-0.19	0.88	0.05	0.20	-0.16	0.90

Table 57. Differential expression of connexins in epilepsy, custom-designed set, includes only the connexins that are expressed on the custom-designed array that are also expressed on the Illumina array for the other diseases. Each of the two epilepsy samples was screened against the normal control sample. LogDif - log difference between the disease sample and the control sample values. FC - fold change between the disease sample and the control sample values. Colours: orange – upregulated; green – downregulated, - grey – no change.

	E113				E118			
Connexins	**E113**	**H109**	**LogDif**	**FC**	**E118**	**H109**	**LogDif**	**FC**
a1 - Cx43	1.18	0.22	0.97	1.96	2.21	1.71	0.50	1.42
a4 - Cx37	1.96	1.85	0.11	1.08	2.01	1.46	0.55	1.47
a5 - Cx40	1.93	2.23	-0.30	0.81	1.49	1.55	-0.06	0.96
b1 - Cx32	3.07	2.70	0.37	1.29	2.21	1.71	0.50	1.42
b2 - Cx26	1.42	1.66	-0.24	0.85	1.38	1.42	-0.04	0.97
b6 - Cx30					1.67	1.06	0.60	1.52
c1 - Cx45	2.01	1.46	0.56	1.47	1.93	1.40	0.53	1.45
c2 - Cx46.6/47	1.32	1.27	0.04	1.03	1.39	1.38	0.01	1.01
d3 - Cx31.9	0.96	1.26	-0.30	0.81	1.34	1.40	-0.05	0.96

Table 58. Differential expression of connexins in epilepsy, MWG-designed set, includes only the connexins that are expressed on the custom-designed array that are also expressed on the Illumina array for the other diseases. Each of the two epilepsy samples was screened against the normal control sample. LogDif - log difference between the disease sample and the control sample values. FC - fold change between the disease sample and the control sample values. Colours: orange – upregulated; green – downregulated, - grey – no change.

	E113				E118			
Connexins	**E113**	**H109**	**LogDif**	**FC**	**E118**	**H109**	**LogDif**	**FC**
a1 - Cx43M	4.01	3.57	0.45	1.36	2.26	1.74	0.51	1.43
a4 - Cx37M	1.76	1.48	0.28	1.21	1.98	1.38	0.60	1.51
a5 - Cx40M	2.49	2.83	-0.34	0.79	1.74	1.82	-0.08	0.95
b1 - Cx32M	1.00	0.24	0.76	1.69	1.82	1.23	0.59	1.51
b2 - Cx26M	1.78	1.07	0.71	1.63	1.88	1.32	0.57	1.48
c1 - Cx45M	1.09	0.84	0.25	1.19	1.77	1.29	0.48	1.40
c2 - Cx46.6/47M	2.45	2.25	0.20	1.15	1.63	1.59	0.04	1.03

Table 59. Differential expression of connexins in epilepsy, cusom-designed set, includes the connexins that are expressed only the custom-designed array. Each of the two epilepsy samples was screened against the normal control sample. LogDif - log difference between the disease sample and the control sample values. FC - fold change between the disease sample and the control sample values. Colours: orange – upregulated; green – downregulated, - grey – no change.

	E113				E118			
Connexins	**E113**	**H109**	**LogDif**	**FC**	**E118**	**H109**	**LogDif**	**FC**
d2 - Cx36	1.00	0.78	0.22	1.17	1.13	1.05	0.08	1.05
b3 - Cx31	0.50	0.36	0.14	1.10	1.11	0.95	0.16	1.12
b4 - Cx30.3	2.68	2.65	0.03	1.02	2.68	2.73	-0.05	0.97
b5 - Cx 31.1	0.97	1.06	-0.08	0.94	1.21	1.03	0.17	1.13
d4 - Cx40.1	-0.02	0.08	-0.10	0.93	0.49	0.54	-0.05	0.97
a10 - Cx62	2.22	2.28	-0.06	0.96	2.14	2.35	-0.22	0.86
c3 - Cx31.3(30.2)	3.41	3.53	-0.12	0.92	2.95	3.10	-0.15	0.90

Table 60. Differential expression of connexins in epilepsy, MWG-designed set, includes the connexins that are expressed only the custom-designed array. Each of the two epilepsy samples was screened against the normal control sample. . LogDif - log difference between the disease sample and the control sample values. FC - fold change between the disease sample and the control sample values. Colours: orange – upregulated; green – downregulated, - grey – no change.

	E113				E118			
Connexins	**E113**	**H109**	**LogDif**	**FC**	**E118**	**H109**	**LogDif**	**FC**
a3 - Cx46M	1.58	1.68	-0.10	0.93	1.11	1.17	-0.07	0.95
b3 - Cx31M	3.32	3.27	0.05	1.04	2.26	2.16	0.10	1.07
b7 - Cx25M	0.88	1.00	-0.12	0.92	0.63	1.09	-0.46	0.73
d4 - Cx40.1M	0.38	0.52	-0.14	0.91	0.74	0.76	-0.02	0.99
a10 - Cx62M	1.90	1.82	0.08	1.06	1.44	1.64	-0.19	0.88
c3 - Cx31.3(30.2)M	0.18	0.22	-0.04	0.97	0.07	0.27	-0.20	0.87

Figures

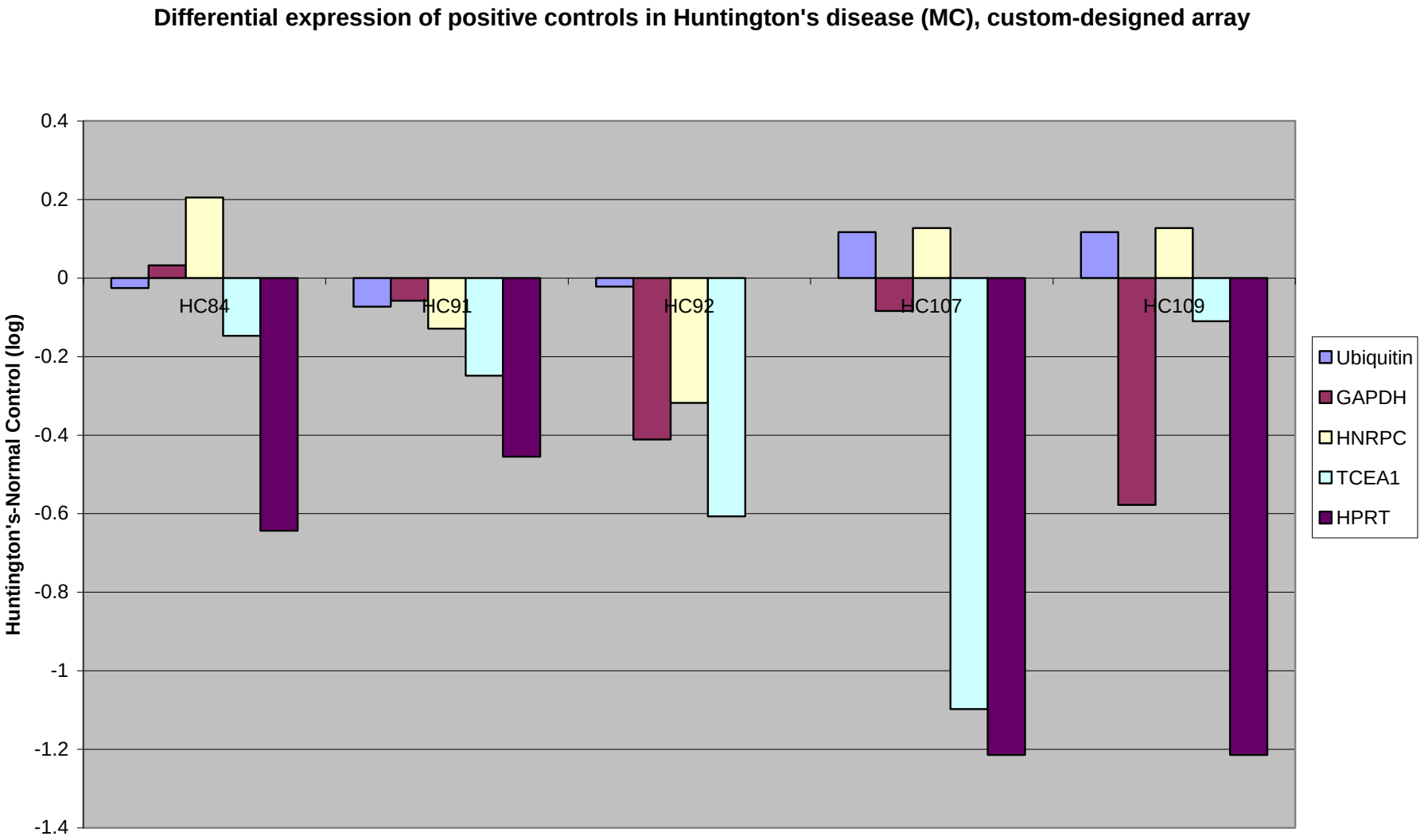

Figure 29. Differential expression of positive controls in Huntington's disease, custom-designed array. Each of the five Huntington's disease samples was screened against the normal control sample. Y axis - the expression level in the diseased sample minus the expression level in the normal control sample.

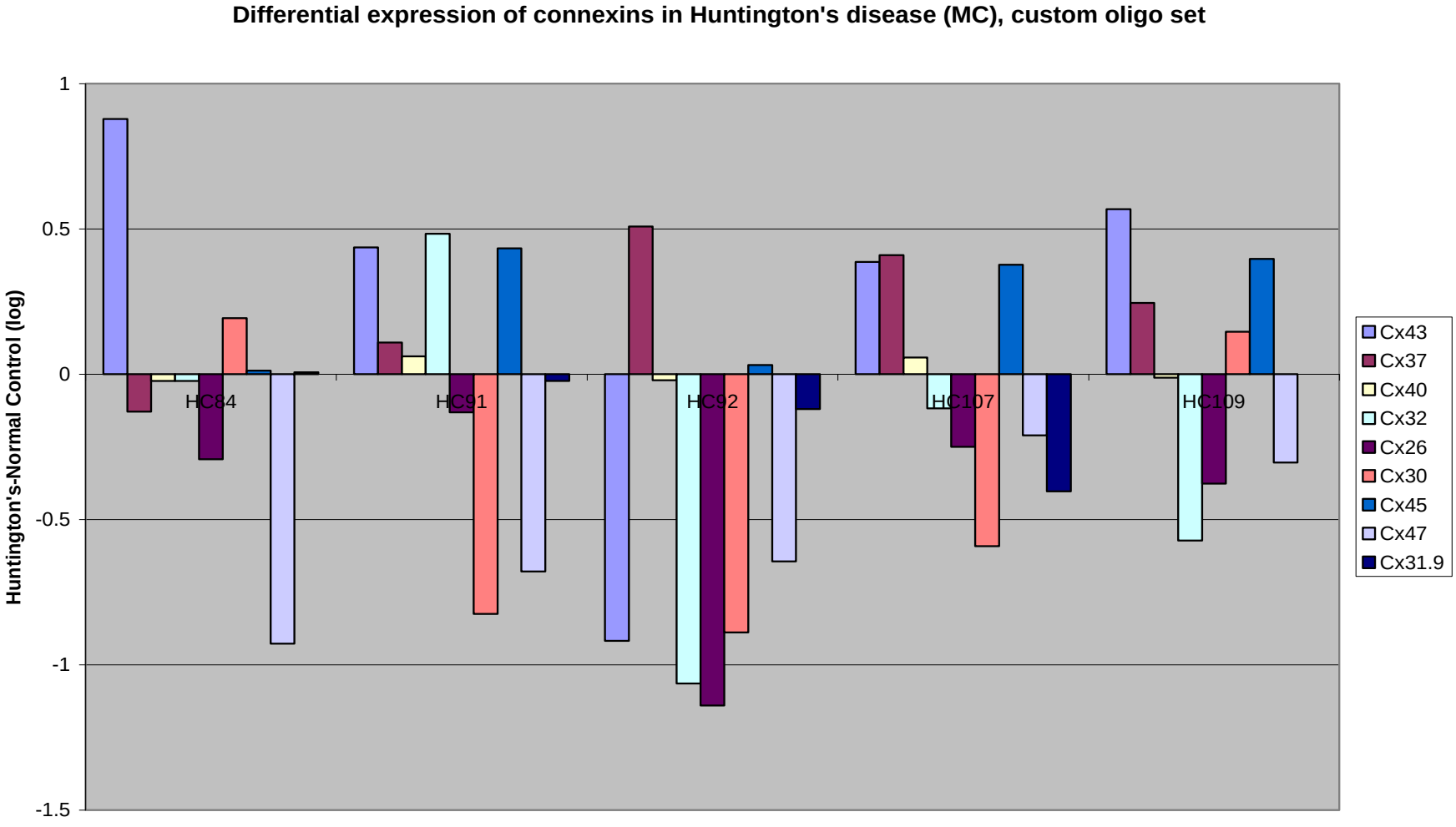

Figure 30. Differential expression of connexins in Huntington's disease, custom-designed set, includes only the connexins that are expressed on the custom-designed array that are also expressed on the Illumina array. Each of the five Huntington's disease samples was screened against the normal control sample. Y axis - the expression level in the diseased sample minus the expression level in the normal control sample.

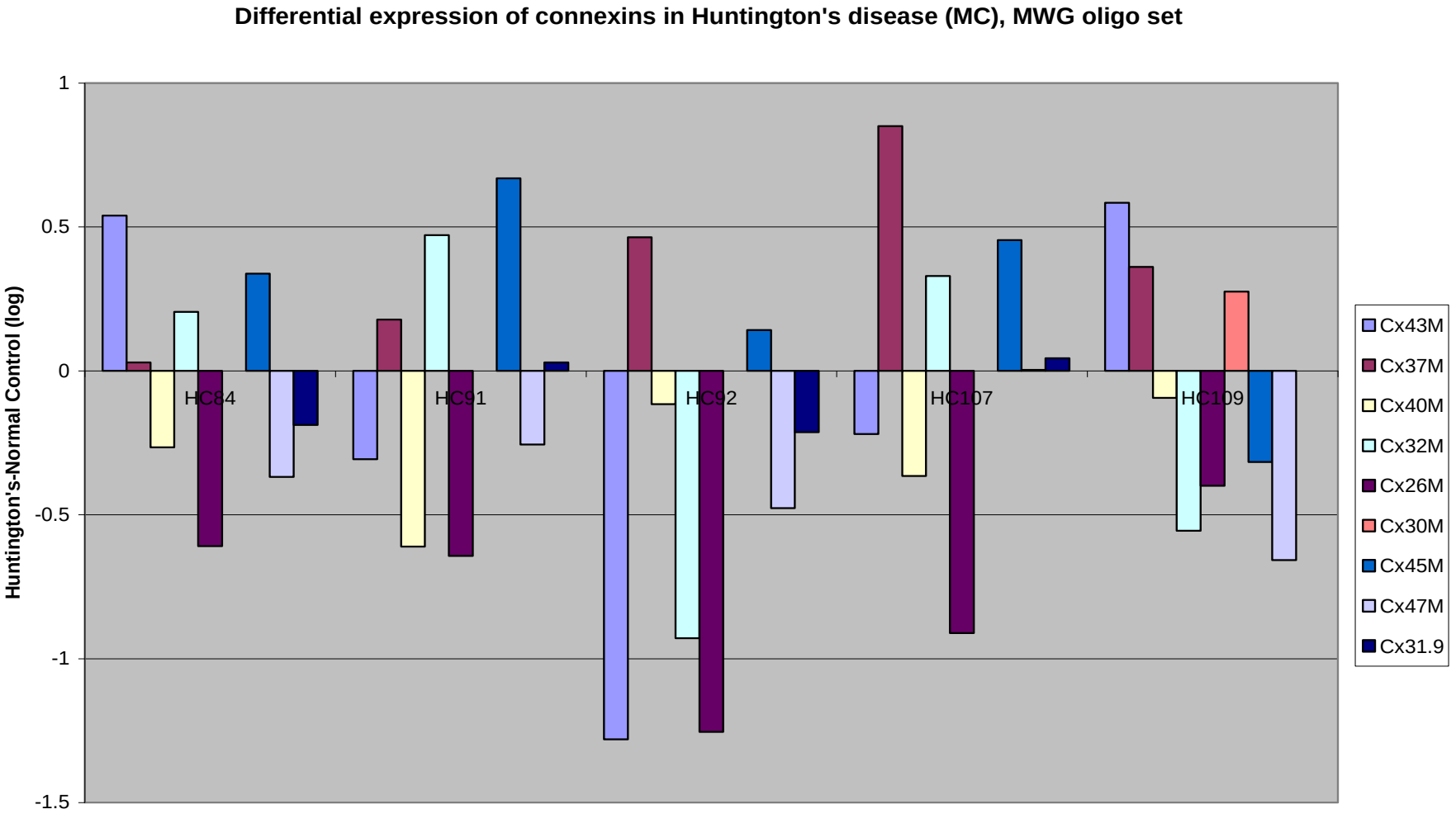

Figure 31. Differential expression of connexins in Huntington's disease, MWG-designed set, includes only the connexins that are expressed on the custom-designed array that are also expressed on the Illumina array. Each of the five Huntington's disease samples was screened against the normal control sample. Y axis - the expression level in the diseased sample minus the expression level in the normal control sample.

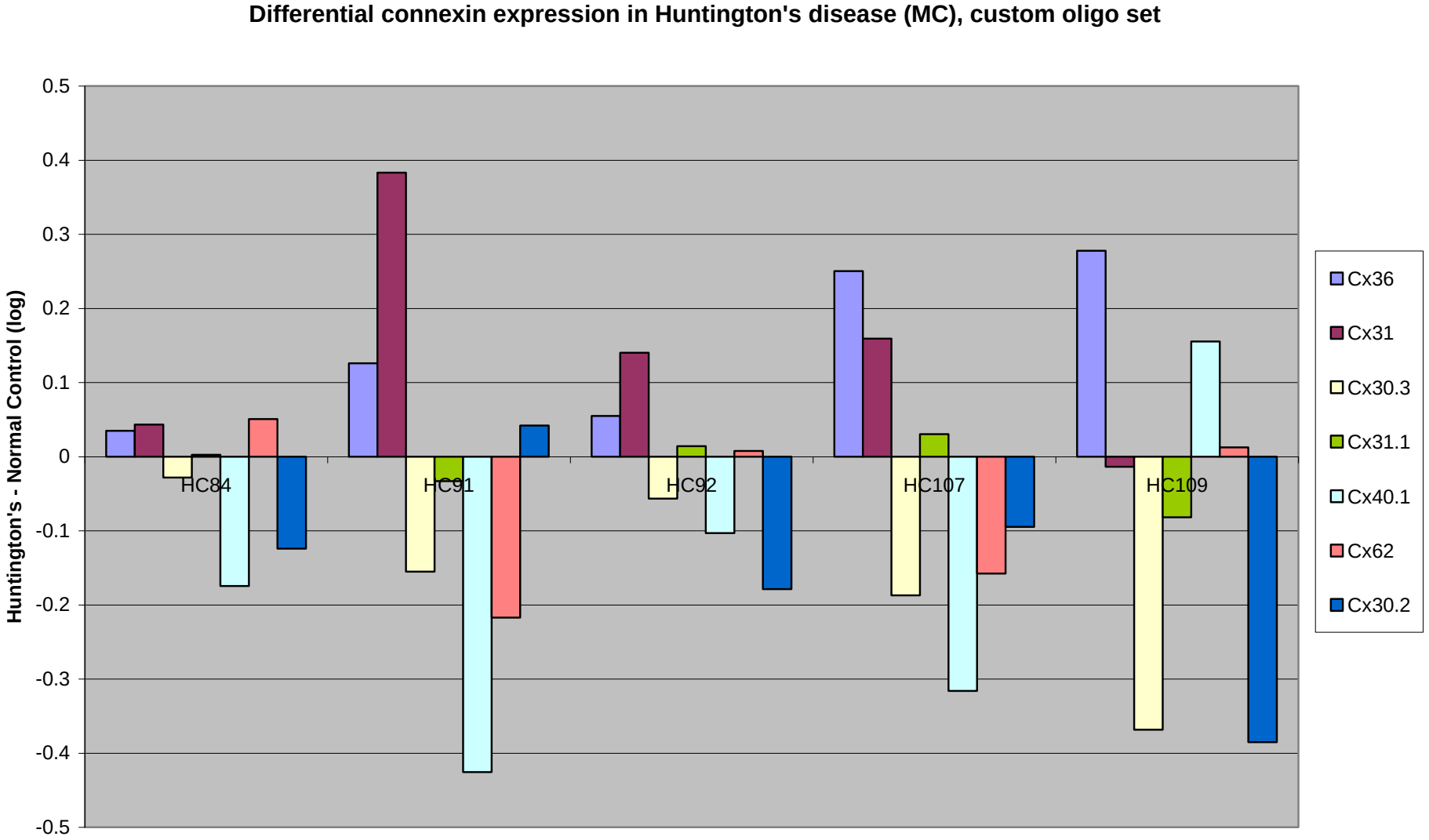

Figure 32. Differential expression of connexins in Huntington's disease, custom-designed set, includes the connexins that are expressed on the custom-designed array but not on the Illumina array. Each of the five Huntington's disease samples was screened against the normal control sample. Y axis - the expression level in the diseased sample minus the expression level in the normal control sample.

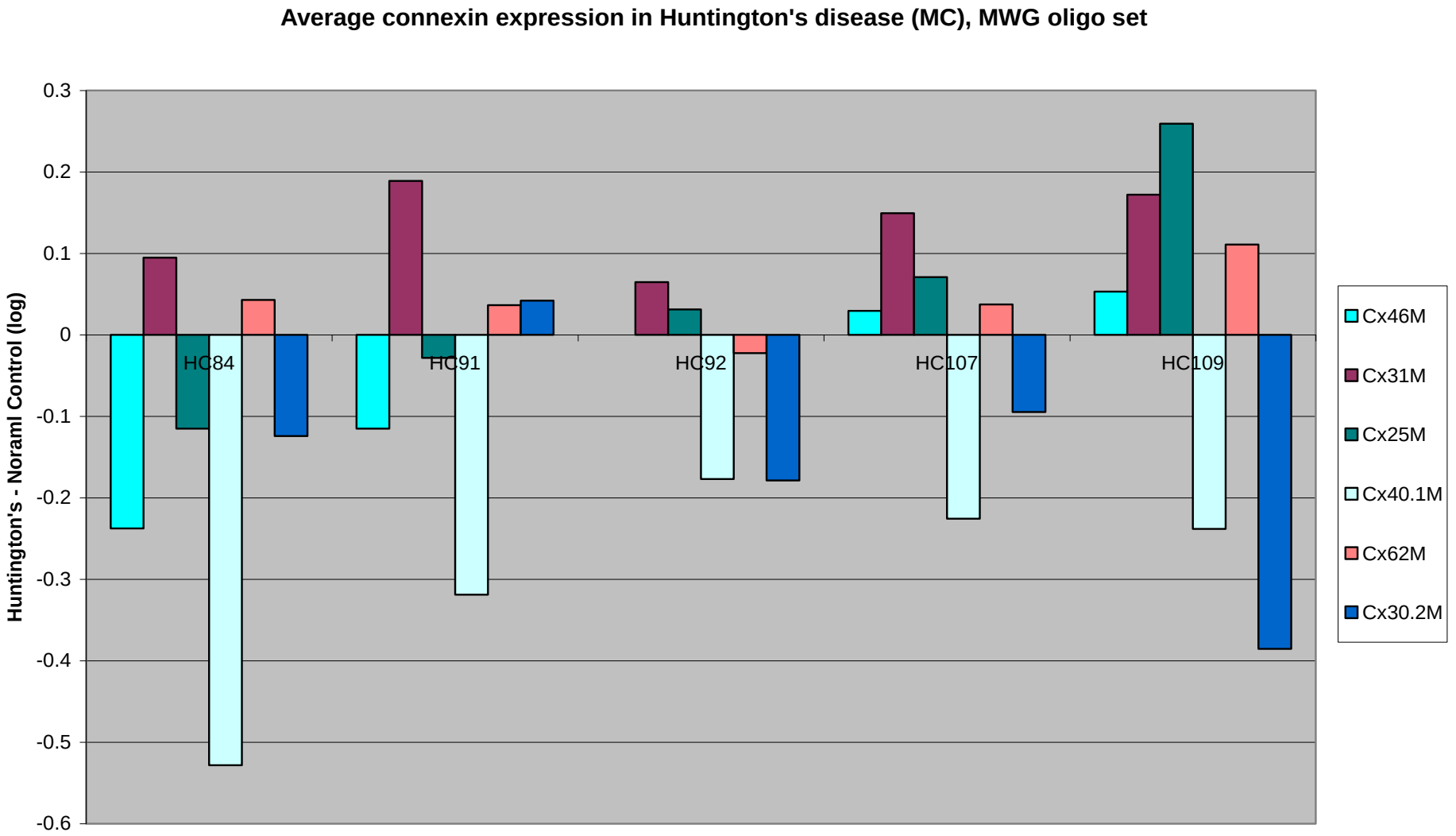

Figure 33. Differential expression of connexins in Huntington's disease, MWG-designed set, includes the connexins that are expressed on the custom-designed array but not on the Illumina array. Each of the five Huntington's disease samples was screened against the normal control sample. Y axis - the expression level in the diseased sample minus the expression level in the normal control sample.

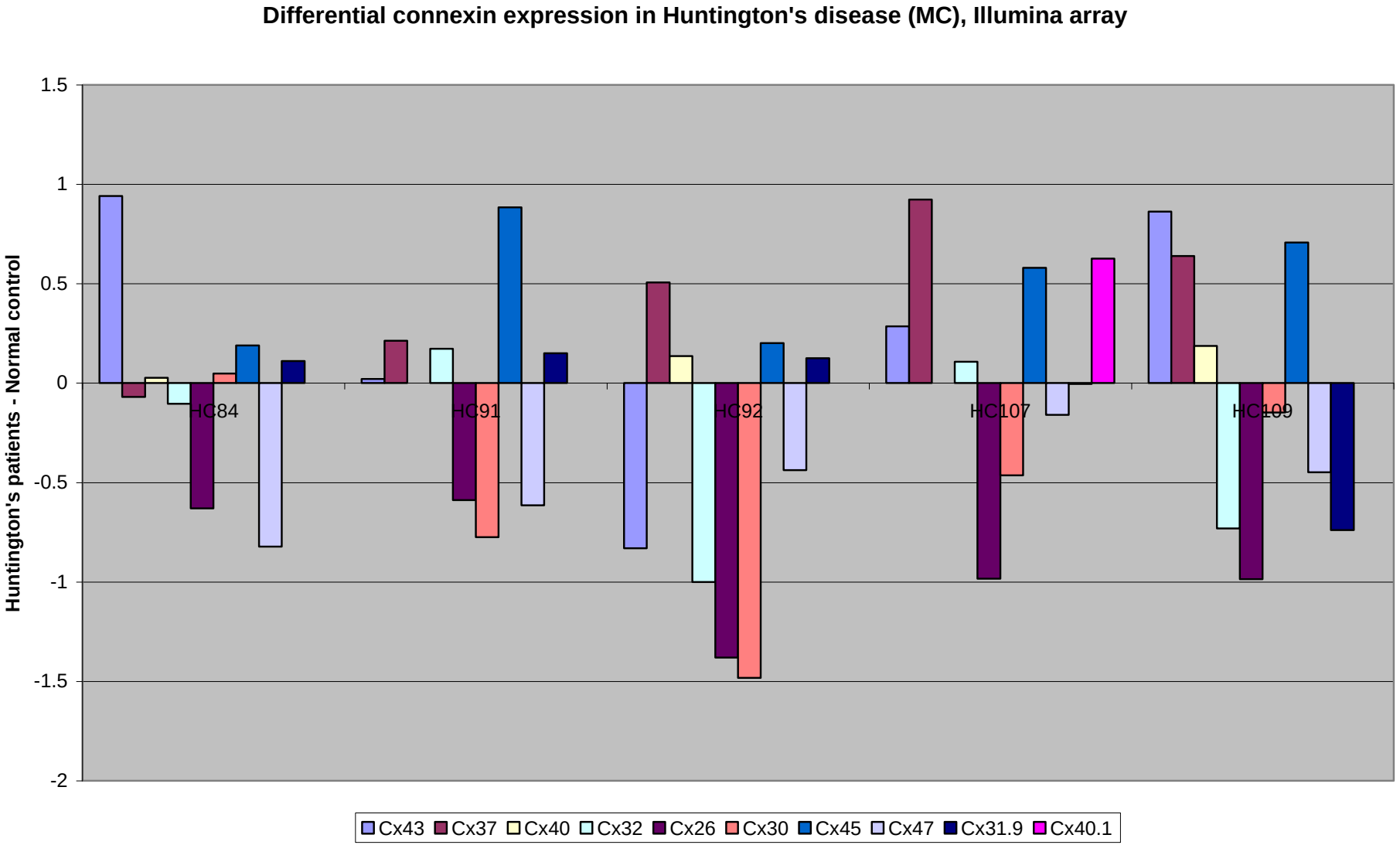

Figure 34. Differential connexin expression in Huntington's disease, Illumina array. Five Huntington's disease samples were screened against one control sample. Y axis - the expression level in the diseased sample minus the expression level in the normal control sample.

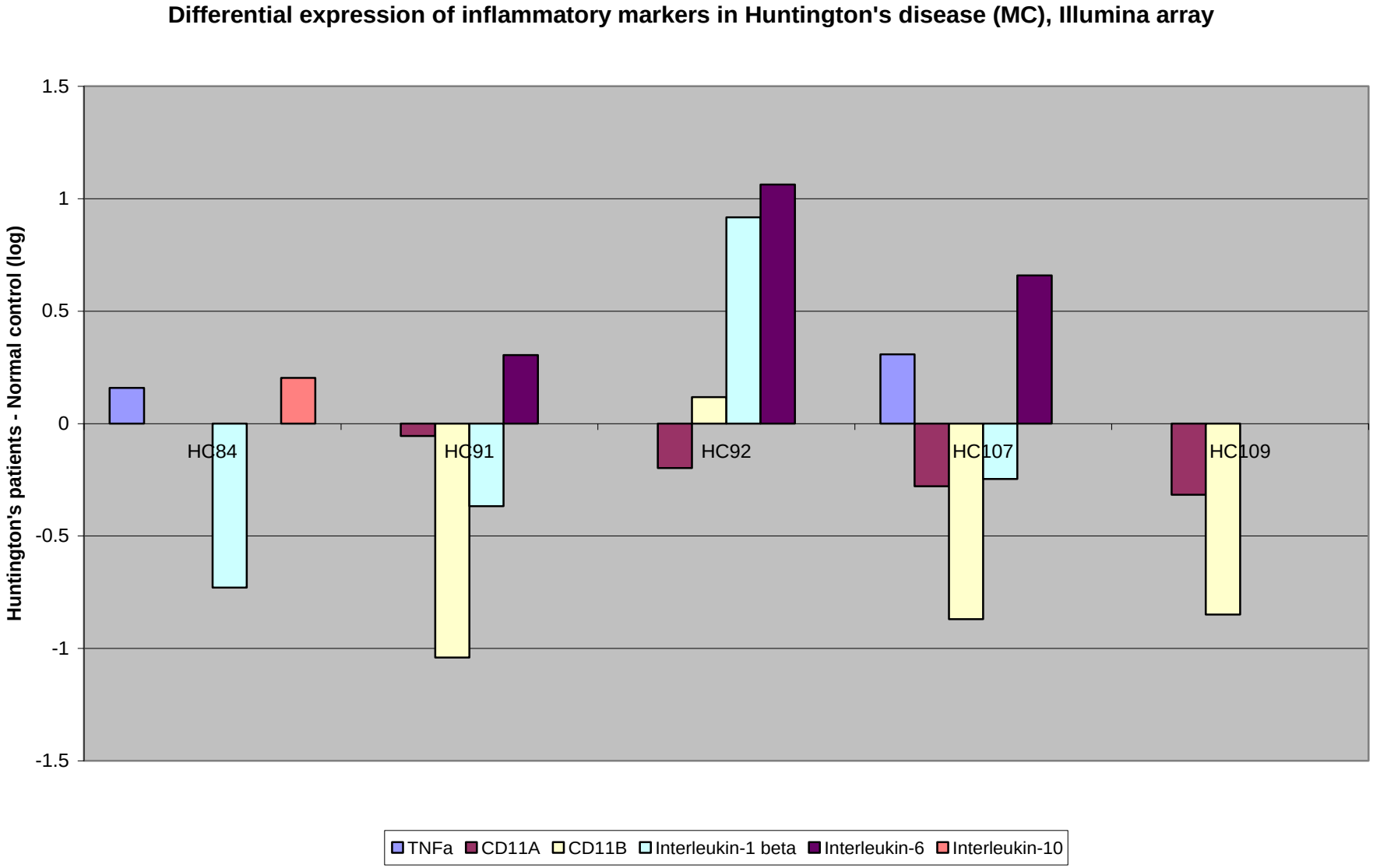

Figure 35. Differential expression of inflammatory markers in Huntington's disease, Illumina array. Five Huntington's disease samples were screened against one control sample. Y axis - the expression level in the diseased sample minus the expression level in the normal control sample.

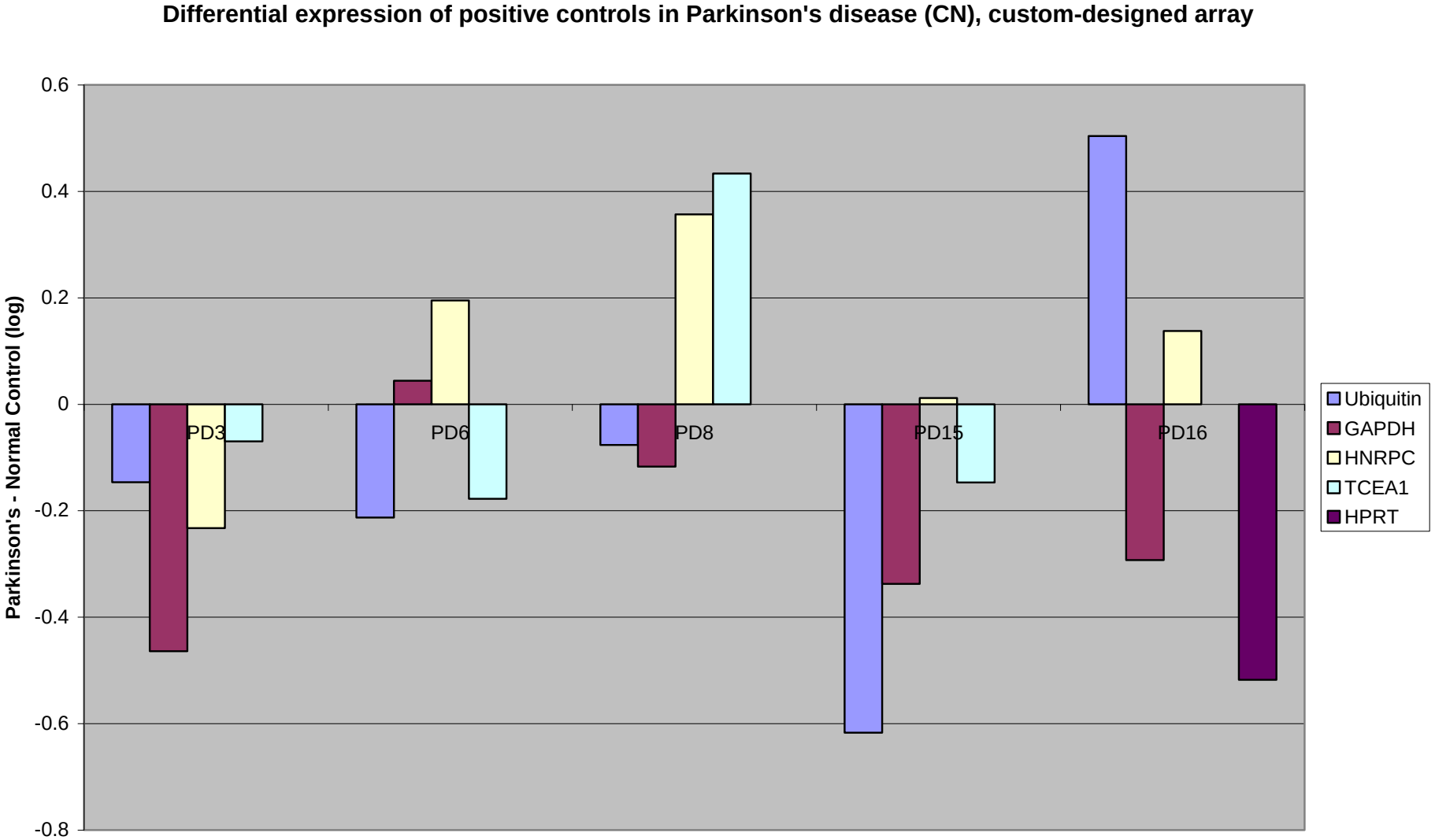

Figure 36. Differential expression of positive controls in Parkinson's disease, custom-designed array. Each of the five Parkinson's disease samples was screened against the normal control sample. Y axis - the expression level in the diseased sample minus the expression level in the normal control sample.

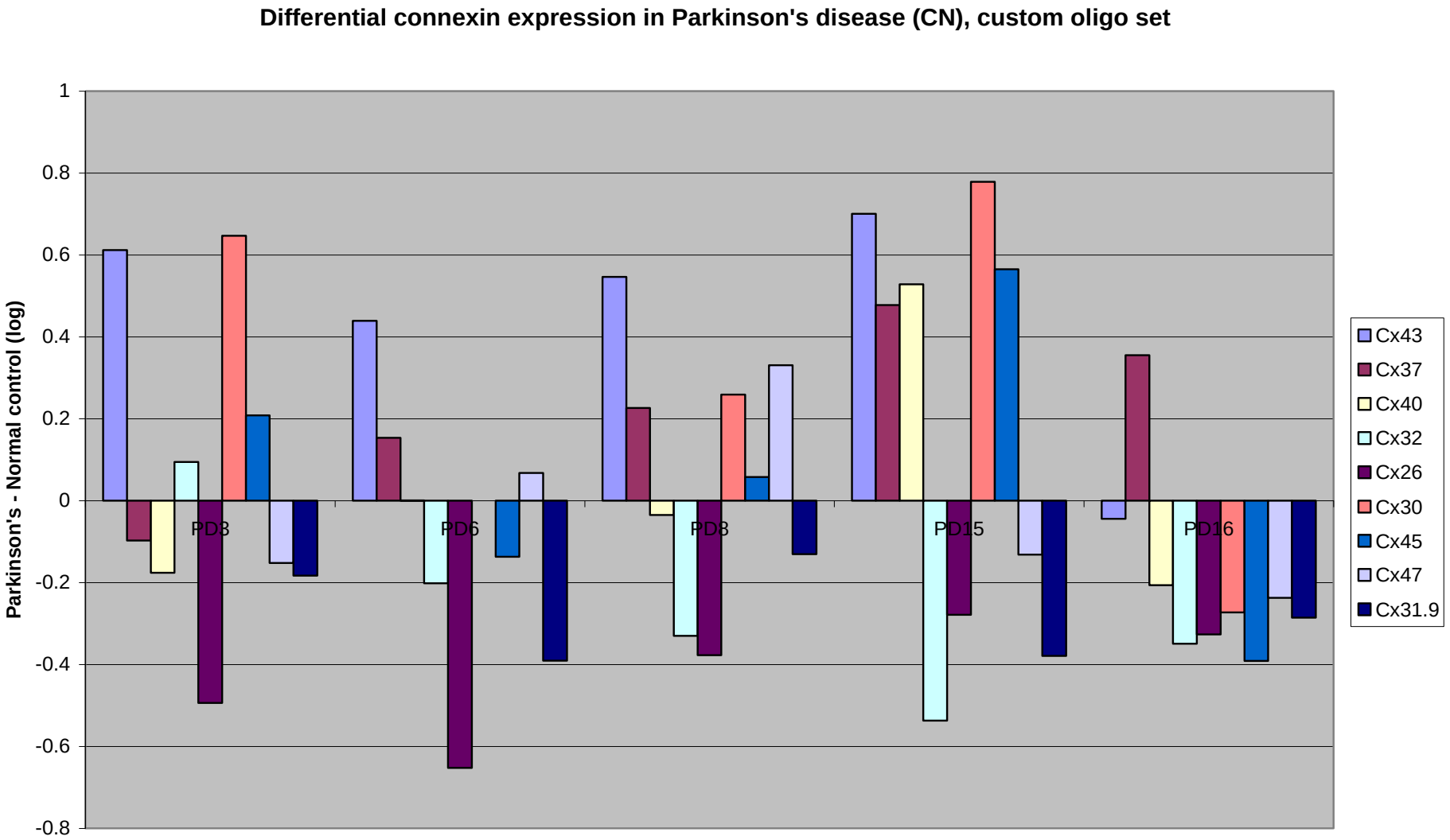

Figure 37. Differential expression of connexins in Parkinson's disease, custom-designed set, includes only the connexins that are expressed on the custom-designed array that are also expressed on the Illumina array. Each of the five Parkinson's disease samples was screened against the normal control sample. Y axis - the expression level in the diseased sample minus the expression level in the normal control sample

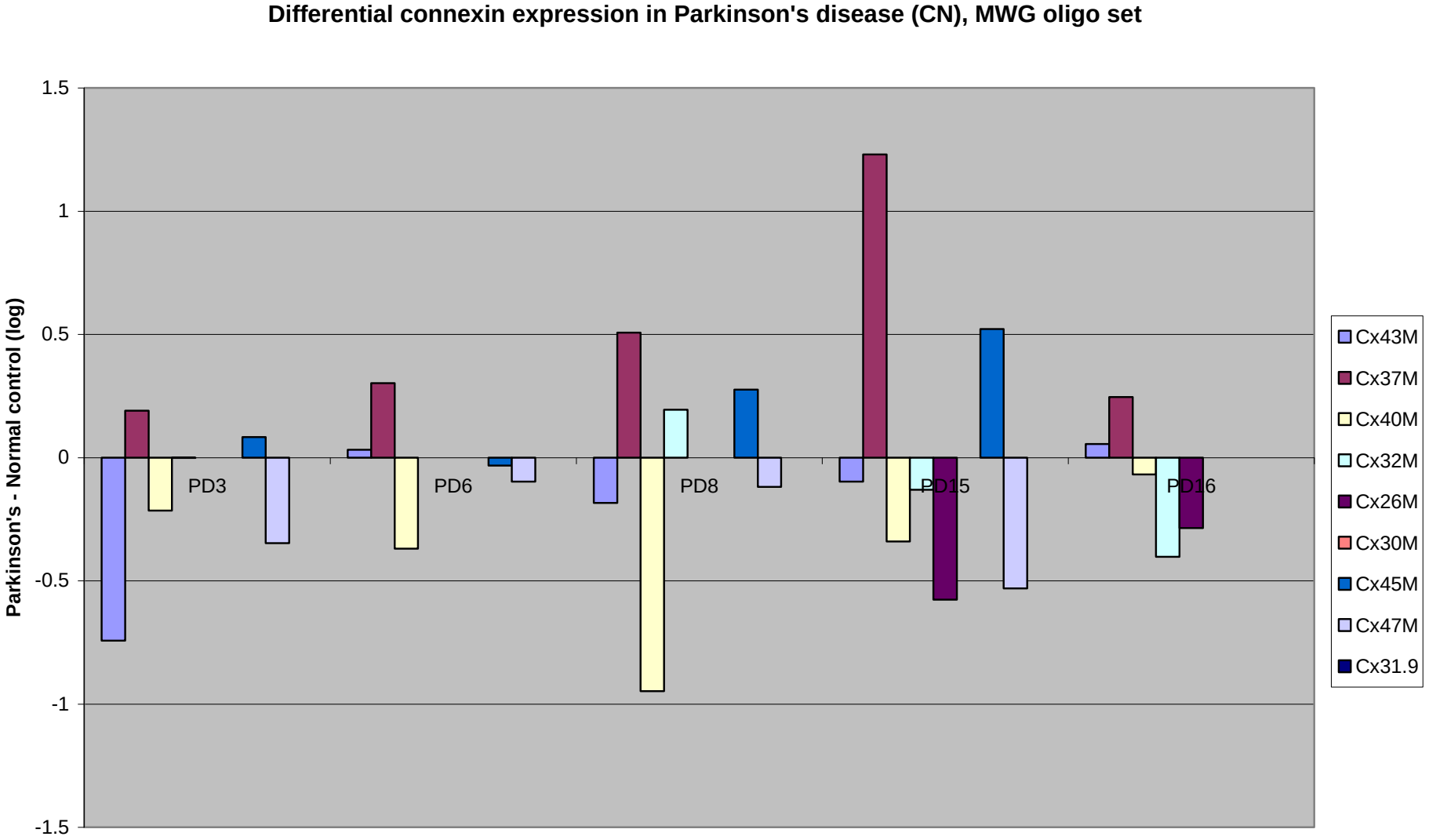

Figure 38. Differential expression of connexins in Parkinson's disease, MWG-designed set, includes only the connexins that are expressed on the custom-designed array that are also expressed on the Illumina array. Each of the five Parkinson's disease samples was screened against the normal control sample. Y axis - the expression level in the diseased sample minus the expression level in the normal control sample.

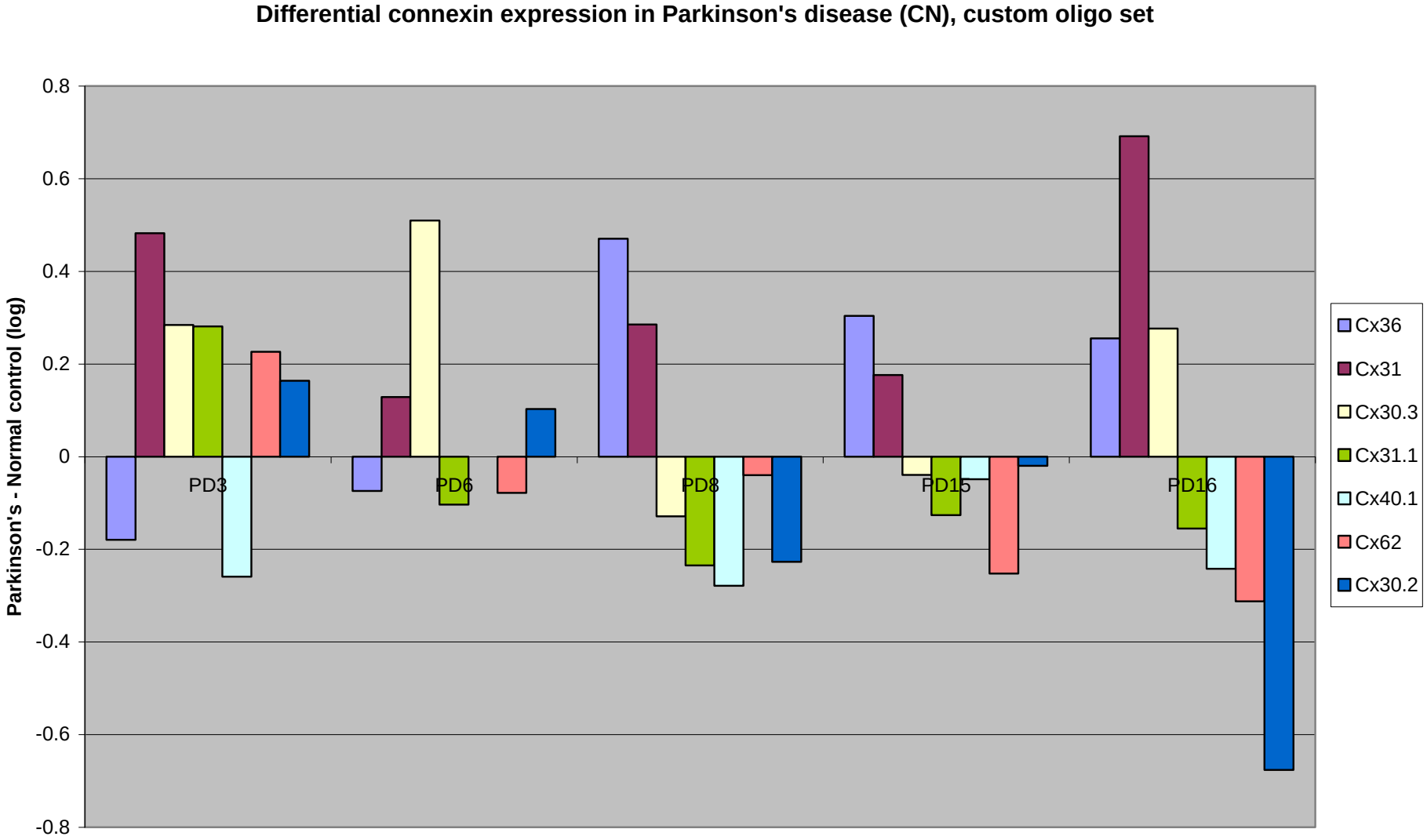

Figure 39. Differential expression of connexins in Parkinson's disease, custom-designed set, includes the connexins that are expressed on the custom-designed array but not on the Illumina array. Each of the five Parkinson's disease samples was screened against the normal control sample. Y axis - the expression level in the diseased sample minus the expression level in the normal control sample.

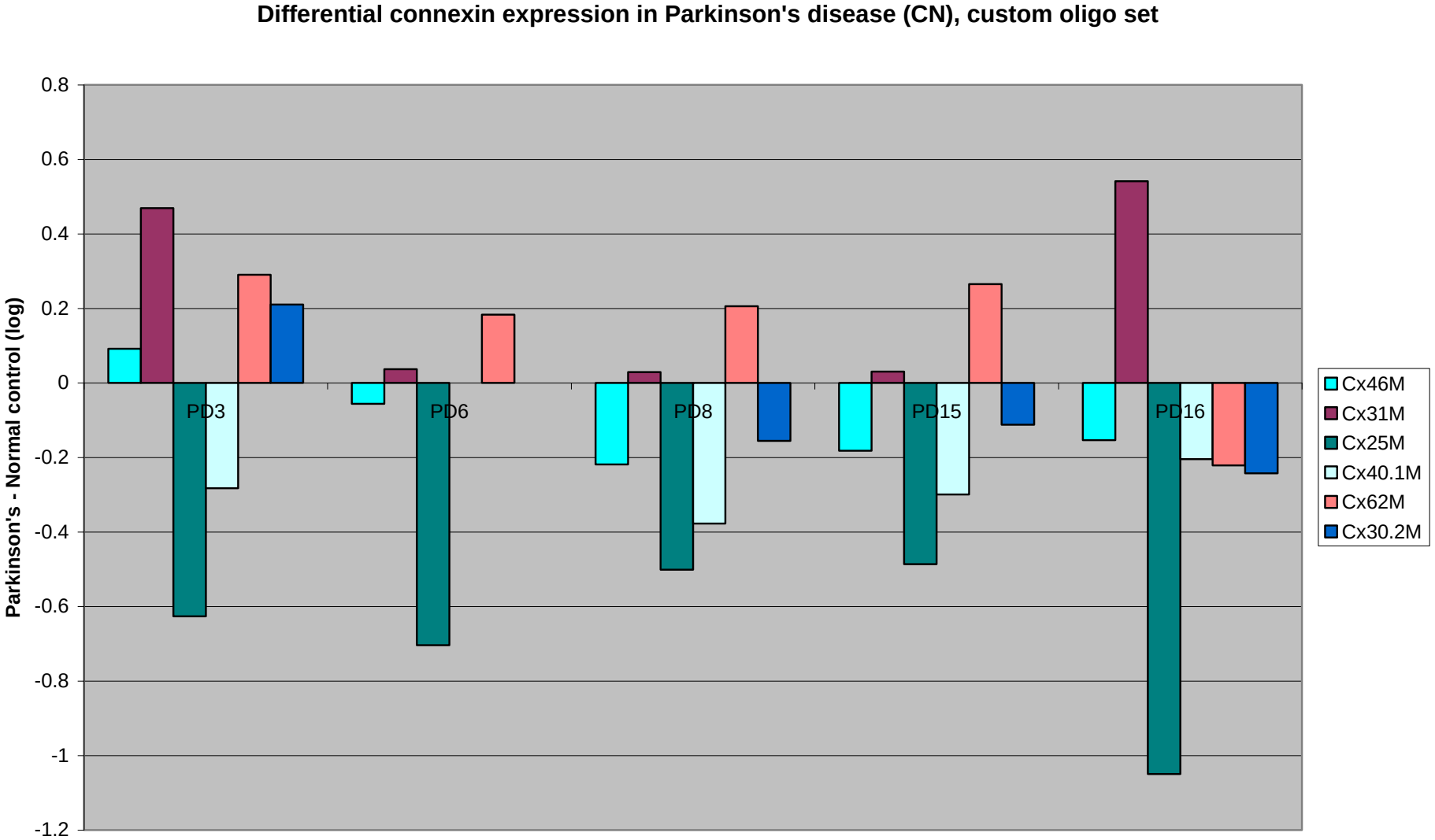

Figure 40. Differential expression of connexins in Parkinson's disease, MWG-designed set, includes the connexins that are expressed on the custom-designed array but not on the Illumina array. Each of the five Parkinson's disease samples was screened against the normal control sample. Y axis - the expression level in the diseased sample minus the expression level in the normal control sample.

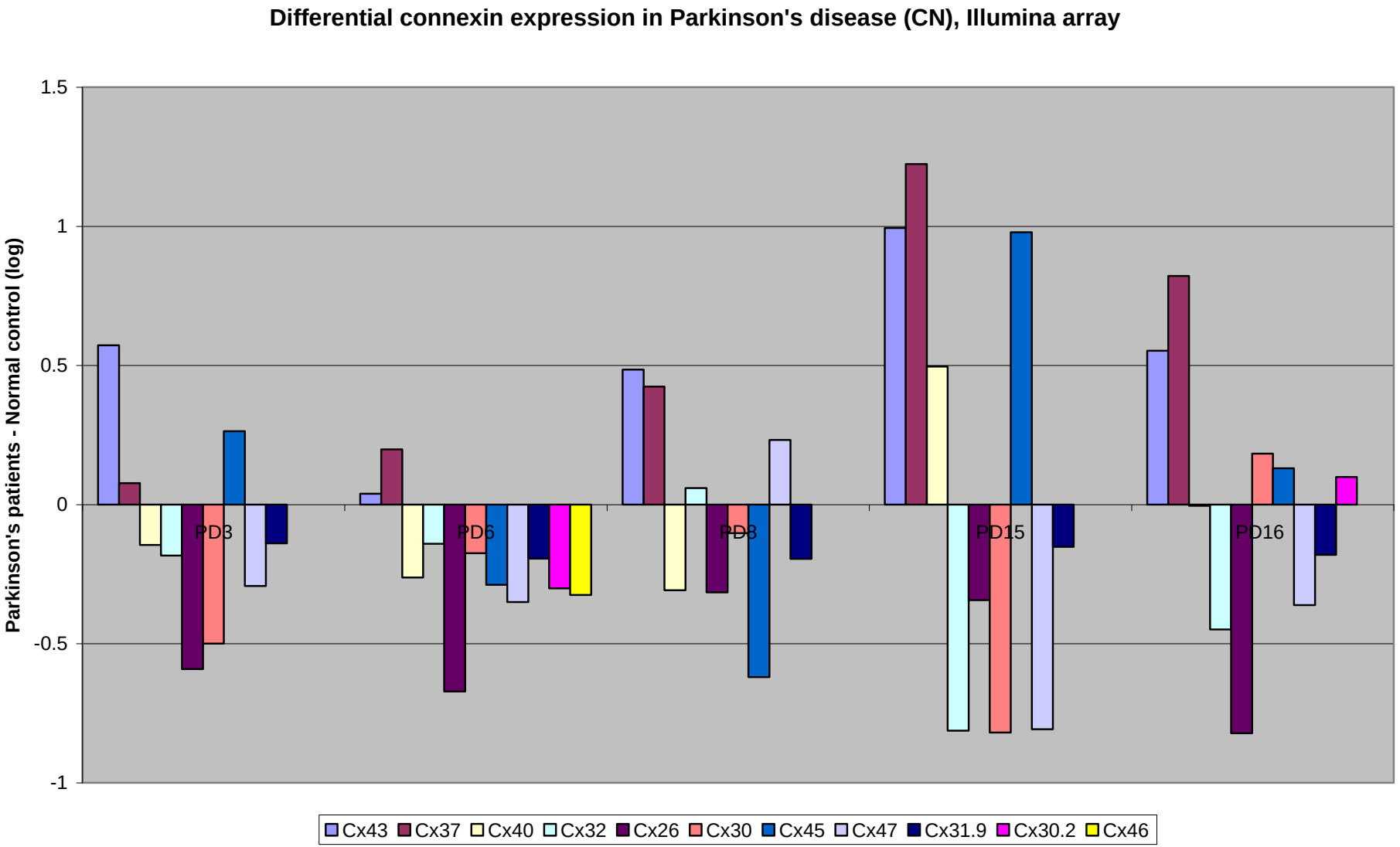

Figure 41. Differential connexin expression in Parkinson's disease, Illumina array. Five Parkinson's disease samples were screened against one control sample. Y axis - the expression level in the diseased sample minus the expression level in the normal control sample.

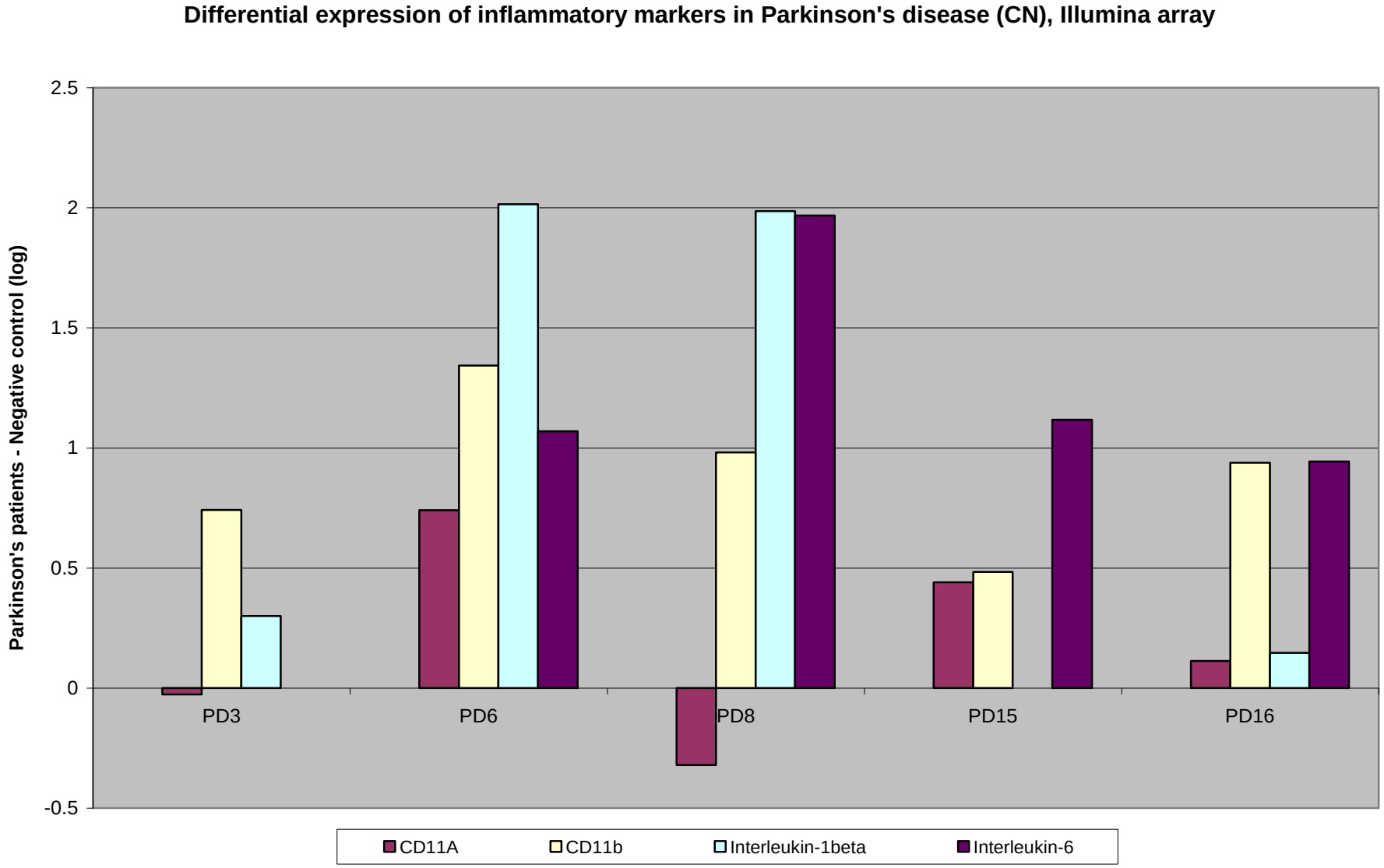

Figure 42. Differential expression of inflammatory markers in Parkinson's disease, Illumina array. Five Parkinson's disease samples were screened against one control sample. Y axis - the expression level in the diseased sample minus the expression level in the normal control sample.

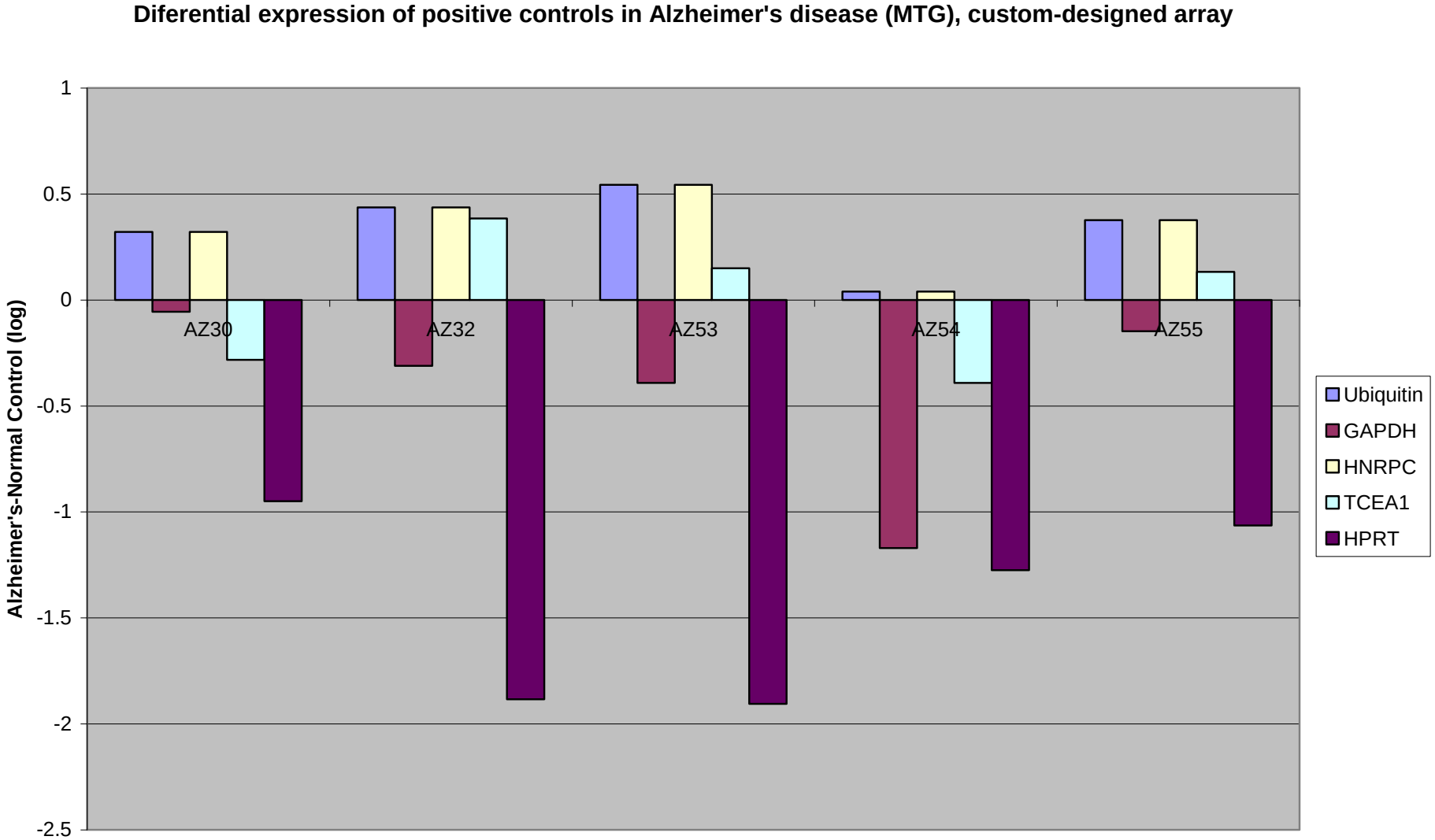

Figure 43. Differential expression of positive controls in Alzheimer's disease. Each of the five Alzheimer's disease samples was screened against the normal control sample. Y axis - the expression level in the diseased sample minus the expression level in the normal control sample.

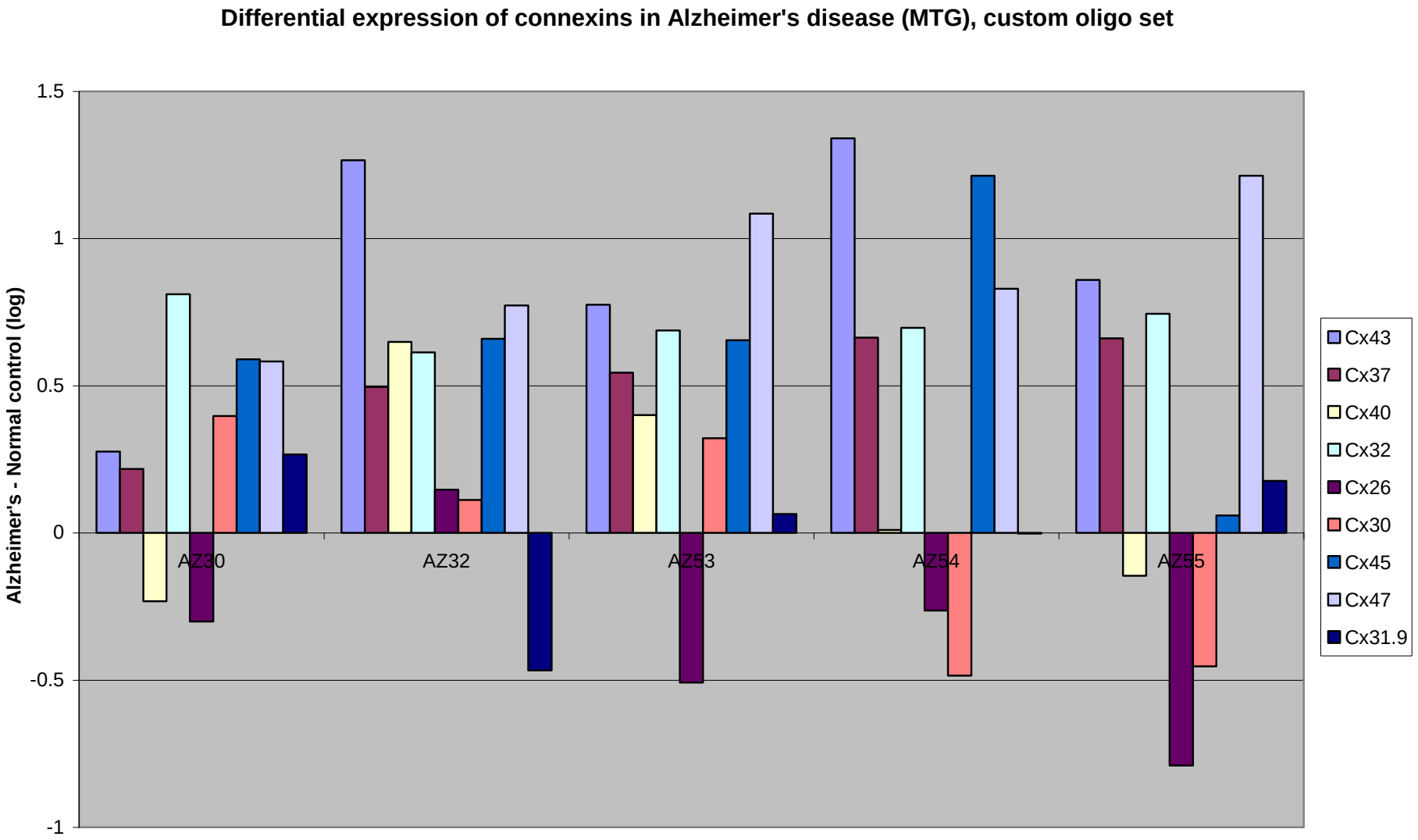

Figure 44. Differential expression of connexins in Alzheimer's disease, custom-designed set, includes only the connexins that are expressed on the custom-designed array that are also expressed on the Illumina array. Each of the five Alzheimer's disease samples was screened against the normal control sample. Y axis - the expression level in the diseased sample minus the expression level in the normal control sample.

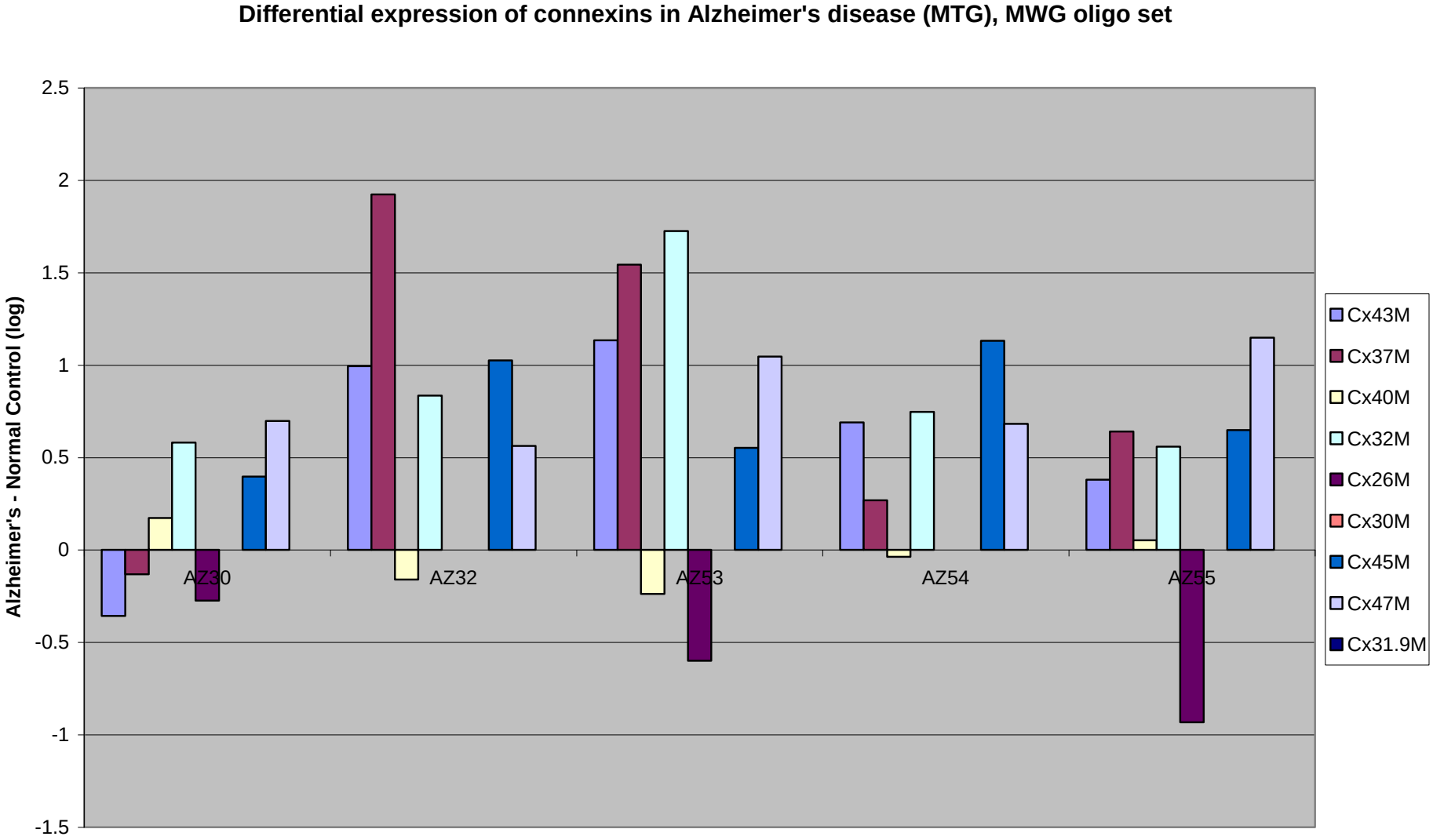

Figure 45. Differential expression of connexins in Alzheimer's disease, MWG-designed set, includes only the connexins that are expressed on the custom-designed array that are also expressed on the Illumina array. Each of the five Alzheimer's disease samples was screened against the normal control sample. Y axis - the expression level in the diseased sample minus the expression level in the normal control sample.

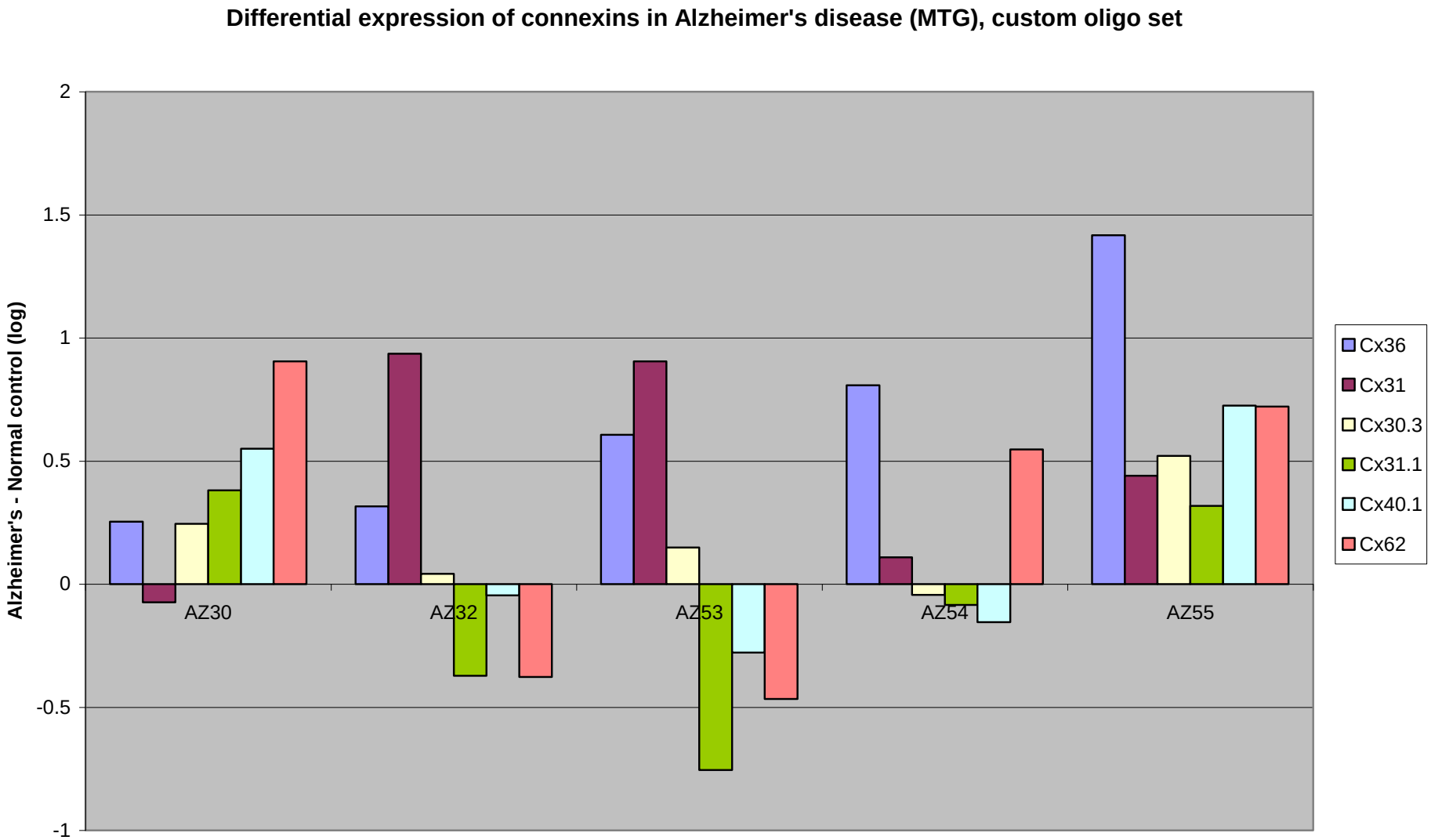

Figure 46. Differential expression of connexins in Alzheimer's disease, custom-designed set, includes the connexins that are expressed only on the custom-designed array but not on the Illumina array. Each of the five Alzheimer's disease samples was screened against the normal control sample. Y axis - the expression level in the diseased sample minus the expression level in the normal control sample.

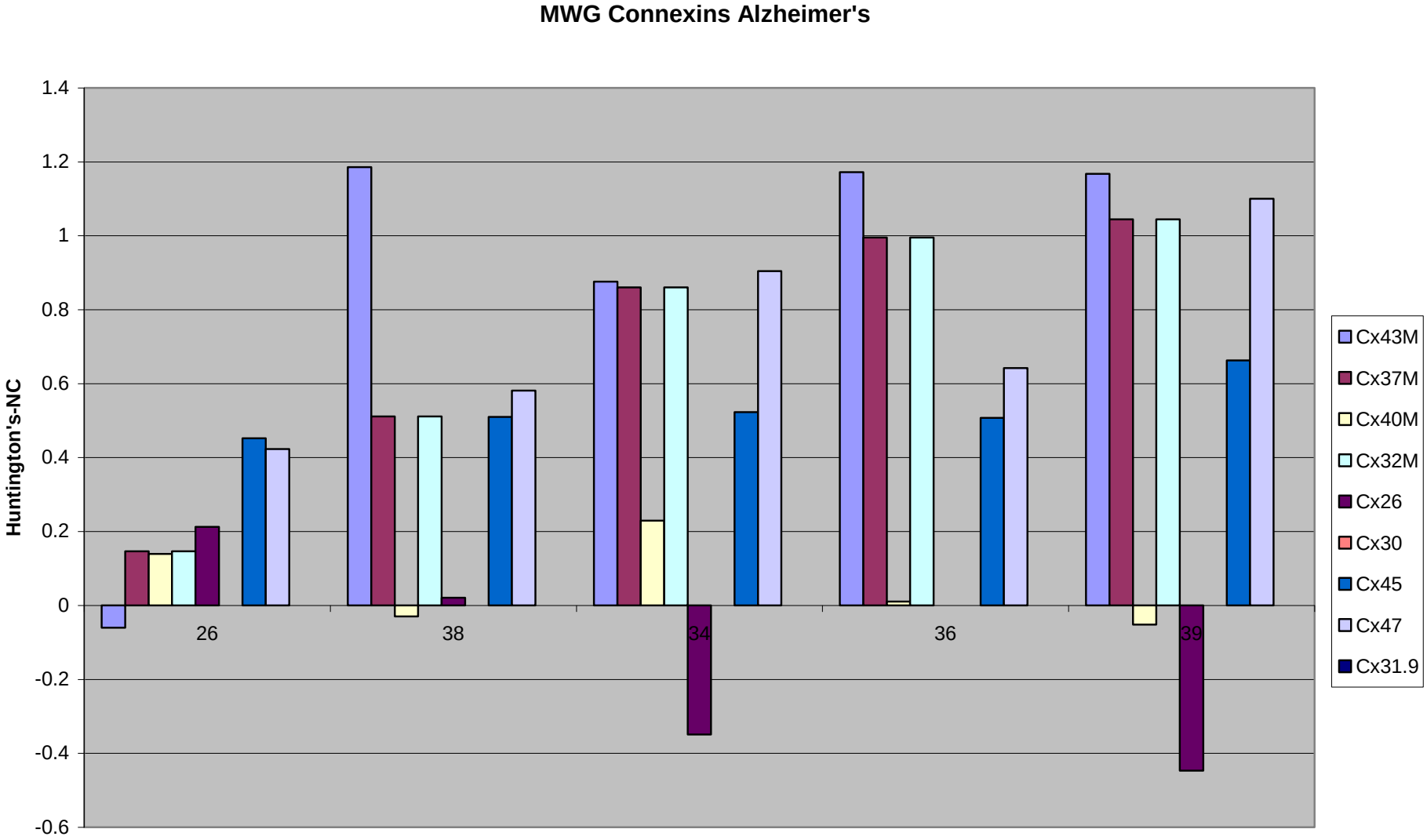

Figure 47. Differential expression of connexins in Alzheimer's disease, MWG-designed set, includes the connexins that are expressed only on the custom-designed array but not on the Illumina array. Each of the five Alzheimer's disease samples was screened against the normal control sample. Y axis - the expression level in the diseased sample minus the expression level in the normal control sample.

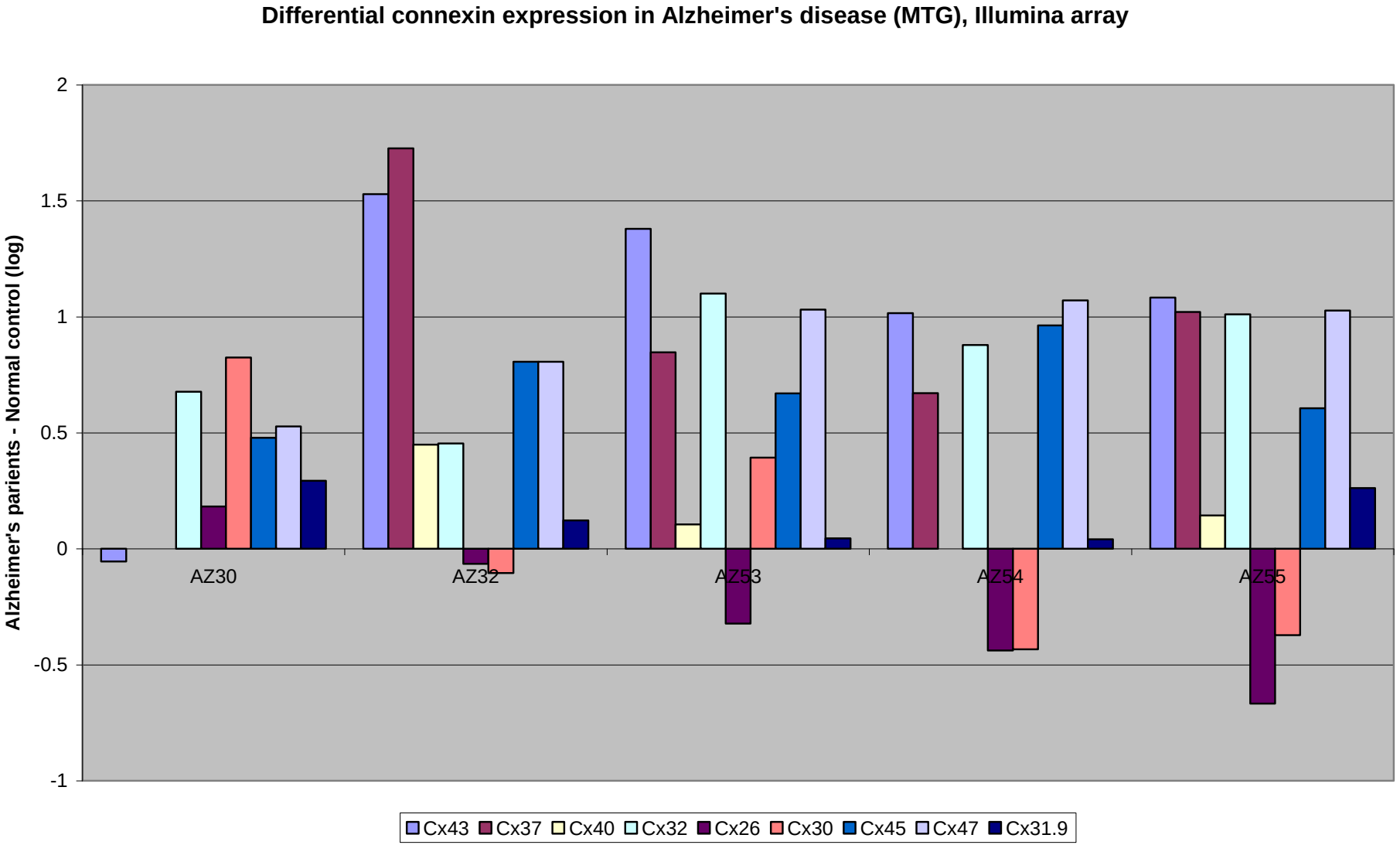

Figure 48. Differential connexin expression in Alzheimer's disease, Illumina array. Five Alzheimer's disease samples were screened against one control sample. Y axis - the expression level in the diseased sample minus the expression level in the normal control sample.

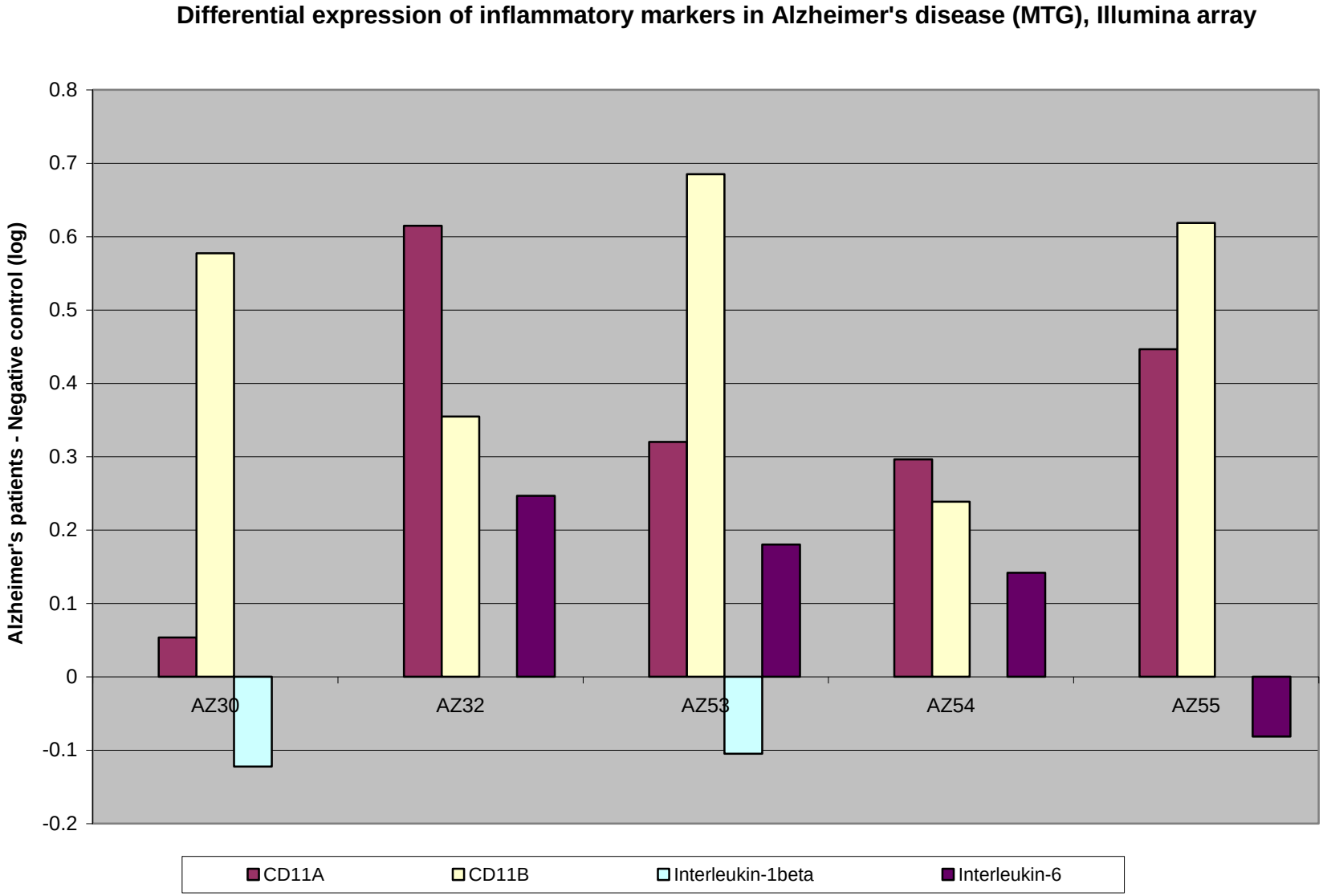

Figure 49. Differential expression of inflammatory markers in Alzheimer's disease. Five Alzheimer's disease samples were screened against one control sample. Y axis - the expression level in the diseased sample minus the expression level in the normal control sample.

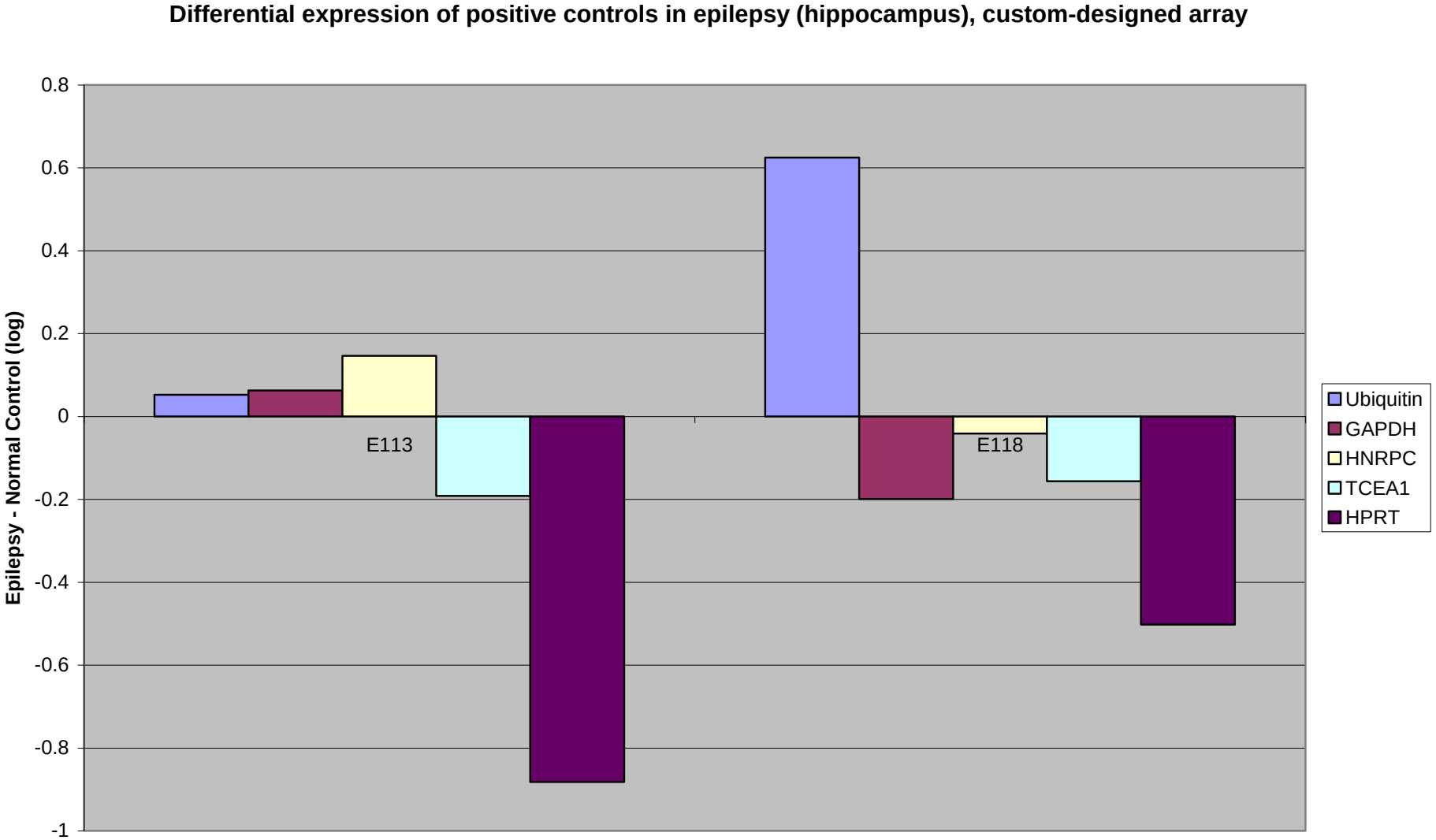

Figure 50. Differential expression of positive controls in epilepsy, custom-designed array. Each of the two epilepsy samples was screened against the normal control sample. Y axis - the expression level in the diseased sample minus the expression level in the normal control sample.

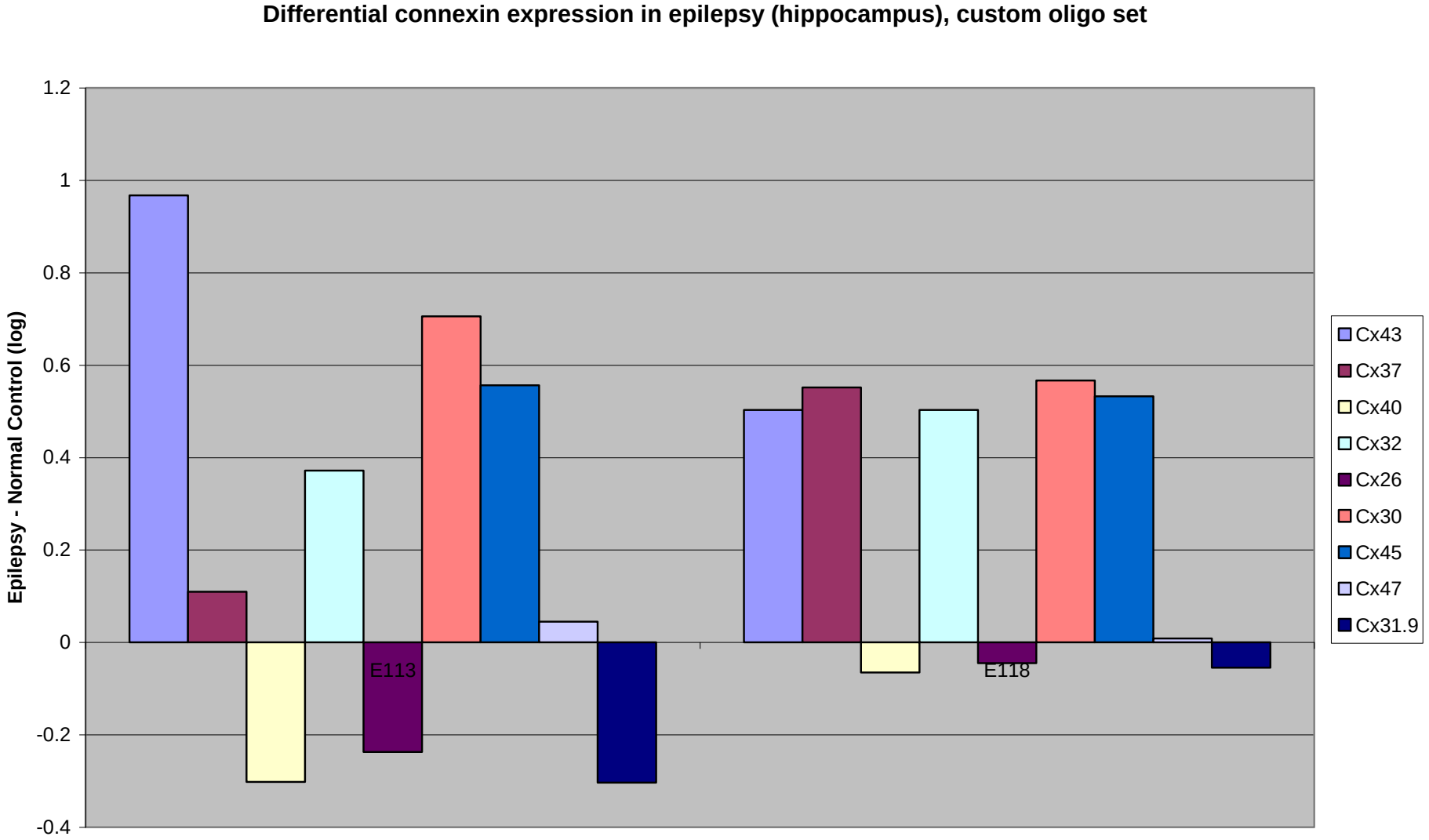

Figure 51. Differential expression of connexins in epilepsy, custom-designed set, includes only the connexins that are expressed on the custom-designed array and the Illumina arrays for the other diseases. Each of the two epilepsy samples was screened against the normal control sample. Y axis - the expression level in the diseased sample minus the expression level in the normal control sample.

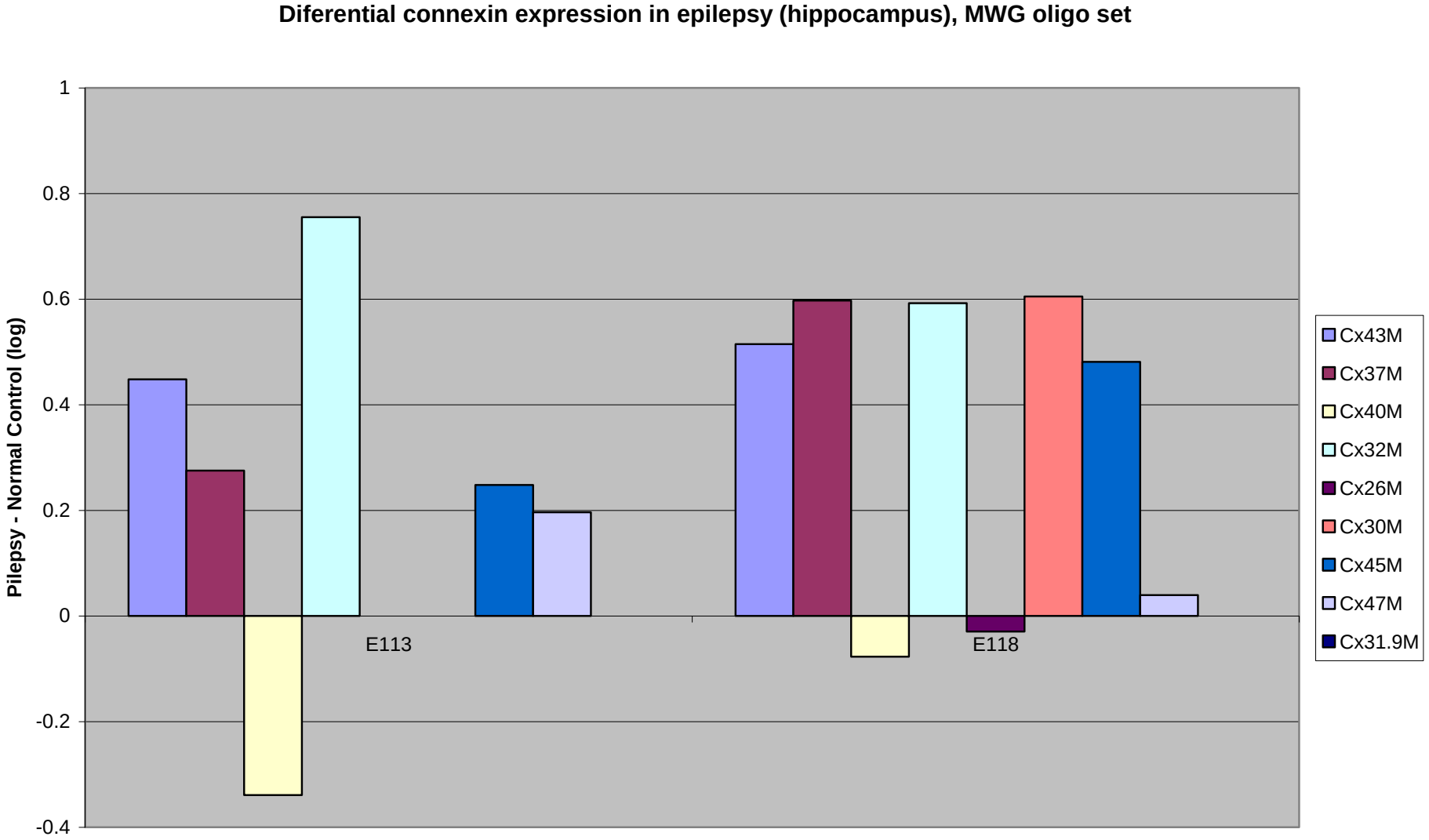

Figure 52. Differential expression of connexins in epilepsy, MWG-designed set, includes only the connexins that are expressed on the custom-designed array and the Illumina arrays for the other diseases. Each of the two epilepsy samples was screened against the normal control sample. Y axis - the expression level in the diseased sample minus the expression level in the normal control sample.

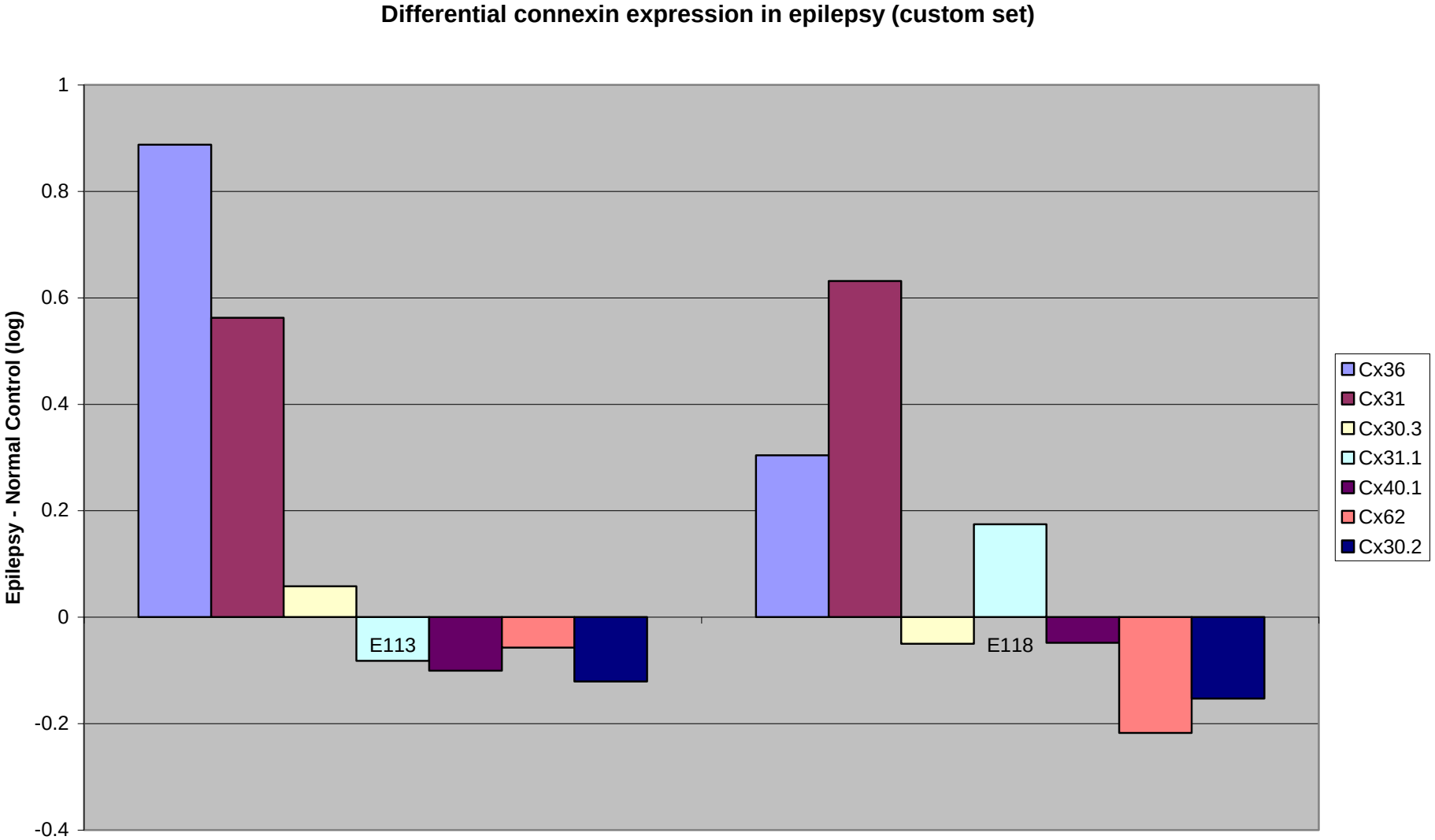

Figure 53. Differential expression of connexins in epilepsy, custom-designed set, includes the connexins that are expressed only in the custom-designed array. Each of the two epilepsy samples was screened against the normal control sample. Y axis - the expression level in the diseased sample minus the expression level in the normal control sample.

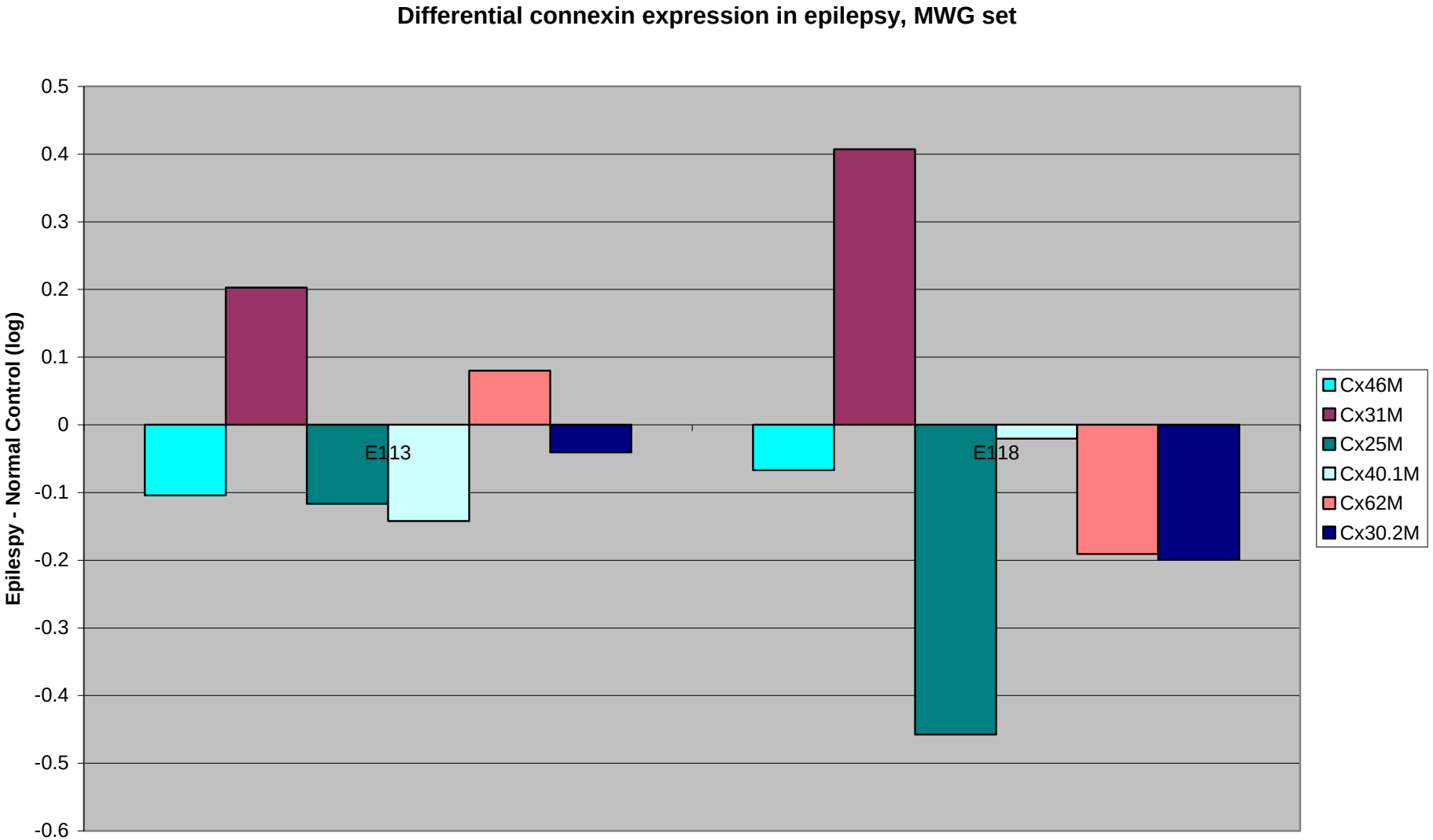

Figure 54. Differential expression of connexins in epilepsy, MWG-designed set, includes the connexins that are expressed only in the custom-designed array. Each of the two epilepsy samples was screened against the normal control sample. Y axis - the expression level in the diseased sample minus the expression level in the normal control sample.

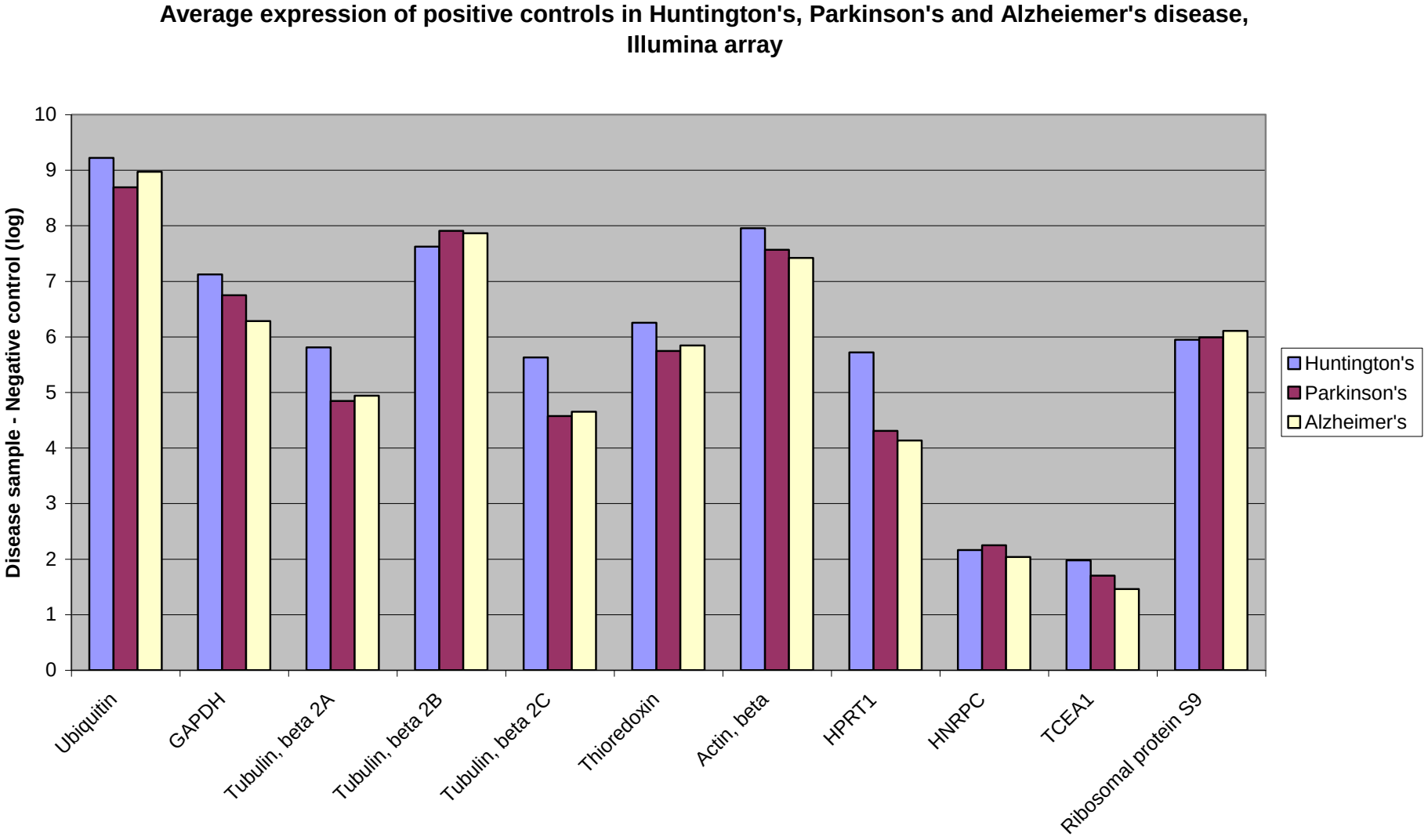

Figure 55. Average differential expression of positive controls in Huntington's, Parkinson's, Alzheimer's disease and epilepsy, custom-designed array. Y axis - the expression level in the diseased sample minus the expression level in the normal control sample.

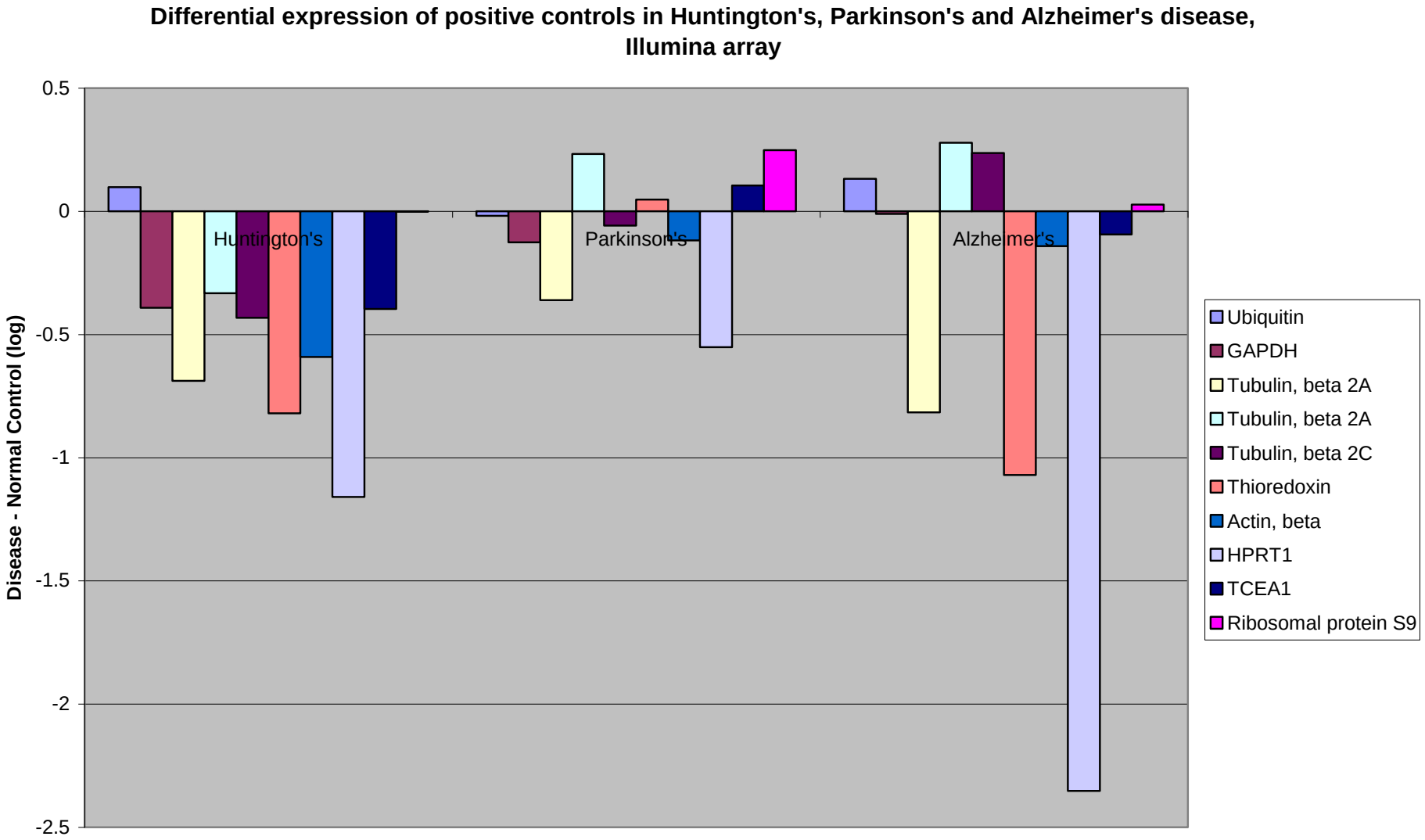

Figure 56. Average differential expression of positive controls in Huntington's, Parkinson's and Alzheimer's disease, Illumina array. Y axis - the expression level in the diseased sample minus the expression level in the normal control sample.

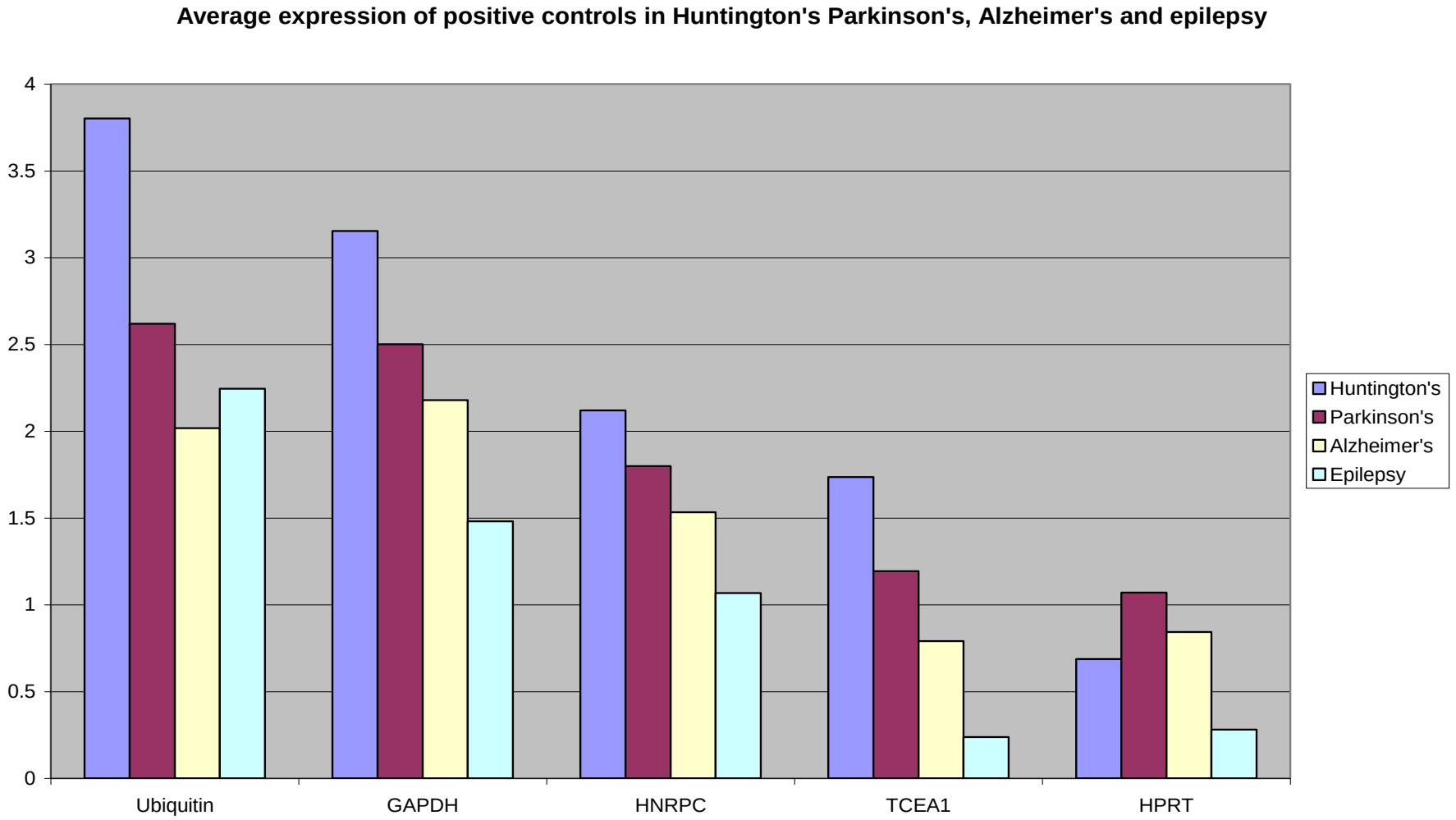

Figure 57. Average positive control expression for Huntington's, Parkinson's, Alzheimer's disease and epilepsy, custom-designed array. Y axis – absolute probe signal in the samples minus the average signal for the negative controls for the disease.

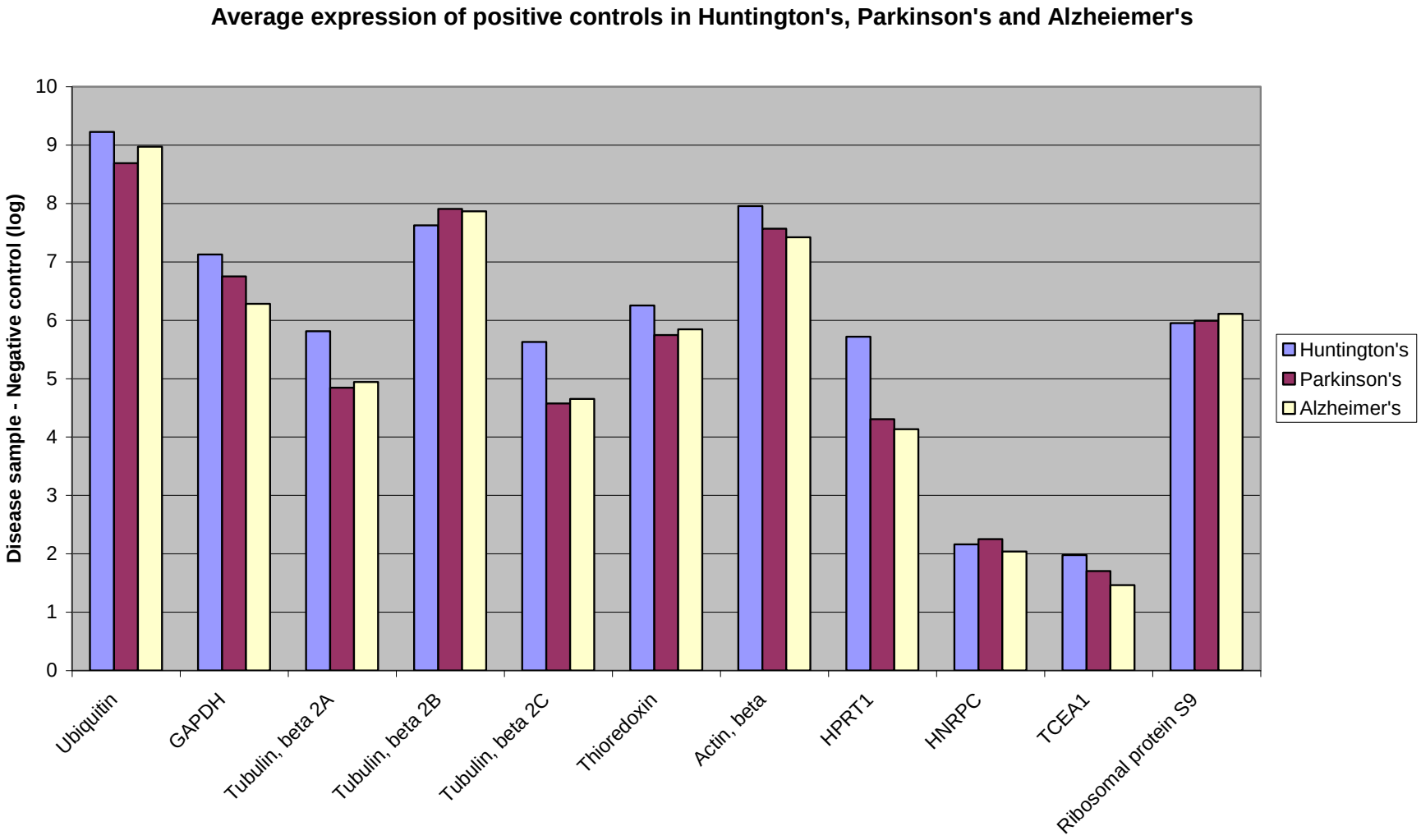

Figure 58. Average expression of positive controls in Huntington's, Parkinson's and Alzheimer's diseases, Illumina array. Y axis – absolute probe signal in the samples minus the average signal for the negative controls for the disease.

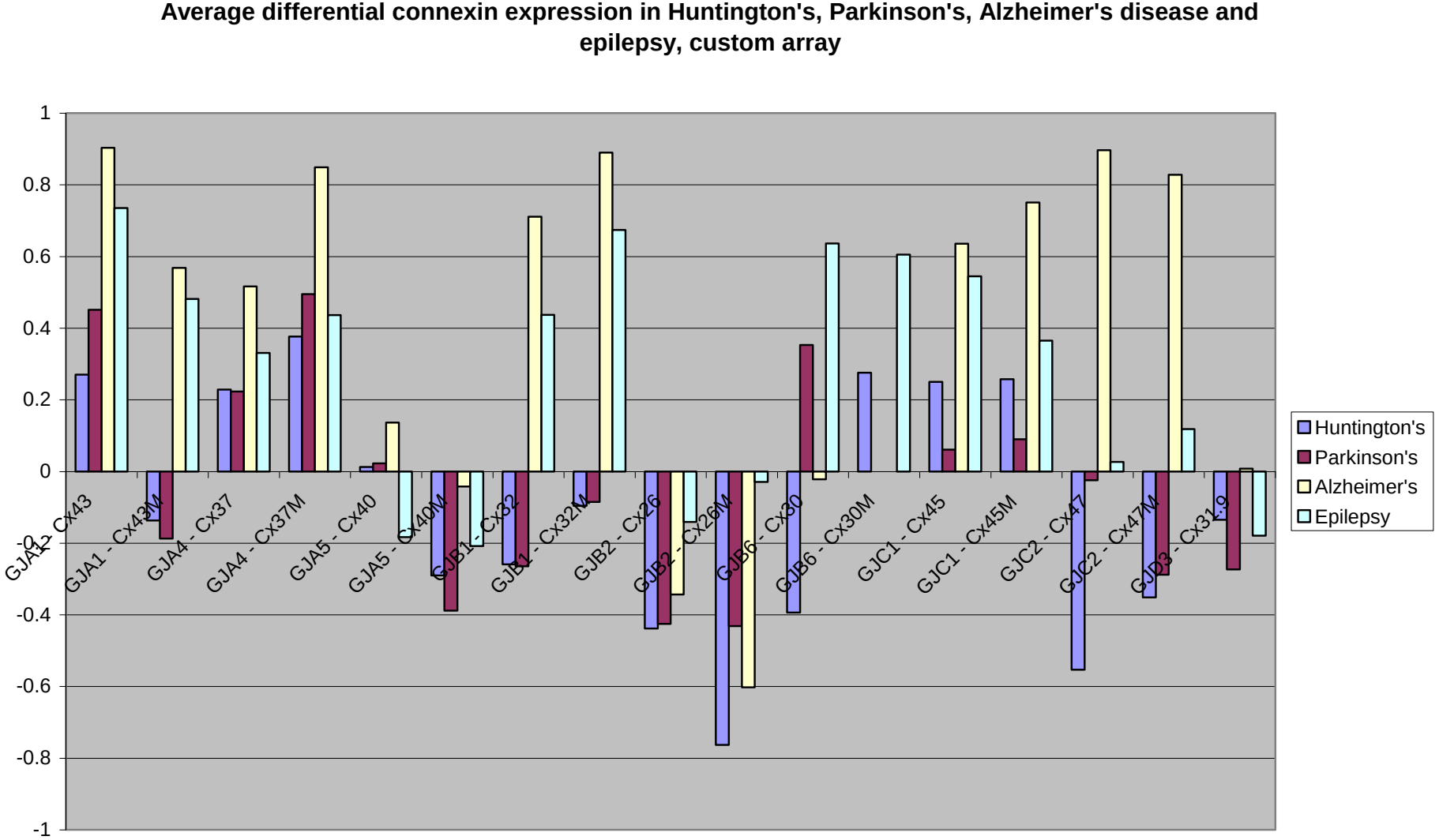

Figure 59. Average differential connexin expression for Huntington's, Parkinson's, Alzheimer's disease and epilepsy, custom-designed array, connexins that are expressed on the custom-designed array that are also expressed on the Illumina array. Y axis – the expression level in the diseased sample minus the expression level in the normal control sample.

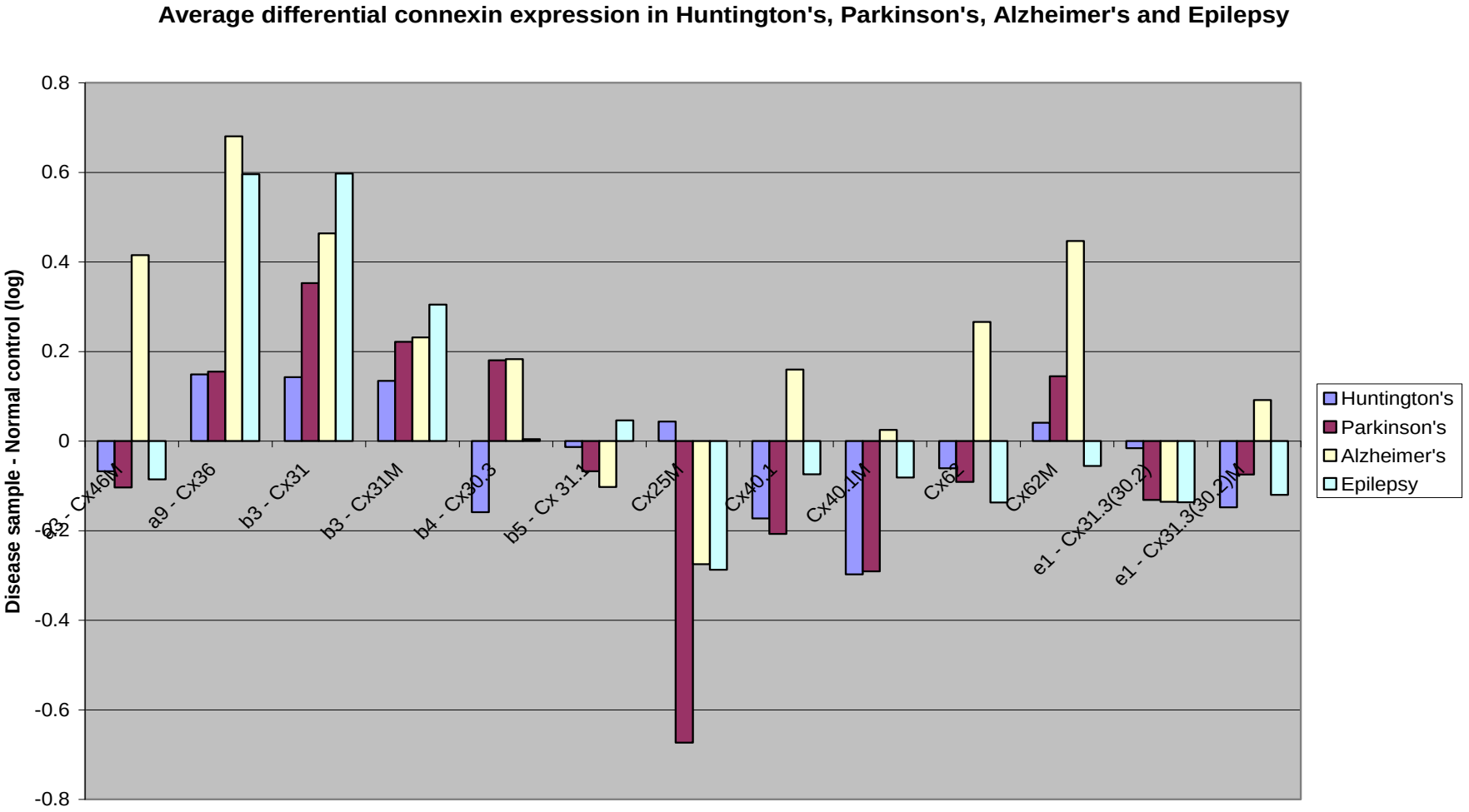

Figure 60. Average differential connexin expression for Huntington's, Parkinson's, Alzheimer's disease and epilepsy, custom-designed array, connexins that are expressed only on the custom-designed array but not on the Illumina array. Y axis - the expression level in the diseased sample minus the expression level in the normal control sample.

6 DISCUSSION

In this discussion I shall cover microarray chip design, validation and performance, then discuss the RNA quality study. In the last section I will discuss the expression of connexins and inflammatory markers in the human brain.

6.1 Microarrays

6.1.1 Oligonucleotide design

The main challenge in the design of custom oligonucleotides proved to be the selection of oligos which were both unique to the particular connexin and had a reasonably high degree of cross-species homology. To a large extent, these tasks were at odds – as stated in the literature (Evans and Martin, 2002; Willecke et al., 2002). There is less homology at the 3' end of the connexin sequences within a connexin family. However, there tends to be less cross-species homology at that part of the coding sequence. The task of cross-species design involved a compromise between these conflicting requirements. The best regions in terms of human-rat homology in most cases proved to not be sufficiently unique across connexin family members. For this reason a significant number of mismatches to the rat sequence are present in some oligonucleotides (up to nine for Cx30.3). This is, however, still far below the 30% mismatch threshold given by Hughes et al. (2001). These researchers have, however, also found that five or more randomly placed mismatches (on a 60-mer) can reduce the fluorescent signal intensity up to 50% of the perfectly matched oligonucleotide. This means that, although the expression of connexins which have mismatched oligonucleotides should be detected in rat tissue, the signal intensity would be considerably below that for the perfectly matched probes. This of course, would affect all tissues equally, so in terms of ratio-based studies in the rat (connexin expression changes in a test sample as compared to control), it should not present a problem. If the amount of gene expression is compared across different connexins in the one sample, however, this will affect the results, and should definitely be taken into account when the chip is used for rat gene expression.

The position of a mismatch on the oligonucleotide probe sequence is also a determinant of its hybridisation properties, with the importance of a base mismatch to hybridisation efficiency roughly corresponding to the distance of the mismatch from the surface (hybridisation is more efficient at the 'free' end of the probe due to a lesser degree of steric interactions further away from the surface (Hughes et al., 2001; Li and Stormo, 2001). Thus the oligonucleotide probes that have rat-human mismatches within the last ten bases at the 3'end (the 5' end being anchored to the surface), may

hybridise poorly even if the total number of mismatches is relatively low. All the oligonucleotides, however, should still be able to detect the presence of connexin expression in the rat tissue, as they all meet the criteria for giving significant hybridisation signal as established previously (>80% sequence similarity and a stretch of contiguous bases of >15 bases long) (Kane et al., 2000).

Due to the confidentiality issues relating to the MWG 30,000 gene array oligonucleotide sequences, these probes could not be aligned against the orthologous rat connexins. This meant that their compatibility with the rat tissue was only speculation. There is also a high chance of cross-hybridisation of the oligos with unrelated sequences from the rat cDNA pool, as they have not been checked against the rat genome. These two considerations effectively render them unsuitable for screening rat tissue with any reliability.

The points mentioned above, together with the fact that a number of rat connexins (Cx46, 33, 29, 39) are not represented on the array, suggests that the chip could only be used for preliminary screening of rat tissue, and that expression studies should be subsequently undertaken using other techniques.

6.1.2 Microarray chips

The overall performance of the array in terms of technical characteristics appears to be satisfactory. The dye intensities across a slide were consistent, demonstrated by the uniform array background and the small standard deviation for all the spots representing a particular oligo in each array block. The connexin expression in different tissues showed a certain degree of consistency across the arrays. Target binding across each array was uniform, and the small amount of variability present seems to be due mainly to technical problems.

The correlation between the two heart samples (rat heart *vs* rat heart) on an array was high, which gives some confidence in the hybridisation properties of the array. Use of the same heart RNA sample, as opposed to two separate heart samples, did not eliminate the small amount of variation, suggesting that this was due to experimental error and not to biological differences. The rat liver *vs* rat heart validation study demonstrated good reproducibility of the results for sample and biological repeats as well as dye reversal experiments.

The high levels of non-specific hybridisation, as represented by the significant intensity of the negative *Arabidopsis* control spots and the presence of oversaturated spots on the array presented a challenge in these experiments. At such high intensities the precise estimation of the target amount is difficult, due to the loss of linear dependence of the amount of detected signal on the amount of

fluorophore present (Hughes et al., 2001). The high fluorescence level was later reduced by optimising the hybridisation and washing condition as well as the scanning settings.

There was also considerably more fluorescence in the Cy3 (green) channel, than in the Cy5 (red) channel on all the slides, as evident both visually and in the intensity data. Cy3 and Cy5 are known to have different quantum yields and to be incorporated at different rates during the reverse transcription reaction. Cy5 is also more sensitive to photobleaching (de Longueville et al., 2002; Armstrong and van de Wiel, 2004). This imbalance required normalisation to correct and underscores the importance of dye reversal experiments.

Global normalisation is customarily used for correcting for colour imbalances. With such a small array, however, it cannot be assumed that overall there is no change in gene expression, i.e. that the log ratios are linear with respect to the signal magnitude. The alternative approach is to construct an MA plot based on the values for positive and negative controls (Yang et al., 2002a; Forster et al., 2003). This is the normalisation procedure which was used in the preliminary validation experiments. This normalisation procedure, however, is not as reliable as the use of the entire set of data, due to the relatively small number of controls, and to the necessity to assume that there was no change in expression between the two samples on a chip, which presents a similar issue to assuming there is no change in overall expression level in the entire set of genes tested. Latter experiments using the commercial microarray platforms confirmed that the expression of in-built housekeeping controls does not remain constant, with both the housekeeping gene expression and the overall signal intensity being related to RNA quality. Thus global normalisation was used in the rat liver *vs* rat heart validation experiments and for the human brain custom-designed array data and appeared to give more consistent results.

The method of binding signal significance estimation based on the brightest negative control which was employed in the preliminary validation experiments appeared to be highly dependent on the amount of intra-slide variation. The two arrays (rat heart *vs* rat lens and human brain *vs* rat brain) with the highest standard deviations for each of the 16-spots per oligo also had the highest cut-off points in terms of the signal intensity significance. The slide with the lowest variability (rat liver *vs* rat brain) has the highest number of expressed connexins of all the arrays. On the rat heart *vs* rat lens array, the expression threshold based on the five negative controls cut off the majority of the connexins, including three of the positive controls which are expressed on all the other arrays. As the RNA quality of the human brain tissue and especially the lens tissue on the respective arrays was considerably below that of the other samples screened, this suggested a potentially serious problem with obtaining results from screening human samples which tend to have a large range of RNA quality, with the significance threshold cutting off most connexins. A possible reason for what seemed to be excessive stringency is

that the variability in the negative control population across the array (which would mirror the overall intra-slide variability) had not been considered in the significance test, i.e. the brightest negative control value was treated as a constant. This was taken into account in the data analysis of the following experiments leading to more consistent results across the range of RNA quality (Tamames et al., 2002; Forster et al., 2003).

A similar problem with estimating differential expression while correlation coefficients between the dye reversals were good, estimation of differential expression varied considerably, being overly dependent on small variations across a slide. Further optimisation of the washing and hybridisation protocol as well as using a different normalisation method appeared to resolve the issue.

The MWG oligonucleotides would also be expected to show a more scattered pattern in terms of binding intensity, as they have a wider CG content and Tm range than our oligonucleotides (30% to 70% GC, with 51% mean, as compared to 50% to 62% GC, with a 56% mean for our oligos). The human brain *vs* rat brain array appeared to bear this out, however the melting temperature did not necessarily show a direct correlation to the binding intensity. The absolute amount of binding for each channel would not be expected to be equal for each pair of oligos designed to the same target within the same platform and cross-platform due to varying labelling methods and probe sequences. This is confirmed by genes which had more than one probe designed to them in the commercial platform (e.g. housekeeping genes on the Illumina array). The relative expression level between a pair of sample types should however be maintained between platforms (Shi et al., 2006).

The five positive controls demonstrated a very constant intensity distribution pattern across all the slides. Ubiquitin demonstrated the highest level of expression, followed by GAPDH. TCEA was third highest, HNRPC was fourth highest, and HPRT the lowest. The expression level of housekeeping controls appeared to correlate with RNA quality which was the most evident in the human brain experiments (both in the Illumina and the custom-designed arrays) as they involved using RNA with a large range of quality. Housekeeping controls were downregulated in all samples in Alzheimer's disease, downregulated in the lowest RIN sample in Parkinson's disease (PD15, RIN=5.3) and in Huntington's disease (HC109, RIN=6.1). HC107 in Huntington's disease was an exception where the housekeeping controls were downregulated in spite of its high RNA quality (RIN=9.1). HPRT, the only positive control gene not showing significant expression on most rat and human custom-designed array slides, had the strongest trend towards downregulation with decreasing RNA quality. On the custom-designed array this could be due to the low sensitivity of the probe (which frequently gives a signal lower than the expression threshold). This trend however was also evident on the Illumina array, thus there could be a real tendency for HPRT mRNA levels to fall with increasing RNA degradation. Differential susceptibility of housekeeping genes to degradation has been previously observed (Lee et

al., 2005; Barrachina et al., 2006). Ubiquitin gave the most consistent performance across the range of RNA quality and from disease to disease, while also giving the highest absolute expression levels on both the custom-designed and the Illumina array, this appears to be the most reliable positive control.

It is encouraging to note that the positive controls, designed for a human MWG array chip, appeared to be largely effective for rat cDNA as well. Since their sequences are not known, there is no way to check whether the oligos have sufficient homology for the rat genome, except by performing such hybridisation experiments. Although the positive control probes likely showed some non-specific cross-binding for the rat target (the human cDNA on the had both a lower level of binding intensity for 4 out of 5 controls and a more differential distribution across the signal strength range when screened against rat cDNA), the overall positive control expression pattern is very similar in the human and rat samples.

The reason why a number of oligonucleotides consistently had high levels of binding, considerably above that of the brightest negative control, is not clear. There appears to be a high amount of non-specific hybridisation. It is not possible to check MWG oligos for cross-hybridisation as their sequences are not known, but the custom-designed oligonucleotides do not appear to align with non-target sequences when checked by a BLAST search.

The rat liver *vs* rat heart validation experiments confirmed that the array can detect changes in connexin expression that are well known to exist even in rat samples in the manner similar to that of the Affymetrix platform which is specifically tailored to rat RNA .The custom-designed oligo for Cx43 gave significantly higher signal in the heart and Cx32 and Cx26 in the liver across both biological and sample repeats. The custom-designed Cx40 oligo was an exception; this would indicate that the three mismatches to the rat sequence it contains prevent it from binding the rat target consistently. The MWG oligos for the same connexins did not give reliable results in rat tissue which would suggest the MWG oligo set is not suitable for obtaining meaningful results when screening rat tissue. Its should be noted that the MWG oligos for Cx43 and Cx40 also performed badly in the human brain tissue not showing concordance with either the custom-designed oligos or the Illumina oligos.

The two sets of oligos (custom-designed and MWG-designed) behaved in a notably more consistent fashion in the human brain experiment than in the rat experiments. MWG oligos hybridised human tissue much better than rat tissue which is not surprising since the MWG oligonucleotides are not rat-specific.

A comparison of two vastly different tissues such as rat heart and liver would be expected to produce much larger fold differences than a comparison of two closely related regions. The rat data

would be also more consistent due to a much lower level of biological variability between laboratory rats and humans. Gene expression changes in the brain also tend to be modest, with a 20-50% change potentially having biological significance and substantially affecting the function of the brain region (Hollingshead et al., 2005). It was possible to select rat tissue of the highest RNA quality, while the amount of RNA degradation in the human brain tissue was much more extensive, thus making the estimation of true gene expression changes more difficult. The Affymterix rat arrays showed considerably higher fold differences for the connexins in the heart and liver samples than the custom-designed and Illumina arrays for either the connexins or the inflammatory markers for the human brain tissue. However, detecting differential expression was still possible with the human brain tissue in spite of the higher degree of variability present.

6.2 RNA quality

One of the salient factors affecting the RNA quality, as determined by this study, was the pH of the tissue. This is in accordance with what has been widely accepted, where pH is taken as a marker of the length and severity of the agonal state, with its concomitant hypoxia leading to acidosis. All of our brain samples had an acidic pH within a relatively narrow range, and lower than is generally reported for guaranteeing good quality RNA (Bahn et al., 2001). This is possibly due to our method of pH measurement (where we avoided the use of buffers to dilute the tissue homogenate; we believe our method provides a more accurate measure of the total tissue pH, both extracellular and cytoplasmic). Unlike the agonal state, the PM delay did not show a correlation with the pH of the tissue in our study, although opposite positive correlation has been reported previously by some authors (Stan et al., 2006).

The cerebellar RIN value is only an approximate indicator of the RNA quality in other brain regions. This is most likely due to differences in the cooling rates of tissue blocks, as well as the handling and the storage condition of the tissue. Cerebellar RIN can, however, be used as a rough guide, as our results have shown that the RNA quality of the brain region of interest is unlikely to be higher than that of the cerebellum, and is, in fact, more commonly lower (range of the difference between the cerebellar RIN and the secondary brain region RIN from -0.9 to 2.6, the mean difference of 0.9). This suggests that there is merit in screening cerebellar tissue for RNA quality and proceeding with good, and even borderline cases, but not with those that are sub-par, as a notable improvement of the RNA quality in the region of interest is unlikely to be found.

It is difficult to conclude, based on the data available, whether the disease itself has any appreciable effect on the RNA quality in the secondarily affected brain region, as the “presumably unaffected” caudate nucleus tissue from normal controls also showed notably lower RNA quality than the

cerebellum samples from the same case. In contrast, the RNA quality of the tissue from the affected region was actually higher than the cerebellar tissue in Parkinson's disease cases.

Our surgical epilepsy tissue yielded RNA of a quality that was generally lower than that of our postmortem tissue, which is at first glance surprising, as surgical tissue is actually processed very quickly. Furthermore, from our own previous work, we know excised mesial temporal lobe hippocampal tissue is densely packed with astrocytes that are highly active and viable cells (Fonseca et al., 2002). Other authors who have looked at neurosurgical epilepsy tissue have reported similar results. The reason for this is not clear, but several things have been suggested, such as active RNAses in surgical tissue and the effects of anaesthesia or exposure to air (Stan et al., 2006).

The effect of age at death, mentioned by Harrison et al. (Harrison et al., 1991), did not overall prove significant in our study, nor did the effect of the sex of the patient. Neither of those factors had been consistently flagged as important in the literature, although each has been investigated (Johnson et al., 1986).

While the difference in the absolute RIN value between the shortest and the longest PM delay cases was not large, multiple regression analysis demonstrated a downward trend. This contradictory relationship is in accordance with what has been reported in the literature, with some authors finding a correlation, and some finding none. Generally, it appears that PM delay has at most a modest effect on RNA quality. It should also be noted that our study used a number of cases with the length of PM delay well outside that usually of interest to researchers. Heinrich et al.(Heinrich et al., 2006) and Schramm et al. (Schramm et al., 1999) also looked at cases with the PM delay of up to 118 h and found no correlation.

It was interesting to observe that, of the four groups of cases for which the cerebellar and the secondarily affected areas were compared, the normal controls had the most cases with the fast mode of death (all except one), and these were also the cases in which the PM delay proved to be the least relevant to RNA quality, with the highest positive correlation (where the expectation was to find a negative one).

This particular part of our study was undertaken with the purpose of investigating whether it was possible to obtain RNA of sufficiently good quality for the purpose of microarray work. It has been encouraging to discover that human brain tissue samples of sufficiently good quality were available, in spite of it being impossible to have optimal handling conditions. Handling human tissue is, however, without a doubt more difficult than dealing with animal tissue, and this factor should be taken into account.

6.3 Connexins Expression and Inflammation in the Human Brain

6.3.1 Expression of connexins

The connexins that appear to be most increased in Huntington's and Parkinson's disease relative to single control for each were Cx37, Cx43 and Cx45, and in Alzheimer's disease – Cx37, Cx43 and Cx47 (with Cx45 being fourth). All of these connexins except Cx47 are expressed in brain endothelial cells, Cx43 is also expressed in astrocytes and microglia, Cx45 in neurons and Cx47 is expressed in oligodendrocytes. The apparently downregulated connexins are Cx26 (astrocytes) and Cx25 (localisation of which has not previously been reported and remains unknown).

It can be hypothesised that upregulation of endothelial connexins, especially Cx43 and Cx37, is connected to vascular leakage, with an increase in coupling of endothelial cells. Alzheimer's and Parkinson's diseases are known to involve pathological changes in the capillaries in the brain (Farkas et al., 2000; Hirsch et al., 2005; Grammas et al., 2006). This would mean that circulating inflammatory cytokines and other reactive species could leak through the blood-brain barrier and the exchange of nutrients and toxic substances may be disturbed, contributing to neuronal damage. Inhibition of Cx43 decreases vascular permeability induced by thrombin. This suggests that blocking other endothelial connexins, such as Cx37 (which does not occur in any other cell type in the brain), could help to decrease the vascular permeability and the disruption of the blood-brain barrier.

Astrocytosis and gliosis take place in Alzheimer's, Parkinson's disease and epilepsy (Hirsch et al., 2005; Shaikh et al., 2007), thus it could be expected that connexins expressed in astrocytes and microglia would be elevated. The highest degree of upregulation of astrocytic connexins in this study occurred in epilepsy and Alzheimer's disease and the lowest in Huntington's disease. The primary astrocytic connexin is Cx43, with smaller contributions from Cx30 and Cx26. Cx30 is believed to comprise approximately 50% of astrocytic connexins in the hippocampus (Kielian, 2008) and Cx30 was upregulated more strongly in the hippocampal epilepsy tissue than in the other diseases. An increase in astrocytic coupling in epilepsy is believed to contribute to synchronisation and propagation of abnormal electrical activity, and a highly significant increase in Cx43 expression has been shown to co-localise with GFAP-positive astrocytes (Fonseca et al., 2002).

It has been widely confirmed that Cx43 expression is increased in chronic and acute inflammation (Fonseca et al., 2002; Cronin et al., 2006; Green and Nicholson, 2008); the present study appears to confirm this, with Cx43 elevated in all diseases. The lowest elevation is present in Huntington's disease and the highest in Alzheimer's disease. Microglial activation is known to play a major role in neurodegenerative diseases. Microglia release inflammatory mediators which damage blood vessels

which in turn exacerbates the leakage of capillaries. Inflammatory mediators also facilitate glial hemichannel opening leading to an increase of bi-directional exchange between the cytoplasm and the extracellular environment (De Vuyst et al., 2007; Retamal et al., 2007). Cx36, which is present in microglia along with Cx43, is notably upregulated in Alzheimer's disease and epilepsy and slightly in Parkinson's and Huntington's disease (this connexin is only present in the custom-designed oligo set on the custom array). Cx36 has been shown to form gap junctions between neurons and microglia in cell cultures (Dobrenis et al., 2005), which raises interesting possibilities in terms of the role its upregulation can play in increased coupling between microglia and astrocytes in Alzheimer's disease.

Of the connexins specific to oligodendrocytes, Cx30.2 did not show change in any of the samples. Mouse Cx29 (human Cx30.2) does not form gap junction plaques or functional gap junction in transfected cells (Ahn et al., 2008). Cx47 was downregulated in Huntington's and Parkinson's disease, upregulated in Alzheimer's disease and unchanged in epilepsy. Cx32, which also occurs in neurons and endothelial cells, was downregulated in Huntington's and Parkinson's disease in a similar fashion to Cx47, and upregulated in Alzheimer's disease and epilepsy. Studies on the function of oligodendrocytes connexins have been conducted on Cx32 and Cx47 knock-out mice which suffered demyelination (Sutor et al., 2000; Odermatt et al., 2003; Li et al., 2008; Sargiannidou et al., 2009), whether there is a relationship between a reduction in the level of expression of these connexins and loss of myelin in neurodegenerative diseases is an interesting question. Cx30/Cx32 and Cx43/Cx47 form heterotypic gap junctions between astrocytes and oligodendrocytes (Nagy et al., 2003; Theis et al., 2005), thus a decrease in the level of expression of Cx32 and Cx47 could be related to uncoupling between astrocytes and oligodendrocytes.

Cx31.9 has been reported in the cerebral cortex (White et al., 2002), but no detailed studies on its localisation and role have been performed. Cx31.9 was downregulated in Parkinson's disease and epilepsy and unchanged in Huntington's and Alzheimer's disease. Regions tested for Parkinson's disease (CN) and epilepsy (hippocampus) are not part of the cerebral cortex. The presence of Cx31.9 in other brain regions has not been investigated and its possible role has not been speculated.

Three connexins that had not been reported in the brain before were detected on the array: Cx30.3 (previously reported in mouse, rat, and rabbit kidney, epidermis and ovarian cells (Plantard et al., 2003; Hanner et al., 2008; Wang et al., 2009a), Cx25 (expressed in embryonic stem cells (Bondarev et al., 2001; Huettner et al., 2006) and 40.1 (expressed in pancreas, kidney, skeletal muscle, liver, placenta, and heart (Sohl et al., 2003; Sohl and Willecke, 2003). This finding should be followed up with further studies to elucidate the precise location and role of these connexins in the brain and neurological diseases.

There appears to be a tendency for the expression level of different connexins to change in the same direction in the Alzheimer's disease and epilepsy. Parkinson's and Huntington's diseases form another such group. One explanation for the former might be the similarity of the brain regions considered for epilepsy (hippocampus) and Alzheimer's diseases (medial temporal gyrus). The reason why Parkinson's and Huntington's diseases group together is not entirely clear. Alzheimer's disease, epilepsy and Parkinson's disease are known to involve inflammation (which is confirmed by our study) and while there is some suggestion that Huntington's disease also involves inflammation, the connection does not seem equally definitive.

6.3.2 Inflammatory cytokines and their relationship to connexin expression

Inflammation is considered one of the important features of pathogenic processes in neurodegenerative diseases. Inflammatory responses have been widely discussed as a possible target of the management of chronic neurodegenerative diseases. In our study we have investigated the expression levels of inflammatory cytokines such as alpha-integrins (CD11A, CD11B and CD11C), IL-1β, IL-6, IL-10, TNF-α, gamma-interferon and GM-CSF. These cytokines are known to be involved in chronic inflammation associated with neurodegenerative diseases. Grammas et al. (Grammas and Ovase, 2001) reported high levels of TNF-α (188% of the control levels), soluble and cell-associated IL-1β (160%) and IL-6 (180%) in microvessels obtained from Alzheimer's disease patients. Mogi et al. (Mogi et al., 1994a) discovered that the level of TNF-α was significantly higher in the striatum (366%) and CSF (432%) of patients with Parkinson's disease compared to controls. In another study by Mogi et al. (Mogi et al., 1994b) IL-1β and IL-6 were elevated in the caudate nucleus of patients with Parkinson's disease (IL-1β by 253% and IL-6 by 517%). IL-1β was found to be elevated in the neocortex of Alzheimer's disease patients by 360% (Colangelo et al., 2002). An increase in the levels of CD11A and CD11B has been associated with microglial activation, a hallmark of neurodegenerative diseases such as Alzheimer's and Parkinson's diseases (McGeer et al., 2000; Ullrich et al., 2001; Imamura et al., 2003; Roy et al., 2008). IL-10 is an anti-inflammatory rather than a pro-inflammatory marker (McGeer et al., 2005; Culpan et al., 2006; Silvestroni et al., 2009). It is only marginally detected in this study.

IL-6 was the only marker that appeared to be elevated in all three diseases. CD11A and CD11B were higher than the single control in Alzheimer's and Parkinson's disease and lower in Huntington's disease. Neither TNF-α nor IL-10 was expressed in Alzheimer's or Parkinson's disease. TNF-α was expressed in the control and two Huntington's disease samples (HC84 and HC107) and IL-10 was only expressed in one control and one disease sample (HC84) (at a level lower than that of the negative control). The expression levels of both were low and the change between the disease and the control

samples small (TNF-α mRNA is known to be especially sensitive to degradation (Ware, 2008)). It is interesting to note that the highest expression level of inflammatory markers in Huntington's disease compared to the control was found in the sample with the lowest Vonsattel disease grade (HC92, Grade 1). The sample with the highest disease grade (HC109, Grade 4) expressed the lowest number of inflammatory markers (only two, CD11A and CD11B). This sample, however also had by far the lowest RNA quality (RIN=6.6 with the average of 8.08 for the disease), thus it is not certain whether the level of expression of inflammatory markers was due to disease grade or the RNA quality. As there was only one sample each with grade 1 and grade 4 (the other three samples were grade 3), these changes might also be due to experimental variation. In Parkinson's and Alzheimer's disease where the range of RNA quality was more extensive than in Huntington's disease, there was no clear pattern of correlation between the level of differential expression of inflammatory markers and RNA quality. There was some tendency however for a lower level of differential expression to co-occur with lower RNA quality. A more extensive study using a larger number of samples would be needed to clarify if there is a genuine correlation.

As the Huntington's diseases samples had the highest RNA quality compared to the Alzheimer's and Parkinson's disease samples (excluding sample HC109), the differences in expression between the samples would be expected to be less due to variability in the tissue quality with the level of differential expression more representative of the actual level of gene expression in the tissue. Thus it is possible to propose that there is in fact no clear pattern of the expression of inflammatory markers in the motor cortex of patients with Huntington's disease.

Huntington's disease had the lowest expression level of connexins and the lowest level of differential expression of inflammatory markers (zero average). Alzheimer's disease had the highest level of connexins and an intermediate level for differential expression of inflammatory markers (three out of the four expressed, 116% average). Parkinson's disease had an intermediate level of change of connexins expressed (virtually zero) and the highest overall upregulation of inflammatory markers (four out of the four expressed, 176%). It would be interesting to conduct further studies to confirm whether the level of inflammatory markers in the caudate nucleus of Parkinson's disease is in fact higher than that in the medial temporal gyrus in Alzheimer's disease.

The apparent elevation in cytokine level in Alzheimer's and Parkinson's disease is in agreement with the literature, although the magnitude of change was lower than in the few studies that have considered precise changes in expression levels. It is difficult to make direct comparisons as the only region considered in the studies published that coincided with the region used in our study was the caudate nucleus in Parkinson's disease (Mogi et al., 1994b). TNF-α was not expressed in our Parkinson's disease samples, IL-1β was elevated by 185% compared to the single control and IL-6 was

elevated by 241% in Parkinson's disease (the largest increase of all the cytokines in the three diseases compared to each brain region's single control). IL-6 was increased by 159% in the motor cortex of Huntington's disease relative to the single control and unchanged in the medial temporal gyrus of Alzheimer's disease. CD11A and CD11B levels appeared to be elevated in Parkinson's and Alzheimer's disease and reduced in Huntington's disease. As CD11A and CD11B are markers of microglial activation, their elevation in Alzheimer's and Parkinson's disease and reduction in Huntington's disease could mean a lower level or absence of microglial activation in the MC in Huntington's disease.

It has been suggested that inflammation is also a feature of Huntington's disease. Silvestroni et al. (Silvestroni et al., 2009) measured the levels of a number of inflammatory markers, including IL-1β, IL-10 in the striatum, cortex and the cerebellum of HD patients. In the cortex IL-1β was not detected, TNF α and IL-10 did not show a consistent expression pattern, where IL-6 was elevated in the cortex. IL-6 was also elevated in our Huntington's disease samples. This pattern is largely similar to the result obtained in our study, where the inflammatory markers did now show a clear pattern of change and thus nothing conclusive could be said about the presence of inflammation in the motor cortex in Huntington's disease.

The finding by Mogi et al. (Mogi et al., 1994b) that IL-1β and IL-6 were elevated in the caudate nucleus of patients with Parkinson's disease suggests that inflammation takes place in the brain regions secondarily affected by neurodegenerative diseases. Our study confirms this for Parkinson's and Alzheimer's disease. How much of this inflammation is local cannot be stated with certainty based on the data available. There is likely a contribution from both circulating inflammatory cytokines and those released by activated astrocytes and microglia. The precise causal relationship between inflammation and connexin expression remains yet to be elucidated. Inflammatory cytokines lead to connexin upregulation and the increased cell coupling contributes to the spread of damage. Inhibiting of Cx43 at the site of acute injury limits local inflammation and lesion spread (Qiu et al., 2003; Coutinho et al., 2005; Cronin et al., 2006). As mentioned above, inhibition of Cx43 decreases vascular permeability induced by thrombin. Pharmacological agents which block gap junctions can abolish neuron-glia signalling and prevent the spread of neurological damage (Theis et al., 2005; Cronin et al., 2006). Inflammatory cytokines released by microglia can however also inhibit connexin expression in astrocytes (Meme et al., 2006; Retamal et al., 2007) and connexins can play a neuroprotective role in ischaemia (Theis et al., 2005)

The upregulation in endothelial connexins in this study seems to be the most closely related to an increase in the level of inflammatory cytokines. Microglial connexins are also elevated. This supports the importance of the vascular leakage and gliosis in neurodegenerative disease. Based on the results

obtained, inflammation seems to be a prominent feature of Alzheimer's and Parkinson's disease, even in the secondary brain regions, with no clear evidence for the presence of inflammation in Huntington's disease (with low levels of both the inflammatory markers and the connexins which appear to accompany inflammation). There was no data on the levels of inflammatory markers in the hippocampal tissue of epilepsy patients, but the pattern of changes in connexin expression which makes it the most similar to Alzheimer's disease suggests that inflammation is present in this brain region as well.

The apparent relationship between the chronic inflammatory response and the changes in connexin expression suggests that regulating connexin expression could provide a potential treatment for neurodegenerative disorders by interrupting the inflammatory cycle (Green and Nicholson, 2008).

6.3.3 Microarray experiments in human neurodegenerative diseases

DNA microarray analysis of brain tissue is highly complex. Although the number of primary cell types in the brain is limited, they demonstrate vast phenotypic diversity, and thus changes in gene expression may affect only subpopulations of cells. Therefore, even extensive transcription changes in a small subpopulation of brain cells may be missed as transcripts from more abundant sources may mask these changes (Mirnics and Pevsner, 2004).

Neurodegenerative diseases are characterised by astrocytosis and gliosis, i.e. both activation and proliferation of astrocytes and microglia, astroglial/neuronal ratios are known to be higher in degenerating brain regions Thus apparent mRNA increases in the expression of genes associated with gliosis and neuroinflammatory processes, such as glial fibrillary acidic protein, gap junction proteins and inflammatory markers may reflect the differences in represented cell populations. Decreases in gene expression in the tissue, on the other hand, may be a consequence of loss of cells, especially neurons (Cha, 2007).

To correlate mRNA expression with the changes at the cellular level a number of techniques have been employed. *In situ* hybridization was used to quantitatively monitor gene expression changes and localise them to particular cells. Levels of different markers were compared to one another, and the expression levels were related to the amount of cellular atrophy suggesting that changes in mRNA levels did not simply mirror cell loss. At present, laser-capture microdissection is employed to isolate particular cells from tissue samples in order to examine mRNA expression and compare different brain regions without any issues regarding regional variability due to cell type distribution. This is particularly important in the case of neurons as larger-scale gene expression changes in glial cells can mask changes in neurons (Mirnics et al., 2006). In our study, for example, it proved difficult to judge

the direction of change in the expression of neuronal connexins as only one of the connexins detected on the arrays is unique to neurons (Cx62) and this does not change except in Alzheimer's disease, where it is upregulated).

In recent years the amount of gene expression data available has been growing at a fast rate. Public repositories of microarrays data such as PubMed Omnibus are now available on the web and can be used by researchers to compare their data with the data obtained in previous studies, to look at genes of interest within the publically available data sets and to combine their own findings with those of the previous studies. This removes the need to conduct as many microarray experiments themselves. At present however the microarray data available on the databases is far from complete and does not cover all of the regions investigated in this study.

A large-scale study of three brain areas (caudate nucleus, motor cortex and cerebellum) was conducted by Hodges et al. (Hodges et al., 2006) who discovered the biggest gene expression changes in the caudate nucleus, the second largest in the motor cortex and the smallest in the unaffected cerebellum, which is in agreement with the established disease pathology. In the list of the top thirty either down-or upregulated genes they list an increase in Cx43 (by 2.64 times) and Cx30 (by 2.3 times) in the motor cortex. No other genes investigated by us made the top thirty in any tissue. However, their data is publically available and it is possible to look up other connexins and inflammatory markers. It is interesting to note that the magnitude of the gene expression changes in their study was quite small, which is in agreement with our results. It should however be noted that microarrays have a compressed dynamic range (Courtney et al., 2010) and may underestimate fold changes.

Both Cx43 and Cx30 are found in astrocytes, Cx30 exclusively, which suggests astrocytosis in the motor cortex in Huntington's disease. Cx43 is elevated in our data as well, but Cx30 is on average downregulated, which could be due to a number of reasons, such as different ways of estimating significance on different array platforms (Affymetrix *vs* Illumina), the actual difference in the samples or the use of only one control. Interestingly, the elevation of connexins was found only in the secondarily affected motor cortex, but not in the caudate nucleus, which possibly suggests that activated astrocytes are a feature of earlier stages of neurodegeneration. The absence of inflammatory markers among the genes with the largest differential expression in any of the tissues points to inflammation not being a prominent feature of Huntington's disease, as opposed to Alzheimer's and Parkinson's diseases, which agrees with our data.

To eliminate the possibility that the observed changes were simply a result of cell loss, Hodges et al. examined mRNA levels in laser-capture microdissected neurons from Grade 1 Huntington's disease caudate nucleus compared to control in addition to whole tissue samples. These analyses confirmed the

changes in expression seen in tissue homogenates. Neuronal expression changes generally paralleled whole tissue expression changes, which gives some confidence in whole tissue studies as to measuring genuine changes in gene expression. It should be noted however that not all connexins and other genes of interest in our study such as inflammatory markers that are found in the tissue occur in neurons. Gene expression in glial cells is of interest in the aetiology of neurodegenerative disease as well**.**

Another important finding was that the gene expression profiles of Huntington's disease caudate nucleus and motor cortex are very similar, suggesting that there may be similar general molecular characteristics to the neurodegenerative process in different regions of the brain. This is encouraging in terms of being able to study secondary regions in order to draw conclusions about neurodegenerative processes. In addition, the confounding effect of previous neuronal loss is likely to be much smaller in the motor cortex: preliminary studies suggest cell loss of only 4–20% in Grades 0–2 (D. Thu and R.L.M Faull, unpublished data).

Microarray studies that have investigated the same brain regions as in our work in Alzheimer's disease include Ray and Zhang (Ray and Zhang, 2010) who studied neurons in entorhinal cortex, hippocampus, posterior cingulate cortex and middle temporal gyrus and found that the degenerative effects of Alzheimer's disease in the MTG was less severe than that in the other brain regions and concluded that entorhinal cortex, posterior cingulate cortex and hippocampus show pathogenesis of late stage Alzheimer's disease while the MTG shows early Alzheimer's disease pathology. Liang et al. (Liang et al., 2008) created a reference data set for six brain regions (the entorhinal cortex, hippocampus, middle temporal gyrus, posterior cingulate cortex, superior frontal gyrus, and primary visual cortex.). As these studies focused specifically on neurons, connexins or inflammatory markers were not in the list of the differentially expressed genes. Earlier microarrays studies which have considered whole tissue samples from regions other than MTG have found an increase in Cx43, TNF and interleukins (Blalock et al., 2005)

The microarrays studies of Parkinson's disease focus on the substantia nigra and differences in individual genes have not been consistent between experiments (Greene, 2010). An elevation in a number of genes involved in TNF and IL signalling pathways has been found (Blalock et al., 2005). Our data obtained from a different brain region also showed evidence of inflammation and correlation with connexin expression.

Finally, it is of note that the technology I started with was appropriate for that time but this has proved to be one of the fastest developing technology fields within molecular biology. If I were to start again today from scratch, I would propose use of a TaqMAN RT-PCR approach which allows analysis of up to 96 different RNAs simultaneously. Two important considerations are the number of genes that

can be analysed with new technologies, and cost. The cost of establishing a TaqMAN RT PCR 96 well array is now minimal compared with approaches available in only recent years. The Illumina microarray approach enables subsequent data mining but this field is moving very quickly, driven by changes in technology. The Institute of Systems biology is currently sequencing the genomes of 100 individuals from families with Huntington's disease and a further 615 individuals from families that have multiple members affected by neurodegenerative disease. (http://www.genomeweb.com/sequencing/isb-orders-615-whole-genome-sequences-complete-genomics-neurodegenerative-disease). Clearly these approaches and the data subsequently available will change the way individuals within research institutes operate. The type of study I have conducted will be possible without entering the wet laboratory at all. This may be not perfect, students doing *in silico* theses may not understand the tissues and diseases processes as well, or the limitations of techniques if they haven't considered how tissue is collected and what tissues are collected. However, there is little doubt that the speed with which the field is changing requires new approaches now.

6.4 Limitations of this study

The primary limitation of this study is the small sample size (only one control sample and five disease samples have been screened for Huntington's, Parkinson's and Alzheimer's disease and only two for epilepsy). Human postmortem tissue has a big range in RNA quality due to different variables such as cause of death and the duration of the agonal state. Genetic and phenotypic diversity of humans is a major source of biological variability. Differences in lifestyle, disease stage, and drug treatment affect gene expression levels. The variability between cases is due to such factors as differences in age and general health (i.e. the presence of other diseases that can have their own effect on the brain tissue studied). This can lead to greater variability between different patients within the same disease group than that between diseases. This is also true for control cases so access to a single control in this study limits the interpretation of data relative to the disease state.

One of the main challenges of work with human tissue is limited tissue availability. This restricts the ability to perform a large number of experiments with biological replicates. A smaller number of replicates make it more difficult to distinguish differential gene expression that is connected to the disease process from differences which are due to biological and environmental variability between particular human patients. This in particular applies to controls where all researchers regardless of the study focus require access to age, sex- and post-mortem delay-matched tissue for their own study. Human postmortem tissue from the areas affected by neurological disease is in addition precious and obtaining large sample sizes may be difficult or impossible. Since this tissue is in high demand, an

attempt to determine the RNA quality of the brain area of interest by using the little-used region of the cerebellum as an indicator was made. The cerebellum however proved only an approximate guide.

Brain cells show immense phenotypic diversity, and gene expression changes can only affect a small population of cells, thus even a profound change in the gene expression level in the population can be missed (Mirnics and Pevsner, 2004). It is impossible to control for all sources of variability and with a small sample size it is difficult to state with confidence to what degree the observed changes are due to the disease process.

The quantity of the human tissue available also limits the number of technical sample replicates that can be hybridised to the arrays, but to a less significant extent as the amount of mRNA required for each arrays is quite small. With technical replication the issue of the cost of each array required for repeated hybridisation comes to the fore. The custom array has the advantage of the low cost that permits a number of technical replicates to be performed in order to deal with variation due to experimental artefacts and measurement error, which can provide better significance estimation. Having two probes for each connexin gene, as opposed to the Illumina array that has only one probe for most transcripts, is a form of internal replication. The multiple number of replicated spots on our array make it possible to test for reproducibility between each connexin and its negative control within that array. With a single control sample source, however, this cannot be extrapolated to the disease condition overall – it provides only an intra-array check.

The two colour array design allows direct comparison of each disease sample with the control sample, rather than comparing the disease samples to reference samples hybridised to a separate array. This minimises inter-array variability. All of our Illumina arrays however were processed together on the same chip which reduced experimental variability as compared to processing each array independently.

The commercial Illumina array data includes gene expression information for the whole genome, and any genes of interest can be investigated when required, as was done with the inflammatory markers in this study. Analysis of an entire 30,000 gene array is a complex undertaking. A more extensive statistical analysis is necessary when using the Illumina arrays due to the complexity of data interpretation from a large number of probes and genes. When simply pulling out genes of interest rather than performing complex statistical analysis on whole arrays, judging statistical significance is impossible, it is only possible to measure fold changes (there are only two data points). It is also only possible to use simple normalisation methods. Basically, a general evaluation is obtained rather than hard statistical data (qualitative rather than quantitative). Using a large number of samples with multiple controls makes cross-comparisons even more difficult logistically. Again, however,

interpretation based upon data mining from this particular study will be limited by the availability of just a single control sample for each brain region.

While it has been possible to obtain meaningful results from screening rat samples on the custom-designed array, the reliability of the data has proved to be limited with many oligos not hybridising the rat target efficiently. This suggest that the array should be used for screening rat tissue very cautiously.

The human brain analysis presented only a snapshot of connexin expression and the level of inflammatory markers at the time of death, it was not possible to determine the precise level and direction of expression changes with the progression of the diseases. The precise causal relationship between the connexins and inflammatory cytokines also could not be established with certainty, as only a correlation in the levels of expression can be seen with postmortem studies such as the present one.

Another limitation of this study is the focus on mRNA without consideration of the concurrent protein changes. In the central nervous system where neuronal projections reach to remote areas, gene expression changes and protein changes may take place in different brain regions (such as grey and white matter). The vast majority of mRNA transcripts are most abundant in the cell body, while the proteins are often localised in axonal projections or nerve terminals a considerable distance away, thus complicating interpretation (Mirnics and Pevsner, 2004). There are a variety of complicated post-transcriptional mechanisms involved in translating mRNA into protein that are not yet sufficiently well defined to be able to calculate protein concentrations from mRNA. It is possible for a mRNA transcript to be up- or down-regulated while the protein amount is significantly changed in the opposite direction (Greenbaum et al., 2003). Proteins may differ substantially in their *in vivo* half lives. Connexin proteins are renewed several times a day, with Cx43 for example having half life of 1.5 – 2.5 hours, and protein turnover rate differs significantly by cell type and can be altered by disturbances in cellular metabolism (Herve et al., 2007). Considering the above, a combined study of RNA and protein levels using high-throughput approaches is desirable. Finally in relation to mRNA and protein expression, while certain trends have been indicated regarding changes in the expression of connexins in particular types of brain cells, the precise localisation of the connexins is not possible and would require immunohistochemical studies or laser microdissection of particular types of cells.

In this thesis it has therefore been possible to observe apparent trends in the secondarily affected regions between endothelial and glial connexins and inflammatory markers in the neurodegenerative diseases that are considered to involve inflammation, such as Alzheimer's and Parkinson's disease. The boutique connexin gene array developed and validated in this study affords low cost, colour design advantages, within chip reproducibility and reduced complexity of analysis as discussed above. It is, however, important to note that the human data presented in Chapter 5 from both this boutique gene

array and the Illumina array must be interpreted with caution owing to the low case numbers and in particular the limitations resulting from a single normal control. The apparent trends though warrant further investigation.

CONCLUSION

The first section of this study (Microarray chip design and validation) has demonstrated the potential for designing a boutique microarray chip; in our case, to screen for connexin gene expression. Despite the substantial similarity within the connexin gene family identification of unique regions within the coding sequences is still possible and oligonucleotides that meet the criteria for microarray probes can be designed in these regions. It proved possible to design the human/rat cross-species screening platform. A compromise, however, had to be made in terms of specificity for the rat sequences due to a relatively large amount of cross-species variation. The data obtained in testing the microarray chip performance has confirmed that the oligonucleotide probes bind both human and rat targets in a consistent manner and that the chip is capable of detecting differential connexin expression in both species.

In the second part of this study (RNA Quality Assessment) it was shown that cerebellar RNA quality was not always an exact predictor of the RNA quality in other brain regions of interest, but it proved to have some predictive value, and can be used as a preliminary indicator. The PM delay was shown to affect the RNA quality adversely, but the magnitude of the effect was small. The major findings from this study were that RNA quality was strongly affected by the pH of the tissue, with both the pH and the RNA quality being influenced by the mode of death.

In the third section of the study the boutique custom-designed microarray chip consistently detected apparent changes in gene expression in the human brain tissue relative to the single control with variable RNA quality across samples within the same disease. Within this array, the custom-designed oligos performed better than the MWG-designed oligos in terms of internal consistency and when compared to the commercial Illumina array.

Taking into account the fact that only one normal control was used, it was nevertheless possible to observe apparent but similar trends in the expression of connexins and the inflammatory marker genes investigated in specific brain regions compared to a single control. While the data obtained is preliminary, these apparent trends warrant further investigation.

FUTURE DIRECTIONS

A much larger number of samples should be screened to provide more reliable data on the changes in gene expression in neurodegenerative diseases to be able to distinguish between alterations due to biological variability from those directly related to the disease process. The samples should then be analysed by qRT-PCR to confirm the results obtained in the microarrays experiments

For correlation of connexin expression changes with cell types known to be present in the brain, immunohistochemistry techniques should be used. Immunohistochemistry would involve staining of brain sections with various antibodies, such as NeuN (neurons), GFAP (astrocytes), Iba (microglia), binding to different cellular components, and using primary anti-connexin antibodies and secondary fluorescence-labelled antibodies to amplify the fluorescence signal.

The expression of a number of other inflammatory cytokines in the brain regions studied should be investigated on the basis of the data available from the Illumina arrays. A more thorough analysis of the Illumina array data using methods such as multivariate analysis would provide a much more comprehensive and detailed picture of gene expression changes in the brain regions so far screened. Other classes of genes besides connexins and inflammatory cytokines could be analysed. The study could possibly be expanded to encompass other brain areas affected by the diseases to look for changes in connexin expression and the level of inflammatory markers. This would help further elucidate the role of connexin expression and inflammation, and the connection between them in neurodegenerative disease, with the ultimate aim of developing therapeutic approaches. The neurodegenerative diseases involve complex molecular interactions and it would ultimately be desirable to perform an integrative study of relative mRNA and protein abundances and their possible interactions.

REFERENCES

(1993) A novel gene containing a trinucleotide repeat that is expanded and unstable on Huntington's disease chromosomes. The Huntington's Disease Collaborative Research Group. Cell 72:971-983.

Aguado F, Ballabriga J, Pozas E, Ferrer I (1998) TrkA immunoreactivity in reactive astrocytes in human neurodegenerative diseases and colchicine-treated rats. Acta Neuropathol 96:495-501.

Ahmad AS, Zhuang H, Echeverria V, Dore S (2006) Stimulation of prostaglandin EP2 receptors prevents NMDA-induced excitotoxicity. J Neurotrauma 23:1895-1903.

Ahn M, Lee J, Gustafsson A, Enriquez A, Lancaster E, Sul JY, Haydon PG, Paul DL, Huang Y, Abrams CK, Scherer SS (2008) Cx29 and Cx32, two connexins expressed by myelinating glia, do not interact and are functionally distinct. J Neurosci Res 86:992-1006.

Alvarez-Maubecin V, Garcia-Hernandez F, Williams JT, Van Bockstaele EJ (2000) Functional coupling between neurons and glia. J Neurosci 20:4091-4098.

Armstrong NJ, van de Wiel MA (2004) Microarray data analysis: from hypotheses to conclusions using gene expression data. Cellular oncology : the official journal of the International Society for Cellular Oncology 26:279-290.

Ausubel FM, et al. (2000) Current Protocols in Molecular Biology. New York: Greene Publishing Associates and Wiley-Interscience.

Bahn S, Augood SJ, Ryan M, Standaert DG, Starkey M, Emson PC (2001) Gene expression profiling in the post-mortem human brain--no cause for dismay. J Chem Neuroanat 22:79-94.

Bal-Price A, Brown GC (2001) Inflammatory neurodegeneration mediated by nitric oxide from activated glia-inhibiting neuronal respiration, causing glutamate release and excitotoxicity. J Neurosci 21:6480-6491.

Baldwin D (2001) MicroArrays: An Introduction. In: DNA Microarrays: The New Frontier in Gene Discovery and Gene Expression Analysis. (Geschwind DH, Van Deerlin V, eds). San Diego, CA: Society for Neuroscience.

Barnes M, Freudenberg J, Thompson S, Aronow B, Pavlidis P (2005) Experimental comparison and cross-validation of the Affymetrix and Illumina gene expression analysis platforms. Nucleic Acids Res 33:5914-5923.

Barrachina M, Castano E, Ferrer I (2006) TaqMan PCR assay in the control of RNA normalisation in human post-mortem brain tissue. Neurochem Int 49:276-284.

Barrett JC, Kawasaki ES (2003) Microarrays: the use of oligonucleotides and cDNA for the analysis of gene expression. Drug Discovery Today 8:134-141.

Barton AJ, Pearson RC, Najlerahim A, Harrison PJ (1993) Pre- and postmortem influences on brain RNA. Journal of Neurochemistry 61:1-11.

Bate C, Boshuizen RS, Langeveld JP, Williams A (2002) Temporal and spatial relationship between the death of PrP-damaged neurones and microglial activation. Neuroreport 13:1695-1700.

Becker KG (2001) cDNA arrays in neuroscience: nylon membrane based arrays. In: DNA Microarrays: The New Frontier in Gene Discovery and Gene Expression Analysis. (Geschwind DH, Van Deerlin V, eds). San Diego, CA: Society for Neuroscience.

Berezikov E, Thuemmler F, van Laake LW, Kondova I, Bontrop R, Cuppen E, Plasterk RH (2006) Diversity of microRNAs in human and chimpanzee brain. Nat Genet 38:1375-1377.

Beyene J, Tritchler D, Bull SB, Cartier KC, Jonasdottir G, Kraja AT, Li N, Nock NL, Parkhomenko E, Rao JS, Stein CM, Sutradhar R, Waaijenborg S, Wang KS, Wang Y, Wolkow P (2007) Multivariate analysis of complex gene expression and clinical phenotypes with genetic marker data. Genet Epidemiol 31 Suppl 1:S103-109.

Beyer M, Gimsa U, Eyupoglu IY, Hailer NP, Nitsch R (2000) Phagocytosis of neuronal or glial debris by microglial cells: upregulation of MHC class II expression and multinuclear giant cell formation in vitro. Glia 31:262-266.

Blalock EM, Chen KC, Stromberg AJ, Norris CM, Kadish I, Kraner SD, Porter NM, Landfield PW (2005) Harnessing the power of gene microarrays for the study of brain aging and Alzheimer's disease: statistical reliability and functional correlation. Ageing research reviews 4:481-512.

Blanc EM, Bruce-Keller AJ, Mattson MP (1998) Astrocytic gap junctional communication decreases neuronal vulnerability to oxidative stress-induced disruption of Ca2+ homeostasis and cell death. J Neurochem 70:958-970.

Bland JM, Altman DG (1986) Statistical method for assessing agreement between two methods of clinical measurement. The Lancet i:307-310.

Bland JM, Altman DG (1999) Measuring agreement in method comparison studies. Statistical Methods in Medical Research 8:135-160.

Bolanos JP, Almeida A, Fernandez E, Medina JM, Land JM, Clark JB, Heales SJ (1997) Potential mechanisms for nitric oxide-mediated impairment of brain mitochondrial energy metabolism. Biochem Soc Trans 25:944-949.

Bondarev I, Vine A, Bertram JS (2001) Cloning and functional expression of a novel human connexin-25 gene. Cell Commun Adhes 8:167-171.

Bowtell D, Sambrook J, eds (2003) DNA Microarrays - A Molecular Cloning Manual. Cold Spring Harbor, NY: Cold Spring Harbor Laboratory Press.

Braun R, Cope L, Parmigiani G (2008) Identifying differential correlation in gene/pathway combinations. BMC Bioinformatics 9:488.

Brisset AC, Isakson BE, Kwak BR (2009) Connexins in vascular physiology and pathology. Antioxid Redox Signal 11:267-282.

Brown DR, Schmidt B, Kretzschmar HA (1996) Role of microglia and host prion protein in neurotoxicity of a prion protein fragment. Nature 380:345-347.

Bruzzone R, Barbe MT, Jakob NJ, Monyer H (2005) Pharmacological properties of homomeric and heteromeric pannexin hemichannels expressed in Xenopus oocytes. J Neurochem 92:1033-1043.

Buesa C, Maes T, Subirada F, Barrachina M, Ferrer I (2004) DNA chip technology in brain banks: confronting a degrading world. Journal of Neuropathology & Experimental Neurology 63:1003-1014.

Bushati N, Cohen SM (2007) microRNA functions. Annu Rev Cell Dev Biol 23:175-205.

Bushati N, Cohen SM (2008) MicroRNAs in neurodegeneration. Curr Opin Neurobiol 18:292-296.

Bussini S, Meda L, Scarpini E, Clementi E, Conti G, Tiriticco M, Bresolin N, Baron P (2005) Heparan sulfate proteoglycan induces the production of NO and TNF-alpha by murine microglia. Immun Ageing 2:11.

Butte A (2002) The use and analysis of microarray data. Nature Reviews Drug Discovery 1:951-960.

Cao F, Eckert R, Elfgang C, Nitsche JM, Snyder SA, DF Hu, Willecke K, Nicholson BJ (1998) A quantitative analysis of connexin-specific permeability differences of gap junctions expressed in HeLa transfectants and Xenopus oocytes. J Cell Sci 111 (Pt 1):31-43.

Carlen PL, Skinner F, Zhang L, Naus C, Kushnir M, Perez Velazquez JL (2000) The role of gap junctions in seizures. Brain Res Brain Res Rev 32:235-241.

Catts VS, Catts SV, Fernandez HR, Taylor JM, Coulson EJ, Lutze-Mann LH (2005) A microarray study of post-mortem mRNA degradation in mouse brain tissue. Brain research Molecular brain research 138:164-177.

Cepko C (2001) A comparison of SAGE and microarray technologies. In: DNA Microarrays: The New Frontier in Gene Discovery and Gene Expression Analysis. (Geschwind DH, Van Deerlin V, eds). San Diego, CA: Society for Neuroscience.

Cha JH (2007) Transcriptional signatures in Huntington's disease. Progress in neurobiology 83:228-248.

Chai HS, Therneau TM, Bailey KR, Kocher JP (2010) Spatial normalisation improves the quality of genotype calling for Affymetrix SNP 6.0 arrays. BMC Bioinformatics 11:356.

Chao CC, Hu S, Sheng WS, Bu D, Bukrinsky MI, Peterson PK (1996) Cytokine-stimulated astrocytes damage human neurons via a nitric oxide mechanism. Glia 16:276-284.

Charles AC, Naus CC, Zhu D, Kidder GM, Dirksen ER, Sanderson MJ (1992) Intercellular calcium signaling via gap junctions in glioma cells. J Cell Biol 118:195-201.

Chen ZJ, Tew KD (2008) Amplified differential gene expression microarrays. In: DNA Microarrays (Schena M, ed), pp 51-64. Bloxham: Scion Publishing Limited.

Cherian PP, Siller-Jackson AJ, Gu S, Wang X, Bonewald LF, Sprague E, Jiang JX (2005) Mechanical strain opens connexin 43 hemichannels in osteocytes: a novel mechanism for the release of prostaglandin. Mol Biol Cell 16:3100-3106.

Cheung VG, Morley M, Aguilar F, Massimi A, Kucherlapati R, Childs G (1999) Making and reading microarrays. Nature Genetics 21:15-19.

Chou CC, Chen CH, Lee TT, Peck K (2004) Optimization of probe length and the number of probes per gene for optimal microarray analysis of gene expression. Nucleic Acids Res 32:e99.

Colangelo V, Schurr J, Ball MJ, Pelaez RP, Bazan NG, Lukiw WJ (2002) Gene expression profiling of 12633 genes in Alzheimer hippocampal CA1: transcription and neurotrophic factor down-regulation and up-regulation of apoptotic and pro-inflammatory signaling. J Neurosci Res 70:462-473.

Colantuoni C, Henry G, Zeger S, Pevsner J (2002a) Local mean normalisation of microarray element signal intensities across an array surface: quality control and correction of spatially systematic artifacts. Biotechniques 32:1316-1320.

Colantuoni C, Henry G, Zeger S, Pevsner J (2002b) SNOMAD (Standardisation and Normalisation of MicroArray Data): web-accessible gene expression data analysis. Bioinformatics 18:1540-1541.

Collignon F, Wetjen NM, Cohen-Gadol AA, Cascino GD, Parisi J, Meyer FB, Marsh WR, Roche P, Weigand SD (2006) Altered expression of connexin subtypes in mesial temporal lobe epilepsy in humans. Journal of neurosurgery 105:77-87.

Condorelli DF, Parenti R, Spinella F, Trovato Salinaro A, Belluardo N, Cardile V, Cicirata F (1998) Cloning of a new gap junction gene (Cx36) highly expressed in mammalian brain neurons. Eur J Neurosci 10:1202-1208.

Cornell-Bell AH, Finkbeiner SM, Cooper MS, Smith SJ (1990) Glutamate induces calcium waves in cultured astrocytes: long-range glial signaling. Science 247:470-473.

Courtney E, Kornfeld S, Janitz K, Janitz M (2010) Transcriptome profiling in neurodegenerative disease. J Neurosci Methods 193:189-202.

Coutinho P, Qiu C, Frank S, Wang CM, Brown T, Green CR, Becker DL (2005) Limiting burn extension by transient inhibition of Connexin43 expression at the site of injury. Br J Plast Surg 58:658-667.

Cronin M, Anderson PN, Green CR, Becker DL (2006) Antisense delivery and protein knockdown within the intact central nervous system. Front Biosci 11:2967-2975.

Culpan D, Prince JA, Matthews S, Palmer L, Hughes A, Love S, Kehoe PG, Wilcock GK (2006) Neither sequence variation in the IL-10 gene promoter nor presence of IL-10 protein in the cerebral cortex is associated with Alzheimer's disease. Neuroscience letters 408:141-145.

Cummings TJ, Strum JC, Yoon LW, Szymanski MH, Hulette CM (2001) Recovery and expression of messenger RNA from postmortem human brain tissue. Modern Pathology 14:1157-1161.

Danesh-Meyer HV, Huang R, Nicholson LF, Green CR (2008) Connexin43 antisense oligodeoxynucleotide treatment down-regulates the inflammatory response in an in vitro interphase organotypic culture model of optic nerve ischaemia. J Clin Neurosci 15:1253-1263.

Davalos D, Grutzendler J, Yang G, Kim JV, Zuo Y, Jung S, Littman DR, Dustin ML, Gan WB (2005) ATP mediates rapid microglial response to local brain injury in vivo. Nat Neurosci 8:752-758.

de Longueville F, Surry D, Meneses-Lorente G, Bertholet V, Talbot V, Evrard S, Chandelier N, Pike A, Worboys P, Rasson JP, Le Bourdelles B, Remacle J (2002) Gene expression profiling of drug metabolism and toxicology markers using a low-density DNA microarray. Biochem Pharmacol 64:137-149.

De Vuyst E, Decrock E, Cabooter L, Dubyak GR, Naus CC, Evans WH, Leybaert L (2006) Intracellular calcium changes trigger connexin 32 hemichannel opening. Embo J 25:34-44.

De Vuyst E, Decrock E, De Bock M, Yamasaki H, Naus CC, Evans WH, Leybaert L (2007) Connexin hemichannels and gap junction channels are differentially influenced by lipopolysaccharide and basic fibroblast growth factor. Mol Biol Cell 18:34-46.

Dere E, Zheng-Fischhofer Q, Viggiano D, Gironi Carnevale UA, Ruocco LA, Zlomuzica A, Schnichels M, Willecke K, Huston JP, Sadile AG (2008) Connexin31.1 deficiency in the mouse impairs object memory and modulates open-field exploration, acetylcholine esterase levels in the striatum, and cAMP response element-binding protein levels in the striatum and piriform cortex. Neuroscience 153:396-405.

Dermietzel R (1998) Diversification of gap junction proteins (connexins) in the central nervous system and the concept of functional compartments. Cell Biology International 22:719-730.

Dermietzel R, Gao Y, Scemes E, Vieira D, Urban M, Kremer M, Bennett MV, Spray DC (2000) Connexin43 null mice reveal that astrocytes express multiple connexins. Brain Res Brain Res Rev 32:45-56.

Dobrenis K, Chang HY, Pina-Benabou MH, Woodroffe A, Lee SC, Rozental R, Spray DC, Scemes E (2005) Human and mouse microglia express connexin36, and functional gap junctions are formed between rodent microglia and neurons. J Neurosci Res 82:306-315.

Draghici S, Khatri P, Eklund AC, Szallasi Z (2006) Reliability and reproducibility issues in DNA microarray measurements. Trends Genet 22:101-109.

Eickhoff B, Korn B, Schick M, Poustka A, van der Bosch J (1999) Normalisation of array hybridization experiments in differential gene expression analysis. Nucleic Acids Research 27:e33.

Eisen MB, Spellman PT, Brown PO, Botstein D (1998) Cluster analysis and display of genome-wide expression patterns. Proc Natl Acad Sci U S A 95:14863-14868.

Ekinci FJ, Linsley MD, Shea TB (2000) Beta-amyloid-induced calcium influx induces apoptosis in culture by oxidative stress rather than tau phosphorylation. Brain Res Mol Brain Res 76:389-395.

Elfgang C, Eckert R, Lichtenberg-Frate H, Butterweck A, Traub O, Klein RA, Hulser DF, Willecke K (1995) Specific permeability and selective formation of gap junction channels in connexin-transfected HeLa cells. J Cell Biol 129:805-817.

Elo LL, Katajamaa M, Lund R, Oresic M, Lahesmaa R, Aittokallio T (2006) Improving identification of differentially expressed genes by integrative analysis of Affymetrix and Illumina arrays. Omics 10:369-380.

Ervin JF, Heinzen EL, Cronin KD, Goldstein D, Szymanski MH, Burke JR, Welsh-Bohmer KA, Hulette CM (2007) Postmortem delay has minimal effect on brain RNA integrity. J Neuropathol Exp Neurol 66:1093-1099.

Evans AL, Sharkey AS, Saidi SA, Print CG, Catalano RD, Smith SK, Charnock-Jones DS (2003) Generation and use of a tailored gene array to investigate vascular biology. Angiogenesis 6:93-104.

Evans WH, Martin PE (2002) Gap junctions: structure and function (Review). Molecular Membrane Biology 19:121-136.

Farkas E, De Jong GI, de Vos RA, Jansen Steur EN, Luiten PG (2000) Pathological features of cerebral cortical capillaries are doubled in Alzheimer's disease and Parkinson's disease. Acta Neuropathol 100:395-402.

Faucheux BA, Bonnet AM, Agid Y, Hirsch EC (1999) Blood vessels change in the mesencephalon of patients with Parkinson's disease. Lancet 353:981-982.

Filipowicz W, Bhattacharyya SN, Sonenberg N (2008) Mechanisms of post-transcriptional regulation by microRNAs: are the answers in sight? Nature reviews Genetics 9:102-114.

Fogal B, Li J, Lobner D, McCullough LD, Hewett SJ (2007) System x(c)- activity and astrocytes are necessary for interleukin-1 beta-mediated hypoxic neuronal injury. J Neurosci 27:10094-10105.

Fonseca CG, Green CR, Nicholson LF (2002) Upregulation in astrocytic connexin 43 gap junction levels may exacerbate generalized seizures in mesial temporal lobe epilepsy. Brain Research 929:105-116.

Forster T, Roy D, Ghazal P (2003) Experiments using microarray technology: limitations and standard operating procedures. Journal of Endocrinology 178:195-204.

Gao HM, Liu B, Zhang W, Hong JS (2003) Novel anti-inflammatory therapy for Parkinson's disease. Trends Pharmacol Sci 24:395-401.

Geschwind DH, Van Deerlin V (2001) Introduction. In: DNA Microarrays: The New Frontier in Gene Discovery and Gene Expression Analysis - 2001 Short Course Syllabus (Geschwind DH, Van Deerlin V, eds). San Diego, CA: Society for Neuroscience.

Gilbert DR, Schroeder M, van Helden J (2000) Interactive visualization and exploration of relationships between biological objects. Trends Biotechnol 18:487-494.

Giorgini F, Moller T, Kwan W, Zwilling D, Wacker JL, Hong S, Tsai LC, Cheah CS, Schwarcz R, Guidetti P, Muchowski PJ (2008) Histone deacetylase inhibition modulates kynurenine pathway activation in yeast, microglia, and mice expressing a mutant huntingtin fragment. J Biol Chem 283:7390-7400.

Goldberg GS, Moreno AP, Lampe PD (2002) Gap junctions between cells expressing connexin 43 or 32 show inverse permselectivity to adenosine and ATP. J Biol Chem 277:36725-36730.

Golub TR, Slonim DK, Tamayo P, Huard C, Gaasenbeek M, Mesirov JP, Coller H, Loh ML, Downing JR, Caligiuri MA, Bloomfield CD, Lander ES (1999) Molecular classification of cancer: class discovery and class prediction by gene expression monitoring. Science 286:531-537.

Goodenough DA, Goliger JA, Paul DL (1996) Connexins, connexons, and intercellular communication. Annual Review of Biochemistry 65:475-502.

Grammas P, Ovase R (2001) Inflammatory factors are elevated in brain microvessels in Alzheimer's disease. Neurobiol Aging 22:837-842.

Grammas P, Samany PG, Thirumangalakudi L (2006) Thrombin and inflammatory proteins are elevated in Alzheimer's disease microvessels: implications for disease pathogenesis. J Alzheimers Dis 9:51-58.

Grammas P, Ottman T, Reimann-Philipp U, Larabee J, Weigel PH (2004) Injured brain endothelial cells release neurotoxic thrombin. J Alzheimers Dis 6:275-281.

Green CR, Nicholson LF (2008) Interrupting the inflammatory cycle in chronic diseases--do gap junctions provide the answer? Cell Biol Int 32:1578-1583.

Greenbaum D, Colangelo C, Williams K, Gerstein M (2003) Comparing protein abundance and mRNA expression levels on a genomic scale. Genome Biol 4:117.

Greene JG (2010) Current status and future directions of gene expression profiling in Parkinson's disease. Neurobiology of disease.

Gunderson KL, Kruglyak S, Graige MS, Garcia F, Kermani BG, Zhao C, Che D, Dickinson T, Wickham E, Bierle J, Doucet D, Milewski M, Yang R, Siegmund C, Haas J, Zhou L, Oliphant A, Fan JB, Barnard S, Chee MS (2004) Decoding randomly ordered DNA arrays. Genome Res 14:870-877.

Haan MN (2006) Therapy Insight: type 2 diabetes mellitus and the risk of late-onset Alzheimer's disease. Nat Clin Pract Neurol 2:159-166.

Hackl H, Sanchez Cabo F, Sturn A, Wolkenhauer O, Trajanoski Z (2004) Analysis of DNA microarray data. Curr Top Med Chem 4:1357-1370.

Hailer NP (2008) Immunosuppression after traumatic or ischemic CNS damage: it is neuroprotective and illuminates the role of microglial cells. Prog Neurobiol 84:211-233.

Hamadeh HK, Afshari CA (2004) Toxicogenomics: Principles and Applications. Hoboken: Wiley-IEEE.

Han BC, Koh SB, Lee EY, Seong YH (2004) Regional difference of glutamate-induced swelling in cultured rat brain astrocytes. Life Sci 76:573-583.

Hanner F, Schnichels M, Zheng-Fischhofer Q, Yang LE, Toma I, Willecke K, McDonough AA, Peti-Peterdi J (2008) Connexin 30.3 is expressed in the kidney but not regulated by dietary salt or high blood pressure. Cell Commun Adhes 15:219-230.

Harrison PJ, Heath PR, Eastwood SL, Burnet PW, McDonald B, Pearson RC (1995) The relative importance of premortem acidosis and postmortem interval for human brain gene expression studies: selective mRNA vulnerability and comparison with their encoded proteins. Neuroscience Letters 200:151-154.

Harrison PJ, Procter AW, Barton AJ, Lowe SL, Najlerahim A, Bertolucci PH, Bowen DM, Pearson RC (1991) Terminal coma affects messenger RNA detection in post mortem human temporal cortex. Brain Res Mol Brain Res Molecular Brain Research. 9:161-164.

Haupt C, Witte OW, Frahm C (2007) Up-regulation of Connexin43 in the glial scar following photothrombotic ischemic injury. Mol Cell Neurosci 35:89-99.

Heales SJ, Bolanos JP, Stewart VC, Brookes PS, Land JM, Clark JB (1999) Nitric oxide, mitochondria and neurological disease. Biochim Biophys Acta 1410:215-228.

Hebert SS, Horre K, Nicolai L, Papadopoulou AS, Mandemakers W, Silahtaroglu AN, Kauppinen S, Delacourte A, De Strooper B (2008) Loss of microRNA cluster miR-29a/b-1 in sporadic Alzheimer's disease correlates with increased BACE1/beta-secretase expression. Proc Natl Acad Sci U S A 105:6415-6420.

Heinrich M, Matt K, Lutz-Bonengel S, Schmidt U (2006) Successful RNA extraction from various human postmortem tissues. International Journal of Legal Medicine.

Heller MJ (2002) DNA microarray technology: devices, systems, and applications. Annual Review of Biomedical Engineering 4:129-153.

Herman B (1998) Fluorescence Microscopy, 2nd Edition. Oxford, UK.: BIOS Scientific Publishers.

Herve JC, Derangeon M, Bahbouhi B, Mesnil M, Sarrouilhe D (2007) The connexin turnover, an important modulating factor of the level of cell-to-cell junctional communication: comparison with other integral membrane proteins. The Journal of membrane biology 217:21-33.

Hester SD, Reid L, Nowak N, Jones WD, Parker JS, Knudtson K, Ward W, Tiesman J, Denslow ND (2009) Comparison of comparative genomic hybridization technologies across microarray platforms. J Biomol Tech 20:135-151.

Hewett SJ, Csernansky CA, Choi DW (1994) Selective potentiation of NMDA-induced neuronal injury following induction of astrocytic iNOS. Neuron 13:487-494.

Hill AA, Brown EL, Whitley MZ, Tucker-Kellogg G, Hunter CP, Slonim DK (2001) Evaluation of normalisation procedures for oligonucleotide array data based on spiked cRNA controls. Genome Biology 2:RESEARCH0055.

Hirsch EC, Hunot S (2009) Neuroinflammation in Parkinson's disease: a target for neuroprotection? Lancet Neurol 8:382-397.

Hirsch EC, Hunot S, Hartmann A (2005) Neuroinflammatory processes in Parkinson's disease. Parkinsonism Relat Disord 11 Suppl 1:S9-S15.

Hirsch EC, Hunot S, Damier P, Faucheux B (1998) Glial cells and inflammation in Parkinson's disease: a role in neurodegeneration? Annals of neurology 44:S115-120.

Hisham K. Hamadeh CAA (2004) Toxicogenomics: Principles and Applications. Hoboken: Wiley-IEEE.

Hodges A et al. (2006) Regional and cellular gene expression changes in human Huntington's disease brain. Human molecular genetics 15:965-977.

Hollingshead D, Lewis DA, Mirnics K (2005) Platform influence on DNA microarray data in postmortem brain research. Neurobiol Dis 18:649-655.

Holloway AJ, van Laar RK, Tothill RW, Bowtell DD (2002) Options available--from start to finish--for obtaining data from DNA microarrays II. Nature Genetics 32:481-489.

Hu J, Ferreira A, Van Eldik LJ (1997) S100beta induces neuronal cell death through nitric oxide release from astrocytes. J Neurochem 69:2294-2301.

Huber W, von Heydebreck A, Sultmann H, Poustka A, Vingron M (2002) Variance stabilization applied to microarray data calibration and to the quantification of differential expression. Bioinformatics 18 Suppl 1:S96-104.

Huettner JE, Lu A, Qu Y, Wu Y, Kim M, McDonald JW (2006) Gap junctions and connexon hemichannels in human embryonic stem cells. Stem Cells 24:1654-1667.

Hughes TR et al. (2001) Expression profiling using microarrays fabricated by an ink-jet oligonucleotide synthesizer. Nature Biotechnology 19:342-347.

Huh Y, Jung JW, Park C, Ryu JR, Shin CY, Kim WK, Ryu JH (2003) Microglial activation and tyrosine hydroxylase immunoreactivity in the substantia nigral region following transient focal ischemia in rats. Neurosci Lett 349:63-67.

Hunot S, Boissiere F, Faucheux B, Brugg B, Mouatt-Prigent A, Agid Y, Hirsch EC (1996) Nitric oxide synthase and neuronal vulnerability in Parkinson's disease. Neuroscience 72:355-363.

Imamura K, Hishikawa N, Sawada M, Nagatsu T, Yoshida M, Hashizume Y (2003) Distribution of major histocompatibility complex class II-positive microglia and cytokine profile of Parkinson's disease brains. Acta Neuropathol 106:518-526.

Imbeaud S, Graudens E, Boulanger V, Barlet X, Zaborski P, Eveno E, Mueller O, Schroeder A, Auffray C (2005) Towards standardisation of RNA quality assessment using user-independent classifiers of microcapillary electrophoresis traces. Nucleic Acids Res 33:e56.

Jain AN, Tokuyasu TA, Snijders AM, Segraves R, Albertson DG, Pinkel D (2002) Fully automatic quantification of microarray image data. Genome Research 12:325-332.

Janitz M, ed (2008) Next-generation genome sequencing - towards personalized medicine. Weinheim: Wiley-VCH.

Johnson SA, Morgan DG, Finch CE (1986) Extensive postmortem stability of RNA from rat and human brain. Journal of Neuroscience Research 16:267-280.

Johnston NL, Cervenak J, Shore AD, Torrey EF, Yolken RH (1997) Multivariate analysis of RNA levels from postmortem human brains as measured by three different methods of RT-PCR. Stanley Neuropathology Consortium.[erratum appears in J Neurosci Methods 1998 Feb 20;79(2):233 Note: Cerevnak J [corrected to Cervenak J]]. Journal of Neuroscience Methods 77:83-92.

Jolliffe I (1986) Principal component analysis. New York: Springer Verlag.

Kalaria RN (1999) Microglia and Alzheimer's disease. Curr Opin Hematol 6:15-24.

Kam Y, Kim DY, Koo SK, Joe CO (1998) Transfer of second messengers through gap junction connexin 43 channels reconstituted in liposomes. Biochim Biophys Acta 1372:384-388.

Kane MD, Jatkoe TA, Stumpf CR, Lu J, Thomas JD, Madore SJ (2000) Assessment of the sensitivity and specificity of oligonucleotide (50mer) microarrays. Nucleic Acids Research 28:4552-4557.

Kang J, Kang N, Lovatt D, Torres A, Zhao Z, Lin J, Nedergaard M (2008) Connexin 43 hemichannels are permeable to ATP. J Neurosci 28:4702-4711.

Kapsimali M, Kloosterman WP, de Bruijn E, Rosa F, Plasterk RH, Wilson SW (2007) MicroRNAs show a wide diversity of expression profiles in the developing and mature central nervous system. Genome Biol 8:R173.

Kaushal V, Schlichter LC (2008) Mechanisms of microglia-mediated neurotoxicity in a new model of the stroke penumbra. J Neurosci 28:2221-2230.

Kielian T (2008) Glial connexins and gap junctions in CNS inflammation and disease. J Neurochem 106:1000-1016.

Kim J, Inoue K, Ishii J, Vanti WB, Voronov SV, Murchison E, Hannon G, Abeliovich A (2007) A MicroRNA feedback circuit in midbrain dopamine neurons. Science 317:1220-1224.

Kim JH, Kim HY, Lee YS (2001) A novel method using edge detection for signal extraction from cDNA microarray image analysis. Experimental & Molecular Medicine 33:83-88.

Kingham PJ, Cuzner ML, Pocock JM (1999) Apoptotic pathways mobilized in microglia and neurones as a consequence of chromogranin A-induced microglial activation. J Neurochem 73:538-547.

Kingsbury AE, Foster OJ, Nisbet AP, Cairns N, Bray L, Eve DJ, Lees AJ, Marsden CD (1995) Tissue pH as an indicator of mRNA preservation in human post-mortem brain. Brain Research Molecular Brain Research 28:311-318.

Kinsner A, Pilotto V, Deininger S, Brown GC, Coecke S, Hartung T, Bal-Price A (2005) Inflammatory neurodegeneration induced by lipoteichoic acid from Staphylococcus aureus is mediated by glia activation, nitrosative and oxidative stress, and caspase activation. J Neurochem 95:1132-1143.

Kleopa KA, Orthmann JL, Enriquez A, Paul DL, Scherer SS (2004) Unique distributions of the gap junction proteins connexin29, connexin32, and connexin47 in oligodendrocytes. GLIA 47:346-357.

Koltai H, Weingarten-Baror C (2008) Specificity of DNA microarray hybridization: characterization, effectors and approaches for data correction. Nucleic Acids Res 36:2395-2405.

Kooperberg C, Fazzio TG, Delrow JJ, Tsukiyama T (2002) Improved background correction for spotted DNA microarrays. J Comput Biol 9:55-66.

Kosik KS (2006) The neuronal microRNA system. Nat Rev Neurosci 7:911-920.

Koyama Y, Ishibashi T, Okamoto T, Matsuda T, Hashimoto H, Baba A (2000) Transient treatments with L-glutamate and threo-beta-hydroxyaspartate induce swelling of rat cultured astrocytes. Neurochem Int 36:167-173.

Kreil DP, Russell RR, Russell S (2006) Microarray oligonucleotide probes. Methods Enzymol 410:73-98.

Kumar NM, Gilula NB (1996) The gap junction communication channel. Cell 84:381-388.

Kuo WP, Jenssen TK, Butte AJ, Ohno-Machado L, Kohane IS (2002) Analysis of matched mRNA measurements from two different microarray technologies. Bioinformatics 18:405-412.

Landgraf P et al. (2007) A mammalian microRNA expression atlas based on small RNA library sequencing. Cell 129:1401-1414.

Lee J, Hever A, Willhite D, Zlotnik A, Hevezi P (2005) Effects of RNA degradation on gene expression analysis of human postmortem tissues.1356-1358, 2005 Aug.

Lee JK, Williams PD, Cheon S (2008) Data mining in genomics. Clin Lab Med 28:145-166, viii.

Lee Y, Kim M, Han J, Yeom KH, Lee S, Baek SH, Kim VN (2004) MicroRNA genes are transcribed by RNA polymerase II. Embo J 23:4051-4060.

Li F, Stormo GD (2001) Selection of optimal DNA oligos for gene expression arrays. Bioinformatics 17:1067-1076.

Li JZ, Vawter MP, Walsh DM, Tomita H, Evans SJ, Choudary PV, Lopez JF, Avelar A, Shokoohi V, Chung T, Mesarwi O, Jones EG, Watson SJ, Akil H, Bunney WE, Jr., Myers RM (2004a) Systematic changes in gene expression in postmortem human brains associated with tissue pH and terminal medical conditions. Hum Mol Genet 13:609-616.

Li X, Penes M, Odermatt B, Willecke K, Nagy JI (2008) Ablation of Cx47 in transgenic mice leads to the loss of MUPP1, ZONAB and multiple connexins at oligodendrocyte-astrocyte gap junctions. European Journal of Neuroscience 28:1503-1517.

Li X, Ionescu AV, Lynn BD, Lu S, Kamasawa N, Morita M, Davidson KG, Yasumura T, Rash JE, Nagy JI (2004b) Connexin47, connexin29 and connexin32 co-expression in oligodendrocytes and Cx47 association with zonula occludens-1 (ZO-1) in mouse brain. Neuroscience 126:611-630.

Liang WS, Dunckley T, Beach TG, Grover A, Mastroeni D, Ramsey K, Caselli RJ, Kukull WA, McKeel D, Morris JC, Hulette CM, Schmechel D, Reiman EM, Rogers J, Stephan DA (2008) Altered neuronal gene expression in brain regions differentially affected by Alzheimer's disease: a reference data set. Physiological genomics 33:240-256.

Lindgren HS, Ohlin KE, Wetsin JE, Cenci MA (2007) L-DOPA-induced angiogenesis in the basal ganglia: a new twist to the pathophysiology of dyskinesia? In: Int Basal Ganglia Soc Congress, pp O-07. Egmont aan Zee, The Netherlands.

Lipshutz R, Fodor S, Gingeras T, Lockhart D (1999) High Density synthetic oligonucleotide arrays. Nature Genetics 21 (Suppl):20-24.

Lipska BK, Deep-Soboslay A, Weickert CS, Hyde TM, Martin CE, Herman MM, Kleinman JE (2006) Critical factors in gene expression in postmortem human brain: Focus on studies in schizophrenia. Biol Psychiatry 60:650-658.

Liu H, Bebu I, Li X (2010) Microarray probes and probe sets. Front Biosci (Elite Ed) 2:325-338.

Lobsiger CS, Cleveland DW (2007) Glial cells as intrinsic components of non-cell-autonomous neurodegenerative disease. Nat Neurosci 10:1355-1360.

Lockhart DJ, Barlow C (2001) Expressing what's on your mind: DNA arrays and the brain. Nature Reviews Neuroscience 2:63-68.

Loo DT, Copani A, Pike CJ, Whittemore ER, Walencewicz AJ, Cotman CW (1993) Apoptosis is induced by beta-amyloid in cultured central nervous system neurons. Proc Natl Acad Sci U S A 90:7951-7955.

Loring JF (2006) Evolution of microarray analysis.[comment]. Neurobiology of Aging 27:1084-1086.

Luo Z, Geschwind DH (2001) Microarray applications in neuroscience. Neurobiology of Disease 8:183-193.

Madrigal JL, Feinstein DL, Dello Russo C (2005) Norepinephrine protects cortical neurons against microglial-induced cell death. J Neurosci Res 81:390-396.

Martin-Magniette ML, Aubert J, Bar-Hen A, Elftieh S, Magniette F, Renou JP, Daudin JJ (2008) Normalisation for triple-target microarray experiments. BMC Bioinformatics 9:216.

Matera AG, Terns RM, Terns MP (2007) Non-coding RNAs: lessons from the small nuclear and small nucleolar RNAs. Nat Rev Mol Cell Biol 8:209-220.

Mayr T, Moser C, Klimant I (2009) Performance of fluorescent labels in sedimentation bead arrays--a comparison study. J Fluoresc 19:303-310.

McGeer EG, McGeer PL (2003) Inflammatory processes in Alzheimer's disease. Prog Neuropsychopharmacol Biol Psychiatry 27:741-749.

McGeer EG, Klegeris A, McGeer PL (2005) Inflammation, the complement system and the diseases of aging. Neurobiol Aging 26 Suppl 1:94-97.

McGeer PL, McGeer EG, Yasojima K (2000) Alzheimer disease and neuroinflammation. J Neural Transm Suppl 59:53-57.

McGeer PL, Itagaki S, Akiyama H, McGeer EG (1988) Rate of cell death in parkinsonism indicates active neuropathological process. Ann Neurol 24:574-576.

McNaught KS, Jenner P (1999) Altered glial function causes neuronal death and increases neuronal susceptibility to 1-methyl-4-phenylpyridinium- and 6-hydroxydopamine-induced toxicity in astrocytic/ventral mesencephalic co-cultures. J Neurochem 73:2469-2476.

Meier C, Dermietzel R (2006) Electrical synapses--gap junctions in the brain. Results and problems in cell differentiation 43:99-128.

Meme W, Calvo CF, Froger N, Ezan P, Amigou E, Koulakoff A, Giaume C (2006) Proinflammatory cytokines released from microglia inhibit gap junctions in astrocytes: potentiation by beta-amyloid. Faseb J 20:494-496.

Mendoza-Naranjo A, Saez PJ, Johansson CC, Ramirez M, Mandakovic D, Pereda C, Lopez MN, Kiessling R, Saez JC, Salazar-Onfray F (2007) Functional gap junctions facilitate melanoma

antigen transfer and cross-presentation between human dendritic cells. J Immunol 178:6949-6957.

Mergenthaler P, Dirnagl U, Meisel A (2004) Pathophysiology of stroke: lessons from animal models. Metab Brain Dis 19:151-167.

Mese G, Richard G, White TW (2007) Gap junctions: basic structure and function. J Invest Dermatol 127:2516-2524.

Metea MR, Newman EA (2006) Glial cells dilate and constrict blood vessels: a mechanism of neurovascular coupling. J Neurosci 26:2862-2870.

Miller CL, Diglisic S, Leister F, Webster M, Yolken RH (2004) Evaluating RNA status for RT-PCR in extracts of postmortem human brain tissue. Biotechniques 36:628-633.

Mirnics K (2001) Microarrays in brain research: the good, the bad and the ugly. Nature Reviews Neuroscience 2:444-447.

Mirnics K, Pevsner J (2004) Progress in the use of microarray technology to study the neurobiology of disease. Nature neuroscience 7:434-439.

Mirnics K, Levitt P, Lewis DA (2006) Critical appraisal of DNA microarrays in psychiatric genomics. Biological Psychiatry 60:163-176.

Mirnics K, Middleton FA, Lewis DA, Levitt P (2001) Analysis of complex brain disorders with gene expression microarrays: schizophrenia as a disease of the synapse. Trends in Neurosciences 24:479-486.

Mogi M, Harada M, Riederer P, Narabayashi H, Fujita K, Nagatsu T (1994a) Tumor necrosis factor-alpha (TNF-alpha) increases both in the brain and in the cerebrospinal fluid from parkinsonian patients. Neurosci Lett 165:208-210.

Mogi M, Harada M, Kondo T, Riederer P, Inagaki H, Minami M, Nagatsu T (1994b) Interleukin-1 beta, interleukin-6, epidermal growth factor and transforming growth factor-alpha are elevated in the brain from parkinsonian patients. Neuroscience letters 180:147-150.

Mortazavi A, Williams BA, McCue K, Schaeffer L, Wold B (2008) Mapping and quantifying mammalian transcriptomes by RNA-Seq. Nat Methods 5:621-628.

Nagalakshmi U, Wang Z, Waern K, Shou C, Raha D, Gerstein M, Snyder M (2008) The transcriptional landscape of the yeast genome defined by RNA sequencing. Science 320:1344-1349.

Nagy JI, Li W, Hertzberg EL, Marotta CA (1996) Elevated connexin43 immunoreactivity at sites of amyloid plaques in Alzheimer's disease. Brain Res 717:173-178.

Nagy JI, Ionescu AV, Lynn BD, Rash JE (2003) Coupling of astrocyte connexins Cx26, Cx30, Cx43 to oligodendrocyte Cx29, Cx32, Cx47: Implications from normal and connexin32 knockout mice. GLIA 44:205-218.

Nakase T, Naus CC (2004) Gap junctions and neurological disorders of the central nervous system. Biochimica et biophysica acta 1662:149-158.

Neijssen J, Herberts C, Drijfhout JW, Reits E, Janssen L, Neefjes J (2005) Cross-presentation by intercellular peptide transfer through gap junctions. Nature 434:83-88.

Nelson SF (2001) Oligonucleotide microarrays for gene expression analysis. In: DNA Microarrays: The New Frontier in Gene Discovery and Gene Expression Analysis. (Geschwind DH, Van Deerlin V, eds). San Diego, CA: Society for Neuroscience.

Niessen H, Harz H, Bedner P, Kramer K, Willecke K (2000) Selective permeability of different connexin channels to the second messenger inositol 1,4,5-trisphosphate. Journal of Cell Science 113:1365-1372.

Noorbakhsh F, Overall CM, Power C (2009) Deciphering complex mechanisms in neurodegenerative diseases: the advent of systems biology. Trends Neurosci 32:88-100.

O'Carroll SJ, Alkadhi M, Nicholson LF, Green CR (2008) Connexin 43 mimetic peptides reduce swelling, astrogliosis, and neuronal cell death after spinal cord injury. Cell Commun Adhes 15:27-42.

Odermatt B, Wellershaus K, Wallraff A, Seifert G, Degen J, Euwens C, Fuss B, Bussow H, Schilling K, Steinhauser C, Willecke K (2003) Connexin 47 (Cx47)-deficient mice with enhanced green fluorescent protein reporter gene reveal predominant oligodendrocytic expression of Cx47 and display vacuolized myelin in the CNS. Journal of Neuroscience 23:4549-4559.

Okamoto T, Akiyama M, Takeda M, Gabazza EC, Hayashi T, Suzuki K (2009) Connexin32 is expressed in vascular endothelial cells and participates in gap-junction intercellular communication. Biochem Biophys Res Commun 382:264-268.

Olson NE (2006) The microarray data analysis process: from raw data to biological significance. NeuroRx 3:373-383.

Orellana JA, Saez PJ, Shoji KF, Schalper KA, Palacios-Prado N, Velarde V, Giaume C, Bennett MV, Saez JC (2009) Modulation of brain hemichannels and gap junction channels by pro-inflammatory agents and their possible role in neurodegeneration. Antioxid Redox Signal 11:369-399.

Orom UA, Nielsen FC, Lund AH (2008) MicroRNA-10a binds the 5'UTR of ribosomal protein mRNAs and enhances their translation. Mol Cell 30:460-471.

Orthmann-Murphy JL, Abrams CK, Scherer SS (2008) Gap junctions couple astrocytes and oligodendrocytes. Journal of molecular neuroscience : MN 35:101-116.

Orthmann-Murphy JL, Freidin M, Fischer E, Scherer SS, Abrams CK (2007) Two distinct heterotypic channels mediate gap junction coupling between astrocyte and oligodendrocyte connexins. Journal of Neuroscience 27:13949-13957.

Ozog MA, Siushansian R, Naus CC (2002) Blocked gap junctional coupling increases glutamate-induced neurotoxicity in neuron-astrocyte co-cultures. J Neuropathol Exp Neurol 61:132-141.

Parenti R, Campisi A, Vanella A, Cicirata F (2002) Immunocytochemical and RT-PCR analysis of connexin36 in cultures of mammalian glial cells. Arch Ital Biol 140:101-108.

Parihar MS, Hemnani T (2004) Alzheimer's disease pathogenesis and therapeutic interventions. J Clin Neurosci 11:456-467.

Patterson TA, Lobenhofer EK, Fulmer-Smentek SB, Collins PJ, Chu TM, Bao W, Fang H, Kawasaki ES, Hager J, Tikhonova IR, Walker SJ, Zhang L, Hurban P, de Longueville F, Fuscoe JC, Tong W, Shi L, Wolfinger RD (2006) Performance comparison of one-color and two-color platforms within the MicroArray Quality Control (MAQC) project. Nat Biotechnol 24:1140-1150.

Paul DL (1995) New functions for gap junctions. Curr Opin Cell Biol 7:665-672.

Paulsen JS, Ready RE, Hamilton JM, Mega MS, Cummings JL (2001) Neuropsychiatric aspects of Huntington's disease. J Neurol Neurosurg Psychiatry 71:310-314.

Pedotti P, t Hoen PA, Vreugdenhil E, Schenk GJ, Vossen RH, Ariyurek Y, de Hollander M, Kuiper R, van Ommen GJ, den Dunnen JT, Boer JM, de Menezes RX (2008) Can subtle changes in gene expression be consistently detected with different microarray platforms? BMC Genomics 9:124.

Perou CM, Sorlie T, Eisen MB, van de Rijn M, Jeffrey SS, Rees CA, Pollack JR, Ross DT, Johnsen H, Akslen LA, Fluge O, Pergamenschikov A, Williams C, Zhu SX, Lonning PE, Borresen-Dale AL, Brown PO, Botstein D (2000) Molecular portraits of human breast tumours. Nature 406:747-752.

Pike CJ, Walencewicz-Wasserman AJ, Kosmoski J, Cribbs DH, Glabe CG, Cotman CW (1995) Structure-activity analyses of beta-amyloid peptides: contributions of the beta 25-35 region to aggregation and neurotoxicity. J Neurochem 64:253-265.

Plantard L, Huber M, Macari F, Meda P, Hohl D (2003) Molecular interaction of connexin 30.3 and connexin 31 suggests a dominant-negative mechanism associated with erythrokeratodermia variabilis. Hum Mol Genet 12:3287-3294.

Popova T, Mennerich D, Weith A, Quast K (2008) Effect of RNA quality on transcript intensity levels in microarray analysis of human post-mortem brain tissues. BMC Genomics 9:91.

Qiagen (2003) The HighLight Microarray System. Helix:10-11.

Qiagen Bench Guide (2001): Qiagen.

Qiu C, Coutinho P, Frank S, Franke S, Law LY, Martin P, Green CR, Becker DL (2003) Targeting connexin43 expression accelerates the rate of wound repair. Curr Biol 13:1697-1703.

Quackenbush J (2001) Computational analysis of microarray data. Nat Rev Genet 2:418-427.

Rana S, Dringen R (2007) Gap junction hemichannel-mediated release of glutathione from cultured rat astrocytes. Neurosci Lett 415:45-48.

Ray M, Zhang W (2010) Analysis of Alzheimer's disease severity across brain regions by topological analysis of gene co-expression networks. BMC systems biology 4:136.

Retamal MA, Froger N, Palacios-Prado N, Ezan P, Saez PJ, Saez JC, Giaume C (2007) Cx43 hemichannels and gap junction channels in astrocytes are regulated oppositely by proinflammatory cytokines released from activated microglia. J Neurosci 27:13781-13792.

Rossi D, Volterra A (2009) Astrocytic dysfunction: insights on the role in neurodegeneration. Brain research bulletin.

Rouach N, Avignone E, Meme W, Koulakoff A, Venance L, Blomstrand F, Giaume C (2002) Gap junctions and connexin expression in the normal and pathological central nervous system. Biology of the cell / under the auspices of the European Cell Biology Organization 94:457-475.

Roy A, Jana A, Yatish K, Freidt MB, Fung YK, Martinson JA, Pahan K (2008) Reactive oxygen species up-regulate CD11b in microglia via nitric oxide: Implications for neurodegenerative diseases. Free Radic Biol Med 45:686-699.

Ruano D, Revilla E, Gavilan MP, Vizuete ML, Pintado C, Vitorica J, Castano A (2006) Role of p38 and inducible nitric oxide synthase in the in vivo dopaminergic cells' degeneration induced by inflammatory processes after lipopolysaccharide injection. Neuroscience 140:1157-1168.

Rufer M, Wirth SB, Hofer A, Dermietzel R, Pastor A, Kettenmann H, Unsicker K (1996) Regulation of connexin-43, GFAP, and FGF-2 is not accompanied by changes in astroglial coupling in MPTP-lesioned, FGF-2-treated parkinsonian mice. J Neurosci Res 46:606-617.

Saez JC, Retamal MA, Basilio D, Bukauskas FF, Bennett MV (2005) Connexin-based gap junction hemichannels: gating mechanisms. Biochim Biophys Acta 1711:215-224.

Sargiannidou I, Vavlitou N, Aristodemou S, Hadjisavvas A, Kyriacou K, Scherer SS, Kleopa KA (2009) Connexin32 mutations cause loss of function in Schwann cells and oligodendrocytes leading to PNS and CNS myelination defects. Journal of Neuroscience 29:4736-4749.

Sargiannidou I, Ahn M, Enriquez AD, Peinado A, Reynolds R, Abrams C, Scherer SS, Kleopa KA (2008) Human oligodendrocytes express Cx31.3: function and interactions with Cx32 mutants. Neurobiology of Disease 30:221-233.

Scemes E, Dermietzel R, Spray DC (1998) Calcium waves between astrocytes from Cx43 knockout mice. Glia 24:65-73.

Schena M, ed (2008) DNA Microarrays. Bloxham, Oxfordshire: Scion Publishing Limited.

Schena M, Friedman MJ, Haje P, Martinsky T, Suzuki G, Costa T, Chung J, Ruiz M, Costa C, Machado L, Raja R, Desai R (2008) Whole human genome microarrays. In: DNA Microarrays (Schena M, ed), pp 1-30. Bloxham: Scion Publishing Limited.

Schramm M, Falkai P, Tepest R, Schneider-Axmann T, Przkora R, Waha A, Pietsch T, Bonte W, Bayer TA (1999) Stability of RNA transcripts in post-mortem psychiatric brains. J Neural Transm 106:329-335.

Shaikh S, Hamilton TM, B NLF (2007) Are connexins important in Parkinson's disease? In: Int Basal Ganglia Soc Congress, pp P-086. Egmond aan Zee.

Sheffler W, Upfal E, Sedivy J, Noble WS (2005) A learned comparative expression measure for affymetrix genechip DNA microarrays. Proc IEEE Comput Syst Bioinform Conf:144-154.

Shi L et al. (2006) The MicroArray Quality Control (MAQC) project shows inter- and intraplatform reproducibility of gene expression measurements. Nat Biotechnol 24:1151-1161.

Shimokawa K, Kodzius R, Matsumara Y, Hayashizaki Y (2008) Methods for increasing the utility of microarray data. In: DNA Microarrays (Schena M, ed), pp 103-114. Bloxham: Scion Publishing Limited.

Shin JY, Fang ZH, Yu ZX, Wang CE, Li SH, Li XJ (2005) Expression of mutant huntingtin in glial cells contributes to neuronal excitotoxicity. J Cell Biol 171:1001-1012.

Shmulevich I, Astola J, Cogdell D, Hamilton SR, Zhang W (2003) Data extraction from composite oligonucleotide microarrays. Nucleic Acids Research 31:e36.

Silvestroni A, Faull RL, Strand AD, Moller T (2009) Distinct neuroinflammatory profile in post-mortem human Huntington's disease. Neuroreport 20:1098-1103.

Singleton AB et al. (2003) alpha-Synuclein locus triplication causes Parkinson's disease. Science 302:841.

SiuYi Leung D, Unsicker K, Reuss B (2001) Gap junctions modulate survival-promoting effects of fibroblast growth factor-2 on cultured midbrain dopaminergic neurons. Mol Cell Neurosci 18:44-55.

Sohl G, Willecke K (2003) An update on connexin genes and their nomenclature in mouse and man. Cell Commun Adhes 10:173-180.

Sohl G, Maxeiner S, Willecke K (2005) Expression and functions of neuronal gap junctions. Nature Reviews Neuroscience 6:191-200.

Sohl G, Nielsen PA, Eiberger J, Willecke K (2003) Expression profiles of the novel human connexin genes hCx30.2, hCx40.1, and hCx62 differ from their putative mouse orthologues. Cell Commun Adhes 10:27-36.

Sproule DM, Kaufmann P (2008) Mitochondrial encephalopathy, lactic acidosis, and strokelike episodes: basic concepts, clinical phenotype, and therapeutic management of MELAS syndrome. Ann N Y Acad Sci 1142:133-158.

Stan AD, Ghose S, Gao XM, Roberts RC, Lewis-Amezcua K, Hatanpaa KJ, Tamminga CA (2006) Human postmortem tissue: what quality markers matter? Brain Res Mol Brain Res 1123:1-11.

Steinhoff C, Vingron M (2006) Normalisation and quantification of differential expression in gene expression microarrays. Brief Bioinform 7:166-177.

Stekel D (2003) Microarray bioinformatics. Cambridge: Cambridge University Press.

Stout CE, Costantin JL, Naus CC, Charles AC (2002) Intercellular calcium signaling in astrocytes via ATP release through connexin hemichannels. J Biol Chem 277:10482-10488.

Stridh MH, Tranberg M, Weber SG, Blomstrand F, Sandberg M (2008) Stimulated efflux of amino acids and glutathione from cultured hippocampal slices by omission of extracellular calcium: likely involvement of connexin hemichannels. J Biol Chem 283:10347-10356.

Sung JY, Lee HJ, Jeong EI, Oh Y, Park J, Kang KS, Chung KC (2007) Alpha-synuclein overexpression reduces gap junctional intercellular communication in dopaminergic neuroblastoma cells. Neurosci Lett 416:289-293.

Suter U, Snipes GJ (1995) Biology and genetics of hereditary motor and sensory neuropathies. Annu Rev Neurosci 18:45-75.

Sutor B, Schmolke C, Teubner B, Schirmer C, Willecke K (2000) Myelination defects and neuronal hyperexcitability in the neocortex of connexin 32-deficient mice. Cereb Cortex 10:684-697.

Szabo A, Boucher K, Carroll WL, Klebanov LB, Tsodikov AD, Yakovlev AY (2002) Variable selection and pattern recognition with gene expression data generated by the microarray technology. Math Biosci 176:71-98.

Taft RJ, Pang KC, Mercer TR, Dinger M, Mattick JS (2010) Non-coding RNAs: regulators of disease. J Pathol 220:126-139.

Tai YF, Pavese N, Gerhard A, Tabrizi SJ, Barker RA, Brooks DJ, Piccini P (2007) Microglial activation in presymptomatic Huntington's disease gene carriers. Brain 130:1759-1766.

Takeuchi H, Jin S, Wang J, Zhang G, Kawanokuchi J, Kuno R, Sonobe Y, Mizuno T, Suzumura A (2006) Tumor necrosis factor-alpha induces neurotoxicity via glutamate release from hemichannels of activated microglia in an autocrine manner. J Biol Chem 281:21362-21368.

Tamames J, Clark D, Herrero J, Dopazo J, Blaschke C, Fernandez JM, Oliveros JC, Valencia A (2002) Bioinformatics methods for the analysis of expression arrays: data clustering and information extraction. Journal of Biotechnology 98:269-283.

Taroncher-Oldenburg G, Griner EM, Francis CA, Ward BB (2003) Oligonucleotide microarray for the study of functional gene diversity in the nitrogen cycle in the environment. Appl Environ Microbiol 69:1159-1171.

Theis M, Sohl G, Eiberger J, Willecke K (2005) Emerging complexities in identity and function of glial connexins. Trends in neurosciences 28:188-195.

Thornton P, Pinteaux E, Gibson RM, Allan SM, Rothwell NJ (2006) Interleukin-1-induced neurotoxicity is mediated by glia and requires caspase activation and free radical release. J Neurochem 98:258-266.

Tomlinson CR, Karyala S, Halbleib D, Medvedovic M, Puga A (2008) Toxicogenomics of dioxin. In: DNA microarrays (Schena M, ed), pp 31-49. Bloxham: Scion Publishing Limited.

Traub RD, Whittington MA, Buhl EH, LeBeau FE, Bibbig A, Boyd S, Cross H, Baldeweg T (2001) A possible role for gap junctions in generation of very fast EEG oscillations preceding the onset of, and perhaps initiating, seizures. Epilepsia 42:153-170.

Tripathy D, Thirumangalakudi L, Grammas P (2007) Expression of macrophage inflammatory protein 1-alpha is elevated in Alzheimer's vessels and is regulated by oxidative stress. J Alzheimers Dis 11:447-455.

Ullrich O, Diestel A, Eyupoglu IY, Nitsch R (2001) Regulation of microglial expression of integrins by poly(ADP-ribose) polymerase-1. Nat Cell Biol 3:1035-1042.

Unsworth HC, Aasen T, McElwaine S, Kelsell DP (2007) Tissue-specific effects of wild-type and mutant connexin 31: a role in neurite outgrowth. Hum Mol Genet 16:165-172.

Vacha SJ (2003) Ten Pitfalls of Microarray Analysis. In: Agilent Technologies, Inc.

Vandecasteele M, Glowinski J, Venance L (2005) Electrical synapses between dopaminergic neurons of the substantia nigra pars compacta. J Neurosci 25:291-298.

Vandecasteele M, Glowinski J, Venance L (2006) Connexin mRNA expression in single dopaminergic neurons of substantia nigra pars compacta. Neurosci Res 56:419-426.

Vandesompele J, De Preter K, Pattyn F, Poppe B, Van Roy N, De Paepe A, Speleman F (2002) Accurate normalisation of real-time quantitative RT-PCR data by geometric averaging of multiple internal control genes. Genome Biol 3:RESEARCH0034.

Vasudevan S, Tong Y, Steitz JA (2007) Switching from repression to activation: microRNAs can up-regulate translation. Science 318:1931-1934.

Venance L, Stella N, Glowinski J, Giaume C (1997) Mechanism involved in initiation and propagation of receptor-induced intercellular calcium signaling in cultured rat astrocytes. J Neurosci 17:1981-1992.

Vis JC, Nicholson LF, Faull RL, Evans WH, Severs NJ, Green CR (1998a) Connexin expression in Huntington's diseased human brain. Cell Biol Int 22:837-847.

Vis JC, Nicholson LF, Faull RL, Evans WH, Severs NJ, Green CR (1998b) Connexin expression in Huntington's diseased human brain. Cell Biology International 22:837-847.

Vis JC, Willecke K, van Roon-Mom WMC, Milham V, Faull RL, Becker DL, Nicholson LF, Green CR (in preparation) Knockdown of gap junction protein connexin43 reduces secondary lesion spread following brain injury, in preparation.

Von Euler H, Khoshnoud R, He Q, Khoshnoud A, Fornander T, Rutqvist LE, Skog S (2005) Time-dependent RNA degradation affecting cDNA array quality in spontaneous canine tumours sampled using standard surgical procedures.979-985, 2005 Dec.

Wang HX, Tong D, El-Gehani F, Tekpetey FR, Kidder GM (2009a) Connexin expression and gap junctional coupling in human cumulus cells: contribution to embryo quality. J Cell Mol Med 13:972-984.

Wang HY, Malek RL, Kwitek AE, Greene AS, Luu TV, Behbahani B, Frank B, Quackenbush J, Lee NH (2003) Assessing unmodified 70-mer oligonucleotide probe performance on glass-slide microarrays. Genome Biology 4:R5.

Wang S, Li J, Xia W, Geng M (2007) A marine-derived acidic oligosaccharide sugar chain specifically inhibits neuronal cell injury mediated by beta-amyloid-induced astrocyte activation in vitro. Neurol Res 29:96-102.

Wang X, Ghosh S, Guo SW (2001) Quantitative quality control in microarray image processing and data acquisition. Nucleic Acids Research 29:E75-75.

Wang Z, Gerstein M, Snyder M (2009b) RNA-Seq: a revolutionary tool for transcriptomics. Nature reviews Genetics 10:57-63.

Ware CF (2008) The TNF Superfamily-2008. Cytokine Growth Factor Rev 19:183-186.

Watakabe A, Sugai T, Nakaya N, Wakabayashi K, Takahashi H, Yamamori T, Nawa H (2001) Similarity and variation in gene expression among human cerebral cortical subregions revealed by DNA macroarrays: technical consideration of RNA expression profiling from postmortem samples. Brain Res Mol Brain Res Molecular Brain Research. 88:74-82.

Webster MJ (2006) Tissue preparation and banking. Prog Brain Res 158:3-14.

Weis S, Llenos IC, Dulay JR, Elashoff M, Martinez-Murillo F, Miller CL (2007) Quality control for microarray analysis of human brain samples: The impact of postmortem factors, RNA characteristics, and histopathology. Journal of Neuroscience Methods 165:198-209.

White TW, Srinivas M, Ripps H, Trovato-Salinaro A, Condorelli DF, Bruzzone R (2002) Virtual cloning, functional expression, and gating analysis of human connexin31.9. Am J Physiol Cell Physiol 283:C960-970.

Willecke K, Eiberger J, Degen J, Eckardt D, Romualdi A, Guldenagel M, Deutsch U, Sohl G (2002) Structural and functional diversity of connexin genes in the mouse and human genome. Biological Chemistry 383:725-737.

Wilson DL, Buckley MJ, Helliwell CA, Wilson IW (2003) New normalisation methods for cDNA microarray data. Bioinformatics 19:1325-1332.

Winer BJ, Brown DR, Michels KM (1991) Statistical Principles In Experimental Design: McGraw-Hill.

Wisniewski HM, Wegiel J (1991) Spatial relationships between astrocytes and classical plaque components. Neurobiol Aging 12:593-600.

Workman C, Jensen LJ, Jarmer H, Berka R, Gautier L, Nielser HB, Saxild HH, Nielsen C, Brunak S, Knudsen S (2002) A new non-linear normalisation method for reducing variability in DNA microarray experiments. Genome Biol 3:research0048.

Xiao Y, Frisina R, Gordon A, Klebanov L, Yakovlev A (2004) Multivariate search for differentially expressed gene combinations. BMC Bioinformatics 5:164.

Xu HL, Pelligrino DA (2007) ATP release and hydrolysis contribute to rat pial arteriolar dilatation elicited by neuronal activation. Exp Physiol 92:647-651.

Yang YH, Dudoit S, Luu P, Lin DM, Peng V, Ngai J, Speed TP (2002a) Normalisation for cDNA microarray data: a robust composite method addressing single and multiple slide systematic variation. Nucleic Acids Research 30:e15.

Yang YH, Dudoit S, Luu P, Lin DM, Peng V, Ngai J, Speed TP (2002b) Normalisation for cDNA microarray data: a robust composite method addressing single and multiple slide systematic variation. Nucleic Acids Res 30:e15.

Yawata I, Takeuchi H, Doi Y, Liang J, Mizuno T, Suzumura A (2008) Macrophage-induced neurotoxicity is mediated by glutamate and attenuated by glutaminase inhibitors and gap junction inhibitors. Life Sci 82:1111-1116.

Ye ZC, Wyeth MS, Baltan-Tekkok S, Ransom BR (2003) Functional hemichannels in astrocytes: a novel mechanism of glutamate release. J Neurosci 23:3588-3596.

Yeager M, Harris AL (2007) Gap junction channel structure in the early 21st century: facts and fantasies. Curr Opin Cell Biol 19:521-528.

Yue H, Eastman PS, Wang BB, Minor J, Doctolero MH, Nuttall RL, Stack R, Becker JW, Montgomery JR, Vainer M, Johnston R (2001) An evaluation of the performance of cDNA microarrays for detecting changes in global mRNA expression. Nucleic Acids Res 29:E41-41.

Zhou F, Yao HH, Wu JY, Yang YJ, Ding JH, Zhang J, Hu G (2006) Activation of Group II/III metabotropic glutamate receptors attenuates LPS-induced astroglial neurotoxicity via promoting glutamate uptake. J Neurosci Res 84:268-277.

Zonta M, Angulo MC, Gobbo S, Rosengarten B, Hossmann KA, Pozzan T, Carmignoto G (2003) Neuron-to-astrocyte signaling is central to the dynamic control of brain microcirculation. Nat Neurosci 6:43-50.